Morphological differences between avian influenza viruses grown in chicken and duck cells, a comparative study

By

Firas Al–Mubarak

BVSc & MSc

Thesis submitted to the University of Nottingham for the degree of Doctor of Philosophy

Division of Infection and Immunity

School of Veterinary Medicine and Science

The University of Nottingham

October 2014

Abstract

The major reservoirs for most influenza A virus subtypes are wild aquatic birds, especially ducks. However, they are typically resistant to the effects of the infection and usually do not develop clinical disease. In contrast, some influenza viruses cause severe illness or even death in susceptible hosts like chickens and turkeys. Paradoxically, infection of primary duck cells results in rapid cell death, whereas in chicken cells, death occurs less rapidly. Duck cells produce fewer infectious virions in comparison with the longer surviving chicken cells. In order to understand this variation in infectious virus production, chicken and duck embryo fibroblast cells (CEF and DEF) were infected with low pathogenic avian H2N3, and the viruses produced from the two hosts ware characterised. Infectious virus production from chicken cells was significantly greater than that observed from duck cells, from 8–48 hr after infection. Influenza matrix gene and protein expression, analysed by quantitative real time PCR and western blotting of culture supernatants, showed comparable levels between species at 8 and 24 hr post infection. These findings led to investigation of virus budding and morphology following infection of duck and chicken cells with the virus. Differences in morphology of released virions were observed. Budding viruses from duck cells were elongated, while chicken cells produced almost spherical virions. There was a similar clear difference in virus morphology in the duck and chicken culture supernatants. Spherical viruses were observed in chicken supernatants while duck cell supernatants contained pleomorphic virions. No differences between any genes of chicken– and duck–derived viruses were found, suggesting that host cell determinants might be responsible for such variations in virus morphology. DEF cells showed extensive production of filamentous or short filament virions following infection with filamentous (equine H3N8) and non–filamentous (avian H2N3) virus strain, respectively. This was observed even after actin disruption

with cytochalasin D (Cyt.D). CEF cells infected with equine H3N8 virus produced extensive filamentous virus, which decreased markedly after disruption of actin with Cyt.D, whereas, following infection with H2N3, spherical virions were observed in the presence or absence of the actin inhibitor. Cells were also transfected with green fluorescent protein – microtubule-associated protein 1A/1B-light chain 3 (GFP–LC3) expression vector and then infected or mock infected with avian H2N3. Short filaments were observed from untransfected and transfected duck cells, while spherical and short filaments were observed from untransfected and transfected chicken cells, respectively. Filamentous virus formation could be enhanced as a result of autophagy which is more marked in duck cells than chicken cells. Further studies such as studying the structure of chicken and duck fibroblast cell membranes, the use of other drugs that inhibit actin in a mechanistically different way, and the role of other cellular proteins in modulating virus morphology should be considered.

Declaration

I declare that the work in this dissertation was carried out in accordance with the regulations of the University of Nottingham.

The work is original and has not been submitted for any other degree at the University of Nottingham or elsewhere.

Name: Firas Al–Mubarak

Signature:

Date:

Conferences, Posters and Oral Presentations:

1. Society for General Microbiology (SGM), Autumn Conference, 3–5 September 2012: attending; University of Warwick.

2. Al–Mubarak FT., Daly JM, Dunham SP (2012). Molecular and morphological differences between avian influenza viruses grown in chicken and duck cells, a comparative study (Poster Presentation). Influenza 2012: One World, One Health. St Hilda's College, Oxford, UK. 17–19 September, 2012.

3. Al–Mubarak FT., Daly JM, Dunham SP (2013). Identification of differences in polymerase basic (PB1 and PB2) proteins of avian influenza A viruses grown in chicken and duck cells (Poster Presentation). Society for General Microbiology (SGM) Spring Conference 2013, Manchester Central 25th – 28th March 2013.

4. Al–Mubarak FT., Daly JM, Dunham SP (2013). Morphological differences between influenza A viruses in avian host cells (Poster Presentation). Influenza 2013: One Influenza, One World, One Health. St Hilda's College, Oxford, UK. 17–19 September, 2013.

5. Postgraduate (PG) research forum: a Research Poster presented; Faculty of Medicine, University of Nottingham, QMC. 15th June 2008.

6. Research Day (first year); Oral Presentation, in Veterinary Medicine and Science; 15th July 2011.

7. Research Day (second year); Oral Presentation, in Veterinary Medicine and Science; 13th July 2012.

8. Research Day (third year); Oral Presentation, in Veterinary Medicine and Science; 11th January 2013.

Acknowledgements

I am very grateful to my supervisors, Dr. Steve Dunham and Dr. Janet Daly for their scientific supervision and support. I thank their guidance throughout my PhD, their invaluable advice and comments for this thesis. I consider working with them both to have been one of the greatest privileges of my professional life.

I am also would like to express my genuine gratefulness to all staff members, who in various ways assisted me throughout my study.

I also wish to thank Denise Christie, the technician in School of Biomedical Science, University of Nottingham for her technical support with the Electron Microscopy work.

I would like to thank my colleague Donna Louise Fountain, and the other virology group members of the Vet School, University of Nottingham for their help and support during the course of this work.

I wish to thank Source Bioscience (Nottingham, UK) for performing the sequencing of my PCR and cloning samples as well as MWG Operon/ UK for supplying the primers used in this study.

I would like to thank Cherry Valley Company Farms Limited, UK for providing ducks eggs and Henry Stewart & Co. Ltd, UK for providing chicken eggs used to propagate viruses and extract cells. I also thank Dr Debra Elton (Animal Health Trust) and Dr Ian Brown (Animal Health Veterinary Laboratory Agency) for providing equine H3N8 and avian H2N3 influenza A viruses, respectively, used in this study.

I wish to express my deepest thankfulness to my beloved mother, brothers, sisters and extended family in Iraq for their motivation and encouragement throughout my career. I

also wish to express deepest love and thankfulness to my wife Abeer, daughter Shatha, and son Abdullah for their support and help during this time.

Finally, I am deeply grateful to the Iraqi government's Ministry of Higher Education and Scientific Research for providing me with an Overseas Scholarship and also for generous funding.

Table of Contents

List of Tables

List of Figures

List of Abbreviations

˚C	Degree Celsius
293T	Human embryonic kidney cells
AI	Avian Influenza
APS	Antigen presenting cells
bp	Base pair
BSA	Bovine serum albumin
CD4	Cluster of differentiation 4
CD8	Cluster of differentiation 8
cDNA	Complementary deoxyribonucleic Acid
CEF	Chicken embryo fibroblasts
CF	Complement Fixation
CPE	Cytopathic effect
Cyt.D	Cytochalasin D
DAPI	4',6–Diamidino–2–phenylindole
DEF	Duck embryo fibroblasts
DEPC	Dimethylpyrocarbonate
DM	Dissociation medium
DMEM	Dulbecco's modified Eagle's medium
DMP–30	Dimethylaminomethyl phenol
DNA	Deoxyribonucleic acid
dNTPs	Deoxynucleotide phosphates
DPBS	Dulbecco's phosphate buffer saline
E.coli	Escherichia coli
EB	Elution Buffer
EDTA	Ethylenediaminetetraacetic acid

ELISA	Enzyme Linked Immunosorbent Assay
EM	Electron Microscopy
ER	Endoplasmic reticulum
FCS	Fetal calf serum
FDA	Food and Drug Administration
FITC	Fluorescein isothiocyanate
g	Gram
GFP	Green fluorescent protein
HA	Haemagglutinin
HEX	Hexagon
HI	Hemagglutination Inhibition
HPAI	High pathogenic avian influenza
hr	Hour(s)
HRP	Horseradish peroxidase
IFN	Interferon
IgG	Immunoglobulin G
IgM	Immunoglobulin M
IgY	Immunoglobulin Y
IL	Interleukin
L	Litre
LC3	Microtubule–associated protein 1A/1B–light chain 3
LLC–MK2	Rhesus monkey kidney epithelial cell line
LPAI	Low Pathogenic Avian Influenza
M	Matrix
MDA 5	Melanoma differentiation–associated gene 5
MDCK	Madin Darby Canine Kidney cells

min	Minute(s)
MIP	Macrophage inflammatory protein
mL	Milliliter
mm	Millimetre
MOI	Multiplicity of infection
mRNA	Messenger Ribonucleic acid
NA	Neuraminidase
NES	Nuclear Export Signal
ng	Nanogram
NK	Natural Killer cells
NLR	NOD like receptor
nm	Nanometer
NP	Nucleoprotein
NS	Non structural
PA	Polymerase acidic
PAGE	Poly acrylamide gel electrophoresis
PB	Binding buffer
PB1	Polymerase basic 1
PB2	Polymerase basic 2
PBS	Phosphate Buffer Saline
PCR	Polymerase Chain Reaction
PE	Washing buffer
pfu	Plaque–forming unit
pml	Picomole
PRRs	Pattern–recognition receptors
PTA	Phosphotungstic acid

RIG–I	Retinoic acid inducible gene–I
RNA	Ribonucleic acid
RNase	Ribonuclease
RNP	Ribonucleoprotein
RT–PCR	Reverse transcriptase Polymerase Chain Reaction
s	Second(s)
SAα2,3–Gal	Sialic acid linked to galactose by α2,3 linkage
SAα2,6–Gal	Sialic acid linked to galactose by α2,6 linkage
SDS	sodium dodecyl sulfate
siRNA	Small interfering RNA
ssRNA	Single stranded RNA
TAE	Tris–acetate–EDTA
TBCK	L–1–tosylamido–2–phenylethyle chloromethyl ketone
TBS	Tris Buffered Saline
TLR	Toll like receptors
TNF	Tumor necrosis factor
U	Unit(s)
UTRs	Untranslated regions
UV	Ultra–violet
V	Volt
VLPs	Virus–like particles
xg	Gravitational force
µg	Microgram
µM	Micromolar
µl	Microlitre
µm	Micrometre

Chapter 1

Introduction and Aims

1.1 Influenza

Influenza, commonly known as the 'flu, is an acute febrile viral illness that affects the respiratory tract of birds and mammals. It usually occurs between autumn to spring and appears in epidemic form in humans which spreads in a specific community and sometimes in pandemic form causing high levels of mortality and economic losses (Timbury, 1997). In humans, it has been documented that epidemic 'flu is responsible for 3–5 million typical infections and 250,000 to 500,000 fatal cases each year (WHO, 2011). New influenza viral strains may be generated over time causing sudden pandemic outbreaks which spread easily among humans especially infants, elderly, and immunocompromised persons (Timbury, 1997, Smith et al., 2001). Several pandemic outbreaks have been recorded and the most significant is the so–called "Spanish flu", which occurred in 1918, killing more than 30 million people around the world. Other significant outbreaks were in 1957 (Asian flu), and in 1968 (Hong Kong flu); but they were less severe than the 1918 pandemic avian influenza (Horimoto and Kawaoka, 2001, Horimoto and Kawaoka, 2005).

1.2 Avian influenza

The first description of avian influenza (AI) was in Italy in 1878 when researchers differentiated a disease of poultry from other diseases with high mortality rates (Alexander and Brown, 2009). The disease is highly contagious for poultry and associated with high mortality. It was named "fowl plague" and it was initially confused with fowl cholera (avian pasteurellosis). In 1880, according to the clinical and pathological properties, the disease was differentiated from fowl cholera and called Typhus exudatious gallinarum. In 1901, scientists determined that a virus causes the

disease, and in 1955, the classical fowl plague virus was confirmed to be a type A influenza virus based on the presence of type–specific ribonucleoprotein (Lupiani and Reddy, 2009). The first isolation of influenza A virus from free–living wild ducks was in 1972 and at that time, numerous surveillance studies showed that wild birds including free–flying and shore birds are the natural hosts for all influenza A subtypes (Slemons et al., 1974).

1.3 Influenza viruses

Influenza viruses belong to the *"Orthomyxoviridae"* family and are classified into five different genera: influenza A, influenza B, influenza C, Thogotovirus, and Isavirus (Cheung and Poon, 2007). They were initially isolated from pigs in 1931 and later from humans in 1933 (Shope, 1931, Smith W., 1995, Juozapaitis and Antoniukas, 2007). The most serious types that cause dangerous outbreaks with high morbidity and mortality are influenza A viruses because they mutate more rapidly and have a wider range of hosts (Khanna et al., 2008). Influenza A viruses infect animals, including birds, pigs, horses, whales, seals, and also humans (Ito and Kawaoka, 2000, Reperant et al., 2009). Type B and C are generally found in humans, in addition to some mammals like seals, with less severity than influenza A. The infection is usually associated with a common cold–like illness, particularly in children (Greenbaum et al., 1998, Osterhaus et al., 2000). Wild aquatic birds of the order of *Anseriformes* (ducks, geese and swans) and *Charadriformes* (gulls, terns, surfbird and sandpiper) are considered to be the natural reservoir of all types of influenza A viruses. In these hosts, viral replication occurs mainly in the gastrointestinal tract, and to a lesser extent in the respiratory tract. The infected birds

generally have no apparent signs of illness, but with some exceptions after infection with highly pathogenic avian influenza viruses (Munster et al., 2007).

The main differences between the three main types of influenza viruses (A, B and C) are outlined in table 1.3–1.

	Influenza A	Influenza B	Influenza C
Number of gene segments	8	8	7
Surface glycoproteins	HA and NA	HA and NA	HEF (Haemagglutinin–Esterase–Fusion)
Host range	Wide range of hosts (humans, pigs, horses, whales, seals and birds)	Humans and seals	Mainly humans (also found in swine)

Table 1.3–1 Comparison of major properties of influenza viruses, adapted from Cheung and Poon (2007)

1.3.1 Structure and molecular biology of influenza A virus

Influenza viruses are roughly spherical with a size of around 100 nm or filamentous in shape, often in excess 300 nm in length (Bouvier and Palese, 2008). Morphological structure is known to be affected by several viral proteins (HA, NA, M1, and M2), in addition to the nature of the host cells (Cheung and Poon, 2007).

Influenza viruses are enveloped with surface glycoprotein spikes and a segmented RNA genome of negative sense (complementary to mRNA). RNA of influenza A virus is organized into 8 segments, in total around 13600 nucleotides long (Hoffmann et al., 2001). These are the polymerase basic (PB1 and PB2), the polymerase acidic (PA), haemagglutinin (HA), nucleoprotein (NP), neuraminidase (NA), matrix (M), and non–structural (NS) genes (Samji, 2009).

Each viral segment contains non–coding regions at both 5´ and 3´ ends. The 5´ terminus of each influenza A viral RNA segment has 13 conserved nucleotides, and the 3´ terminus has 12. The extreme ends are conserved among all segments, and this is followed by a segment–specific noncoding region (Hoffmann et al., 2001). These unique noncoding regions (U12 and U13) contain the promoter components, which are important for the initiation of transcription and replication as they are recognized by the polymerase complex consisting of PB1, PB2, and PA proteins (Hsu et al., 1987, Coloma et al., 2009). In between these highly conserved noncoding regions and the long central coding region of each gene there are additional untranslated regions (UTRs) at both 5´ and 3´ ends. Specific nucleotides and the UTRs and terminal coding regions act as the viral packaging signal (Hutchinson et al., 2010). Figure 1.3–1 shows the typical structure of influenza viral RNA.

Figure 1.3–1 Schematic diagram of a typical influenza viral RNA segment.

A large open reading frame (green box) which represents the coding region is flanked by short untranslated region (UTRs) (black lines) containing terminal promoter sequences (blue boxes) that form the polymerase binding site. Those sequences are comparable between all genome segments and all virus subtypes. Specific nucleotide segments (red wedges), which overlap the UTRs and the terminal coding regions act as viral packaging signal. Figure adapted from Hutchinson et al. (2010).

Influenza A viral gene segments are known to encode at least ten proteins which are the RNA polymerase complex proteins (PA, PB1, and PB2), surface glycoproteins (HA, and NA), nucleoprotein (NP), matrix proteins (M1 and M2), and nonstructural proteins (NS1,

NS2) (Samji, 2009, Wang and Taubenberger, 2010). In addition, PB1–F2 and a new viral protein (N40) which is translated from segment 2 have been recently identified in some influenza A virus isolates (Chen et al., 2001, Wise et al., 2009). Moreover, two more proteins, PA-X and M42 which are translated from segment 3 and 7, respectively, have been recently found (Jagger et al., 2012, Wise et al., 2012) (Figure 1.3–2).

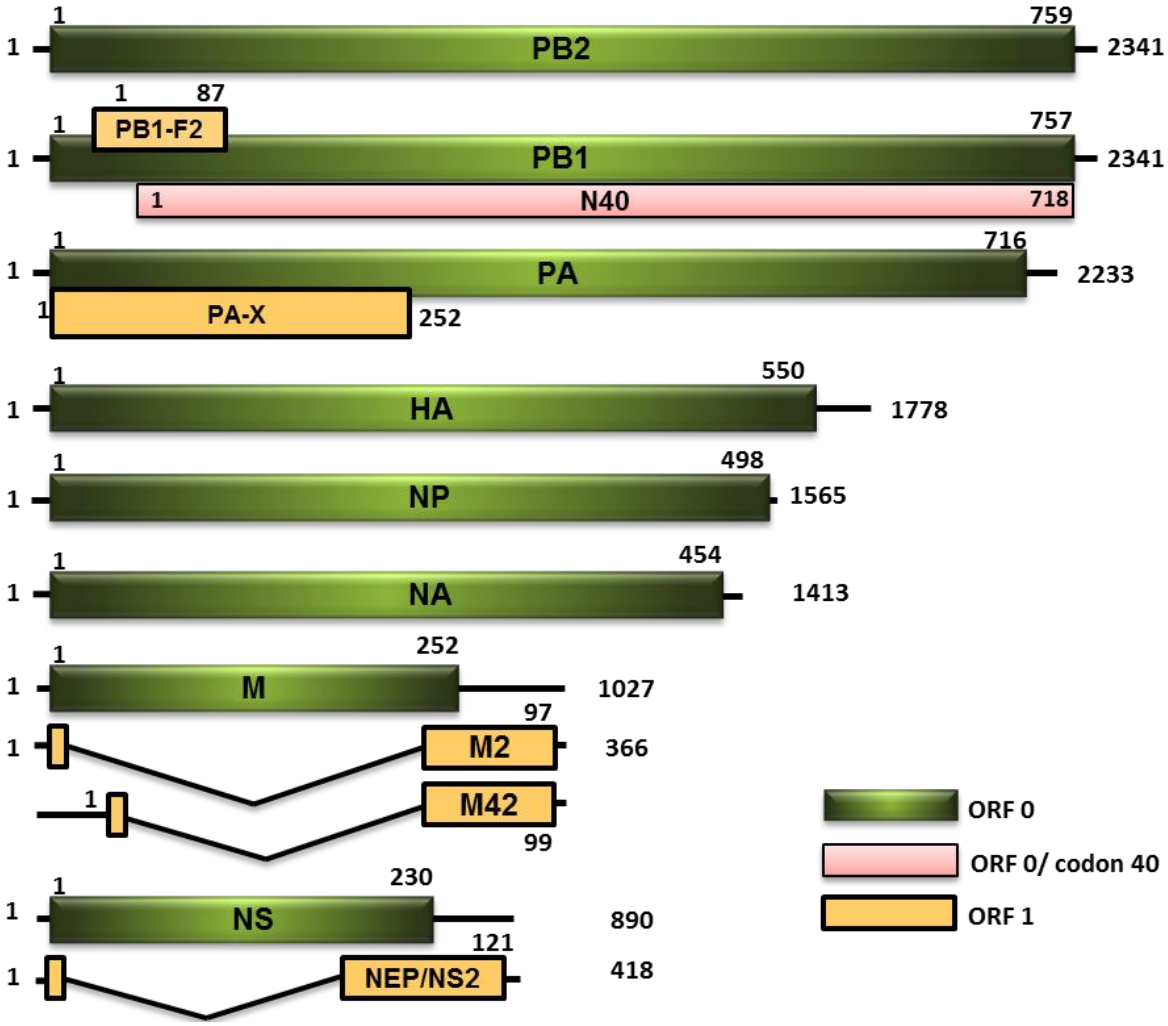

Figure 1.3–2 Genomic structure of influenza A virus.

RNA segments (in nucleotides) shown in positive sense and their encoded proteins (in amino acids). The lines at the 5´ and 3´ termini represent the coding regions. The PB1 segment encodes three proteins, two of them (PB1 and N40) translated from ORF 0, and PB1–F2 protein translated from ORF 1. The M2, M42 and NEP/NS2 proteins are encoded by spliced mRNAs (the introns are indicated by the V–shaped lines). Figure modified from (David M. Knipe, 2007, Jagger et al., 2012, Wise et al., 2012).

Each viral RNA segment is surrounded by nucleoprotein (NP) forming ribonucleoprotein (RNP) and encapsidated by one copy of trimeric polymerase (PB1–PB2–PA complex) which is essential for viral replication (Digard et al., 1999). The lengths of the rod–like RNPs are varied (30–100 nm) and correlate with the length of each viral segment (Noda and Kawaoka, 2010). By longitudinally and transversally sectioning budding virions of different virus strains, a study has shown that the eight RNPs are highly organized in a distinct pattern; a central segment is surrounded by seven segments of different lengths (Noda et al., 2006). Such an organization is also observed in the isolated virion (Calder et al., 2010). The structural organization of viral ribonucleoprotein can be seen in figure 1.3–3.

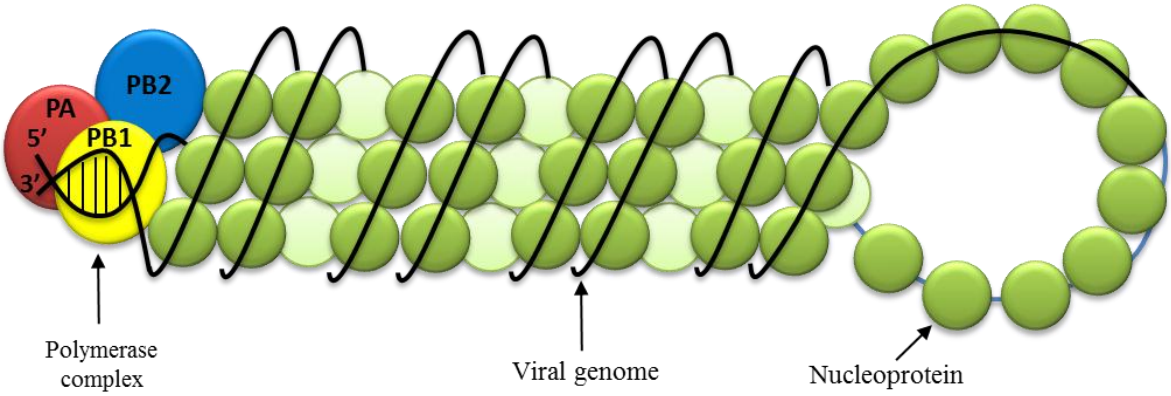

Figure 1.3–3 Structure of influenza virus ribonucleoprotein (vRNP).

Green spheres represent NP monomers, and the black line shows the associated single–stranded vRNA molecule. Influenza RNP folds into a double–helical hairpin structure. A short duplex formed between the 5′ and the 3′ ends provides the binding site for the heterotrimeric RNA–dependent RNA polymerase. Figure adapted from Portela and Digard (2002).

Four virus proteins (PB2, PB1, PA, and NP) are responsible for virus transcription and replication of the viral genome in the nuclei of infected cells. PB1–F2 protein plays a role in pro–apoptotic activity, while N40 protein, which is encoded by the same gene (PB1),

interacts with the polymerase complex in the cellular environment but does not contribute to transcription function (Wise et al., 2009). PA-X protein has been shown to modulate host response and viral virulence (Jagger et al., 2012). Haemagglutinin (HA or H) plays a role in virus attachment to the host cell and subsequent fusion with cell membranes, while neuraminidase (NA or N) supports the release of viruses from the host cell surface by hydrolyzing sialic acid from glycoproteins which helps to release the progeny virus particles from host cells (McCauley and Mahy, 1983, Odagiri, 1992). Non–structural protein 1 (NS1) has a major role in inhibition of host immune response via limitation of interferon (IFN) production (Hale et al., 2008). NS2 (also called nuclear export protein or NEP) plays a role in the export of RNPs from the nucleus to the cytoplasm during viral replication, in addition, it also regulates virus transcription and replication processes (Robb et al., 2009). Matrix protein 1 (M1), the major structural protein, is the dominant protein in determining virus morphology and also plays an important role in virus assembly and budding (Rossman and Lamb, 2011). Matrix protein 2 (M2) is the ion channel that regulates the pH, and is responsible for virus uncoating, the step that follows virus entry into the host cell (Holsinger et al., 1994). In addition, this protein also plays an important role in membrane scission in the last stage of virus life cycle (Roberts et al., 2013). Matrix protein 42 (M42) can functionally replace M2 and support efficient replication in null M2 influenza viruses (Wise et al., 2012). Table 1.3–2 summarizes the length of each viral segment and the function of protein(s) encoded by each segment.

Segment	Segment length in nucleotides	Encoded protein(s)	Protein length in amino acids	Protein function
1	2341	PB2	759	Polymerase subunit; plays a role in RNA replication by mRNA cap recognition
2	2341	PB1	757	Polymerase subunit; RNA elongation during replication
		PB1–F2	87	Pro–apoptotic activity
		N40	718	Polymerase complex interaction
3	2233	PA	716	Polymerase subunit; endonuclease activity
		PA-X	252	modulates the host response and viral virulence
4	1778	HA	550	Major surface antigen, receptor binding and fusion activities, main target for neutralizing antibodies
5	1565	NP	498	RNA binding protein; nuclear import regulation
6	1413	NA	454	Minor surface glycoprotein for neutralizing antibodies; sialic acid activity, cleavage of progeny virions from host cell receptors and virus release
7	1027	M1	252	Major component of virion; RNA nuclear export regulation, viral assembly and budding
		M2	97	Ion channel for controlling pH during virus uncoating and HA synthesis (viral release)
		M42	99	functionally replace M2 in M2-null viruses
8	890	NS1	230	Interferon antagonist protein; regulation of host gene expression
		NEP	121	Control export of RNP from nucleus

Table 1.3–2 Influenza A virus gene segments, their proteins and functions. Modified from Bouvier and Palese (2008). Typical gene and protein sizes shown, though strain variation occurs.

The viral envelope is made of a lipid bilayer which is derived from the host cell's plasma membrane. Three surface viral antigens are embedded in the lipid bilayer: the HA spike, which has a rod like–shape, represents approximately 80% of the total surface proteins; the NA spike, which is almost mushroom–shaped, represents 17%; with minor components of M2 represented by few molecules (only 16 to 20 molecule per virion) (Schroeder et al., 2005, Nayak et al., 2009). Underneath the lipid bilayer, the M1 protein forms a layer that separates the viral segments from the virus membrane. Inside the virion, 8 segments of different length are associated with the nucleocapsid protein (NP) and three large proteins (PB1, PB2, and PA). NEP is also associated with the virus but in low amounts (Cheung and Poon, 2007). Figure 1.3–4 illustrates the typical structure of influenza A virus.

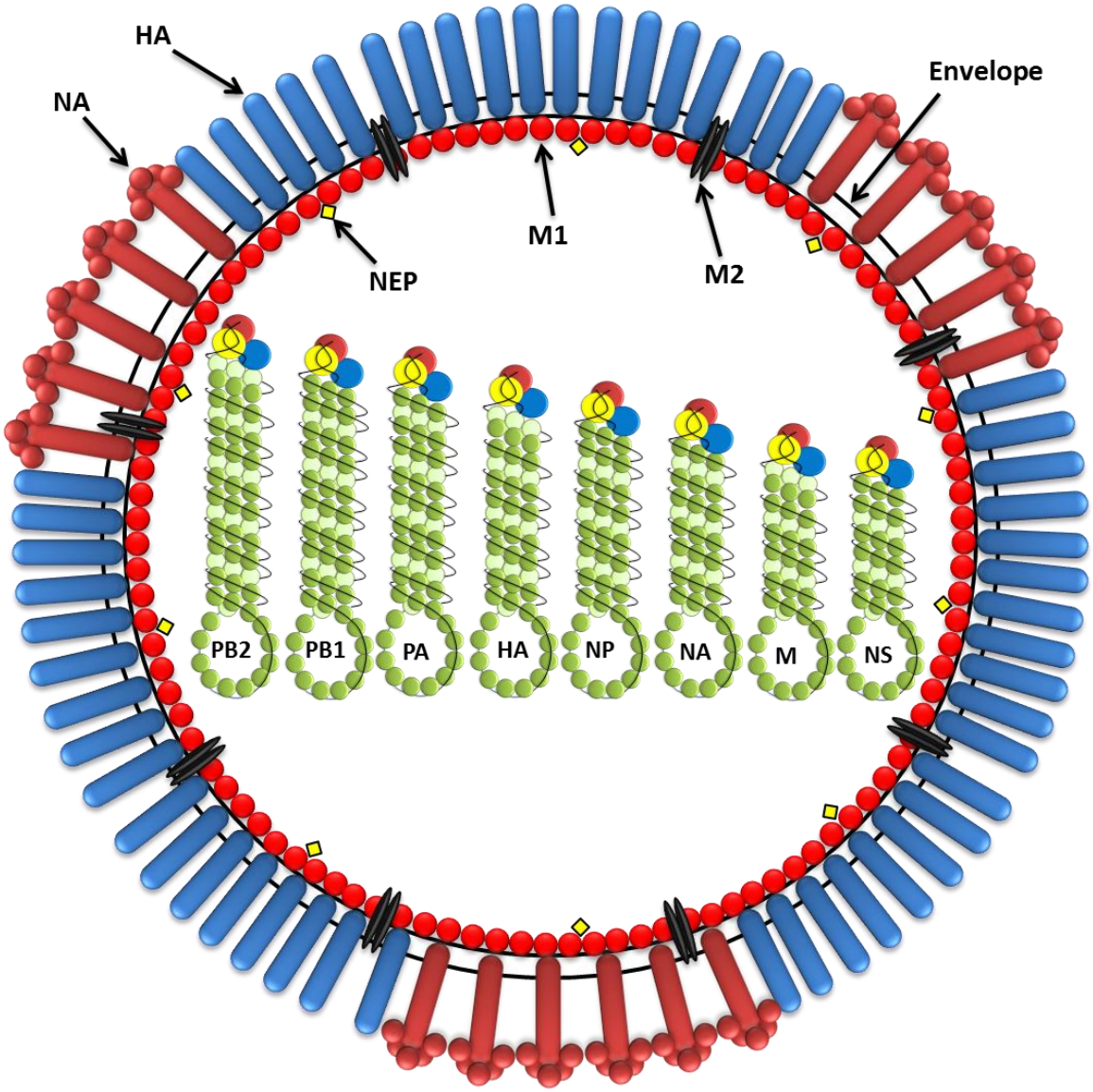

Figure 1.3–4 Schematic diagram of influenza virus A particle.

The RNA is segmented and each segment encodes one or more proteins. The segments are not identical in length (ranging from 2341 to 890 nucleotides). The longest segment encodes PB2 protein and the shortest encodes NS protein. The RNA segments are coated with nucleoprotein forming ribonucleoprotein (RNP), and a small amount of transcriptase (polymerase complex) represented by PB1, PB2, and PA is also associated with it. The haemagglutinin (HA), neuraminidase (NA), and M2 proteins are inserted into the host–derived lipid envelope. The matrix (M1) protein underlies the lipid envelope. A nuclear export protein (NEP) is also associated with the virus.

Both NA and HA genes encode surface glycoproteins and influenza A virus can be classified into several subtypes according to the antigenic diversity of those surface antigens. There are 18 HA and 11 NA subtypes described as H1–H18 and N1–N11 with amino acid sequences differing by 30% or more between subtypes (Hampson and Mackenzie, 2006). Of those subtypes, 16 HA (HA1–HA16) and 9 NA (NA1–NA9) circulate in waterfowl and two of HA and NA (HA17–HA18 and NA10–NA11) have been isolated from bats (Tong et al., 2012, Tong et al., 2013). The most frequently circulating subtypes of influenza A viruses in the human population are H1N2, H3N2 and H1N1 (Nelson and Holmes, 2007).

In addition, many different subtypes have been generated over time because of the genetic reassortment (antigenic shift). In the last few years, humans have been infected with swine and bird flu in different parts around the word, raising concerns for public health for humans as well as for pork and poultry production worldwide (Metzgar et al., 2010, Van-Tam and Sellwood, 2010).

1.3.2 Replication of influenza A viruses

1.3.2.1 Virus attachment and entry

The first step of viral replication is virus attachment to its host cell through N–acetyl neuraminic (sialic) acid, a nine–carbon acidic monosaccharide (Couceiro et al., 1993). The most common linkages of sialic acids are α 2,3 and α 2,6 linkage with which influenza viruses have the affinity to bind. The different sialic acid linkages can be one factor in host specificity. Both types of receptors are wide spread in many organs in chickens, ducks, cats, and pigs (Kuchipudi et al., 2009, Nelli et al., 2010, Trebbien et al., 2011, Wang et al., 2013); with a dominant expression of SA α 2,6Gal in the respiratory

tissues of humans including epithelial cells in the nasal mucosa, paranasal sinuses, pharynx, trachea, bronchi and bronchioles; while SA α 2,3Gal is occasionally detected in the nasal mucosa and on the non–ciliated cuboidal bronchiolar cells at the junction between the respiratory bronchiole and alveolus (Shinya et al., 2006).

Once a host cell is infected with influenza virus, the HA glycoprotein is produced as a precursor, HA0, which is cleaved into two subunits (HA1 and HA2) by host serine proteases before virus particles become infectious (Klenk and Garten, 1994). The H1 portion contains the antigenic sites (the receptor binding domain), while the H2 portion mediates fusion of the virus envelope and cell membranes (Figure 1.3–5) (Steinhauer, 1999). Virulent and avirulent avian influenza A viruses can be differentiated by the sequence of a few basic amino acids at the point where the HA0 is cleaved (cleavage site); the so–called cleavage sequence (Zambon, 1999).

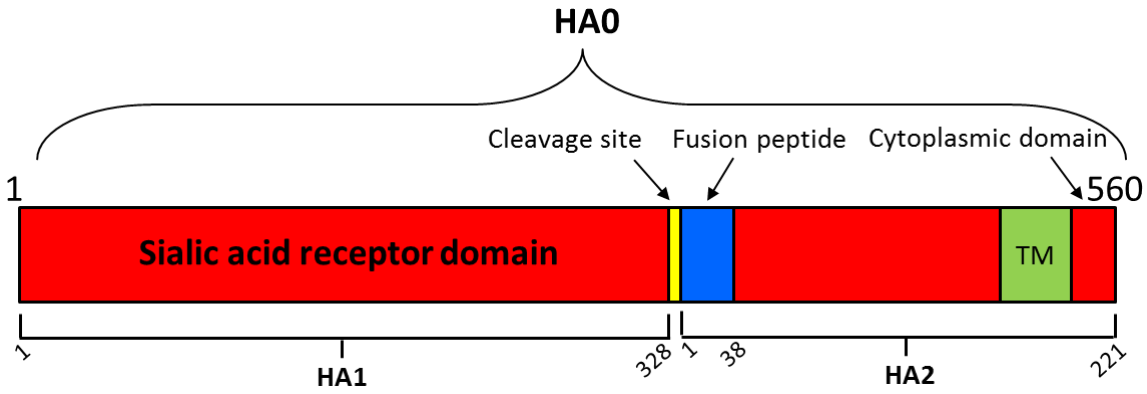

Figure 1.3–5 Schematic structure of HA of influenza A virus.

The HA0 monomer of approximately 560 amino acid length is cleaved into HA1 and HA2 at the cleavage site (yellow). Fusion peptide (blue) mediates fusion of the virus envelope and cell membranes. TM: transmembrane domain.

The virus enters the host cell via receptor (clathrin) mediated endocytosis at the inside face of the plasma membrane forming an endosome (Rust et al., 2004). Although other

endocytic routes (non–clathrin–dependent) may provide additional entry pathways, the endocytic pathway seems to be the most common (Sieczkarski and Whittaker, 2002). The endosome has a low pH of around 5 to 6, which induces a conformational change in HA0, displaying the HA2 fusion peptide. This fusion peptide inserts itself into the endosomal membrane and mediates the fusion of the viral envelope with the endosomal membrane, reviewed in Stegmann (2000). This mechanism is not only important for inducing the conformation change in HA0, but also opens up the M2 ion channel during fusion of viral and endosomal membranes, allowing the virion interior to become acidic which releases the vRNP from M1. This permits the vRNP to enter the host cell's cytoplasm, reviewed in Pinto and Lamb (2006).

1.3.2.2 Transcription, replication and protein synthesis

Transcription and replication occur inside the nucleus. Because of the negative sense of the viral genome, the viral RNA is copied into positive sense mRNA by the polymerase complex to act as a template for the production of the viral RNAs. The polymerase complex responsible for viral transcription and replication is formed by PB1, PB2, and PA. The viral RNA transcription is catalyzed by the RNA dependent RNA polymerase. The mRNA acquires a 5´ capped primer in a process known as "cap snatching". The PB2 protein has a role to capture this primer from host mRNA. The cap is cleaved by PA endonuclease into short sequence which is polymerized by RNA dependent RNA polymerase PB1.The resultant positive sense viral mRNA is exported to the cytoplasm through nuclear pores to start viral translation by ribosomes (Figure 1.3–6). Positive sense viral mRNA also serves as a template to produce the negative sense RNA that is packaged into new virions (Bouloy et al., 1978, Swayne, 2008).

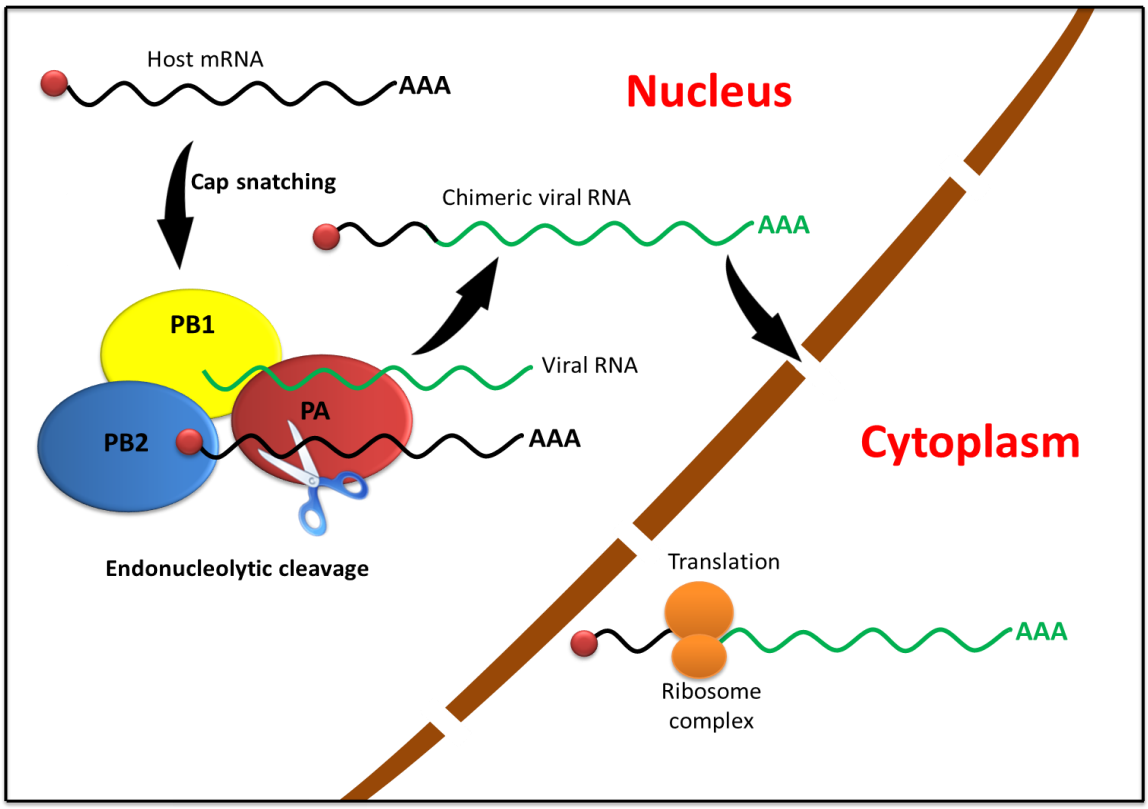

Figure 1.3–6 Cap–snatching transcription mechanism of influenza A virus polymerase.

The polymerase complex (PB1, PB2, and PA) is localized in the nucleus of infected host cell. The PB2 subunit steals short 5´ capped host mRNA molecule (black). The cap is cleaved by PA endonuclease into a short fragment (10–15 nucleotides) which is used to initiate polymerization by RNA dependent RNA polymerase of the PB1 subunit using viral RNA as a template (green), resulting in capped, polyadenylated, chimeric mRNA molecule (black and green). The resultant molecule is exported to the cytoplasm via nucleus pores for translation into viral proteins. Figure adapted from Boivin (2010).

Polymerase basic (PB1 & PB2), nonstructural (NS1 & NS2), NP, PA, and M1 proteins are synthesized in the host cell cytoplasm then transported to the nucleus to participate in matrix and nonstructural splicing, transcription and replication. Surface glycoproteins (HA and NA) are synthesized by ribosomes and then enter the endoplasmic reticulum (ER), where they are glycosylated, and then folded in the Golgi apparatus. These proteins are incorporated in the cell membrane and assembled with vRNP complex, (reviewed in Sidorenko and Reichl (2004)). Matrix 2 (M2) protein is modified by palmitoylation and it also plays a part in membrane association (Grantham et al., 2009).

1.3.2.3 Virus packaging, budding and release

Influenza progeny virions are not infectious unless they have all eight genome segments (Bancroft and Parslow, 2002). Formation of new vRNP complexes from the newly synthesized PB1, PB2, PA, NP, and NS2 proteins occurs in the nucleus of the infected host cell. M1 proteins catalyze the transport of vRNP to the cytoplasm after forming M1–vRNP complexes. Nuclear export of vRNA complexes is directed by NEP protein and the nuclear export signal (NES) carried by NP proteins and inhibited by the M1 proteins. Consequently, newly synthesized vRNA accompanied by M1 proteins are unable to penetrate into the nucleus again (Portela and Digard, 2002).

Two models for the packaging of the segmented influenza A virus genome have been identified: random and segment specific packaging (Hutchinson et al., 2010). In the random model, the segments of the viral genome are distinguished from cellular RNA and also non–genomic viral RNAs and then integrated into a new virion; however, this mechanism does not distinguish between different segments. In this case, the possibility of the formation of fully infectious virus might be through chance by acquiring 8 different segments, or by packaging with more segments than the minimum. Conversely, in a mechanism of the specific packaging model, one copy of each viral segment is specifically selected producing fully infectious virus, (cited by Bancroft and Parslow (2002)).

The final step of viral replication is budding and release. Budding occurs at the apical plasma membrane of the host cell, possibly initiated by the accumulation of M1 protein at the cytoplasmic side of the lipid bilayer. The protein complexes represented by M1 interact with the cytoplasmic tail of envelope proteins (M2, HA, and NA proteins). This interaction leads to the formation of a bud and assembly site in the cellular membrane (Bouvier and Palese, 2008). The most important step occurring before the new virion

leaves the plasma membrane is the cleavage of sialic acid residues by NA from glycoproteins and glycolipids to facilitate release of virus particles into the extracellular medium (Palese et al., 1974). In addition, the cytoplasmic tail of M2 protein facilitates virion scission and is also required for filamentous particle formation (Roberts et al., 2013).

1.3.2.4 The role of cell polarity on virus assembly and morphology

Cell polarity is a characteristic feature in many cell types, in particular epithelial cells, which enables them to perform specialized functions. Cytoskeleton proteins, in particular the actin, play a dominant role in establishment and maintenance of this feature. Differences in the structure and organisation of actin cytoskeleton exhibit differences in the level of cell polarity. Cell polarity was shown to play an important role in determining influenza virus morphology, in particular, the filamentous form. Polarized epithelial cells produce high levels of filamentous virus while non-polarized fibroblasts were found to support the production of spherical virions (Roberts and Compans, 1998). The assembly of filamentous virions, but not the spherical, requires an intact actin cytoskeleton because filaments grow by incorporating multiple lipid raft domains in cell membrane. Disruption of actin cytoskeleton with actin inhibitors leads to aggregation of lipid raft domains into annuli surrounding actin cores. This blocks the production of filamentous virions but the spherical viruses are not affected because of the much smaller raft domains necessary for the formation of a single virus particle (Simpson-Holley et al., 2002).

The stages of influenza virus replication start from attachment of the virus onto host cells and end with the release of the progeny particles (Figure 1.3–7).

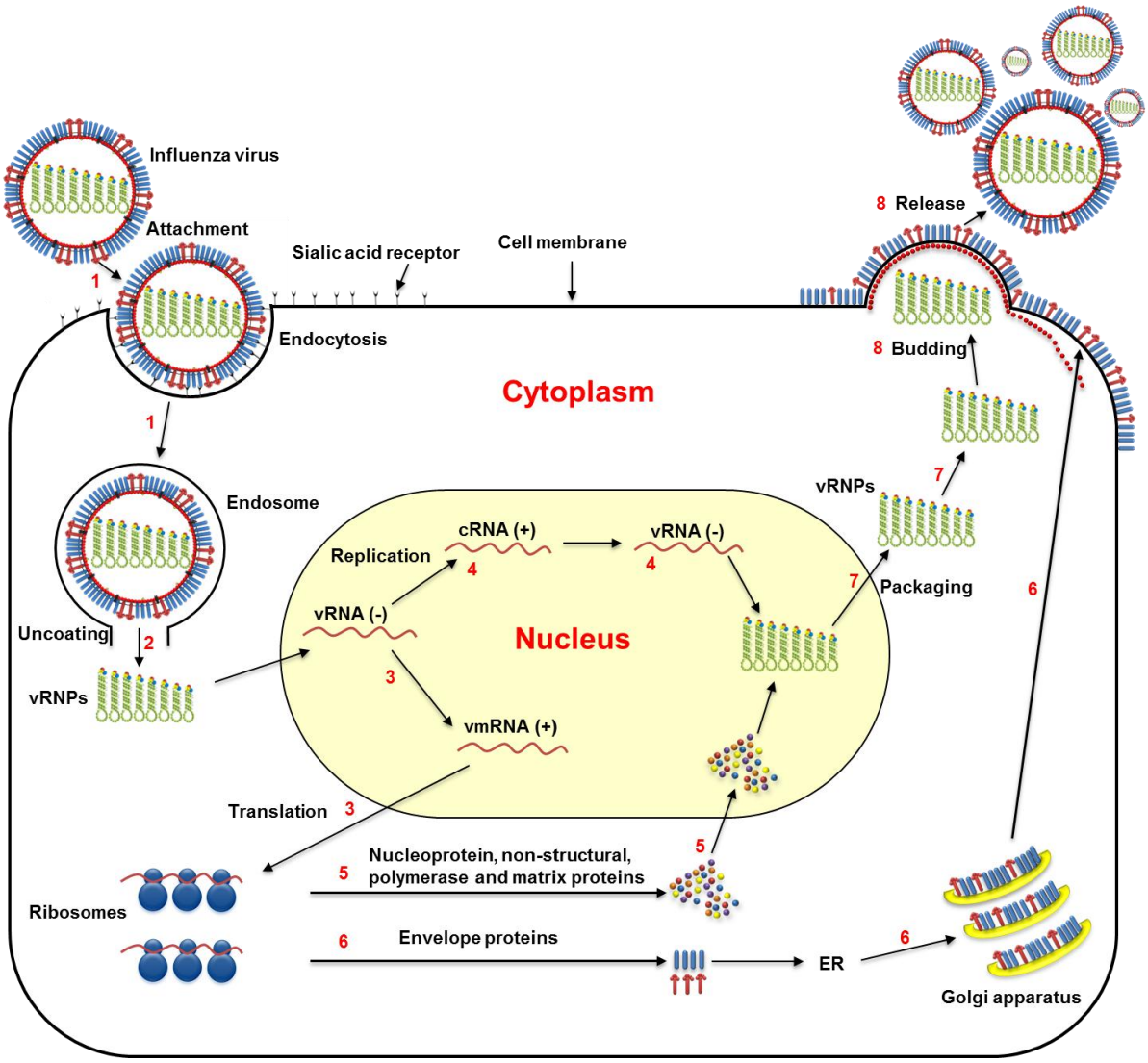

Figure 1.3–7 Life cycle of influenza viruses.

Stages involved in the replication process are:

1. Attachment to host receptor and entry to host cell via endocytosis.

2. Virus uncoating and releasing RNPs to the cytoplasm.

3. Transcription and translation of viral RNA.

4. Replication of viral RNA.

5. Production of nucleoprotein, non-structural, matrix, polymerase acidic, and polymerase basic proteins.

6. Production of envelope proteins (surface glycoproteins HA and NA, and M2) and their transportation to cell membrane.

7. Viral RNPs packaging and assembly.

8. Virion budding and release from the cell membrane.

1.4 Pathogenicity of influenza A viruses

According to the pathogenicity and severity of the disease in chickens, avian influenza A viruses can be classified into two pathotype groups: highly pathogenic avian influenza (HPAI) and low pathogenic avian influenza (LPAI). The mortality rates of the poultry flocks infected with HPAI viruses may reach to 100%, while infection with LPAI cause only milder and primarily respiratory disease (Capua and Alexander, 2009).

In HPAI viruses, the region that encodes the cleavage site of the surface glycoprotein (HA) molecule contains multiple basic amino acids (arginine and lysine) which allows cleavage of the HA molecule by cellular endogenous proteases widely distributed throughout the cells of the body (Wood et al., 1993, Senne et al., 1996). This molecular structure is important in determining the virulence of these strains because it allows the virus to replicate in a considerably broader tissue range, causing widespread damage in tissues and death of the bird, with a mortality rate approaching 100% (Kim et al., 2009, Adams and Sandrock, 2010). The most pathogenic subtypes of avian influenza are restricted to subtypes H5 and H7 (Hampson and Mackenzie, 2006). On the other hand, LPAI viruses have only one basic amino acid (arginine) in the cleavage site of the HA molecule. This limits the site for the viral cleavage by host proteases such as trypsin–like enzymes, and as a consequence, the replication process occurs in limited tissues and organs, particularly in respiratory and digestive tracts, causing only mild disease (Alexander, 2000). LPAI viruses which cause asymptomatic or low pathogenic infection may mutate and convert to HPAI viruses through an adaptation process after infection of poultry (Mundt et al., 2009). This also reflects the importance of the role of wild birds as a primary source of zoonotic introduction of influenza and spreading the pandemics (Causey and Edwards, 2008).

1.5 Genetic variations

During influenza viral replication, genetic variations occur frequently. This is due to the structure of the viral RNA (segmented) and the low fidelity of the RNA dependent RNA polymerase which generates replication errors during virus life cycle (Zambon, 1999, Zambon, 2001). Consequently, influenza A viruses can undergo recurrent antigenic changes (Shors, 2009). The resultant change in structure allows the virus to evade neutralizing antibody, the main mechanism of protective immunity against influenza infection. Such changes may lead to the creation of a new virus strain distinctive from those previously circulating viruses (Zambon, 1999, Smith et al., 2001).

1.5.1 Antigenic shift

Antigenic shift is a result of reassortment and it occurs when two or more different influenza A viruses subtypes infect a single cell simultaneously. Because influenza A viruses are segmented, it is possible to produce new viruses with a variety of segment combinations by the acquisition of entirely new gene segments. The newly assembled progeny virions may have mixed genes from the two parent viruses (Holmes et al., 2005, Nelson et al., 2008). Genome segmentation therefore confers evolutionary advantages by allowing genetic reassortment. This may result in the emergence of new subtypes which may be more pathogenic than the original parent viruses and may be associated with pandemics (Neumann et al., 2009b, Van-Tam and Sellwood, 2010).

Pigs are thought to have an important role in reassortment because of their ability to become infected with different types of influenza A viruses (avian and human viruses), and thus they act as an intermediate host, or “mixing vessel” (figure 1.5–1). The new reassortant strain may cause a pandemic or panzootic because the hosts (humans or birds)

have little or no immunity against it (Smith et al., 2001, Van-Tam and Sellwood, 2010). Such a scenario happened recently in April 2009 where a swine origin H1N1 virus originated from a triple reassortant, composed of genes from avian, porcine and human virus origin (Michaelis et al., 2009).

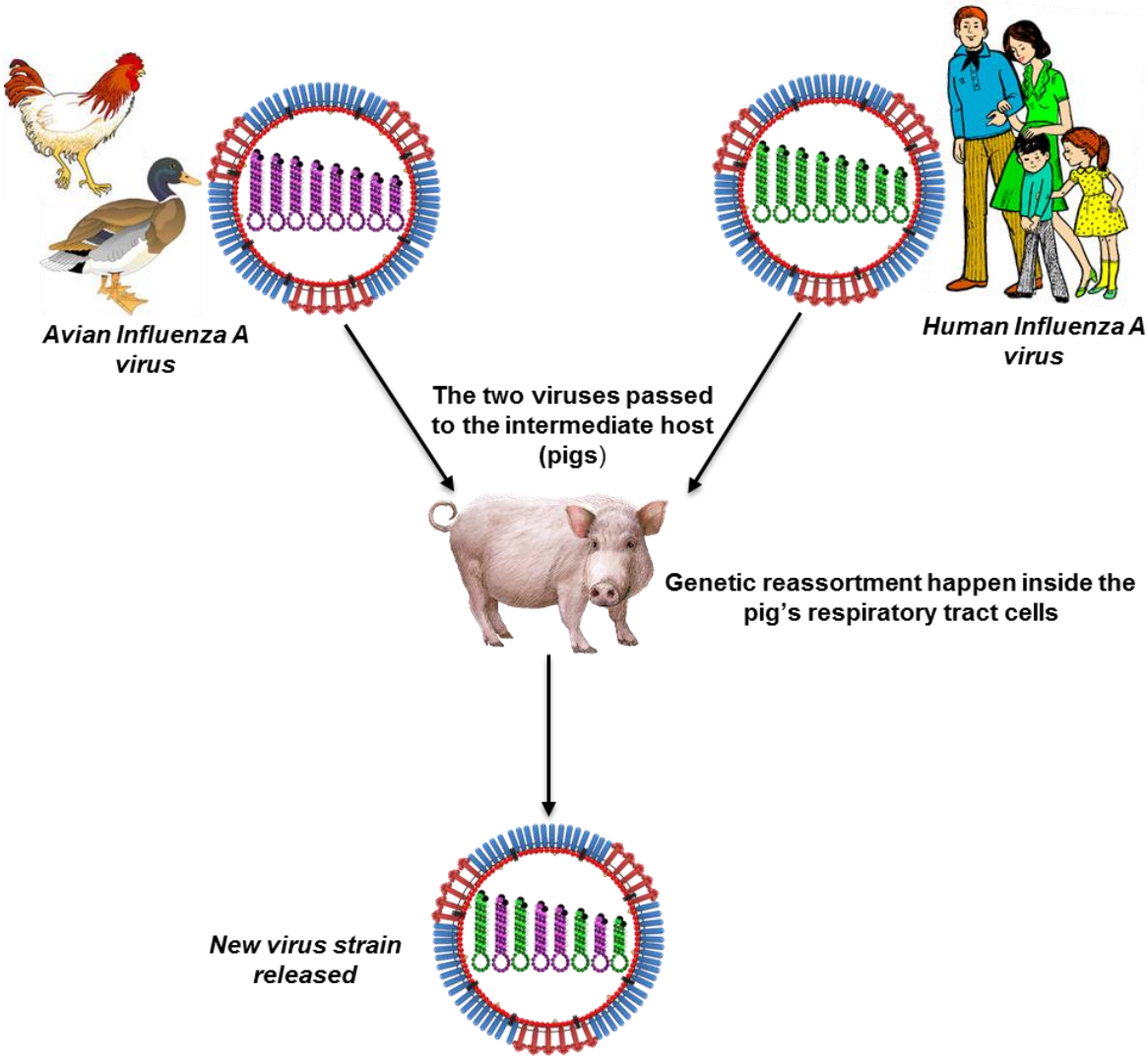

Figure 1.5–1 Schematic diagram of the antigenic shift process.

Both avian and human influenza A strains co–infect the pig's respiratory tract cells where the reassortment may occur. The new virus strain is released and can infect humans and also spread from person to person.

As a consequence of such genetic changes, many pandemic outbreaks have been recorded. The most severe outbreak was in 1918 which is known as 'Spanish flu'; Asian and Hong Kong flu occurred in 1957 and 1968 respectively (Timbury, 1997). The very recent global outbreak is named swine flu or 2009 flu pandemic which is caused by a H1N1 subtype which derived from triple reassortment of human, avian and swine viruses (Trifonov et al., 2009).

1.5.2 Antigenic drift

Genetic change in influenza A virus also occurs by 'antigenic drift'. This is due to the accumulation of point mutations over time, which results from a lack of proofreading mechanism in the RNA polymerase, leading to incorrect ribonucleotide insertions during replication (Zambon, 1999, Adams and Sandrock, 2010). Such changes occur progressively over a period of time accompanied by a gradual change in surface glycoproteins (HA and/ or NA). The accumulation of basic amino acids in the HA gene product may result in the transition of low pathogenic viruses to high pathogenic forms (Adams and Sandrock, 2010). The newly created viruses can escape immunity acquired after infection or vaccination and cause seasonal epidemic influenza, in humans, which usually occurs in winter every year and can infect the same person multiple times (figure 1.5–2). As a result of this, influenza vaccines must be updated each year with changes in the circulating influenza viruses to achieve the best match with the circulating strain possible (Chen and Deng, 2009). These changes can be confirmed by phylogenetic analysis of H and N gene sequences (Hampson and Mackenzie, 2006). Influenza viruses produced as a result of antigenic drift are usually not changed much in their virulence in comparison with those produced from antigenic shift (Timbury, 1997). However, such viral gene mutations may play a role in virus evolution and spread.

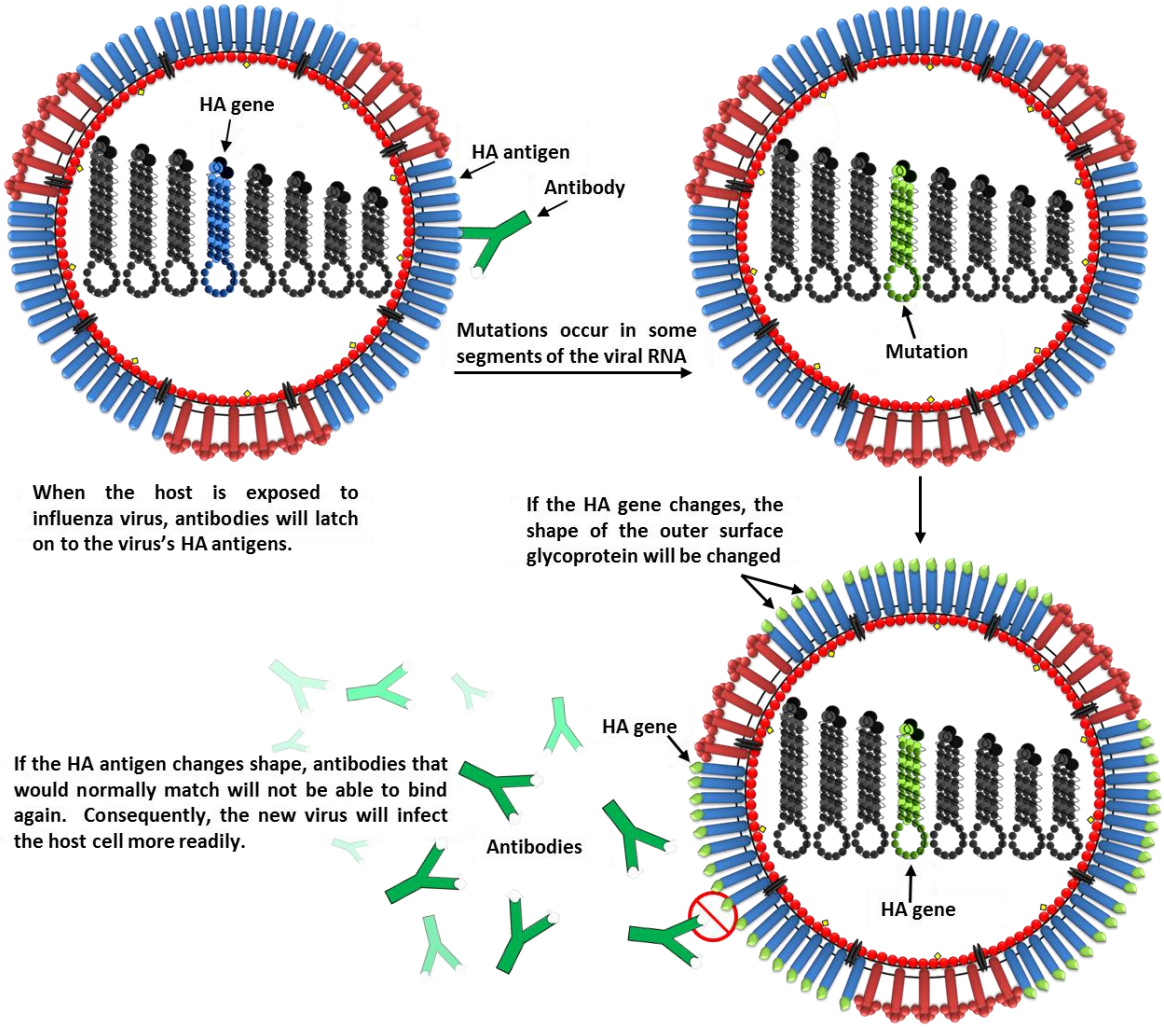

Figure 1.5–2 Schematic diagram of antigenic drift process.

This occurs when the genes encoding viral surface antigens undergo progressive mutation which leads to antigenic changes in the protein. Such changes allow the newly formed viruses to infect the host because of the absence of the specific antibodies against the altered surface antigen.

1.6 Host range and cell receptors

Influenza A viruses' subtypes have been isolated from an expansive range of hosts including avian and mammalian species. The avian host range includes both wild aquatic and terrestrial birds particularly ducks, geese, and chickens. The mammalian host range includes humans, pigs, and horses (Webster, 1998, Adams and Sandrock, 2010). The host

specificity of each type of influenza virus is mainly determined by differences in the host cell receptors (Naeve et al., 1984).

There are two main types of host cell receptors with which influenza viruses have the affinity to bind. The linkage between neuraminic acid and the sugar (galactose) determines whether influenza virus binds to avian or mammalian cells (Figure 1.6–1). Avian influenza viruses preferentially bind to the neuraminic acid α 2,3 galactose receptors while mammalian influenza viruses bind to neuraminic acid α 2,6 galactose(Auewarakul et al., 2007, Pillai and Lee, 2010).

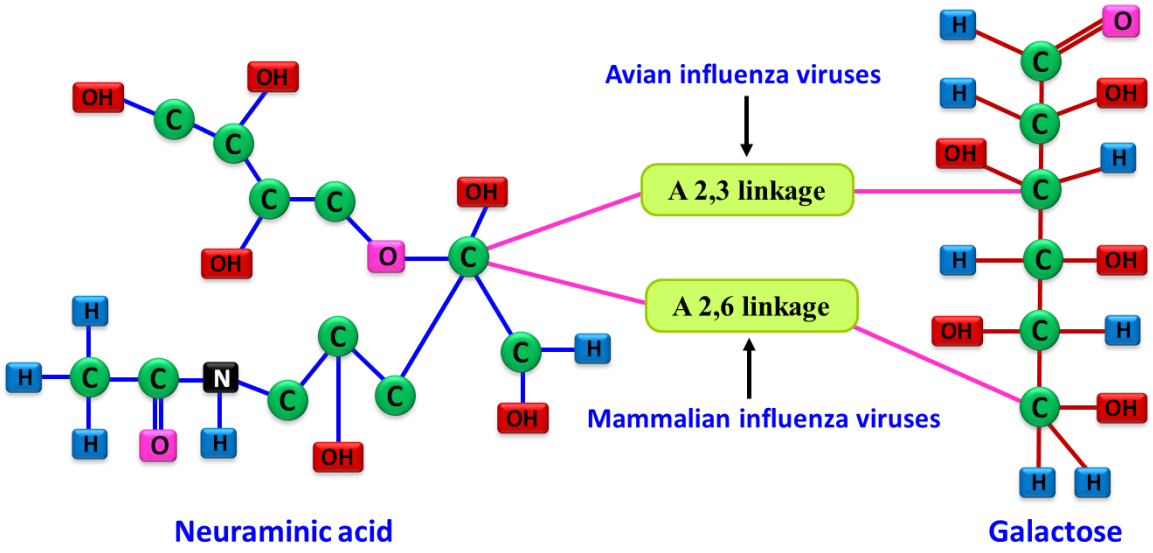

Figure 1.6–1 Overview of receptor predilections of avian and mammalian influenza viruses.

Nelli et al (2010) showed that both receptors are present extensively in different organs in pigs, providing evidence why such mammals can act as mixing vessels for human and avian influenza virus. These two types of receptor are also distributed in many organs in chickens and ducks (Kuchipudi et al., 2009). The presence of these receptors on the same cells of the host may provide the environment for genetic reassortment and the production of new viruses by antigenic shift that may be more virulent than the original viruses.

Genomic mutations of avian influenza viral HA may play a role in changing the affinity of receptor binding from sialic acid– α 2,3 galactose to sialic acid– α 2,6 galactose, which leads to extension of the viral host range (Yu et al., 2011).

Figure 1.6–2 shows the natural reservoirs of influenza A viruses and how transmission occurs between hosts, which might lead to increase virulence after mixing in the pig.

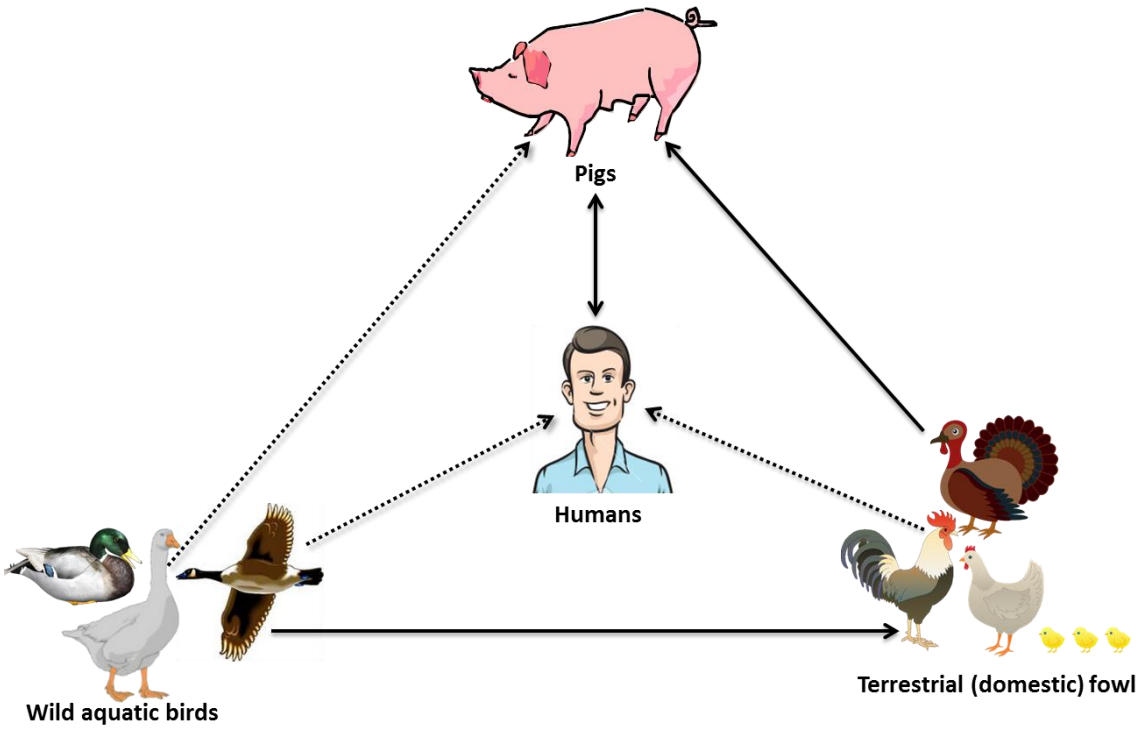

Figure 1.6–2 The reservoir of influenza A viruses.

Wild aquatic birds are the natural reservoir for all influenza A subtypes. Avian influenza A viruses are frequently transmitted to domestic fowl from the natural wildlife reservoirs, and also to pigs from domestic fowl. Pigs can be frequently infected from human and domestic fowls, and virus reassortment can occur in pigs between avian, swine and human influenza A viruses. Influenza A viruses from pigs can also infect humans. Pigs act as "mixing vessel" for influenza A viruses. Transmission of influenza A viruses can be either frequent (solid lines), or occasional (dotted line). Figure adapted from Maw et al. (2008)

1.7 Pathological findings

Avian influenza A viruses can be classified into two fundamental groups: high and low pathogenic viruses, based on the severity of infection. In seasonal and acute outbreaks of low pathogenic viruses in chickens, the major areas affected with pathological lesions are the respiratory and urogenital systems. These pathological lesions include pulmonary congestion, air saculitis, pneumonia, congestion of the ovary, and hemorrhagic ovarian follicles. During the latter stages of outbreaks, gross or histologic lesions which are identified within the urinary system include visceral urate deposition, nephritis, renal tubule necrosis, and swollen kidneys (Swayne and Slemons, 1994).

In contrast, during infection with high pathogenic viruses in chickens, the pathological lesions are more prominent in comparison with low pathogenic viruses. The lesions may also involve the intestine, liver, spleen, and the brain. The major lesions are congestion and neuronal degeneration in brain tissues and severe congestion, edema and hemorrhage in lung tissues. The main pathological findings in the liver, spleen, and kidneys are hyperemia, cell degeneration and necrosis (Vascellari et al., 2007).

1.8 Mode of transmission

All influenza A subtypes can be transmitted in two main ways: inhalation of contaminated aerosols and by direct contact. Many studies have shown that inhalation of aerosol and infectious respiratory droplets play an essential role in the spread of the disease (Tellier, 2009, Tellier, 2006). Transmission by contact may occur directly from the infected persons or animals or indirectly by touching contaminated tissues and surfaces (Collier and Oxford, 2006, Tellier, 2006, Van-Tam and Sellwood, 2010).

Persons who are in contact with infected birds may be infected with the highly pathogenic strains (Khanna et al., 2008). Such transmission could happen in wet markets where live birds are sold, leading to direct close contact with infected poultry, via feather plucking and preparation of poultry for consumption, as well as poultry slaughtering facilities, commercial poultry farms, and eating of raw or poorly cooked animal parts (Paul Tambyah and Leung, 2006, Ma et al., 2008).

Transmission between birds usually occurs by the faeco–oral route which is the predominant means of spread in wild bird reservoirs (University Jawa State, 2010). The stability of avian influenza viruses in water supplies may spread the infection to other birds such as shore birds and also to aquatic mammals such as seals and whales (Stallknecht et al., 1990). Mallard ducks are of great interest because they are widely distributed and can travel large distances carrying the viruses from one region to another (Achenbach and Bowen, 2011). Transmission also occurs through inhalation of respiratory secretions contaminated with influenza virus particles (Zambon, 1999).

1.9 Clinical signs and symptoms

1.9.1 Clinical signs and symptoms in humans

Generally signs and symptoms appear directly after the incubation period which is 24 to 48 hr after being exposed to infection, but sometimes they may take four days to appear (Van-Tam and Sellwood, 2010). The severity of symptoms varies with virus subtype. A person who is infected with the disease starts to spread the viruses to other people one day prior to the beginning of symptoms and remains infectious for five to seven days (Collier and Oxford, 2006, Van-Tam and Sellwood, 2010). The typical symptoms of influenza A in people include fever (38˚C or more), rhinitis, runny nose, cough,

headache, myalgia (muscle pain), body aches especially joints and throat, nasal congestion, chills, tiredness, watering eyes, loss of appetite, weakness and general discomfort, diarrhoea or vomiting (especially in children) (Collier and Oxford, 2006, Van-Tam and Sellwood, 2010). The common symptoms (fever, headache and fatigue) are caused by the secretions of large amounts of cytokines, including interferons and interleukins which are produced from influenza infected cells (Hampson and Mackenzie, 2006).

1.9.2 Clinical signs in birds

The incubation period of influenza A in birds extends from one to seven days followed by the appearance of clinical signs (University Jawa State, 2010). The main clinical signs which appear in poultry infected with HPAI include decreased food and water consumption, loss of appetite, sudden drop in egg production, rales, sinusitis, ruffled feathers, excessive lacrimation, respiratory signs, cyanosis of the head and skin (purplish–blue coloring), edema of the face and head, diarrhea and nervous system disorders, including loss of the ability to walk and stand. The birds can be markedly depressed and sudden death of large number of poultry is common (Peiris et al., 2007, Neumann et al., 2009a). Other signs include sneezing, coughing, blood tinged oral and nasal discharges, loss of egg pigmentation and shell less eggs (University Jawa State, 2010). Usually HPAI viruses cause significant mortality in chickens but are typically benign in ducks and geese with some exceptions of highly pathogenic avian H5N1 which may cause dark green diarrhea, anorexia and sometimes neurological signs (Neumann et al., 2009a).

Infection of poultry with LPAI is usually subclinical (asymptomatic), however, it may cause decreased egg production and mild respiratory signs (University Jawa State, 2010).

1.10 Laboratory diagnosis

Laboratory diagnosis is important to detect and confirm influenza virus infection either in the case of seasonal outbreaks or in a pandemic (Dwyer et al., 2006). Laboratory investigations should confirm the suspected cases and differentiate them from flu–like diseases which may be caused by other respiratory viruses including adenovirus, picornaviruses, parainfluenza viruses, respiratory syncytial viruses, rhinovirus, and also by bacterial agents such as chlamydia, legionella and mycoplasma (Allwinn et al., 2002, Patrick and Richard, 2003).

Many diagnostic techniques for influenza virus infection have been used and are classified into direct and indirect techniques. The direct methods include direct detection of viral particles, rapid antigen detection such as immunofluorescence techniques, and Enzyme Linked Immunosorbent Assay (ELISA). The indirect methods involve conventional and rapid cell culture, eggs or animal inoculation for growing and also typing of the viruses. Hen's eggs are usually used for such propagation (Dwyer et al., 2006, Khanna et al., 2008).

Further investigations of influenza virus have been done by nucleic acid testing (RT–PCR), and serological diagnostic tests (complement fixation (CF), haemagglutination inhibition (HI), and neutralization tests). All of these diagnostic tests have different sensitivity rates with some advantages and disadvantages (Dwyer et al., 2006). RT–PCR is generally more sensitive and specific and is not time consuming. It provides accurate detection, and facilitates the typing and subtyping of influenza viruses (Ellis et al., 1997).

In addition, multiplex PCR can be used to detect the infection by including a universal primer set in one amplification reaction, to determine the presence of more than one genome segment in the same reaction (Hoffmann et al., 2001, Ellis and Zambon, 2002). Furthermore, quantitative RT–PCR (qRT–PCR) is considered the more sensitive and accurate method for influenza A virus detection and quantitation. This test is usually used for the detection of viral M gene, the most conserved gene for all influenza A virus subtypes (Spackman and Suarez, 2008).

Serological tests, particularly haemagglutination inhibition and complement fixation are not only used for detection of infection, but also to determine the host's response to influenza vaccination (Prince and Leber, 2003).

Influenza viruses can be isolated by using cell culture techniques whereby a specimen is inoculated in a live culture system and the virus is then detected after a given period of incubation. Madin Darby Canine Kidney (MDCK) cells are frequently used to detect viral replication by observing the cytopathic effects (CPE) on infected cells (Dwyer et al., 2006). Embryonated hen's eggs, 10 to 12 days old, are also used to grow and isolate influenza virus by inoculating the amniotic cavity with the specimen. It usually requires 3 days or more to grow the viruses inside the eggs before harvesting (Wang and Taubenberger, 2010).

1.11 Treatment

Treatment of influenza infection using antiviral medication plays an important role in modulating disease severity and in prevention and management of the disease. There are two main antiviral classes for influenza: adamantanes (M2 blockers), and neuraminidase inhibitors (Hurt et al., 2006).

1.11.1 M2 blockers

M2 protein plays an essential role in virus uncoating, the process that follows virus entry. It is activated by the low PH of endosome prior HA mediated fusion; however, this mechanism can be inhibited using effective M2 blockers (Wharton et al., 1994). Amantadine (Symmetrel®) and rimantadine (Flumadine®) were the first effective drugs licensed for influenza treatment (Montalto et al., 2000). They inhibit viral replication during the early stage of infection by preventing H^+ protons from flowing into the inner part of the virion through the M2 ion channel, thereby preventing viral uncoating, a process necessary for release of the transcriptionally active ribonucleoprotein complex for transport to the nucleus (Figure 1.11–1). As a consequence of the M2 blocking, viral RNA is not released to the cytoplasm of infected cell (Suzuki et al., 2003).

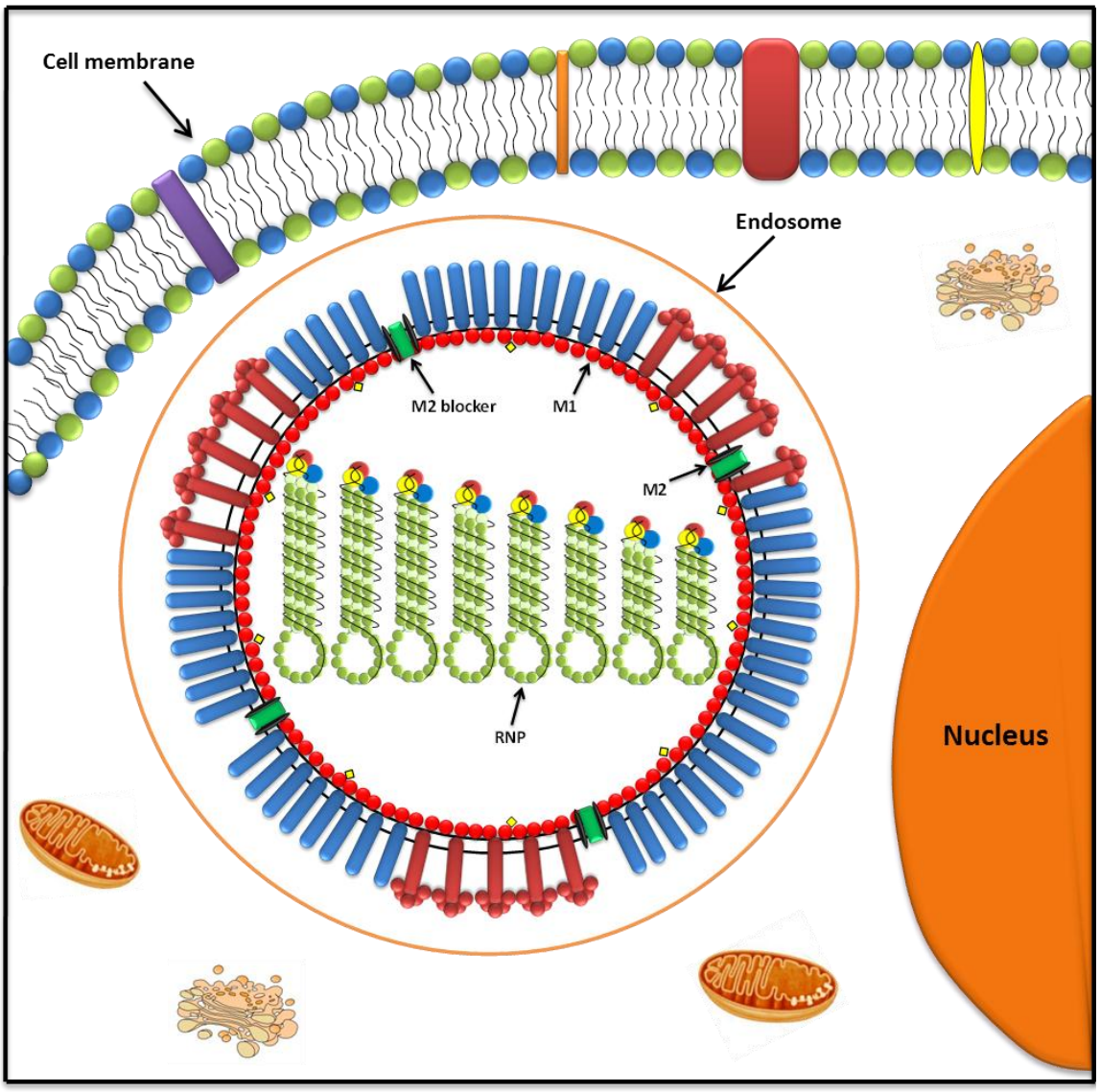

Figure 1.11–1 Inhibition of influenza virus uncoating.

Amantadine (green bars) blocks the M2 ion channel preventing H^+ protons from entering the inside of the virion. Viral RNP is not released from matrix protein 1, which therefore stops viral replication.

In 1966, the Food and Drug Administration (FDA) approved amantadine for prophylaxis, and then in 1976, it started to administer this anti–viral for adults and children from one year and older. Rimantadine was then approved in 1993 by FDA for prevention of the disease in adults and for prophylaxis in children more than one year of age (Montalto et al., 2000). These two antiviral medications, in particular amantadine, are not widely used

because of their side effects on the central nervous system and the high incidence of drug resistance (Hayden et al., 1981, Du et al., 2012). Mutations in the viral M gene which happens through a single amino acid substitution in the M2 transmembrane domain can cause resistance to amantadines, and the resistant virus isolates can be transmitted to susceptible contacts. This potential of drug resistance limits the use of this drug for the treatment of influenza (Hay et al., 1986, Moscona, 2005).

1.11.2 Neuraminidase inhibitors

Neuraminidase is a glycoprotein expressed on the surface of influenza virus. It helps the progeny viral particles to be released from a host cell by cleaving the terminal neuraminic acid (sialic acid) residues from HA receptors on the cell membrane (Figure 1.11–2). This supports the spread of the new viral particles from the host cell to the uninfected surrounded cells (Air and Laver, 1989). Neuraminidase inhibitors are effective against all influenza viruses through inhibiting the release of virions from the host cell (Thorlund et al., 2011).

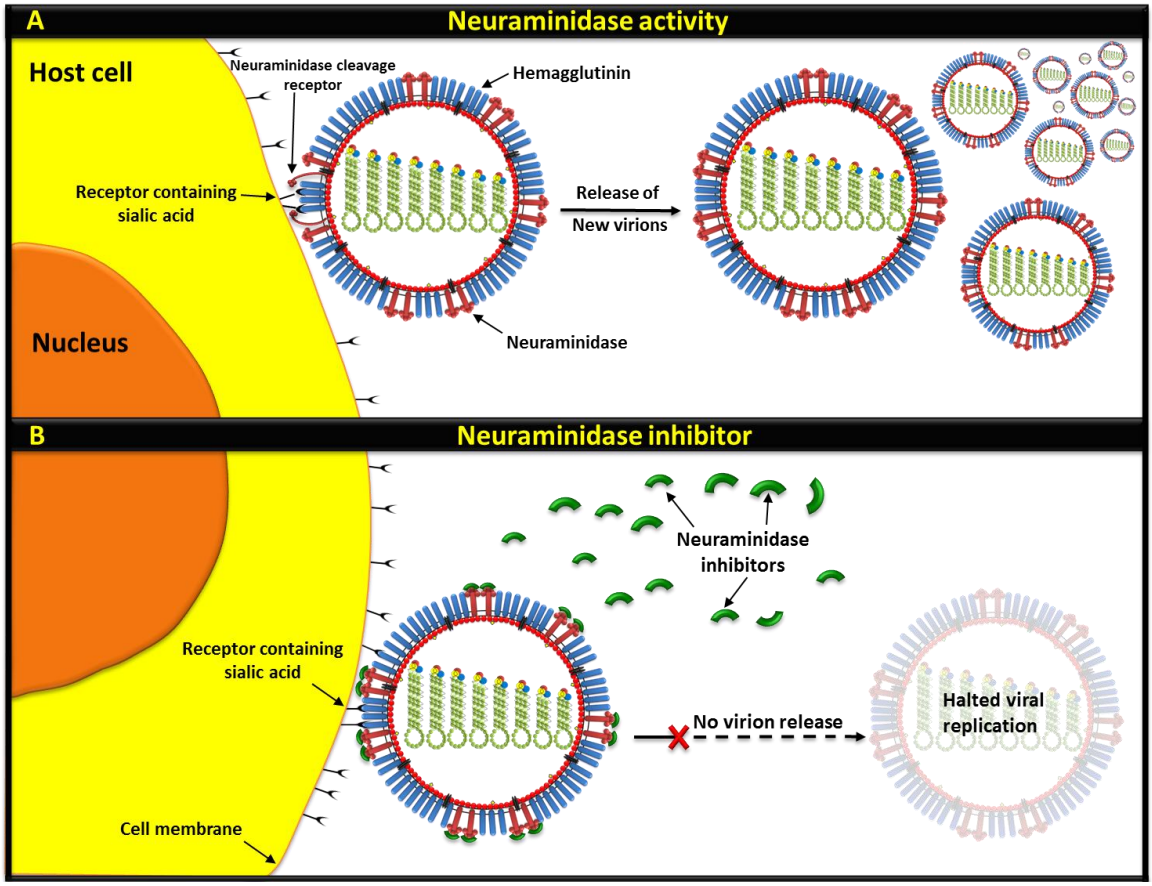

Figure 1.11–2 Mechanism of action of neuraminidase inhibitors.

(A) Neuraminidase function during influenza virus replication cycle. (B) Neuraminidase inhibitors block the replication of the virus, preventing the release of virions from the surface of infected cells. Adapted from Moscona (2005).

Two main neuraminidase inhibitors Zanamivir (Relenza®) and oseltamivir (Tamiflu®) have been approved to limit the severity and spread of influenza infections. They were first introduced in 1999 by the FDA for the treatment of uncomplicated acute influenza (Montalto et al., 2000). Both drugs are also effective for preventing the spread of the disease (chemoprophylaxis). These drugs are preferable to the M2 blockers because of their wider effectiveness (effective against influenza A and B), in addition to the absence of nervous system side effects (Gubareva et al., 2000). Other antivirals, Peramivir and laninamivir have been recently introduced in Japan (Thorlund et al., 2011).

1.12 Immunity and host response

1.12.1 Innate immunity and viral strategies to avoid the innate response

The first line of host defense against influenza virus infection is the innate immune response, and it is activated within a few hours of infection. There are three major components used by the host: antigen presenting cells (APCs), pattern recognition receptors (PRRs), and cytokines (Kreijtz et al., 2011).

The main function of APCs is the engulfment of foreign particles through phagocytosis, as well as the production of inflammatory cytokines such as interferons. In addition, they have a role to ingest and breakdown the pathogen to clear the infection. Interferons produced from these cells can stimulate dendritic cells (DCs) resulting in enhancement of antigen presentation to CD4+ and CD8+ (helper) T cells which further promote the adaptive immune response (Kreijtz et al., 2011).

Influenza virus infection can be recognized by some PRRs such as toll like receptors (TLRs), retinoic inducible gene–I (RIG–I), melanoma differentiation–associated gene 5 (MDA5), as well as NOD–like receptors (NLR). These receptors recognize pathogen–associated molecular patterns (PAMPs), in addition NLR can also recognize the activity of the virus replication strategy (Pang and Iwasaki, 2011).

Of the 11 TLRs known, TLR–3 and TLR–7 have been shown to play an important role in recognizing double–stranded and single–stranded viral RNA, respectively. Both RIG–I and MDA5 have been shown to bind double stranded RNA. Signaling by these receptors leads to production of inflammatory cytokines from infected host cells including interferon (IFN), tumor necrosis factor (TNF), and macrophage inflammatory protein (MIP) released by natural killer (NK) cells (Alexopoulou et al., 2001, Lund et al., 2004, McGill et al., 2009). These cytokines have such a strong antiviral activity that they can

kill virus–infected cells and limit viral replication. Such immunity is a starting point of the cellular immune response to limit viral replication and viral load (Achdout et al., 2003).

Although the host organism develops sophisticated antiviral responses in order to defeat emerging viruses following infection, influenza viruses can avoid or subvert these responses by evolving various immune evasion strategies to replicate efficiently. This involves binding of influenza virus proteins to various components of the innate immune system leading to their inhibition. For example, NS1 protein plays an important role to block interferon production by inhibiting RIG-I receptor signaling. In addition, PB2 and PB1-F2 limit the production of IFN-β through the association with mitochondrial antiviral signaling protein (MAVS) (van de Sandt et al., 2012). Recently, a study has shown that autophagy which is considered an important defence process against influenza A infection, is manipulated by the virus itself via the interaction of M2 with the essential autophagy protein, Microtubule–associated protein 1A/1B–light chain (LC3). This interaction subverts autophagy and promotes the relocalization of LC3 to the plasma membrane in virus–infected cells. This could provide suitable resources for viral budding and to enhance the stability of filamentous viruses (Beale et al., 2014).

1.12.2 Adaptive immune response

The adaptive immune response represents the second line of host defense. It consists of a cellular response represented by T lymphocytes, and a humoral response which is represented by specific antibodies produced by B lymphocytes.

1.12.2.1 Cellular immune response

During infection, CD4+ and CD8+ T lymphocytes may be induced. Antigen presenting cells (dendritic cells, macrophages, and monocytes) express the major histocompatibility complex class II (MHC II) on their surfaces. When the virus has been engulfed, a lysosome containing digestive enzymes combines with the phagosome to process the antigens. The processed antigens combine with the MHC II proteins forming an MHC II–antigenic peptide complex and are presented on the surface of the APC. Helper T cells (CD4+) recognize the displayed antigen and bind to the complex. T helper cells are divided into several subsets including Th1 and Th2. Th2 cells produce cytokines which further promote the humoral response (Soghoian and Streeck, 2010). In contrast, Th1 cells promote the development of cellular immunity via stimulation of CD8+ lymphocytes. Some viral peptides are expressed on major histocompatibility complex class I (MHC I) of antigen–presenting cells. In this case, peptides are transported to the endoplasmic reticulum where they associate with MHC I, then this complex (peptide/MHC I) is transported via the Golgi apparatus to the plasma membrane. CD8+ cells (cytotoxic T cells) recognise this complex as abnormal resulting in the activation of these cells which eventually lyse virus–infected cells (Yewdell et al., 1985).

1.12.2.2 Humoral immune response (antibody response)

Humoral immunity (antibody based) is a specific type of immune response which helps to eliminate disease and also prevents reinfection in hosts previously exposed to the same strain (Hampson and Mackenzie, 2006). Antibodies against HA have been shown to increase host resistance to influenza. They bind to the trimeric globular head of the HA and inhibit virus attachment and entry. The virus can be neutralized by facilitating

phagocytosis (Kreijtz et al., 2011). Antibodies against NA are not protective but may limit the spread of infection by inhibiting NA enzymatic activity (Hampson and Mackenzie, 2006). Both proteins have high sequence differences and antigenic variations between subtypes. Thus protection provided by humoral immunity is type and subtype dependent and is not effective against different HA and NA subtypes or newly emerging viruses after antigenic shift and antigenic drift, even among healthy young adults. This is the main reason that influenza vaccines should be updated annually to generate humoral immunity against the HA molecule of the newly emerging viruses. Antibodies against M2 might have an impact on virus neutralization, but to a limited extent in comparison with antibodies against HA and NA (Suarez and Schultz-Cherry, 2000, Chen and Deng, 2009). The main antibody types secreted following influenza infection are the mucosal antibodies (IgA), and the circulatory antibodies (IgM and IgG). All have a major role in virus neutralization and clearance (Mazanec et al., 1995).

The humoral immune response in poultry which follows natural infection includes systemic and mucosal antibody production. The circulatory antibody response is measured by the production of immunoglobulin M (IgM) after 5 days of infection. The immunoglobulin Y (IgY), which is equivalent to the mammalian IgG in terms of function, but slightly different in structure, is detected shortly after. The antibodies target surface viral proteins (HA, NA, and M2) that are of importance for protection from disease (Suarez and Schultz-Cherry, 2000).

1.12.3 Acquired immunity

Although vaccination in poultry is possible and effective, it may cause some concerns. It poses problems for international trade, as animals with positive antibodies against

influenza either due to vaccination or infection may not be imported to many countries. In addition, if vaccination is not administered correctly, it may allow the virus to mutate and spread the infection (Savill et al., 2006).

Haemagglutinin (HA) antigen is considered the main component in vaccines which stimulate virus neutralizing antibodies. Most current influenza vaccines used for poultry contain inactivated virus, and are produced through a series of chemical and physical processes. Such vaccines are very effective in inducing antibody against highly pathogenic influenza without causing any dangers because the virus cannot replicate (Rao et al., 2009).

Many other kinds of influenza vaccines have been introduced recently by applying reverse genetic technology, such as fowl–pox recombinant vaccines (Suarez and Schultz-Cherry, 2000). DNA vaccines have received much attention to induce protective immune responses. Polyvalent DNA vaccines have also been developed recently since they elicit broad protection against different H5N1 sublineages in poultry (Rao et al., 2009).

Vaccine immunogenicity is enhanced by the use of adjuvants which regulates the adaptive immune response. Adding an adjuvant triggers the immune system non–specifically to become more sensitive to the vaccine (Atmar and Keitel, 2009). Adjuvanticity (the effect of adjuvant) can be measured by comparing the immunogenicity of vaccine containing adjuvant, with vaccine without adjuvant. Most adjuvants that have been used worldwide are aluminum salts, followed by MF59 and AS03. Although adjuvants play a role in improving vaccine immunogenicity, they can cause adverse reactions ranging from slight to moderate. However, no serious reactions have been reported, indicating that the use of adjuvanted vaccines is generally safe (Kohhei T. and Ishii, 2012).

1.13 Differences in influenza infection outcome between chicken and ducks

Aquatic birds such as ducks are considered to be the major natural reservoirs of all recognized subtypes of influenza A viruses (Webster et al., 1992) in which the virus is maintained in a low pathogenic form. LPAI viruses usually cause asymptomatic infection in those birds, and they replicate mainly in their epithelial cells of the digestive tracts following a faeco–oral route of transmission. Large amounts of virus are shed in faeces of reservoirs which contaminates the environment for prolonged periods of time (Webster et al., 1978). In contrast, when LPAI viruses are transmitted to domestic poultry such as chickens, turkeys and quail, subclinical infection or mild respiratory signs are typically observed (Pillai et al., 2010). In addition, in experimentally infected ducks, most HPAI virus infections are non–lethal and produce subclinical or no clinical signs (Shortridge et al., 1998, Kishida et al., 2005, Jeong et al., 2009). In contrast, HPAI viruses infecting chickens (naturally and experimentally) are very lethal causing high mortality rate reaching to 100% of the animals, often within 2 days.

Paradoxically, Kuchipudi et al. (2011) observed that duck cells undergo rapid cell death following *in vitro* infection with H2N3 viruses, while cell death occurs less rapidly after infection in chicken cells. This study also showed that the number of infectious virions produced in chicken cells was significantly higher than the number of infectious virions produced from duck cells. However there was no significant difference between virus RNA output measurements from the two species.

1.14 Hypothesis

The different outcomes of H2N3 infection in chicken versus duck cells, which are accompanied by a reduction in infectious virus titre from duck cells, may be due to changes in virus morphology, defects in the viral structure, or host cell factors.

1.15 Aim and objectives

The overall aim was to study the molecular and morphological differences between influenza viruses grown in chicken and duck cells *in vitro*. The aim was achieved by the following objectives:

1. To determine the difference in infectivity of viruses produced from chicken and duck cells at different time points and also to monitor viral RNA replication and protein synthesis by absolute real time PCR and western blotting, respectively.

2. To determine the differences in the viral budding and morphology between chicken and duck cells via electron microscopy, and also to examine virus morphology in culture supernatants of both cell types.

3. To investigate the molecular changes of an avian influenza A virus cultured on chicken and duck embryo fibroblasts by whole genome sequencing.

4. To determine the influence of the host cell on virus morphology by growing viruses with different morphology on MDCK, chicken, or duck cells.

Chapter 2

General Materials and Methods

2.1 Introduction

This chapter describes the general materials and methods that were used in the study. Further specific methods are described in the appropriate chapters thereafter.

2.2 Virus production and titration

2.2.1 Viruses

Two LPAI influenza A subtypes were used in this study: avian influenza H2N3 (A/mallard duck/England/7277/06) and equine influenza H3N8 (A/equine/Newmarket/5/03) that were kindly provided by Dr Ian Brown (AHVLA) and Dr Debra Elton (Animal Health Trust), respectively. They were grown in allantoic fluid of embryonated hen's eggs to propagate the viruses.

2.2.2 Virus propagation

Influenza viruses are efficiently propagated in the laboratory, which has allowed them to be widely studied. Embryonated chicken eggs are efficient and commonly used for this purpose (Stanley, 1944, Veeraraghavan and Sreevalsan, 1961, Monto et al., 1981). This method is still being used for vaccine production and diagnostic purposes.

Viruses used in this study were propagated in fertile hen's eggs provided by Henry Stewart & Co. Ltd, UK. Eggs were produced from Dekalb white hens, which were originally selected from the light Sussex strain. Working virus concentration was prepared by diluting the stock virus 1:2000 for H2N3 and 1:200 for H3N8 in Dulbecco's phosphate buffer saline (DPBS, Invitrogen) containing 2% tryptose phosphate broth

solution (Sigma) and 1% antibiotics (100 U/ mL penicillin and 100 ug/ mL streptomycin, Invitrogen). The number of virus passages of both strains is unknown; however, the available information assumes that it is relatively low passage.

The fertilized eggs were incubated for 8 days and 10 days (for H2N3 and H3N8, respectively) at 37.5˚C then inoculated with the virus. At the end of this period of incubation, the embryos were candled using an Egg–Lume Candling Lamp in a dark room and the air sacs were outlined with a pencil in order to determine the site for injection. Eggs without developing embryos were discarded. After wiping the egg surface with ethanol, a small hole was made in the shell at the site of injection with a specific drill without damaging the shell membranes, and a second hole was made above the air sac to alleviate the pressure during inoculation. A hypodermic syringe (1 mL) fitted with a fine needle was used for virus inoculation. The needle was passed through the hole in the egg shell, through chorioallantoic membrane, and the virus (0.1 mL) was injected in the allantoic cavity, which is filled with allantoic fluid. The hole was carefully sealed with wax or tape, and the eggs were placed at 37.5˚C for 48 hr. Figure 2.1–1 shows the structure of the embryonated egg and the specific site of inoculation.

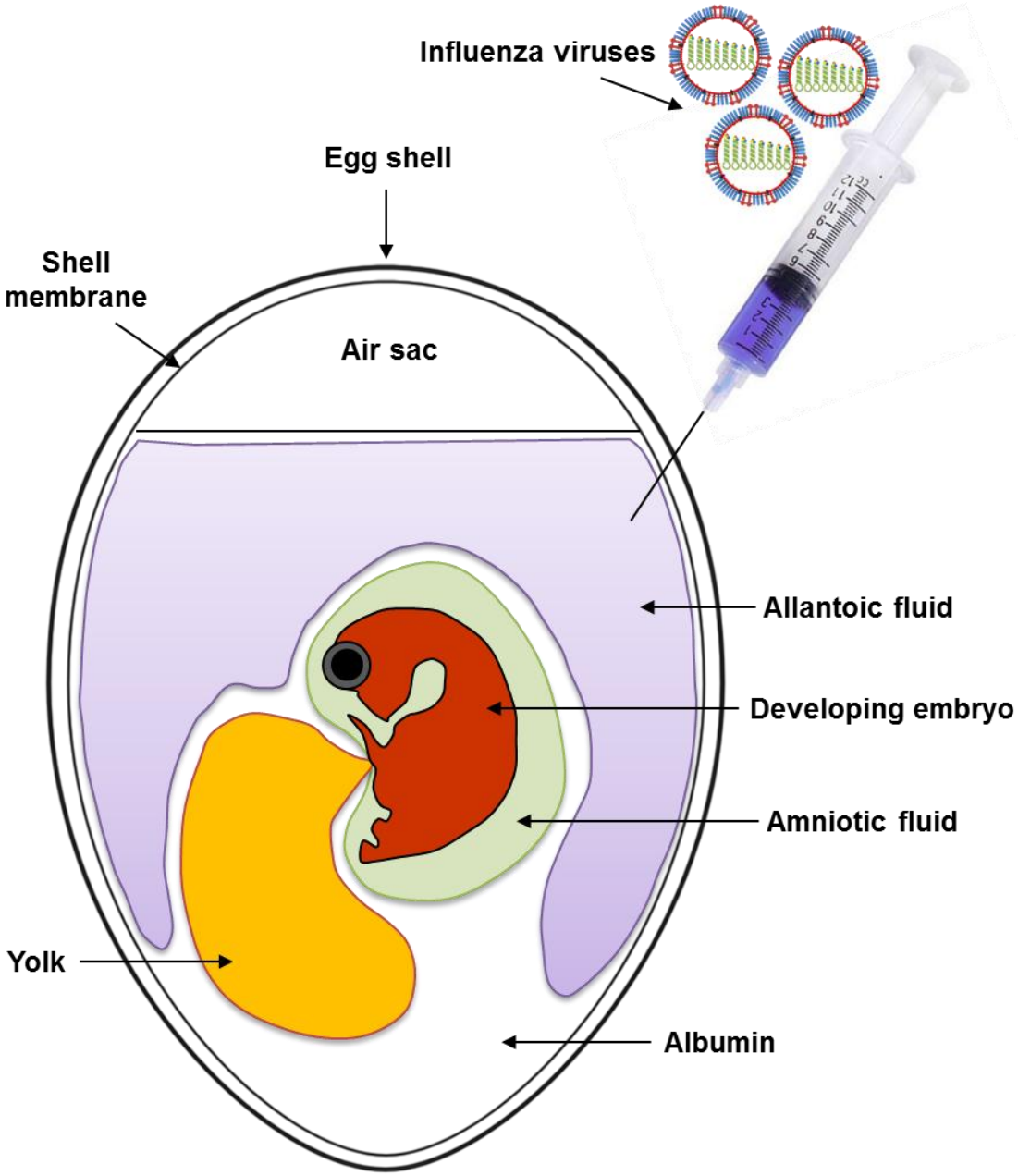

Figure 1.1–1 Inoculation of influenza virus into chicken embryo.

A healthy embryo was inoculated with 0.1 µl of virus in to the allantoic cavity as indicated with a syringe.

Eggs were candled again 24 hr after inoculation, in the dark room, in order to discard any embryos killed by the inoculation procedure. The embryos were chilled at 4˚C for 30 min or overnight before harvesting the virus at 48 hr post–inoculation. The top of the egg shell (at the air sac) was carefully opened using scissors, and the flap of the shell was removed by tweezers. Allantoic fluid was then carefully aspirated with a disposable pipette. The harvested viruses were clarified at 1000 xg for 5 min, aliquoted into small tubes, and then stored frozen at –80˚C until further use.

2.2.3 Virus titration

2.2.3.1 Primary cell culture

Embryo fibroblast cells were extracted from 8 day old chickens provided by Henry Stewart & Co. Ltd, UK, and 10.5 day old Pekin duck embryos provided by Cherry Valley Farms Ltd (Rothwell, Lincs, UK). The egg shell was opened and the embryo was pulled out with a sterile blunt ended curved forceps and placed in a Petri dish and rinsed with PBS (Invitrogen). The head, limbs and internal organs were removed, and the bodies were transferred to a new petri dish containing PBS. The embryos were minced and digested in 0.25% trypsin in dissociation medium (DM) (F12 Hams + 1% penstrep + 1.5% fungizone) at 37˚C for 1 hr. Large undigested tissue pieces were removed using a cell strainer and the remaining suspension was centrifuged at 400 x g for 5 min. Cells were seeded into cell culture flasks (Nunc) and maintained in Dulbecco's modified Eagle's medium (DMEM) containing 10% fetal calf serum (FCS) (Invitrogen) and supplemented with 1% antibiotics (100 U/mL penicillin and 100 ug/mL streptomycin) (Invitrogen).

2.2.3.2 Cell line

Madin Darby canine kidney (MDCK) cells were used for the determination of infectious virus production from chicken and duck fibroblasts, and for immunofluorescence experiments (Chapter 3 and 6).

2.2.3.3 Sub–culturing of cells

Confluent monolayers of cells were washed three times with pre–warmed PBS and trypsinised with pre–warmed 0.5% and 1% trypsin/EDTA solution (Invitrogen) in PBS for primary and MDCK cells, respectively. Cells were incubated at 37°C until they detached from the flask surface, then trypsin was neutralised using pre–warmed DMEM–Glutamax containing 10% FCS and 1% antibiotics. The cell suspension was centrifuged at 400 xg for 5 min and the supernatant was discarded. The cell pellet was re–suspended in DMEM–Glutamax supplemented with 10% FCS and 1% antibiotics, and then inoculated into new plates after cell counting.

For later use, cells were frozen at –196°C in liquid nitrogen. Freezing solution was prepared using DMEM–Glutamax supplemented with 50% FCS and 10% dimethyl sulphoxide (DMSO) (Sigma). Cell–freezing solution was aliquoted into 1.8 mL cryovials and put in Mister Frosty containing isopropanol and stored at –80°C for 24 hr, prior to moving to liquid nitrogen.

2.2.3.4 Cell counting

Cells were counted using the microscope chamber slide (haemocytometer). The slide has two chambers, each divided into 9 large squares. Each square has the same dimensions and accommodates 10^{-4} mL of cell suspension (Figure 2.2–1 A). The cell suspension was first diluted enough to be uniformly distributed and not overlapping. The slide mirror–like polished surface and its cover slip were cleaned gently using lens paper and 70% ethanol. A volume of 10 microlitres of the diluted cell suspension was mixed thoroughly with 10 µl of 0.4% trypan blue in microcentrifuge tube, and incubated for a few minutes. Ten microlitres of the mixture was gently loaded onto the edge of the cover slip and allowed to distribute under the cover slip by capillary action. The slide was placed under the light microscope stage, and the viable cells (unstained with trypan blue) were counted using the x10 objective lens. Cells were counted in four large squares (top left, top right, bottom left, and bottom right) and the centre square. Cells touching lines were included on two sides only (see figure 2.2–1 B). The concentration of viable cells per millilitre was calculated using the following formula:

Number of viable cell in top left square = A

Number of viable cell in top right square = B

Number of viable cell in bottom left square = C

Number of viable cell in bottom right square = D

Number of viable cell in centre square = E

The total number of viable cells = A+B+C+D+E = F

Average number of viable cell per square = F/5 = G

Dilution factor = final volume of sample (cell volume + Trypan Blue) / cell volume = H

Concentration of viable cells per millilitre = G x H x 10^4

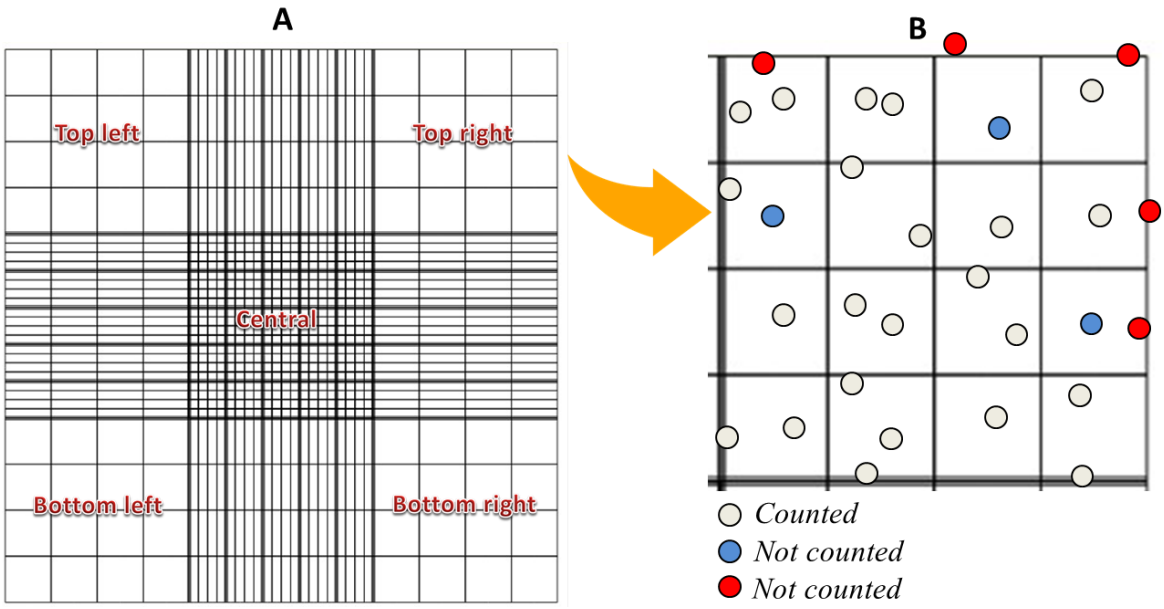

Figure 2.2–1 Haemocytometer Cell Counting Chamber.

(A) Diagram showing the dimensions of a haemocytometer grid when viewed under the microscope. The slide consists of 9 large squares, and cells were counted in the five labelled squares. (B) Diagram showing one of the largest squares. To ensure consistency of counting, cells that crossed the edges were counted in two sides only (indicated by transparent circles), while those located on the other sides were excluded (indicated by red circles). Dead cells (indicated by blue circles) were also excluded.

2.2.3.5 Determination of multiplicity of infection (MOI)

Confluent monolayers of MDCK cells in T75 flasks (Nunc) were split with trypsin and seeded to a 96 well plate (Nunc) at a seeding density of approximately 5000 cells per cm^2 in DMEM with 10% FCS, and 1% penicillin/streptomycin (P/S). The plates were incubated at 37˚C until they were 100% confluent (usually after 24 hr). The medium was removed and cells were rinsed three times with PBS. The cells were infected with 50 µl of each virus dilution in triplicate using serum free infection media (DMEM/F–12, Invitrogen) supplemented with 2% Ultroser G (Pall Biosepra), 1% antibiotics, and 500 ng/mL TPCK trypsin (Sigma–Aldrich), and incubated initially for 2 hr. They were then

washed thoroughly three times with PBS followed by addition of 50 µl fresh infection medium to each well. At 6 hr post–infection, cells were washed three times with PBS and fixed with cold (4°C) 1:1 acetone–methanol. The plates were then kept in the fridge with PBS or TBS until they were stained (2.2.3.6).

In practice, if a plaque assay is used, the MOI used in this study was at least 3. For 95% infection, the proportion of cells uninfected (P_0) = 0.05. The multiplicity of infection (m) can be calculated using the formula for the Poisson distribution as follows:

$P_0 = e^{-m} = 0.05$

$m = 3$

2.2.3.6 Immunocytochemical staining

Detection of influenza viral protein expression was carried out by using the Envision + system–HRP (DAB; DAKO, Ely, UK) for immunocytochemical staining. The fixed cells were first blocked with peroxidase block for 40 min at room temperature, and then washed three times with 1x TBS–T. The cells were then incubated with a primary mouse monoclonal antibody to influenza nucleoprotein (NP) (Abcam, UK) for 50 min at room temperature. After washing three times with TBS–T, the cells were incubated with peroxidase labelled anti–mouse IgG antibody for 50 min at room temperature. During incubation time, substrate–chromogen solution was prepared by mixing 1 drop of DAB chromogen to 1 mL of substrate buffer, according to the manufacturer instructions. Cells were washed three times and incubated with the solution for 5 min, and then were rinsed with water and examined under the microscope. The amount of virus that produced 95–100% positive cell labelling for NP was established as MOI of 1.0.

2.2.3.7 Virus infection of cells

Cells were seeded in flat culture well plates (Nunc) at a seeding density of 5000 cells/cm^2 in DMEM containing 10% FCS, 100 U/mL penicillin and 100 µg/mL streptomycin. The plates were incubated at 37˚C until cells became 100% confluent. The cells were rinsed twice with PBS and then infected with virus in serum free Ham's 12 (infection media) containing 2% Ultroser G (Pall Biosepra, Portsmouth, UK), 500 ng/mL TPCK Trypsin (Sigma–Aldrich Ltd.) and antibiotics. The plates were incubated at 37˚C for 2 hr to allow virus attachment. The cells were rinsed three times with PBS, and then a fresh infection media was added to all the wells. They were then further incubated up to 48 hr. Supernatants were collected either for viral RNA extraction or for virus titration.

2.3 Viral RNA Extraction and quantification

Extraction of viral RNA from chicken and duck culture supernatants was performed using a QIAamp viral RNA purification kit (Qiagen) following the manufacturer's instructions (Appendix IV). The concentration of purified RNA was determined using NanoDrop8000 spectrophotometer (Thermoscientific, UK) by UV absorption. Eluted viral RNA samples were stored at –80˚C until further use.

Chapter 3

Influenza A virus production in chicken and duck cells

3.1 Summary

In this chapter, comparisons of infectious virus production, viral RNA production, and matrix protein expression were made following infection of chicken and duck embryo fibroblasts (CEF and DEF) with avian LPAI H2N3 (A/mallard duck/England/7277/06). DEF cells produced significantly lower numbers of infectious viruses compared to CEF cells. This difference was observed at 24 to 48 hr post infection. Influenza matrix gene expression, analysed by absolute real time PCR on culture supernatants, was comparable between species at 8 and 24 hr post infection. Matrix protein expression of viruses produced from both cells at 8 and 24 hr post infection was measured by western blotting. No significant difference in viral M protein expression was detected. These findings suggest that neither replication of viral RNA nor inefficient virus budding is responsible for the lower infectious virus production from duck cells. Other factors such as differences in the molecular structure of virions could have an impact in decreasing virus infectivity.

3.2 Introduction

Various laboratory *in vitro* models have been widely employed for studying influenza virus infection. Both organ and tissue cultures have been shown to support the growth of influenza virus. Avian organ cultures such as chicken embryo tracheal cultures are very sensitive to influenza infection and they have been used for the propagation of viruses (Blaskovic et al., 1972). Human organ cultures such as nasal polyps have been shown to support the growth of both human and avian influenza strains (Suptawiwat et al., 2010). In addition, other mammalian organ cultures such as hamster trachea were also used for

studying virus infection and metabolic activity following infection with different influenza viruses (Reeve et al., 1978).

Cell cultures are a good model to study influenza virus isolation and determination of virus titre. Madin Darby Canine Kidney (MDCK) cells are the most efficient cell system for this purpose because of the high susceptibility to infection and the production of high virus titres (Reina et al., 1997, Li et al., 2009). In addition, avian cell cultures such as CEF and DEF cells made from 10–day old chicken embryos and 12–day old Pekin duck embryos, respectively, have also been used to study influenza virus infection and host responses (Liang et al., 2011).

3.2.1 Cytopathic effect

The growth of viruses in cell culture is often associated with microscopically visible morphologic changes in the infected cells. These changes are referred to as cytopathic effect (CPE) of the virus, and they consist of cell rounding and detachment from the surface, disorientation, swelling, shrinking, necrosis, and vacuolization. Examples of CPE caused by influenza A virus are shown in Figure 3.2–1. Influenza virus infection, in particular infection with highly pathogenic strains, causes death of infected tissue culture cells (Daidoji et al., 2008). Apoptotic (programmed) cell death following influenza virus infection plays a major role in tissue damage during infection (Brydon et al., 2005), and is usually associated with low yields of infective virus particles (Takizawa et al., 1993, Kuchipudi et al., 2011).

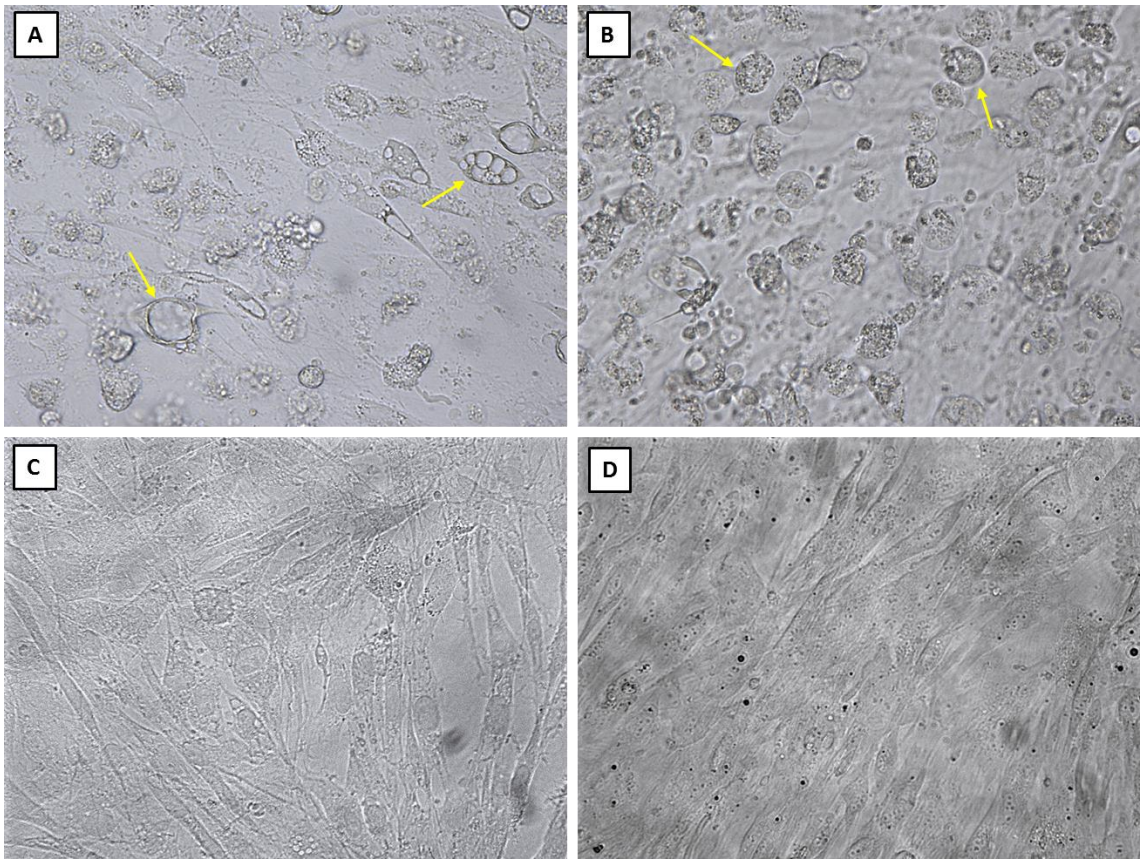

Figure 3.2–1 Cytopathic effects caused by influenza A virus.

Different cytopathic changes following infection of embryo fibroblasts with H2N3 virus for 24 hr are shown. Chicken cell culture (A) shows some swelling cells and vacuole formation while duck cell culture (B) shows cells rounding and detaching from the surface (indicated by arrows). Uninfected control chicken and duck cells (C and D) show no evidence of CPE.

3.2.2 Measurement of virus production in infected cells

3.2.2.1 Focus forming assay

Focus forming assays are widely used to determine the virus concentration. Madin Darby canine kidney (MDCK) cells are often used for this purpose because of their high susceptibility to infection with most influenza A strains (Gaush and Smith, 1968, Govorkova et al., 1999). In this method, cell monolayers are infected with serial dilutions of the virus and incubated for about 8 hr. Detection of infected cells is determined by

immunostaining technique using a virus–specific primary antibody such as an NP specific monoclonal antibody, and then the infected cells can be easily observed using either fluorescently or enzyme (e.g. horse radish peroxidase, HRP) labelled secondary antibodies (Figure 3.2–2). Results are expressed as Focus Forming Unit (FFU) per microlitre.

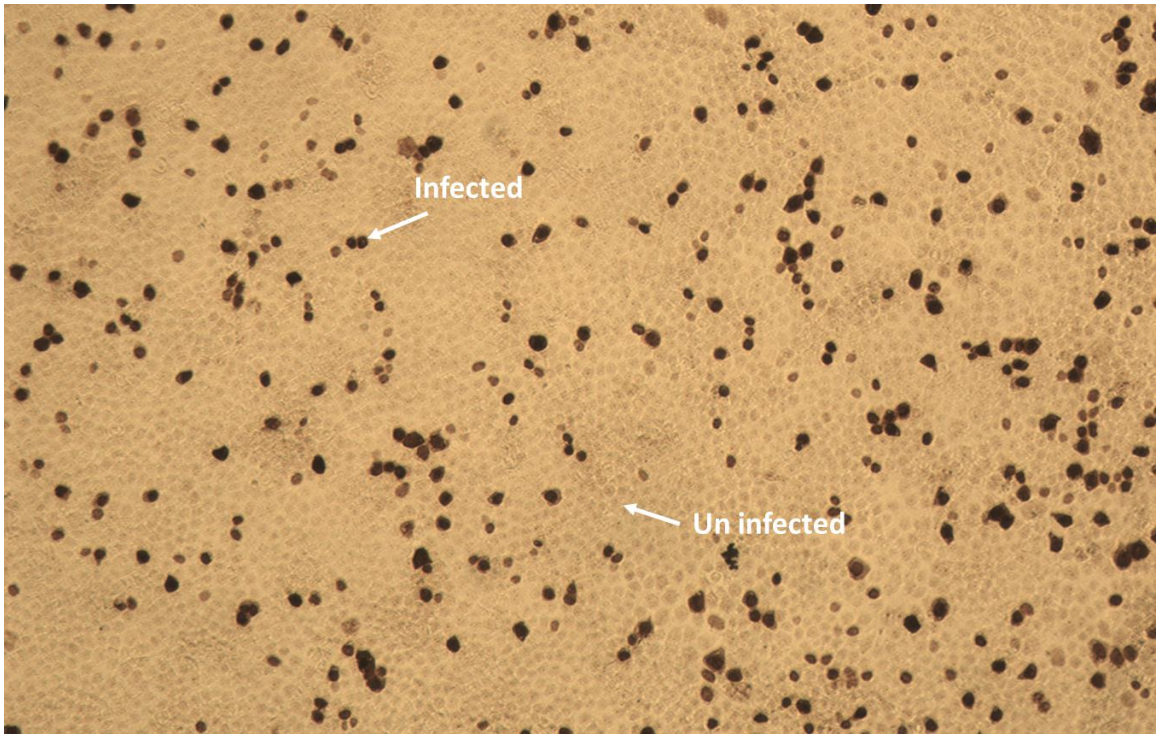

Figure 3.2–2 Immunocytochemical staining of MDCK cells.

Cells are infected with unknown concentration of influenza A virus for 8 hr. Infected cells (dark brown) can be easily differentiated from uninfected cells (unstained).

3.2.2.2 Quantification of viral gene expression by qRT–PCR

Quantitative reverse transcription polymerase chain reaction (qRT–PCR) enables quantification of gene expression and RNA copy number measurements (Heid et al., 1996). It allows exponential amplification of RNA sequences to be detected and measured as the reaction progresses in real time. This technique is based on the reaction of fluorescent molecules with the amplified DNA to produce a fluorescent signal (Figure

3.2–3). The main fluorescent chemistries that have been used are DNA binding dyes (such as SYBR green) and fluorescently–labelled sequence specific primers or probes (such as TaqMan).

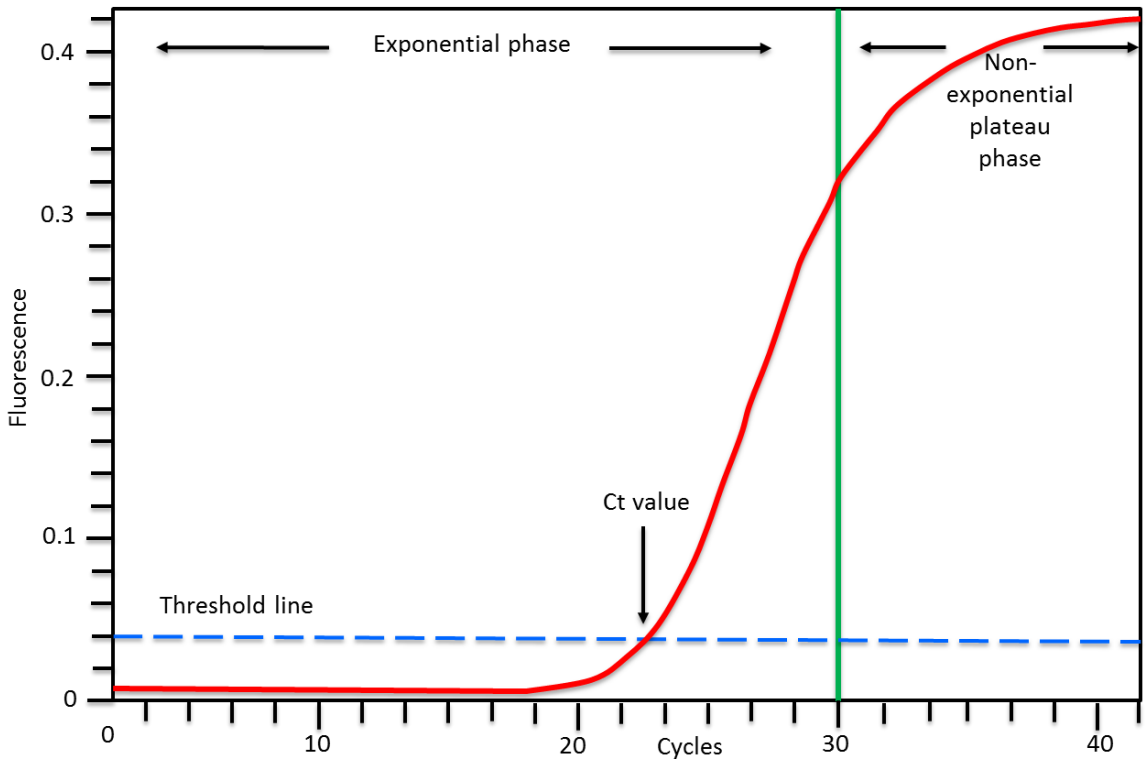

Figure 3.2–3 Graphical representation of real–time PCR data. Cycle number is shown on the X–axis, and the amplification of fluorescence is shown on y–axis. Exponential phase represents the period of time where the PCR product is approximately doubled each cycle. Non–exponential plateau phase (cycles 30–40) starts when one or more PCR component becomes limited. The number of cycles at which the fluorescent signal becomes detectable is called Threshold cycle (Ct).

Previous studies have described qRT–PCR methods to detect influenza A virus by amplifying a part of the matrix gene, the most conserved gene among all influenza A subtypes (Fouchier et al., 2000, Ward et al., 2004, Youil et al., 2004). This technique is considered to be faster and more sensitive in comparison with the other traditional isolation and quantification procedures (Fouchier et al., 2000).

3.2.2.3 Measurement of virus protein production from culture supernatants

The final step of the influenza A life cycle is budding and release. M1 protein plays a critical role in this step, and it is impossible for virus budding to occur in the absence of this protein (Lohmeyer et al., 1979, Nayak et al., 2004). Therefore measurement of M1 protein expression from culture supernatants is valuable to measure virion production from different host cells. Protein expression can be measured by western blotting, a widely accepted technique for visualization and identification of proteins. Western blotting was first documented by Towbin et al (1979), and has since become a routine technique for protein analysis. It is based on building up an antibody:protein complex using a specific primary antibody followed by detecting this complex using a labelled secondary antibody. The procedure involves electrophoretically separating proteins in an appropriate gel such as sodium dodecyl sulfate–poly acrylamide gel electrophoresis (SDS–PAGE) (Laemmli, 1970), and then the separated proteins are blotted onto a solid matrix such nitrocellulose membrane. Before immunological detection, membranes are blocked to prevent the non–specific binding (high background) of antibodies to the membrane surface. Immunological staining (Figure 3.2–4) is performed by incubating membranes with primary antibody targets for the specific protein. The produced protein:antibody complex is then exposed to conjugated secondary antibody such as HRP–linked, and the detected signal from the labelled secondary antibody is proportional to the amount of protein on the membrane.

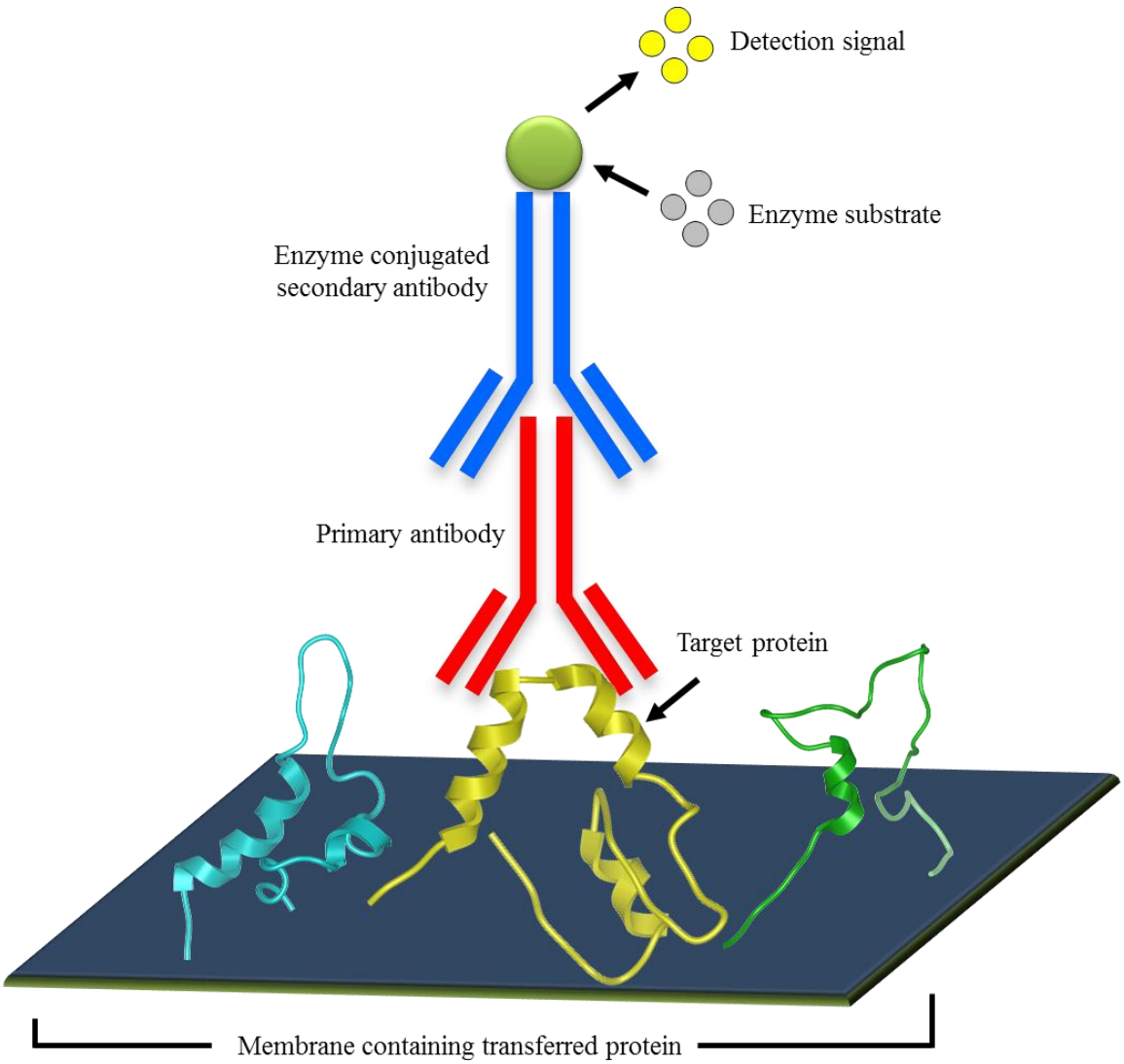

Figure 3.2–4 Illustration of target protein detection in western blot.

Specific antibody binds with the protein of interest on the blotted membrane. Enzyme– labelled secondary antibody interacts with protein–primary antibody, forming protein–primary antibody–secondary antibody complex. When this complex is exposed to an appropriate substrate, the enzyme drives a chemiluminescence reaction and produces a colour.

3.2.3 Replication of influenza A in chicken and duck cell cultures

Previous work showed that the number of infectious virions produced in CEF cells is significantly higher than the number of infectious virions produced from DEF cells, however there was no significant difference between virus RNA output measurements from the two cell types (Kuchipudi et al., 2011). The experimental aims of the work outlined in this chapter were to confirm these findings and additionally measure virus protein production to determine whether the decrease in virus protein expression may be responsible for the decreased infectivity of the virus.

3.2.4 Hypothesis

The reduction of infectious virus production from duck cells might be a consequence of disruption in RNA replication and decrease in the level of viral M1 protein expression.

3.2.5 Aim and objectives

To determine the difference in infectivity of viruses produced from chicken and duck cells.

For this objective, culture supernatants of infected chicken and duck cells were collected at different times post–infection to detect infectious virus production at each time point. Viral RNA replication and protein synthesis were monitored by absolute real time PCR and western blotting, respectively.

3.3 Materials and methods

3.3.1 Growth curves

3.3.1.1 Infection of chicken and duck cells

Monolayers of chicken and duck embryo fibroblast cells were grown in 24–well plates as described in (2.2.3.7). Cells were infected with the LPAI H2N3 (A/mallard duck/England/7277/06) in triplicate at multiplicity of infection (MOI) of 1.0 in serum free media (infection media) supplemented with 2% Ultroser G (Pall Biosepra), 1% P/S, and 500 ng/mL TPCK trypsin (Sigma–Aldrich), and incubated initially for 2 hr. After 2 hr, the cells were carefully washed three times with PBS followed by addition of fresh media. Supernatants were collected at 2, 4, 6, 8, 24, and 48 hr post infection and were stored at –80°C until use.

3.3.1.2 Virus infectivity assay

Confluent MDCK cells grown on 96–well plates were infected in triplicate with virus collected from chicken and duck cells at each time point to measure the virus infectivity, which was expressed as focus forming units per µl. Immunological staining with influenza mouse anti–NP antibody was performed (as described in 2.2.3.6) to differentiate between infected and non–infected cells.

3.3.1.3 Focus forming units calculation

Focus forming units (ffu) per microlitre of the virus were calculated. The well was divided into four equal parts (A1, A2, A3, and A4). Pictures were taken for each part of the well and all positively–stained cells were counted using image J software (http://imagej.en.softonic.com).

Total number of positive cells in the well = A1+A2+A3+A4 = B

Amount of undiluted virus used in the well = C (microlitres)

The number of infective virus particles per microlitre = B/C

3.3.2 Quantification of virus production (measurement of M gene copy number)

RT–PCR was employed to quantify influenza virus matrix gene in culture supernatants as described before (Slomka et al., 2009). Viral RNA from culture supernatants of infected chicken and duck cells was extracted using QIAamp viral RNA purification kit (Qiagen) following the manufacturer's instructions. A one step absolute quantification of viral M gene expression was performed using SuperScript® III Platinum® One–Step qRT–PCR Kit (Invitrogen). A sense primer (5'–3') 24–AGA TGA GTC TTC TAA CCG AGG TCG–47 and antisense primer 124–TGC AAA AAC ATC TTC AAG TCT CTG–100 were used to amplify a 101 bp fragment of M gene, along with a hydrolysis probe (5'–3') 74–FAM–TCA GGC CCC CTC AAA GCC GA–TAMRA–93 which anneals to a part of the amplicon amplified by the two primers. The master mix components were prepared in RNase–free conditions using the amounts of reagents in Table 3.3–1.

Component	Volume/reaction (µl)
DEPC–treated water	4.4
Enzyme mix	0.4
Reaction mix (2X)	10
RNase OUT (40 units/µl)	0.2
Probe (used at final concentration of 0.2µM)	0.4
Sense primer (used at final concentration of 0.4µM)	0.8
Anti–sense primer (used at final concentration of 0.4µM)	0.8
Template RNA	3
Total	**20**

Table 3.3–1 Components and concentrations of one–step real–time PCR for M gene.

Table showing list of components used to perform a one–step real–time PCR reaction. The volumes and concentrations of reagents were optimized as shown in the table. Enzyme mix consisted of SuperScript® III Reverse Transcriptase and a hot start Platinum® Taq DNA Polymerase. Reaction mix consisted of a proprietary buffer system, magnesium ions (Mg^{+}), deoxyribonucleotide (dNTPs), and stabilizers.

Seventeen microlitres of master mix was added to each required well (in triplicate) of the 96–well plate (Thermo Scientific), followed by adding 3 µl of RNA sample (diluted 1:300 or 1:500). Amplification and detection of specific amplicons was performed by using LightCycler® 480 (Roche). A relative standard curve was constructed using 5 different dilutions (10,000 to 100,000,000 copy/µl) of M gene standards (a kind gift from Dr. Suresh Kuchipudi, The University of Nottingham, UK). These standard dilutions were prepared by cloning the amplified influenza M gene cDNA into the TOPO–TA cloning system followed by *in–vitro* transcription to produce M gene RNA (Kuchipudi, 2010). Quantitative RT–PCR conditions and cycling parameters for samples were as follows: one cycle at 50°C for 30 min, one cycle at 95°C for 2 min, and 40 cycles of 95°C for 15 s and 60°C for 1 min. M gene copy number was calculated using LightCycler® 480 software release 1.5.0, and statistical analysis was done by using GraphPad Prism software, version 6.02.

3.3.3 Western blotting

3.3.3.1 Samples of viruses

Supernatants collected from chicken and duck cells infected with H2N3 at MOI 1.0 for 8 and 24 hr were used. They were first centrifuged for 10 min at 1000 xg to remove cell debris. Samples were then either used directly or kept at –80°C.

3.3.3.2 SDS–PAGE

Polyacrylamide Novex® 14% Tris–Glycine Mini Gels (Invitrogen) was used to detect M1 protein from culture supernatants. Samples to be tested, 1 µl of chicken or duck virus supernatant was suspended in 5 µl of 2X Tris–glycine SDS sample buffer (Invitrogen) with 1 µl of 2X reducing agent (DTT, Invitrogen) and distilled water (to 10 µl) to lyse viral protein. The mixture was incubated at 95°C for 5 min, and then cooled and spun briefly. Ten microlitres of each sample along with a pre–stained protein marker (Invitrogen) were loaded into lanes. Samples were then electrophoresed in 1X Novex® Tris–Glycine SDS running buffer (Invitrogen) at 125 V until the final band of the samples had reached the bottom of the gel. Gels were then taken out from electrophoresis apparatus and washed briefly with electro–transfer buffer.

3.3.3.3 Transfer

Samples were transferred to a 0.2 µm Amersham Hybond ECL Nitrocellulose Membrane (GE Healthcare, Life Sciences) by wet blotting. Membrane was first submerged with 100% methanol for 30 s, and then washed briefly with water. Tris–glycine gel, membrane, Hybond blotting paper (GE Healthcare, Life Sciences) and foam stacks

(Invitrogen) were pre–soaked in 100 mL of transfer buffer (1X Novex® Tris–Glycine Transfer buffer (Invitrogen) with 10% methanol) for about 15 min. Pre–wetted blotting paper was placed on three foam stacks followed by the gel. The membrane was then placed on the gel, and further blotting paper and foam stacks were placed on top. Air bubbles were removed after adding each layer using a serological pipette to push air bubbles outward. The gel "sandwich" was placed in the transfer cassette and then loaded to the transfer apparatus. Cold transfer buffer was poured into the apparatus, and the power supply was then set at 40V for 90 min.

3.3.3.4 Immunological staining

After transfer, the membranes were removed and rinsed briefly with ultrapure water. They were then treated with blocking buffer (5% skimmed dried milk in 1x TBS) for 50 min at room temperature with gentle shaking. Without washing, membranes were then incubated with diluted primary antibody: a mouse monoclonal antibody to influenza M1 protein (ABD Serotec) diluted 1:2000 with blocking solution and incubated at 4°C overnight. The membranes were washed 5 times with 1x TBS–T (10 min each time) with shaking. Following this step, HRP–linked anti–mouse IgG antibody (Cell Signaling Technology) diluted 1:2000 with blocking buffer was added and incubated for 1 hr at room temperature with gentle shaking. After 5 times washing, the membranes were subjected to ECL prime reagent (GE Healthcare, Life Sciences) to detect the antigen antibody complexes. The membrane was exposed to photographic film (GE Healthcare, Life Sciences) for about 10 s. The film was then processed with a SRX–101A Konica Minolta processer and protein molecular weight was marked on the film. M protein expression was determined by optical densitometry using Image J 1.47 software.

3.3.4 Statistical analysis

All data were analysed using GraphPad Prism software, version 6.02. The data from infectious virus production in chicken and duck cells was compared using two–way ANOVA. The data from M1 gene and protein expressions were analysed using student's *t* test.

3.4 Results

3.4.1 Measurement of stock virus titre on MDCK cells

MDCK cells infected with serial dilutions of H2N3 were stained with NP specific monoclonal antibody to influenza A. The lowest dilution that showed around 95% of positive cell was an MOI of 1.0 (Figure 3.4–1 A), and that dilution was used for the followed experiments. Uninfected cells showed no staining (Figure 3.4–1 B).

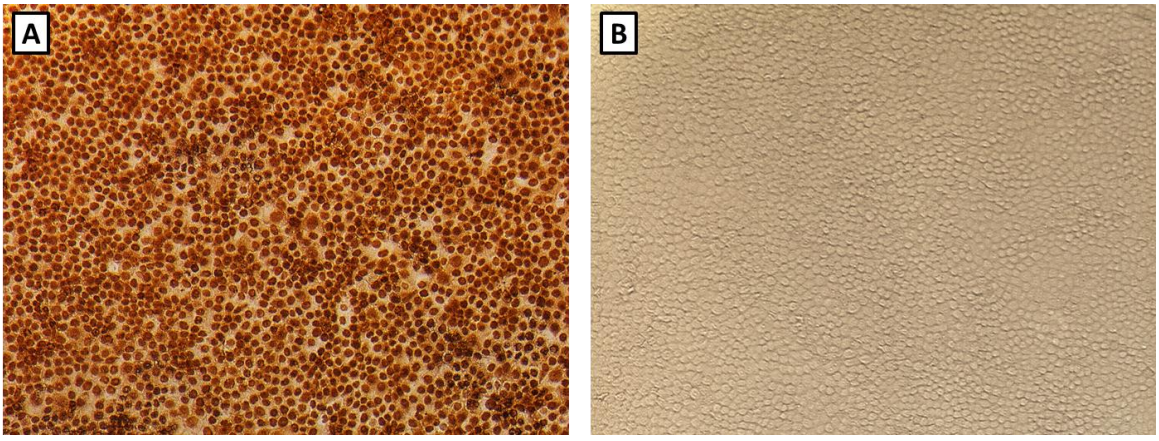

Figure 3.4–1 Measurement of multiplicity of infection 1 (MOI 1.0) of H2N3 on MDCK cells.

Cells infected with H2N3 and stained with a monoclonal antibody to virus nucleoprotein. (A) The lowest dilution of virus that infected 95–100% of cells was considered as MOI of 1.0. (B) Uninfected control cells did not show any staining with antibody.

3.4.2 Chicken and duck cell susceptibility to H2N3

The effect of virus infection on chicken and duck cells was assessed by infection with H2N3. Comparable levels of infection were obtained following infection of the two cells with the virus at MOI of 1. Uninfected cells did not show any evidence of infection (Figure 3.4–2).

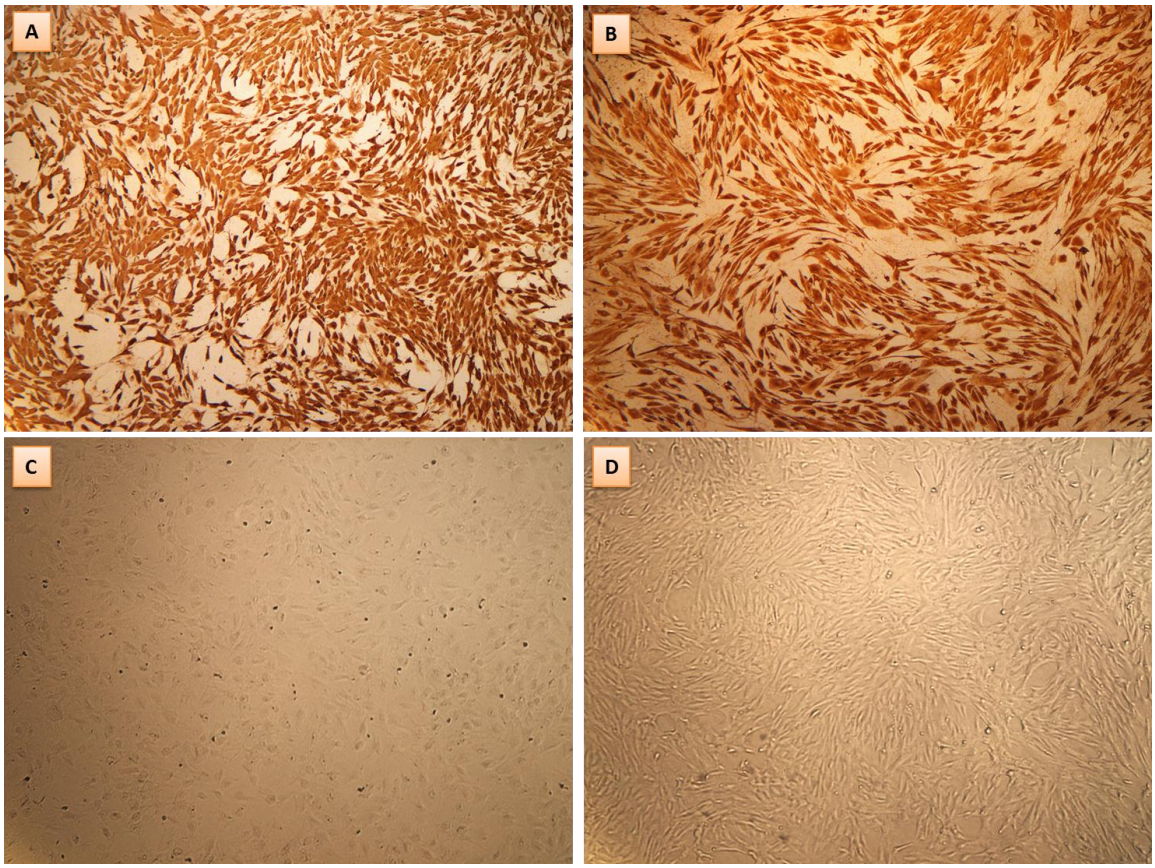

Figure 3.4–2 Susceptibility of avian embryo fibroblasts to H2N3 influenza at MOI of 1.

(A) Chicken and (B) duck cells show similar susceptibility to infection with the virus (8 hr post infection at MOI of 1.0). Cell infection is detected by immunostaining for viral nucleoprotein antigen to influenza A virus. (C) Chicken and (D) duck uninfected controls show no staining with antibody.

3.4.3 Infectious virus production from chicken and duck cells

To determine the level of infectious virus production at different time points, supernatants were collected from infected chicken and duck cells at 2, 4, 6, 8, 24, and 48 hr post

infection, and titrated on MDCK cells. The results showed a highly significant difference in the number of infectious viruses after 8 hr between infected chicken and duck cells (Figure 3.4–3). Chicken cells produced four– to five–fold more infectious virus, 24–48 hr post infection, than duck cells.

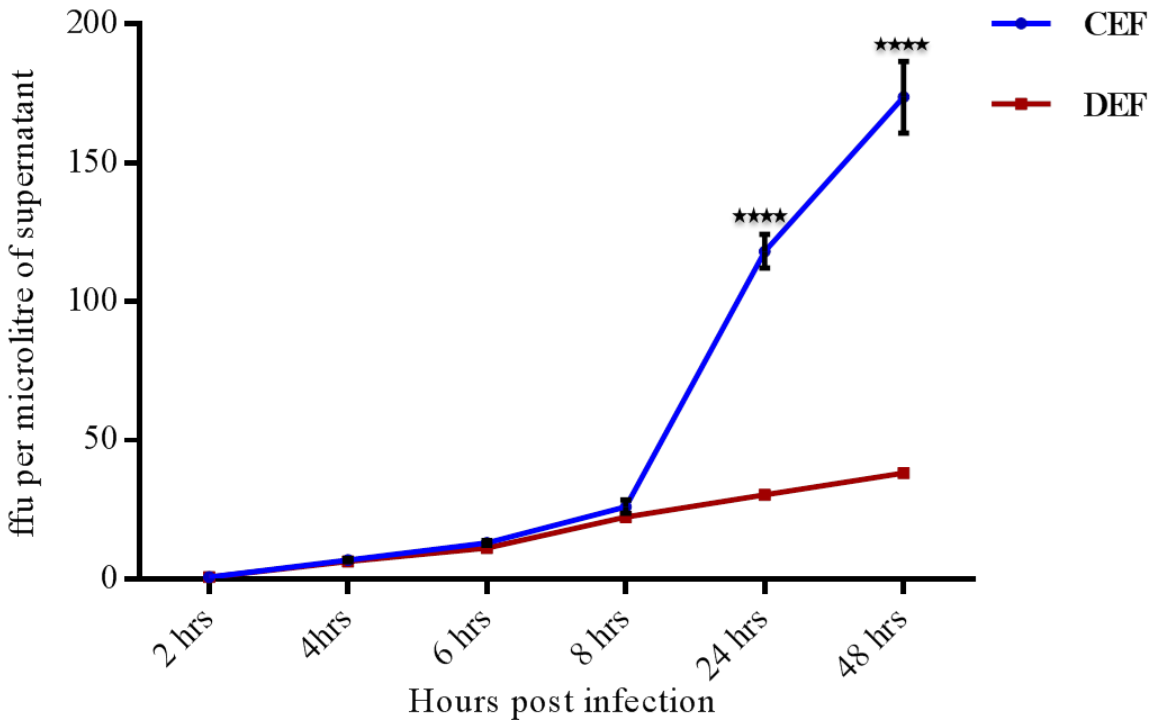

Figure 3.4–3 Levels of infectious virus production in supernatants of infected chicken and duck embryo fibroblasts. Cells were infected with avian H2N3 at a MOI of 1.0 and supernatants collected at six different time points. The infectious viral titre was measured by titration on Madin Darby canine kidney (MDCK) cells. Significant differences ($p<0.0001$) in infectious virus production between species was detected at 24 and 48 hr post infection. Level of infectious viruses showed no difference between species following infection for 2, 4, 6, and 8 hr. Data shown represent the mean of triplicate wells with error bars showing SD. ffu, focus–forming unit. CEF: chicken embryo fibroblasts, DEF: duck embryo fibroblasts.

3.4.4 Viral RNA production from chicken and duck cells

To investigate whether the reduction of infectious virus production from duck cells was a consequence of the disruption of viral RNA replication, matrix gene copy number (M

gene) was measured using qRT–PCR technique on culture supernatants collected at 8 and 24 hr post infection. M gene copy number of tested samples was calculated using the constructed standard curve with five dilutions of matrix gene RNA (Figures 3.4–4 and 3.4–5). Viral RNA output (M gene) at the two time points (8 and 24 hr post infection) was comparable between infected chicken and duck cells (*p>0.05)*.

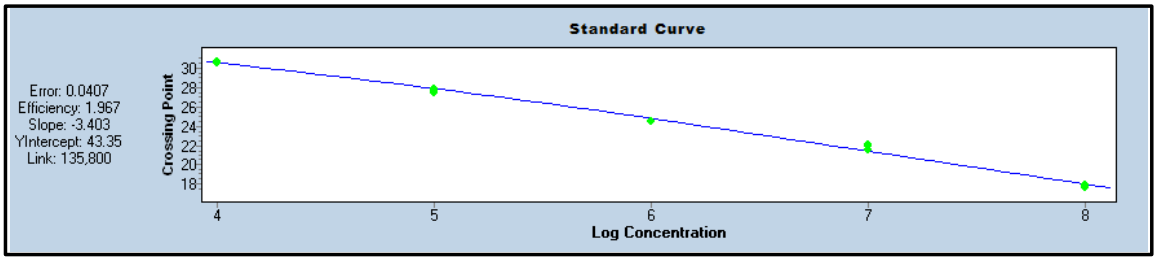

Figure 3.4–4 Standard curve for the calculation of M gene copy number. X axis represents M gene copy number which can be predicted using the average of Ct values (crossing points) on Y axis.

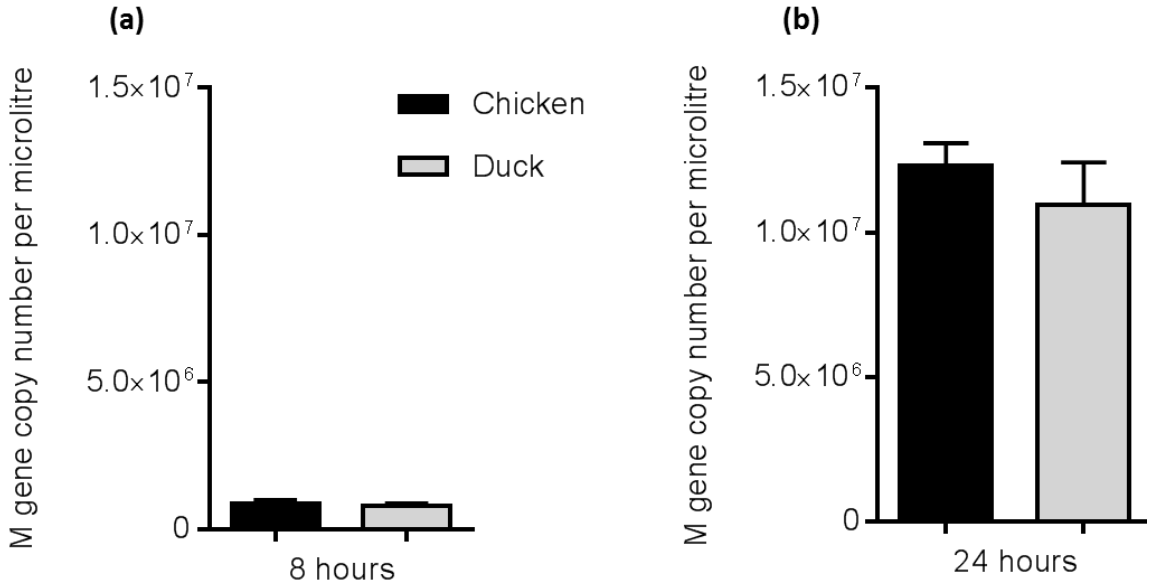

Figure 3.4–5 Measurement of influenza A matrix gene copy number using real time PCR. Figure shows matrix gene copy number in culture supernatants of chicken cells (black bars) and duck cells (grey bars) infected with avian H2N3 for 8 hr (a) and 24 hr (b). Results did not show any significant difference in M gene production between host cells at the two time points following infection with the virus (p>0.05). Data shown represent the mean of triplicate wells with error bars showing SD.

3.4.5 Matrix protein expression in chicken and duck cell supernatants

The level of viral M1 protein expression was determined following infection, using western blotting. Viral proteins were prepared from culture supernatants at 8 and 24 hr post infection. The amount of matrix protein production at the two time points, measured by the optical density, was similar between chicken and duck cell produced viruses (Figure 3.4–6 a and b).

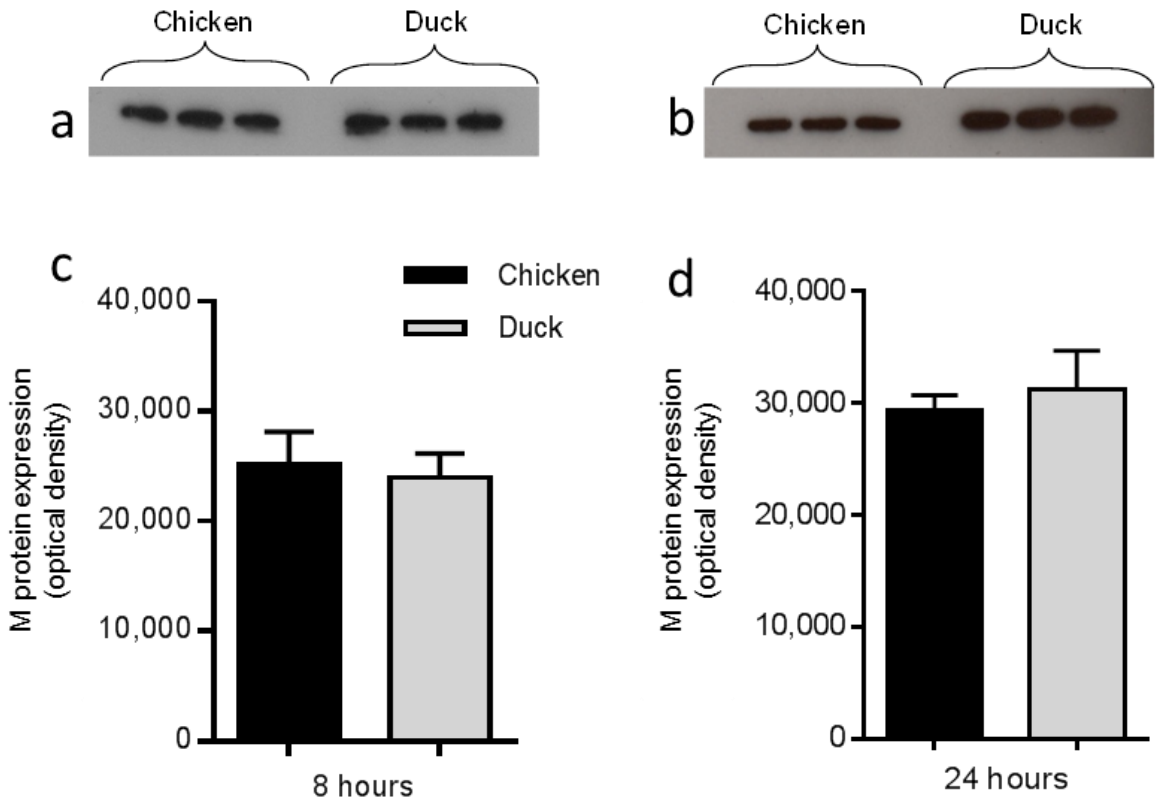

Figure 3.4–6 Western blot analysis of viral matrix protein.

Viral protein, extracted from culture supernatants, and subjected to SDS–PAGE. (a) M protein expression from infected chicken and duck cells at 8 hr, and (b) at 24 hr. Quantitative analysis showed no difference in M protein expression between chicken cells (black bars) and duck cells (grey bars) at both time points (c and d; $p>0.05$). Data shown represent the mean of triplicate wells with error bars showing SD.

3.5 Discussion

In this chapter, differences in the production of infectious virus from chicken and duck fibroblasts were studied. Results revealed that duck cells produced significantly less infectious virus than chicken cells, at 24 and 48 hr post infection. The number of infectious viruses in supernatants of chicken cell cultures was dramatically increased by increasing the time of incubation, in contrast, the production of infectious virus from duck cells did not increase greatly with further incubation. However, viral M gene RNA production was comparable between chicken and duck cells. Matrix protein expression (M1) was also similar in supernatants from chicken and duck cells.

It is well known that influenza virus requires host cell factors and components to facilitate productive infection and to produce infectious progeny virions. Cell type and virus strain may play a role in supporting different levels of influenza virus replication. For example MDCK and Vero (African green monkey kidney) cells have different viral growth kinetics (Youil et al., 2004). In addition, different strains of influenza viruses target different cell types in cultured human airway epithelial cells because of the differences in cell receptors (Matrosovich et al., 2004). In the current study, the same virus strain (avian H2N3) was used to infect the same cell type of chicken and duck. Interestingly, chicken and duck fibroblasts showed similar viral antigen expression of H2N3 based on antibody staining of cells for virus nucleoprotein expression. This suggests that the viral antigen expression on both cell types at a similar level. Therefore, the significant decrease in the number of infectious virions produced following infection of duck cells was not a consequence of a lower number of infected cells. The number of infectious viruses produced from duck cells was significantly lower than that produced from chicken cells at 24 and 48 hr post infection while it was similar between the two cell types at time point 2 to 8 hr post infections. This observation is associated with rapid cell

death which is induced to a greater degree in duck cells than in chicken cells following infection with influenza viruses (Kuchipudi et al., 2011). Cell death was also associated with low yields of infective virus particles following infection of HeLa cells with influenza virus (Takizawa et al., 1993).

Supernatants collected at 8 and 24 hr post infection were used to determine viral M gene RNA production and viral matrix protein expression. The two time points were selected as representatives of a significant (24 hr) and non–significant (8 hr) difference in infectious virus production between chicken and duck cells. Influenza viral M gene production in the infected cell cultures at 8 and 24 post infection was comparable in chicken and duck cells virions. Further, matrix protein expression in culture supernatants at the two time points was also comparable between chicken and duck cells. The matrix protein of influenza A virus has been shown to play a major role in mediating the budding of virus–like particles (VLPs) in the absence of other viral proteins (Gomez-Puertas et al., 2000, Latham and Galarza, 2001). However, it would be interesting to measure the level of all viral proteins in culture supernatants using western blotting. In addition, immunofluorescence of budding viruses and electron microscopy of immunogold–labeled virions with monoclonal antibodies against viral surface proteins is important to evaluate VLPs formation (Latham and Galarza, 2001). Moreover, further studies are required to measure the levels of the other viral RNA segments and the resultant protein expression associated with replication in chicken and duck cells. It is possible that the replication of one of the other segments is the rate limiting step for virus replication in duck cells. In addition, genetic factors such as mutations or deletions in some virus genes or the production of defective interfering viruses might have a role in decreasing virion infectivity following infection of duck cells with the virus.

Chapter 4

Electron microscopy of viruses produced from chicken and duck embryo fibroblasts

4.1 Summary

Differences in the cellular response to influenza A infection between chicken and duck embryo fibroblast (CEF and DEF) cells, with duck cells producing less infectious virus, have led to investigate virus assembly and morphology in chicken and duck fibroblasts following infection with avian H2N3. Cells were infected with a spherical H2N3 virus strain, and the differences in morphology of budding virions were observed. Viruses budding from duck cells were elongated, while chicken cells produced almost spherical virions. This difference was also seen in viruses purified from the duck and chicken culture supernatants. Spherical viruses were observed in chicken supernatants while duck cell supernatants showed pleomorphic virions. These results suggest that factors such as differences in gene sequences of structural genes (M1, M2, HA, and NA) or host cell determinants might be the reason for the production of such variations in virus morphology.

4.2 Introduction

4.2.1 Influenza A virus morphology

Influenza A viruses are not uniform in their morphological features. They have different shapes ranging from spherical to elliptical with about 100 nm in diameter to elongated or filamentous with a diameter reaching to more than several micrometres, and occasionally they are pleomorphic (Calder et al., 2010). They have two membrane–associated glycoproteins: haemagglutinin (HA), neuraminidase (NA), with small amount of matrix protein 2 (M2), which are embedded in a cell–derived lipid envelope. Beneath the lipid envelope, there is a matrix protein 1 (M1) layer. All these proteins play an important role

in virus morphogenesis (Palese and Shaw, 2007, Bouvier and Palese, 2008). Diversity of virus morphology is thought to be a genetic trait, in particular the seventh segment (M) which encodes the matrix proteins plays a dominant role in determining virus shape (Roberts et al., 1998, Elleman and Barclay, 2004). In addition, surface glycoproteins (HA and NA) have also been implicated to modulate virus shape (Jin et al., 1997, Zhang et al., 2000). Although genetic traits play a major role in determining morphology, these traits can be lost after serial passages in the laboratory (Chu et al., 1949, Ada et al., 1958).

Non–viral factors are also involved in determining influenza A virus morphology. Newly isolated clinical strains usually contain a certain percentage of filamentous forms, while laboratory adapted viruses especially with many passages on eggs or cells, are almost spherical particles (Cox et al., 1980). Cellular factors such as cell polarity and actin cytoskeleton can play a major role in determining virus morphology (Sun and Whittaker, 2007). Epithelial cells have been shown to produce more filamentous particles than fibroblasts and intact actin cytoskeleton is important for forming filamentous, but not spherical virions (Roberts and Compans, 1998, Simpson-Holley et al., 2002). Furthermore, endocytic trafficking regulator and its effector Rab11–family interacting protein 3 (Rab11–FIP3) are also required to support the formation of filamentous virions (Bruce et al., 2010).

4.2.2 Electron Microscopy

Electron Microscopy (EM) was first described by Ruska et al. (1939) for investigating the nature of viruses; however it is still used in different purposes, particularly in the field of virology (Goldsmith and Miller, 2009). It allows detection and classification of viruses

based on their structure and morphology, in addition to studies of virus pathogenesis and life cycle (Schramlova et al., 2010, Zhang et al., 2013). It can be employed for viewing pathogens (usually viruses) either by performing routine thin sections of tissue culture or by testing body fluids directly (Hazelton and Gelderblom, 2003).

Thin tissue sectioning is considered a valuable method used in cells or tissues for virus detection and examining the effect of the virus on the host cell (Miller, 1986). In this technique, cells are usually grown and infected on plastic coverslips, followed by fixation with EM fixative buffer, such as 2–4% glutaraldehyde, then washing in buffers, and positive staining with 1% buffered osmium. The sample is then completely dehydrated with graded ethanol series and acetone followed by embedding in resin, ultrathin sectioning, and multiple staining incubations. Viruses can also be viewed in fluids using negative staining. Samples are first clarified to remove large particles (e.g. bacteria and cell debris) by centrifugation at a low speed and for diluted samples, ultracentrifugation is usually performed. Samples are adsorbed on coated grids and floated to allow negative staining such as Urenyle acetate or phosphotungstic acid (PTA) and examined under an electron microscope (Hazelton and Gelderblom, 2003, Goldsmith and Miller, 2009).

Transmission electron microscopy (TEM) has had a major contribution in the discovery of many viruses and in the diagnosis of various virus infections. Although more sensitive molecular methods such as PCR and immunofluorescence have gradually replaced TEM, it remains essential for certain aspects in virology particularly in the diagnosis of unknown pathogens and also to study the cellular changes associated with viral infection (Roingeard, 2008). Transmission electron microscopy of influenza viruses has been used to study the morphology and the ultra–structural components of viruses (Noda et al., 2006, Khanna et al., 2008), and for the detection of new virus strains (Kang et al., 2006).

TEM can be used to observe budding of influenza virions by ultra–thin sections, and also detection of virus morphology using negative staining of culture supernatants or body fluids (Bachi et al., 1969, Rodriguez Boulan and Sabatini, 1978, Wrigley, 1979, Nayak et al., 2009).

4.2.3 Hypothesis

The reduction in infectious virus titre from duck cells may be due to changes in virus assembly and morphology.

4.2.4 Aim and objectives

To determine the differences in influenza virus assembly and morphology in duck or chicken cells via electron microscopy.

For this objective, chicken and duck cells infected with influenza virus were detected by electron microscopy to visualise the differences in viral budding and assembly. Culture supernatants were tested to compare the morphology of viruses produced from both cell types.

4.3 Materials and Methods

4.3.1 Viruses

Avian influenza H2N3 A/mallard duck/England/7277/06 was used. This was grown in allantoic fluid of embryonated hen's eggs (as described in 2.2.2).

4.3.2 Virus infection and fixation of cells

Chicken and duck embryo fibroblast cells (as described in 2.2.3.1) were grown on Thermanox Plastic Coverslips (13 mm in diameter) in 24–well plates in DMEM with 10% FCS and 1% antibiotics, and then incubated at 37°C until confluent. The cells were then infected with H2N3 in serum–free Ham's 12 containing 2% Ultroser G, 500 ng/mL TPCK trypsin and antibiotics at a multiplicity of infection (MOI) of 1.0 for 7 hr, or at a MOI of 0.1 for 24 hr. They were then fixed with EM fixative buffers (3% glutaraldehyde in 0.1M cacodylate buffer) at room temperature for 10 min, washed with cacodylate buffer, and stored at 4°C until TEM processing.

4.3.3 Processing cells for transmission electron microscopy

4.3.3.1 Preparing resin

Resin used for cell infiltration and embedding was prepared by mixing 25 mL Araldite CY212 resin, 15 mL Agar 100 resin and 55 mL of dodecenylsuccinic anhydride (DDSA) in a tri–pour beaker. The mixture was stirred well, and then 2 mL dibutyl phthalate and 1.5 mL DMP–30 were added and mixed. The beaker was covered with foil and incubated for 20 min at 60°C to eliminate air bubbles that formed during mixing.

4.3.3.2 Cell dehydration and infiltration with resin

Cultured cells were fixed with 1% aqueous osmium tetroxide for 30 min, and then washed with distilled water 5 x 1 min. Dehydration in graded ethanol series was performed using the following ethanol concentrations and times: 2 x 5 min 50% ethanol,

2 x 5 min 70% ethanol, 2 x 5 min 90% ethanol, followed by 3 x 10 min 100% ethanol. The coverslips were then transferred to glass vessels and infiltrated with 100% dried acetone for 2 x 5 min. The dried cells were infiltrated with resin in three steps: 30 min in 1:3 resin:acetone mix, 1 hr in 1:1 resin : acetone mix, and then 3 x 1 hr in pure resin.

The coverslips containing the cell layer were inverted on a capsule filled with fresh resin and then incubated in the embedding oven for 48 hr at 60°C. The resin block polymerized, and the coverslip was removed from the cells by immersing the block in liquid nitrogen and snapping the coverslip leaving the cells on the surface of the block. The resin block was removed from its plastic tube using a beam capsule press. Then the block was embedded in an eppendorf tube containing fresh resin so that the cell layer was nearest the bottom, and the sides of the tube were marked where the cell layer of the block was. Then it was polymerized as before.

After polymerization, the cell layer was enclosed in a resin block. The layer was cut out of the block by sawing either side of it to give a disc of resin with the layer running through the middle. The disc was cut in half to form 2 semi–circles, and those were stuck onto the top of a blank resin block using super glue.

4.3.3.3 Sample cutting

The block–tissue was placed into a chuck of a Leica EM UC6 ultramicrotome system and tightened securely. A sharp knife was fixed on the stage of the microscope and gradually advanced to the front until it has almost touched the block. The block was the carefully trimmed several times until the tissue was being sectioned. The knife was then replaced with a fresh one attached with a plastic boat. The boat was filled with sterile water to the

level of the knife edge. The block was advanced by 0.5 µm and green–pink sections were cut and floated out onto the water. A drop of water was placed on a 3–aminopropyltriethoxysilane (APES)–coated slide, and a section was removed from the boat using a fine paintbrush and placed on the drop of water on the slide. The slide was then placed on a hotplate to flatten out and dry the section, and then a few drops of 1% toluidine blue–O in 1% sodium borate were added, and the slide was placed again on the hotplate. After 1 min, the slide was rinsed with distilled water and replaced on the hotplate to dry, and then was viewed under the light microscope. Once the cells were seen clearly, the area of interest was determined.

The whole chuck holder (including the block) was removed and placed into the flat holder in place of the knife holder. The surface of the block was trimmed into a trapezium shape using a single–edged blade. The sample was then sectioned as above using a diamond knife. The sections this time were cut thinner (90 nm) and they appeared pale gold–silver in color. Sections were separated in the boat using a fine eyelash and flattened using chloroform vapour. Sections were picked up on G200HH 3.05 mm copper grids, 100 HEX (TAAB). Using fine forceps, the grid was held dull side up and introduced to the water at an angle, and then was brought under the section and lifted clear of the water with the section on the upper surface. Grids were put in a labelled petri dish containing filter paper for 1 hr at room temperature for air drying.

4.3.3.4 Sample staining

A square of parafilm slightly smaller than a petri dish was prepared and attached to the bottom of the dish. Using a syringe and filter, 1 drop of ethanolic urenyle acetate was put on the parafilm, and the grid was then placed on the drop with the sample facing down.

Drops were then incubated in the dark for 5 min at room temperature. The grid was then retrieved from the drop with a pair of fine forceps and quickly dipped ten times in each of a series of three disposable beakers, the first beaker containing 50% ethanol and the other two containing sterile water. It was then blotted on clean filter paper, and then a fresh piece of filter paper was slid between the forceps blades and also used to push the grids out of the forceps and onto a clean dry piece of filter paper on a petri dish. Using another clean petri dish, a square of parafilm was placed on the base, and by the use of syringe and filter, 1 drop of Reynold's Lead Citrate was put on the parafilm. The grid was placed on the drop, and the dish was quickly covered and incubated in dark for 8 min at room temperature. It was then rinsed with sterile water and dried as above, and then placed in a clean labelled petri dish.

4.3.4 Processing supernatants for electron microscopy

Chicken and duck cells were grown in T75 flasks in DMEM with 10% FCS and 1% antibiotic at a seeding density of 2.5 x 10^6 cells per flask. They were incubated at 37°C until confluent. They were then infected with H2N3 in serum–free Ham's F12 containing 2% Ultroser G, 500 ng/mL TPCK trypsin and antibiotics, at a MOI of 1.0. The flasks were initially incubated at 37°C for 2 hr. They were then rinsed three times with PBS, and 5 mL of fresh infection media without Ultroser G and TPCK trypsin was added. The cells were then further incubated up to 24 hr. Viral supernatants were then harvested, and clarified by centrifugation at 500 xg for 10 min. They were then concentrated by Amicon® Ultra 100K NMWL (National Molecular Weight Limit) Centrifugal Filter Device (Millipore) at 3000 xg for 30 min. Virus concentration was confirmed by titrating with chicken red blood cells. Samples were then prepared for negative staining. Briefly,

10 µl of concentrated sample were absorbed to Formvar carbon support film 3.05 mm copper grids, 100 HEX (TAAB) and incubated for 1 min then the excess fluid was carefully wicked away using a filter paper. Ten microlitres of negative stain (2% phosphotungstic acid) were then added to the grid and incubated for 30 s, then removed with filter paper. Grids were then left to air dry for 30 min at room temperature.

4.3.5 EM imaging

Samples were imaged using Tecnai G212 Bio Twin Digital TEM system. Photographs were taken from different areas of the grid at a range of image magnifications.

4.4 Results

4.4.1 The morphology of avian H2N3

Avian H2N3 viruses that were used to infect chicken and duck fibroblasts were visualized by negative stain transmission electron microscopy. Virions appeared spherical to slightly ovoid in shape of a diameter about 100 nm (Figure 4.4–1).

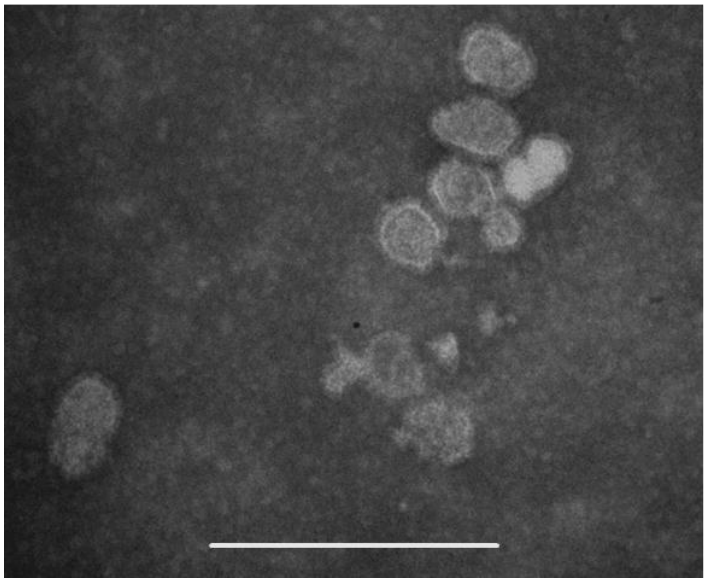

Figure 4.4–1 : Electron micrographs of negatively stained avian H2N3 virions grown in allantoic fluid of hen's eggs. Spherical particles were detected after testing the allantoic fluid under transmission electron microscope. Scale bar 500 nm.

4.4.2 EM imaging of infected chicken cells

To observe the first generation of viruses produced from chicken fibroblasts, cells were infected at MOI of 1.0 and incubated at 37°C for 7 hr. The majority of cell membrane budding viruses showed spherical virus morphology with a diameter of about 100 nm (Figure 4.4–2). Very similar results were observed in the second viral generation which was obtained after infecting cells at MOI of 0.1 for 24 hr (Figure 4.4–3).

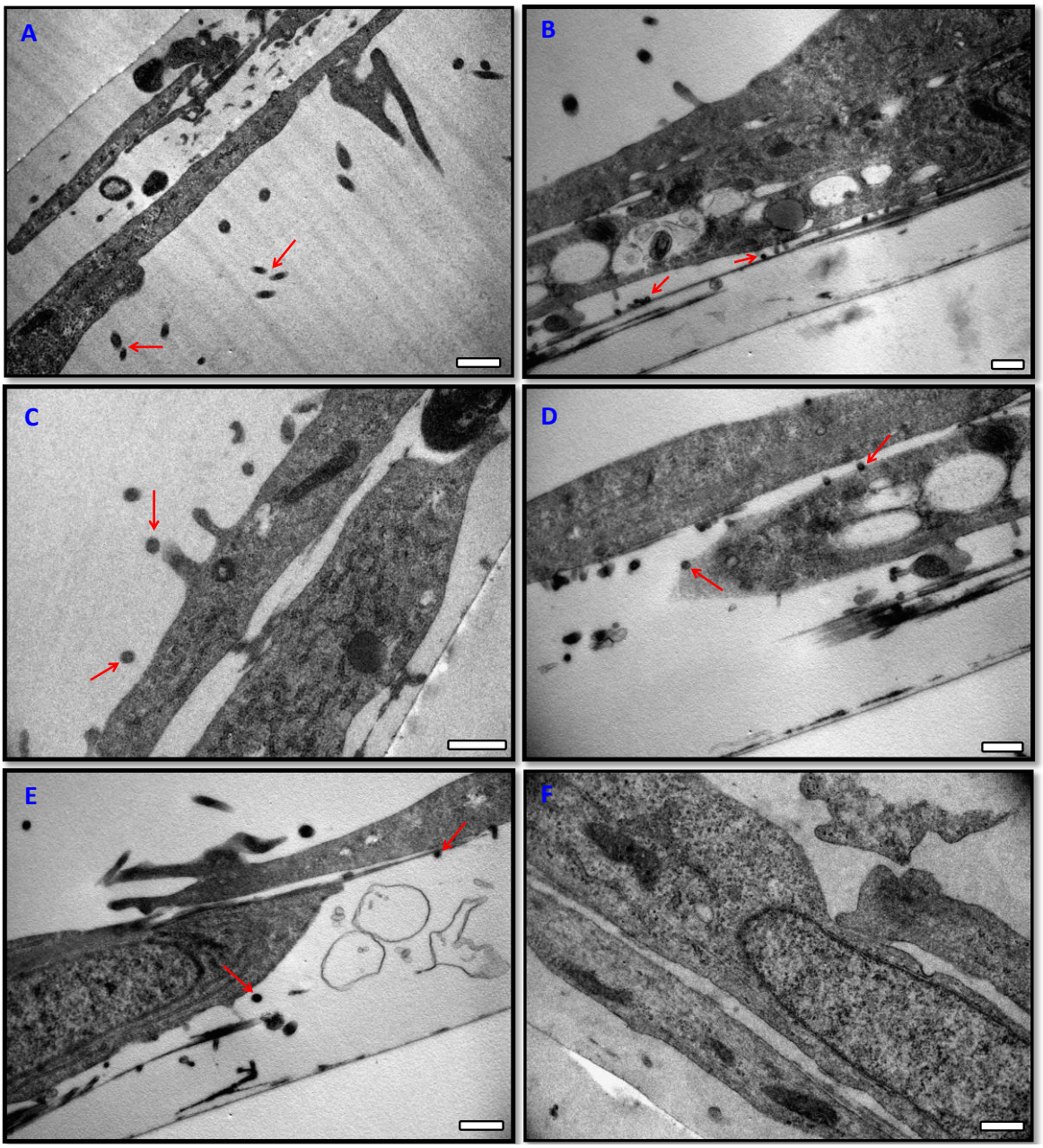

Figure 4.4–2 Budding influenza virus particles from infected chicken cells 7 hr post infection. Electron micrographs showing the presence of spherical virions budding from the surface of H2N3 infected chicken fibroblasts at MOI of 1.0 at 7 hr post infection (A, B, C, D and E) (indicated by arrows). Uninfected control (F) showed no virions. Scale bars 500 nm.

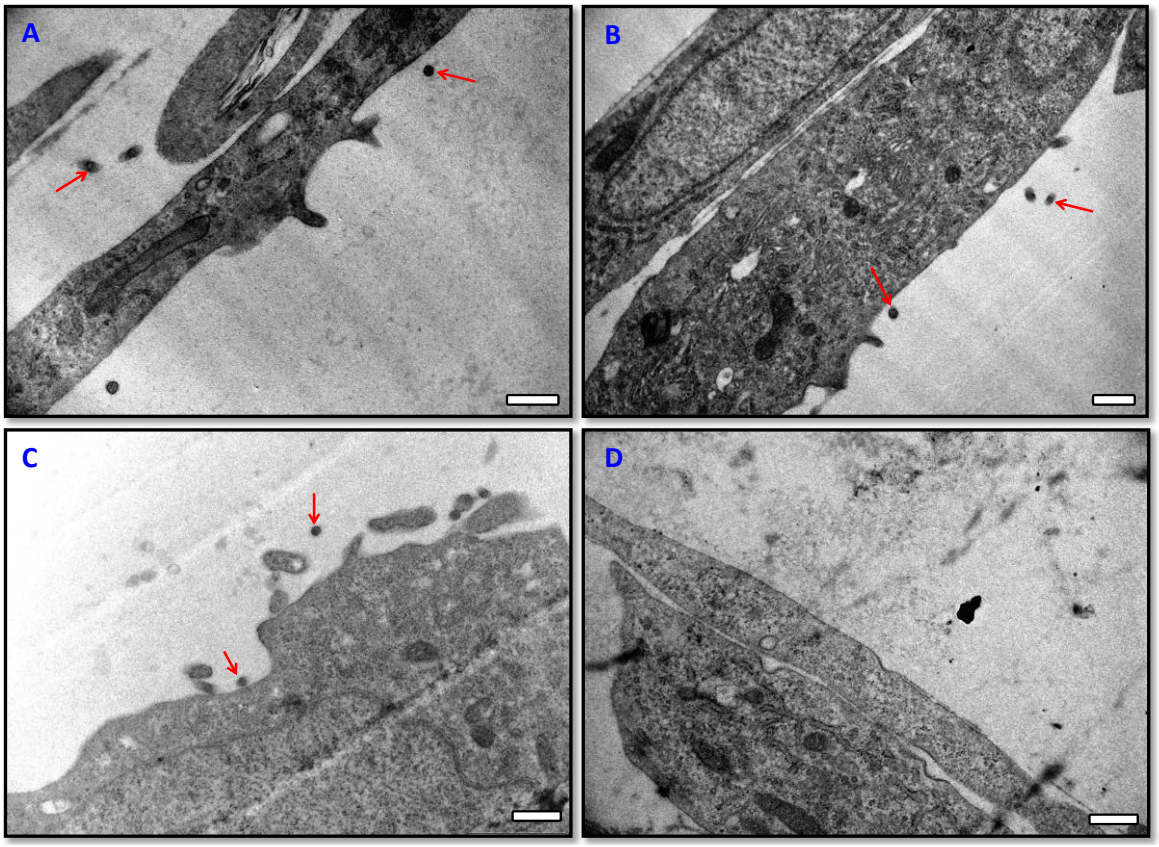

Figure 4.4–3 Budding influenza virus particles from infected chicken cells 24 hr post infection. Electron micrograph showing the presence of spherical virions budding from the surface of H2N3 infected chicken fibroblasts at MOI of 0.1 after 24 hr post infection (A, B, and C) (indicated by arrows). Uninfected control (D) showed no virions. Scale bars 500 nm.

4.4.3 EM results of infected duck cells

Two viral generations were also studied following infection of duck cells with the H2N3. The first generation was generated by infecting cells at MOI of 1.0 for 7 hr, while the second generation was observed following infection at MOI of 0.1 for 24 hr. Although the virus used to infect cells is spherical in shape, the majority of budding viruses were elongated over 500 nm length and almost filamentous up to few micrometres in length (Figure 4.4–4 and 4.4–5).

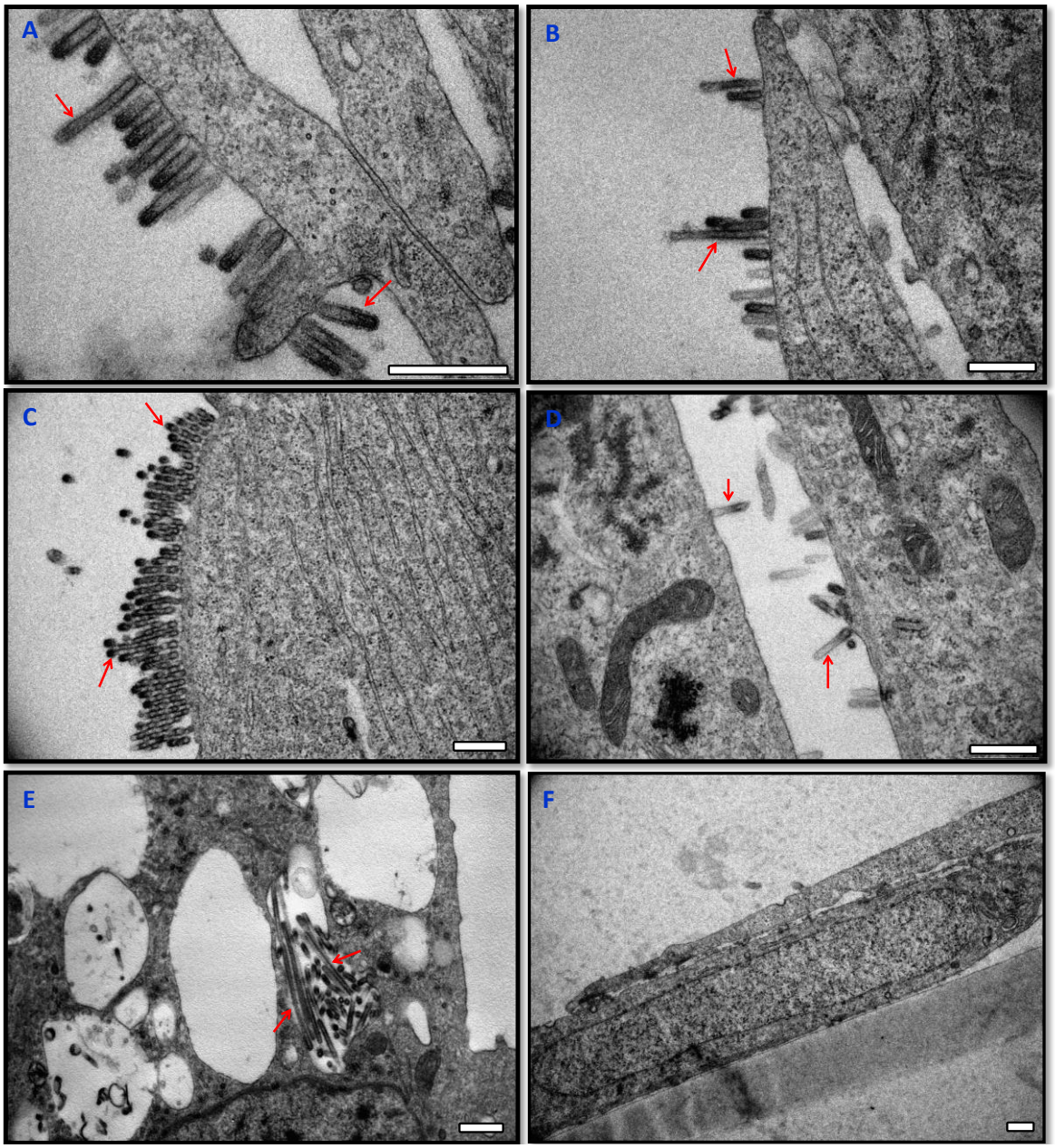

Figure 4.4–4 Budding influenza virus particles from infected duck cells 7 hr post infection.

Electron micrograph showing the presence of numerous virions budding from the surface of H2N3 infected duck fibroblasts at MOI of 1.0 after 7 hr post infection. Most of the budding particles are elongated or short filaments (A, B, C and D) with some filamentous bundles (E) (indicated by arrows). Uninfected control (F) showed no virions. Scale bars 500 nm.

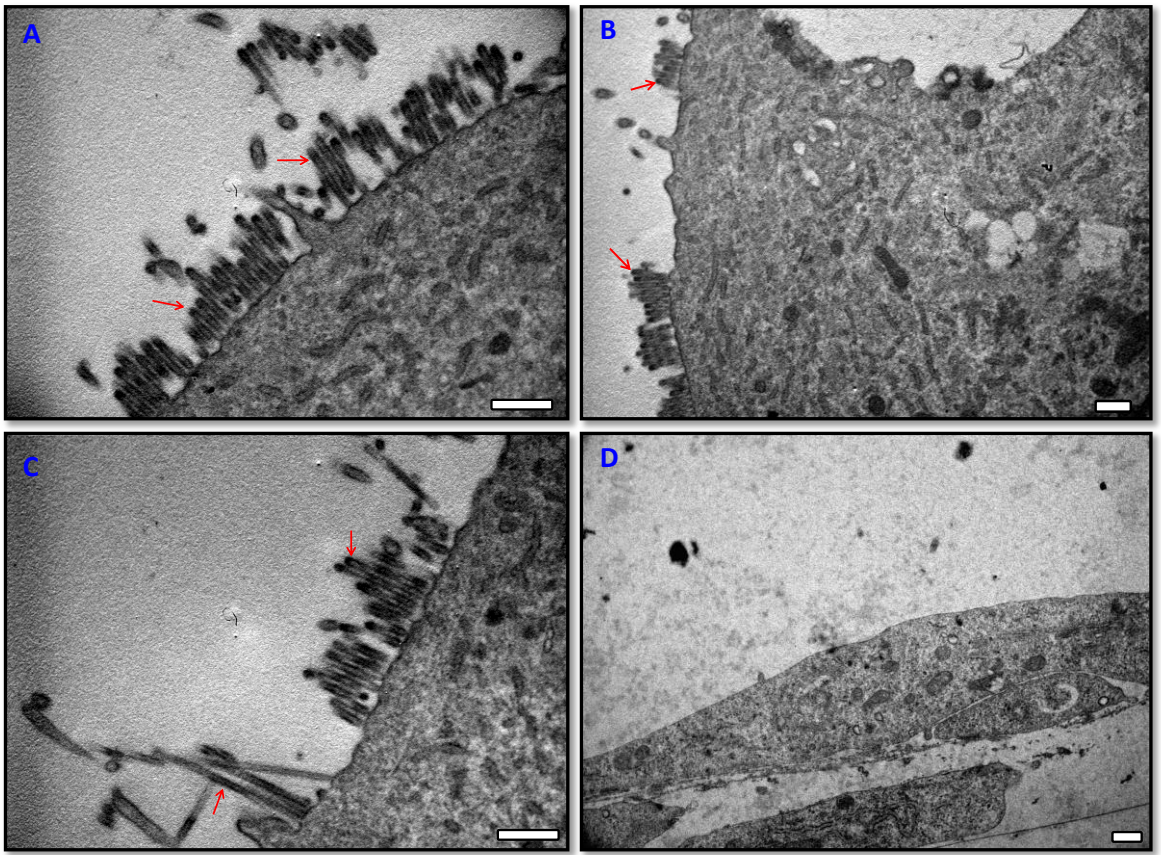

Figure 4.4–5 Budding influenza virus particles from infected duck cells 24 hr post infection.

Electron micrograph showing the presence of elongated to filamentous virions budding from the surface of H2N3 infected duck fibroblasts at MOI of 0.1 after 24 hr post infection (A, B, and C) (indicated by arrows). Uninfected control (D) showed no virions. Scale bars 500 nm.

4.4.4 EM results of culture supernatants

To achieve a further overview of the variations in virion morphology between viruses grown in chicken and duck embryo fibroblasts, concentrated viruses from culture supernatants of infected cells were examined under the electron microscope at different magnifications (Figure 4.4–6 and 4.4–7). Morphological differences were clearly observed between the two cell supernatants. Viruses derived from chicken cells were almost spherical while those obtained from duck cells were elongated to pleomorphic with sizes similar to those budding from cells. Very similar results were observed after imaging the non–concentrated viruses (Figure 4.4–8).

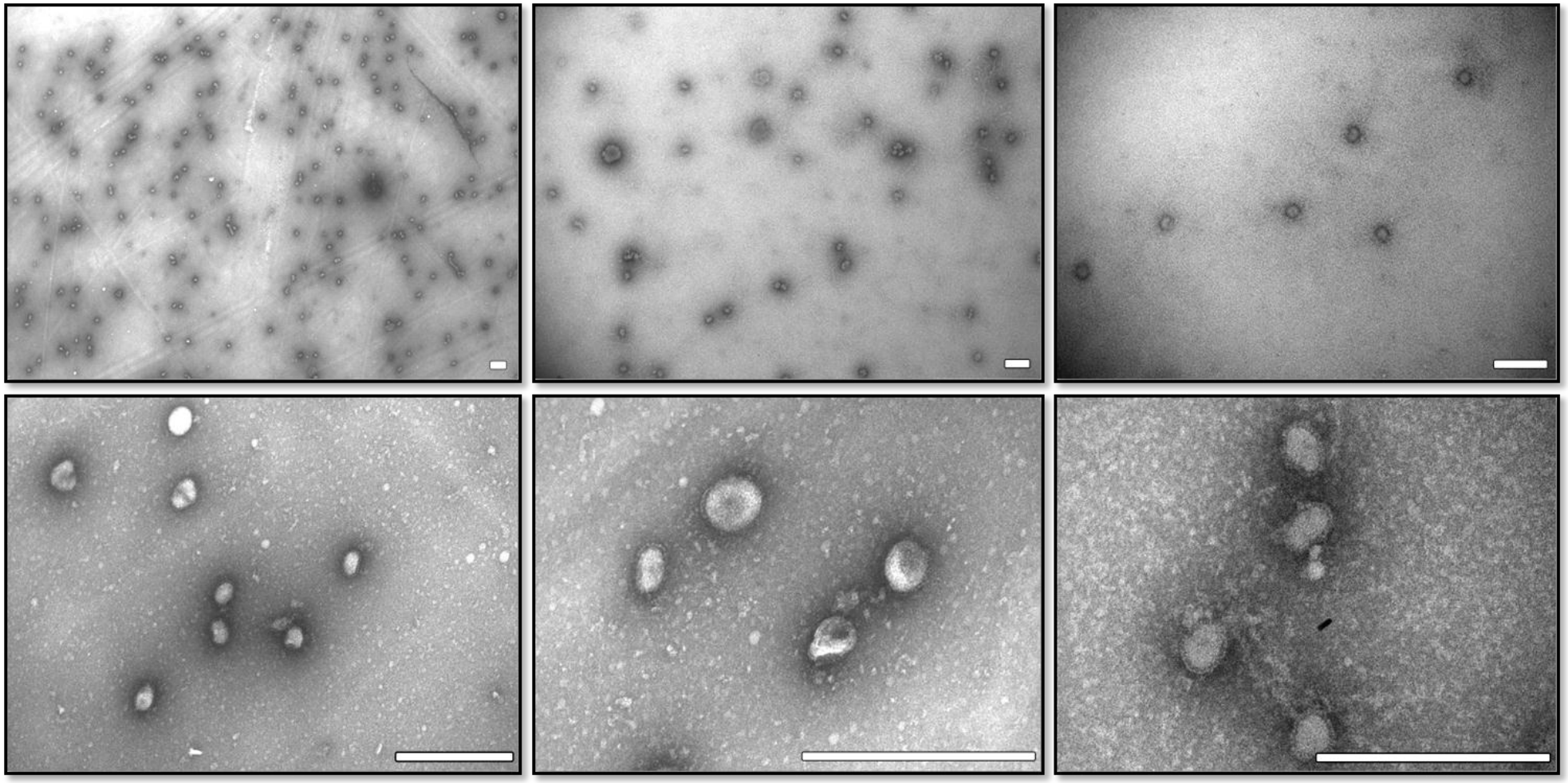

Figure 4.4–6 Electron micrographs of concentrated and negatively stained virions released from chicken fibroblasts.

Spherical particles were detected after testing culture supernatants of infected chicken cells under an electron microscope. Scale bars 500 nm.

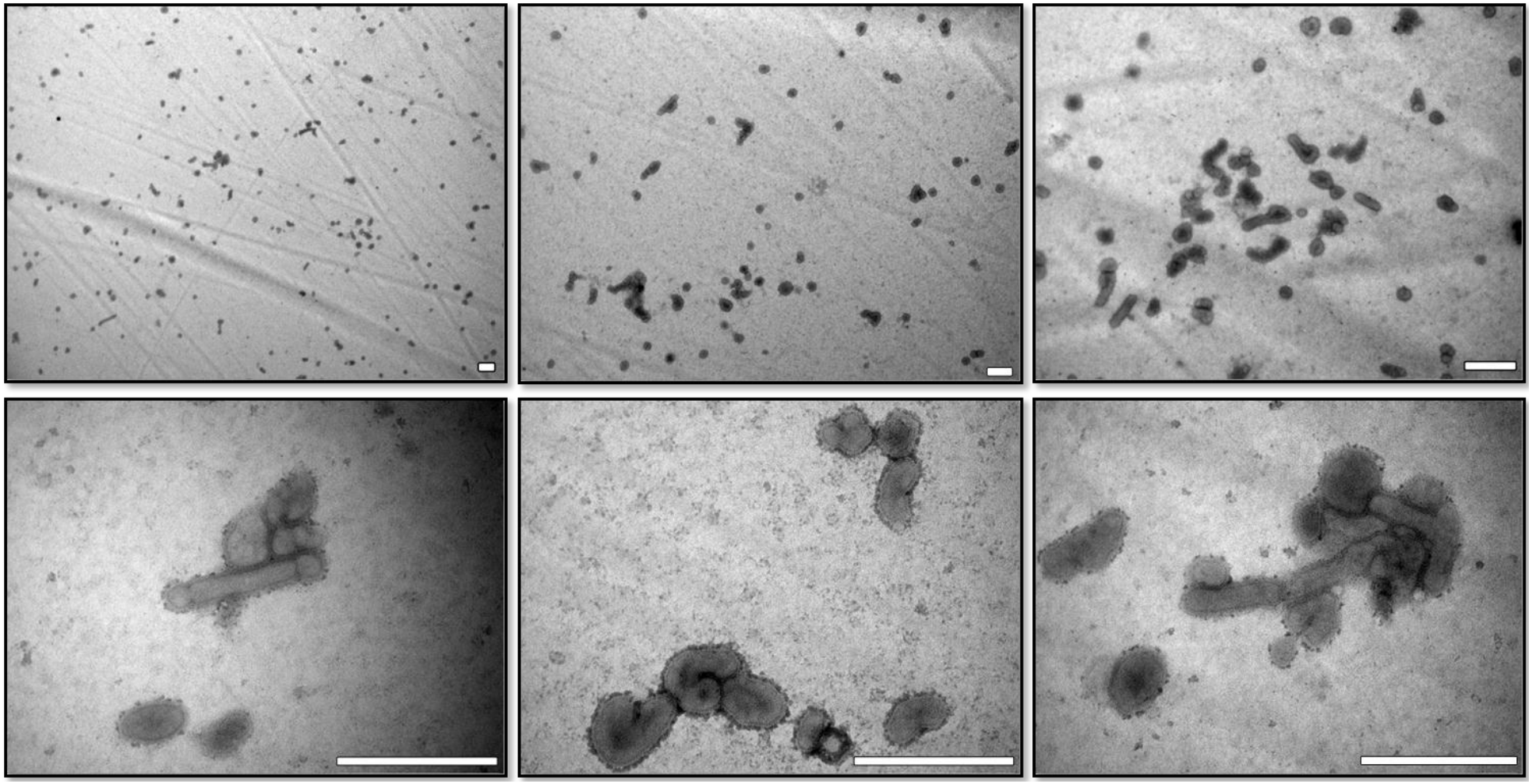

Figure 4.4–7 Electron micrographs of concentrated and negatively stained virions released from duck fibroblasts.

Pleomorphic particles were frequently observed after testing culture supernatants of infected duck cells under electron microscope. Scale bars 500 nm.

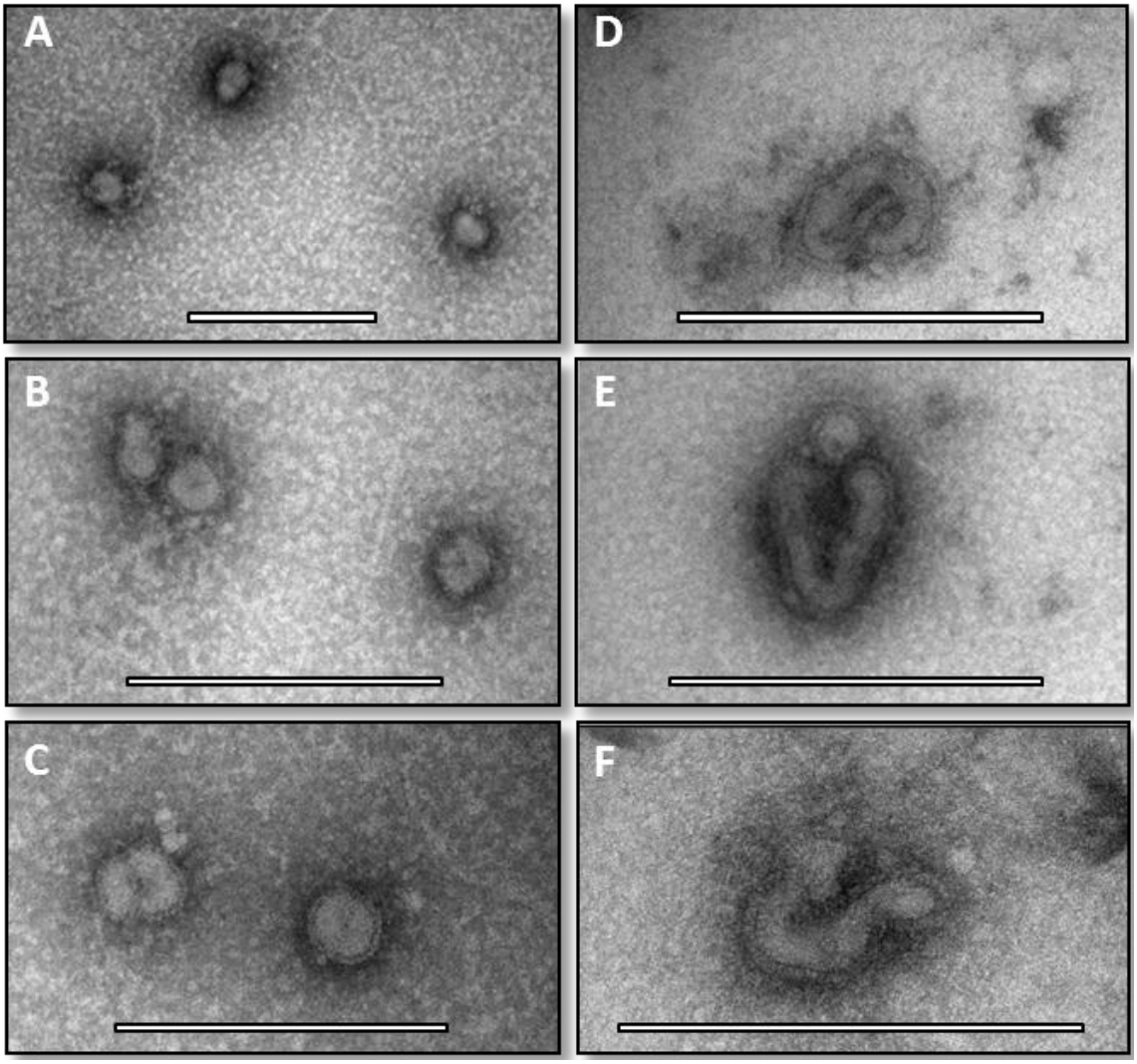

Figure 4.4–8 Electron micrographs of non–concentrated and negatively–stained virions released from chicken and duck fibroblasts.

The figure showing non–concentrated viruses obtained from chicken (A, B and C) and duck (D, E and F) fibroblasts. Similar virus morphology with concentrated virions was observed. Chicken and duck cells produced spherical and pleomorphic virion shapes, respectively. Scale bars 500 nm

4.5 Discussion

Differences in virus morphology between chicken and duck fibroblasts following infection with avian H2N3 were studied using a transmission electron microscope. Results revealed that there is a clear difference in assembly of viruses from chicken and duck cells, and also in the morphology of viruses within culture supernatants. Longer virions were observed in duck cells compared with those budding from chicken cells. Viruses observed from culture supernatants of chicken cells were mostly spherical in shape with a similar diameter to the inoculum virions, while viruses produced from duck cells were slightly elongated or pleomorphic.

Sample preparation processes may play a role in producing pleomorphic virus particles (Noda, 2011). Studies have shown that pleomorphic morphology is introduced during the storage of virions at 4°C after they are harvested (Choppin et al., 1961). In addition, virus morphology can be substantially disrupted by ultracentrifugation of non–fixed samples which results in production of irregular virions (Sugita et al., 2011). To avoid these possibilities, viruses were concentrated using an alternative method that should keep the virus shape without any changes. This method is based on the filtration of culture supernatants at a lower centrifugation speed. In addition, non–concentrated viruses were also tested under an electron microscope and no obvious differences to the concentrated samples were observed.

It is well known that influenza A viruses exhibit different morphological structures. Most clinical isolates are predominantly filamentous (Chu et al., 1949), while the laboratory–adapted strains are mostly spherical or elliptical (Kilbourne and Murphy, 1960). Matrix (M gene) which encodes two proteins (M1 and M2) has been shown to play an essential role in modulating filamentous versus spherical virus morphology (Hughey et al., 1995,

Bourmakina and Garcia-Sastre, 2003, Elleman and Barclay, 2004). In addition, viral morphology, genome packaging, and incorporation of NA and M1 into virions are also reported to be affected by changes in the amino acid sequences (Burleigh et al., 2005) or deletion in the cytoplasmic tails of the other viral transmembrane proteins (HA, NA) (Jin et al., 1997, Zhang et al., 2000). Therefore, sequencing of these genes (M, HA, and NA) is important to determine whether the difference in virus morphology is accompanied by with some mutations or deletions in these genes during virus replication (see chapter 5).

Cellular factors such as cell polarity and actin cytoskeleton network are important in determining the production of filamentous virions. Filamentous particles up to 30 µm can be observed on the surface of polarized cells following infection with a filamentous strain such as A/Udorn/72 virus while spherical or slightly elongated particles are usually detected from the infection of non–polarized cells (Roberts and Compans, 1998). However, duck fibroblast cells used in this study produced short filaments after infecting with spherical strain (H2N3) while chicken fibroblast cells produced only spherical virions. Intact actin of chicken and duck fibroblasts might have a potential role in determining virus morphology, particularly the filamentous form.

Chapter 5

Molecular analysis of H2N3 virus produced in chicken and duck cells

5.1 Summary

Molecular differences between H2N3 viruses produced in chicken and duck cells were investigated. All the eight viral segments were amplified by one–step polymerase chain reaction (PCR) and sequenced directly. Six of the viral gene sequences (PA, HA, NA, M, NS, and NP) showed identical sequences in viruses produced by chicken and duck cells, but some differences in viral sequences were found in two of the polymerase (P) genes (PB1, and PB2). However, these differences were due to the production of non–specific PCR products rather than viral mutations, which was confirmed by cloning the PCR products using the TOPO® TA Cloning system, and also by loading a large volume of PCR products on agarose gel, enabling detection of the non–specific bands. Taken together, these results demonstrate that there is no difference between gene sequences of influenza viruses grown in chicken or duck primary cells. As a consequence, any differences in virus morphology, between chicken and duck grown viruses must be due to host cell factors.

5.2 Introduction

5.2.1 Genetics of influenza A virus

The influenza A virus is lipid–enveloped with eight separate single–stranded RNA segments, which are the polymerase genes (PA, PB1, and PB2), haemagglutinin (HA), nucleoprotein (NP), neuraminidase (NA), matrix (M), and non–structural (NS) genes (Cheung and Poon, 2007). Each segment encodes one or more proteins. The polymerase protein complex (PB1–PB2–PA) encodes RNA–dependent RNA polymerase and is found as a heterotrimer within the whole virions or in the nuclei of infected host cells

(Detjen et al., 1987). In addition to the three polymerase subunits that are encoded by the three polymerase genes, PB1 also encodes two minor products: N40, which is N–terminally truncated from the same PB1 protein reading frame (Wise et al., 2009) and PB1–F2, a short peptide expressed from open–reading frame 1 (McAuley et al., 2010). The NP with the polymerase complex forms the ribonucleoprotein (RNP) that each viral segment is associated with (Naffakh et al., 2008). The HA gene encodes the major surface protein which binds with the sialic acid of the host cell leading to virus uptake, while the NA gene encodes the enzymatic surface protein which is important for viral release at the end of virus replication. The seventh segment (M) encodes two proteins: M1 that lines the internal surface of the virus lipid membrane; and M2, which is the ion channel that mediates virus uncoating (Mitnaul et al., 2000). The shortest segment also encodes two proteins: NS1 which mediates evasion of the innate immune response and NS2 (also called nuclear export protein, NEP) that plays a role in exporting RNA from the nucleus into the cytoplasm (Iwatsuki-Horimoto et al., 2004).

Every viral protein has specific binding sites that are essential in the virus life cycle, to facilitate production of a fully infectious virion. These domains have a role in each of the life cycle, including virus attachment, transcription, replication, nuclear import and export, packaging, budding and release. Mutations and deletions in any of influenza viral genes might affect virus replication and the production of a completely infectious virion. Figure 5.2–1 shows the main influenza A viral protein domains and their role in virus replication, pathogenicity and morphogenesis.

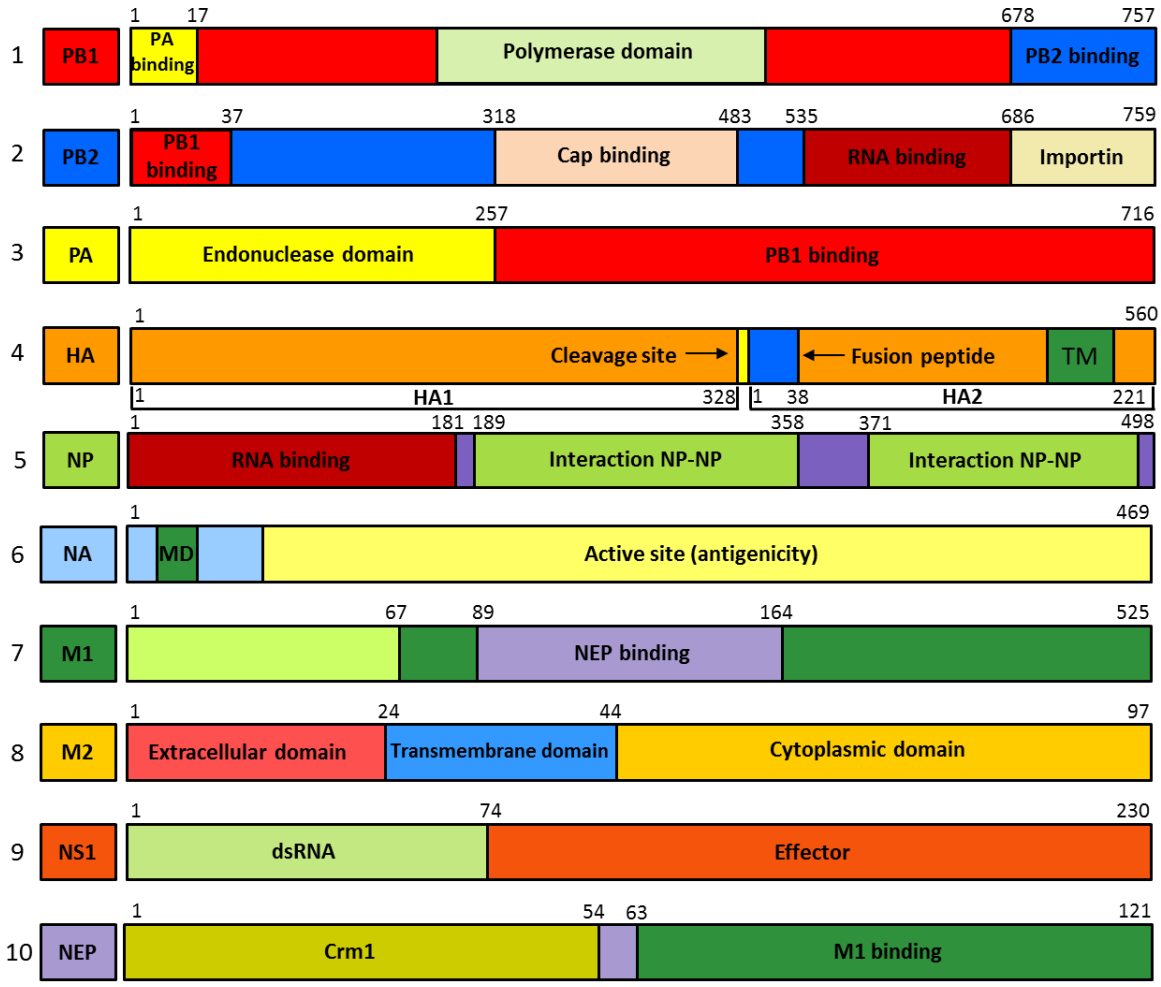

Figure 5.2–1 Domain organisation and structures of influenza A viral proteins.

The figure shows a linear representation of the viral protein molecules. Numbers refer to the amino acid positions. PB1 protein (1) represents the core subunit of the polymerase complex as it interacts with both PB2 and PA proteins (2 and 3, respectively), which results in the production of a PA–PB1–PB2 complex which plays an essential role in viral RNA transcription and replication. In addition, PB2 forms the cap–binding and putative RNA domains; and also a domain that binds human importin α. NP protein (5) has a tail–loop binding site, which is important in NP–NP binding, in addition to the RNA binding site. NP is also incorporated into the polymerase complex via interaction with the PB2 protein. The HA protein (4) consists of two main parts; the HA1 subunit containing the sialic acid receptor–binding domain and the ectodomain HA2 subunit, which contains a fusion peptide that mediates the fusion of the virus envelope and endosomal membranes, and transmembrane (TM) domains, which interact with M1 at the end of the virus life cycle. There is a protease cleavage site between the HA1 and HA2 subunits characterised by a specific multibasic amino acid sequence. The biggest part of the NA protein (6) is the active site, which plays a role in cleaving the terminal sialic acid from the HA receptors on cell membranes. It also contains a

membrane domain that interacts with M1. The main structural component of the M1 protein (7) is the nuclear export protein (NEP) binding site, which is important in the nuclear export of ribonucleoprotein particles. The M2 protein (8) has three regions: the extracellular domain which is highly conserved between the different influenza in all known influenza strains, transmembrane domain which forms the core of the ion channel and is the target of anti–influenza drugs, and cytoplasmic domain, which plays a role in virus budding and assembly. The NS1 protein (9) can be divided into the N–terminal domain that binds double–stranded RNA and the C–terminal effector domain that binds multiple cellular proteins. NEP (10) is also divided into two regions; the N–terminal domain that binds the cellular protein Crm1, or exportin 1, which mediates the export of many proteins, and the C–terminal region which has been identified as pivotal for the M1 binding site. Figure assembled from (Kong et al., 2006, Boulo et al., 2007, Cady et al., 2009, Das et al., 2010, Du et al., 2012).

5.2.2 Polymerase chain reaction and nucleotide sequencing

The polymerase chain reaction (PCR) is an *in vitro* biochemical technique used to amplify a single copy of DNA, generating billions of specific sequences from a DNA template in a simple enzymatic reaction (Mullis, 1990). It has now became one of the most common molecular techniques used for a variety of applications such as detection and diagnosis of infectious diseases, identification by "finger printing", and DNA cloning for sequencing. It has frequently been used in the detection and screening of influenza A viruses (Pisareva et al., 1992, Fouchier et al., 2000). Viral mutations can also be detected using this technique (Liu et al., 2009). Sequencing of PCR amplification products can provide valuable information about the identity of a virus. The process of obtaining nucleotide sequence data from PCR reactions can be achieved through the use of a cycle sequencing reaction that utilizes Taq polymerase and dideoxynucleotides in the PCR reaction mixture (Innis et al., 1988). Removal of unincorporated primers and nucleotides from the PCR product is a necessary step before DNA sequencing. This can

be achieved by performing PCR purification by centrifugal ultrafiltration devices. While most of primer dimers are removed using such devices, large nonspecific amplicons (>50 bp) will not be removed and they can interfere with DNA sequencing (Krowczynska and Henderson, 1992).

5.2.3 Hypothesis

The reduction in infectious influenza virus titre from duck cells and the variation in virus morphology may be due to defects or changes in the viral genome.

5.2.4 Aim and objectives

To investigate the molecular changes of influenza viruses cultured on chicken and duck embryo fibroblasts by whole genome sequencing.

To achieve this objective, viral nucleotide and amino acid sequence alignment between viruses derived from chicken and duck fibroblasts will be performed to determine any differences which might have a role in decreasing viral infectivity and changing virus morphology. Sequences of parent viruses (grown in hens' eggs) will also be compared with virus sequences following culture in chicken or duck cells.

5.3 Materials and Methods

5.3.1 Polymerase chain reaction (PCR)

Amplification of each gene segment of influenza virus was performed using One Step Super Script III RT–PCR kit (Invitrogen). Viral RNA was extracted from culture supernatant following the procedure described in chapter 2 (2.3).

5.3.1.1 Oligonucleotide primers used in PCR

Highly conserved sequences among several strains of H2N3 influenza A viruses were used to design the primers that were used for amplification (Appendix II). The influenza research data base (http://www.fludb.org/brc/home.do?decorator=influenza) was used for primer design of all viral genes together with another freely available software program (http://www.premierbiosoft.com/servlet/com.pbi.crm.clientside.FreeToolLoginServlet#) for checking the possibilities of primer dimer, cross dimer, and hair pin loops. Primers were designed to amplify all eight H2N3 viral segments in the genome. In order to amplify the whole virus genome, two or three sets of primers were designed for each gene (Table 5.3–1). All these primers were supplied by Eurofins WMG Operon, London, UK.

Gene	*Forward primer*	*Reverse primer*	*Amplicon sizes(bp)*
PB2	PB2–53–For 5'–ATCTAATGTCGCAGTCCCGCAC–3'	PB2–2278–Rev 5'–TCGCTGTCTGGCTGTCAGTAAG–3'	2226
PB2	PB2–1–For 5'–CTCAGCGAAAGCAGGTCAA–3'	PB2–106–Rev 5'–GGTCCACAGTGGTCTCTTAG–3'	106
PB2	PB2–2233–For 5'–AACGGAAACGGGACTCTA–3'	PB2–2341–Rev 5'–TAGAGTAGAAACAAGGTCGT–3'	109
PB1	PB1–25–For 5'–ATGGATGTCAATCCGACTTTAC–3'	PB1–2298–Rev 5'–CTATTTCTGCCGTCTGAG–3'	2274
PB1	PB1–1–For 5'–CTC AGCAAAAGCAGG CAAA–3'	PB1–120–Rev 5'– ATGGCTGTATGGAGGATCTC–3'	120
PB1	PB1–2222–For 5'– ACGGATTAAGAAGGAGGAGT–3'	PB1–2341–Rev 5'– AGAGTAGTAGAAACAAGACATT–3'	120
PA	PA–1–For 5'–AGCGAAAGCAGGTACTGA–3'	PA–2217–Rev 5'–TTTTGGACAGTATGGATAGC–3'	2217
HA	HA–1–For 5'–AGCAAAAGCAGGGGTTATAC–3'	HA–1711–Rev 5'–GCAGAGACCCATTAGAACAC–3'	1711
HA	HA–1366_For 5'–TGGAGAATGAGAGGACA–3'	HA–1778–Rev 5'–CTAGAGTAGTAGAAACAAGGGTGT-3'	413
NP	NP–1–For 5'–AGCAAAAGCAGGGTAGATAA–3'	NP–1525–Rev 5'–CTGCATTGTCTCCGAAGA–3'	1525
NP	NP–1356–For 5'–TCAGACATGAGAACAGAAATCA–3'	NP–1565–Rev 5'–TAGAGTAGTAGAAACAAGGGTATT–3'	210
NA	NA–11–For 5'– GGTGCGAGATGAATCCAAAT–3'	NA–1374–Rev 5'–CCGATCCAGGTTCATTGTCT–3'	1364
NA	NA–1–For 5'–AGCAAAAGCAGGTGCGAGAT–3'	NA–420–Rev 5'–GAGAGCAAAGGACCAGCAAT–3'	420
NA	NA–1220–For 5'–ATTGGTCAGGCTATTCAGG–3'	NA–1453–Rev 5'–TAGAGTAGTAGAAACAAGGTGG–3'	234
M	M–1–For 5'–AGCAAAAGCAGGTAGATATTG–3'	M–999–Rev 5'–GCTCTATGTTGACAAAATGACC–3'	999
M	M–857–For 5'–AATGCATTTATCGTCGCCT–3'	M–1027–Rev 5'–TAGAGTAGTAGAAACAAGGTAGT–3'	171
NS	NS–20–For 5'–AWACATAATGGAYTCCAACAC–3'	NS–677–Rev 5'–CTTTGGAGGGAGTGGAG–3'	658
NS	NS–575–For 5'-GGACTTGAATGGAATGATAACAC-3'	NS–890–Rev 5'–TAGAGTAGTAGAAACAAGGGTG–3'	316

Table 5.3–1 Primers designed for RT–PCR amplification of the eight viral segments of H2N3 avian influenza A. Two or more sets of primers were designed for each gene to amplify and sequence the whole genome. Some non–influenza nucleotides were added in some primers (underlined) to ensure that the whole amplicon can be sequenced, to increase annealing temperature at 5'–end and also to decrease the possibility of primer dimer formation.

5.3.1.2 PCR conditions

For amplifying each of the 8 viral genes, SuperScript® III one step RT–PCR system with platinum® Taq high fidelity was used. Both cDNA synthesis and PCR amplification were performed in a single tube using this system. Gene–specific primers (Table 5.3–1) were used for cDNA synthesis and PCR amplification. Starting material of viral RNA used in cDNA synthesis of all genes was 100 ng/µl, and the final concentration of Mg^{+2} ions (which is included in the 2X reaction mix) was 1.2 mM. The volumes and final concentrations of components used in the PCR are shown in Table 5.3–2.

Component	*Volume*	*Final Concentration*
2X Reaction Mix	25 µl	1X
Template RNA	n µl (100 ng)	–
Sense primer	1 µl	0.2 µM
Anti–sense primer	1 µl	0.2 µM
Enzyme mix	1 µl	1.0 unit
PCR grade water	To 50 µl	–

Table 5.3–2 One–step RT-PCR reaction.

Table showing list of components used to perform one–step RT–PCR. The amount of viral RNA used in the reaction was 100 ng/µl. Reaction mix consisted of a proprietary buffer system, deoxyribonucleotide phosphate (dNTPs), magnesium ions (Mg^{+2}), and stabilizers. Enzyme mix consisted of SuperScript® III Reverse Transcriptase and Platinum® *Taq* DNA Polymerase High Fidelity.

The tube was capped and then placed in a thermal cycler (XP cycler), and the following program was used for RNA transcription (cDNA synthesis) and PCR amplification:

1) For amplicons more than 400 bp, PCR conditions were: cDNA synthesis at 55°C for 30 min, initial denaturation at 95°C for 2 min followed by 35 cycles of: denaturation at 95°C for 30 s, annealing at 58°C for 40 s, extension at 68°C for 2 min. The reaction was then held at 68°C for 10 min, and then cooled down at 4°C for 5 min. The extension time of 2

min in PCR cycles was employed to increase the yield of the large (polymerase) genes. The above concentrations and PCR conditions were employed for all viral gene amplicons more than 400 bp with differences in the annealing temperature for NS and PB2 genes which were 53°C and 62°C, respectively.

2) For amplicons less than 400 bp, PCR conditions were: cDNA synthesis at 55°C for 10 min, initial denaturation at 95°C for 2 min followed by 35 cycles of: denaturation at 95°C for 15 s, annealing at 57°C for 30 s, extension at 68°C for 30 s. The reaction was then held at 68°C for 1 min, and then cooled to 4°C for 5 min. The above concentrations and PCR conditions were employed for all viral gene amplicons less than 400 bp with a difference in the annealing temperature for M gene, which was 55°C instead of 57°C.

5.3.1.3 Agarose gel electrophoresis

The amplified PCR products were detected using 1% (w/v) agarose gel prepared with agarose (Sigma) in TAE buffer. The mixture was stirred well and melted in a microwave oven, and mixed once or twice during microwaving. The gel was then cooled to 55°C, and one microgram per milliliter of Nancy–520 (Sigma) was added. The gel was then poured into a gel casting tray, and a 10 well gel comb was inserted, and then left for 30 to 45 min to set. The comb was then carefully pulled out and the gel was placed in the electrophoresis tank. Running buffer was added into the tank up to 2 to 3 mm over the gel. The sample was then prepared for loading on the gel by adding 8.5 µl of PCR product and 1.5 µl of 6X loading dye (New England BioLabs). A 1 kb or 100 bp DNA ladder (New England BioLabs) was loaded in one of the side well. The lid was placed on the gel box and the electrical current was connected for around 1 hr with 90 V. The gel was then carefully removed from the tray and examined under a UV trans–illuminator

(ImageQuant 300 imager, GE healthcare, UK). The size of the gene was estimated by comparison with the standard DNA ladder.

5.3.2 Sequencing

5.3.2.1 PCR purification and determination of DNA concentration

PCR products were cleaned up using QIAquick PCR purification kit (Qiagen) according to manufacturer's instructions (Appendix IV). The volume of the DNA elution buffer (10 mM Tris Cl, pH 8.5) was 50 µl. The concentration of cleaned up DNA was determined using NanoDrop8000 spectrophotometer (Thermo Scientific, UK) by UV absorption. The purified PCR products were sent for sequencing.

5.3.2.2 Nucleotide sequencing

One nanogram per microliter per 100 bp of purified DNA with 3.2 pml/µl of forward and reverse primers that were used to amplify the viral genes was sent to Source BioScience LifeSciences for sequencing. Additional primers for polymerase (PB1, PB2, and PA) genes (Table 5.3–3) were also used to obtain full coverage of these genes. The sequences were edited using Chromas Lite software and then were assembled and aligned by Geneious Inspirational Software for Biologists (www.geneious.com).

Gene	*Forward primer*	*Reverse primer*
PB2	PB2–738_For (seq) 5'–AGCGAAAGCAGGTCAAATA–3'	PB2–1501_Rev (seq) 5'–AATTCGACACTAATTGATGGC–3'
PB1	PB1–784_For (seq) 5'–ATGGATGTCAATCCGACTTTAC–3'	PB1–1585_Rev (seq) 5'–CTATTTCTGCCGTCTGAG–3'
PA	PA–712_For (seq) 5'–AGCGAAAGCAGGTACTGA–3'	PA–1404_Rev (seq) 5'–TTTTGGACAGTATGGATAGC–3'

Table 5.3–3 Primers designed for sequencing the "middle" of the polymerase genes of H2N3 avian influenza A.

5.3.2.3 Amino acid sequences

The assembled sequences were translated to amino acids using the same software (Geneious Inspirational Software for Biologists). Sequence differences were identified by alignment of the amino acid sequences (chicken– and duck–produced genes) and also by comparison with amino acid sequences available from GenBank.

5.3.3 Cloning

5.3.3.1 Cloning of PCR products into a plasmid vector

For cloning the amplified influenza A virus PB1 and PB2 genes, TOPO® TA Cloning system for Sequencing (Invitrogen), a specialized cloning kit designed for Taq polymerase–amplified PCR products was used. The plasmid vector (pCR™4–TOPO®) is 3956 bp and supplied linearized with single 3'thymidine (T) residue overhangs allowing any PCR product with any adenosine (A) residues overhanging to be ligated into the vector. Topoisomerase is also covalently bound to the vector. The cloning reaction was performed following the manufacturer's instructions. Fresh PCR product was first

purified as described in 5.3.2.1, and the DNA concentration was determined by NanoDrop quantification. Fifteen to twenty nanograms of purified PCR product, 1 µl of TOPO vector, 1 µl of salt solution (containing 1.2 M NaCl and 0.06 M $MgCl_2$) and water (to a final volume of 6 µl) were added to a 0.5 mL centrifuge tube and mixed gently. The mixture was incubated at room temperature for 5 min, and then was placed on ice.

The amount of purified PCR product needed for the cloning reaction was calculated using the following formula:

$$\frac{10 \text{ ng/ vector} \times \text{kb insert}}{\text{Kb vector (3956)}} \times \frac{3}{1} = \text{ng of PCR needed}$$

5.3.3.2 Transformation of bacteria with plasmid

Four microlitres of TOPO cloning reaction were added into one vial of One Shot® TOP10 chemically competent *E. coli* and mixed gently. The contents were then incubated on ice for 30 min. The cells were then subjected to heat shock for 30 s at 42°C in a water bath without shaking and then immediately moved on to ice. Two hundred and fifty microlitres of pre–warmed S.O.C medium (0.5 g of tryptose, 5 g of yeast extract and 200 Mm glucose in 1 L of sterile distilled water) was added to the tube. The tube was incubated at 37°C for 1 hr in an orbital shaker at 225 rpm. Following incubation, 100–200 µl from each transformation were spread on pre–warmed Luria–Bertani (LB) agar (Thermo Scientific) supplemented with 50 µg/mL kanamycin and incubated overnight at 37°C. Single clones were transferred to 8 mL of LB broth (Thermo Scientific)

supplemented with 50 µg/mL kanamycin and incubated overnight at 37°C in an orbital shaker at 150 rpm prior to isolation of plasmid DNA.

5.3.3.3 Plasmid DNA purification

Plasmid purification was performed using PureLink® Quick Plasmid DNA Miniprep system (Invitrogen) following the manufacturer's instructions (Appendix IV). The volume of the plasmid elution buffer (10 mM Tris–HCl, pH8.0; 0.1 mM EDTA) was 75 µl. The Concentration of DNA from purified plasmid was determined using NanoDrop8000 spectrophotometer (Thermoscientific, UK) by UV absorption.

5.3.3.4 Restriction digestion

To determine the insert size of transformants, plasmid DNA was digested with the restriction enzyme *EcoRI*. Two micrograms of plasmid DNA was mixed with 1 µl of *EcoRI* (Invitrogen) and 2 µl of 10x reaction buffer REACT®3 (Invitrogen) and PCR grade water for a final volume of 20 µl. The mixture was incubated in water bath at 37°C for 1 hr. The reaction was stopped by adding 3 µl of loading buffer (New England BioLabs) and then was run on an agarose gel as described in 5.3.1.3 using a 1 kb ladder (New England BioLabs) to determine the sizes of the bands. Samples containing inserts of the appropriate size were then used for sequencing.

5.3.3.5 Plasmid sequencing

Plasmids were sent to Source Bioscience for sequencing. Fifteen positive plasmids of each gene were used for this purpose. One hundred microgram per microlitre of plasmid with 3.2 pml/µl of M13 Forward '5–GTAAAACGACGGCCAG–3' and M13 Reverse '5–CAGGAAACAGCTATGAC–3', which are supplied as a part of the TOPO–TA cloning system (Invitrogen), were used for sequencing. The sequence data was edited using Chromas Lite software and the area of differences determined using Geneious Inspirational Software for Biologists.

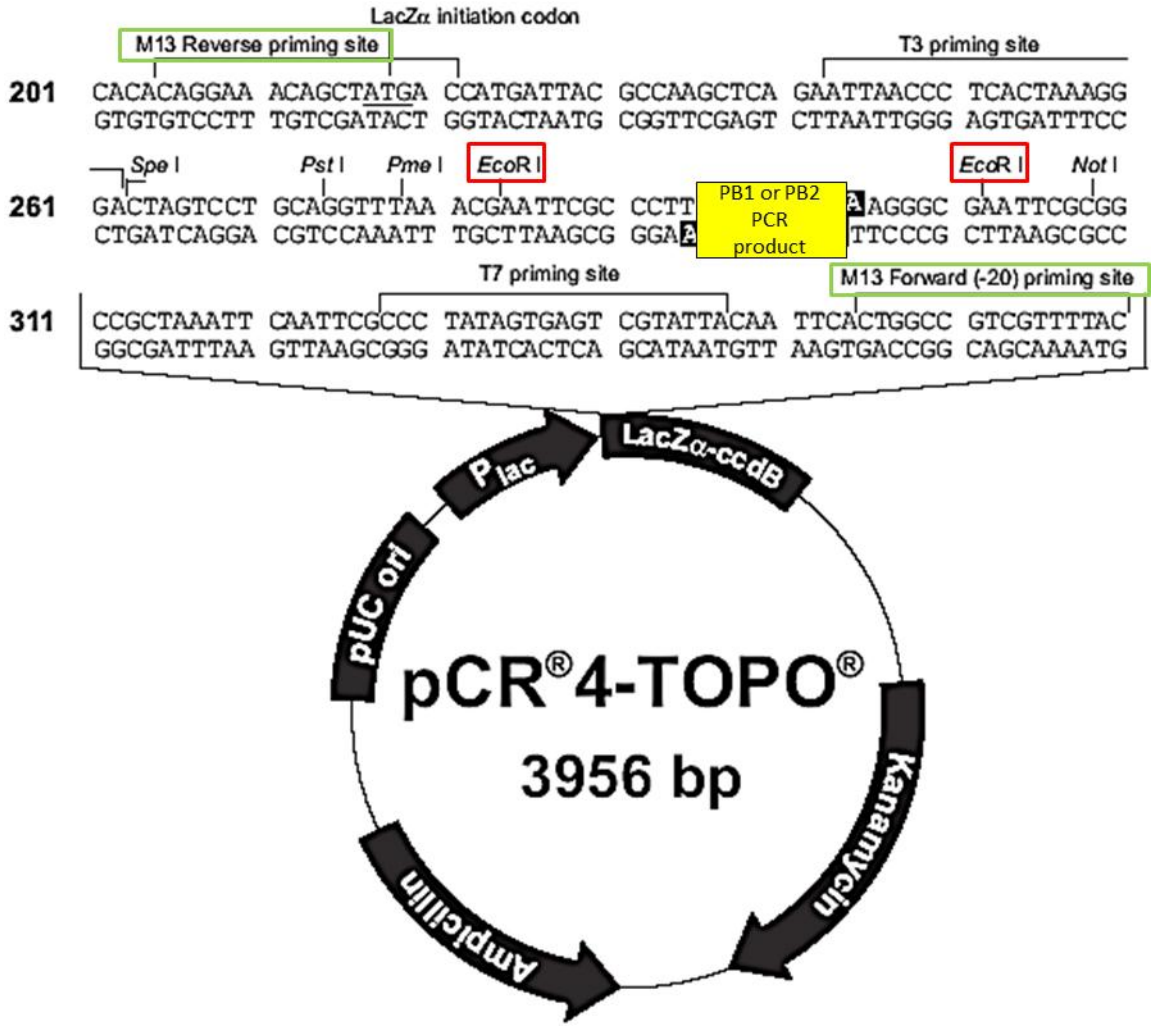

Figure 5.3–1 pCR™ 4–TOPO® vector map.

The map shows the features of pCR™ 4–TOPO® that was used for cloning and sequencing of influenza PB1 and PB2. After cloning the vector was digested at EcoRI restriction sites (red boxes) in order to confirm gene ligation onto the vector. Forward and reverse M13 priming sites (green boxes) were used for sequencing. The yellow box indicates the site where PB1 and PB2 were inserted.

5.4 Results

5.4.1 Gene amplification

All viral genes were successfully amplified by using one step RT–PCR. Genes were amplified using one or more sets of primers in order to cover the whole genome. All results showed single and clear bands following loading of 10 µl of the product stained with 1 µg/mL of Nancy–520. Figure 5.4–1, A and B shows the largest amplicons of all viral genes; product sizes were determined by comparison with 1 kb ladder. Figure 5.4–2 shows the small DNA amplicons which are located at the ends of viral genes, and the sizes were detected using 100 bp ladder.

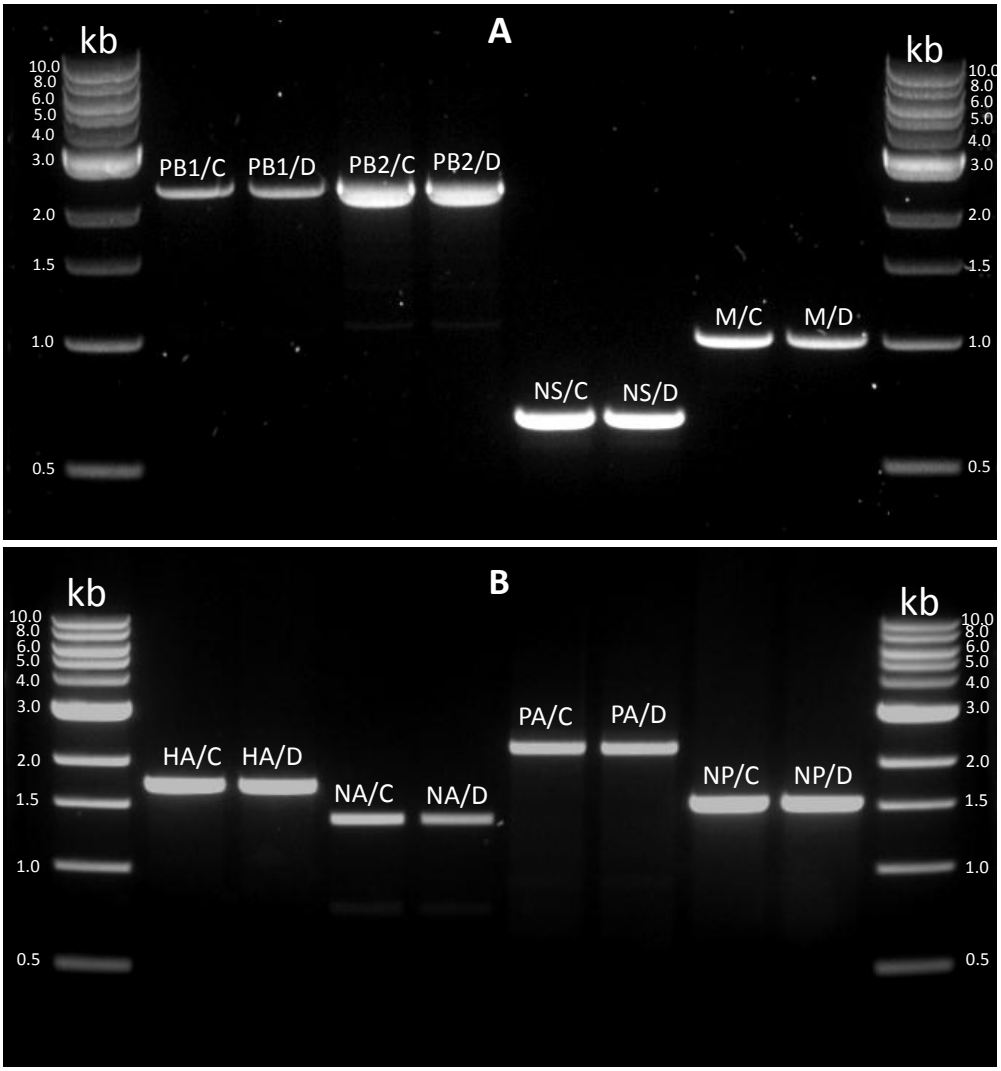

Figure 5.4–1 PCR products of large DNA amplicons of influenza virus visualized by Nancy–520 stained agarose gel electrophoresis.

The PCR products were separated using a 1% agarose gel pre–stained with 1 µg/mL Nancy–520. (A) Amplification of PB1, PB2, NS, and M genes from chicken and duck produced viruses /C and /D. (B) Amplification of HA, NA, PA, and NP genes from chicken and duck produced viruses /C and /D.

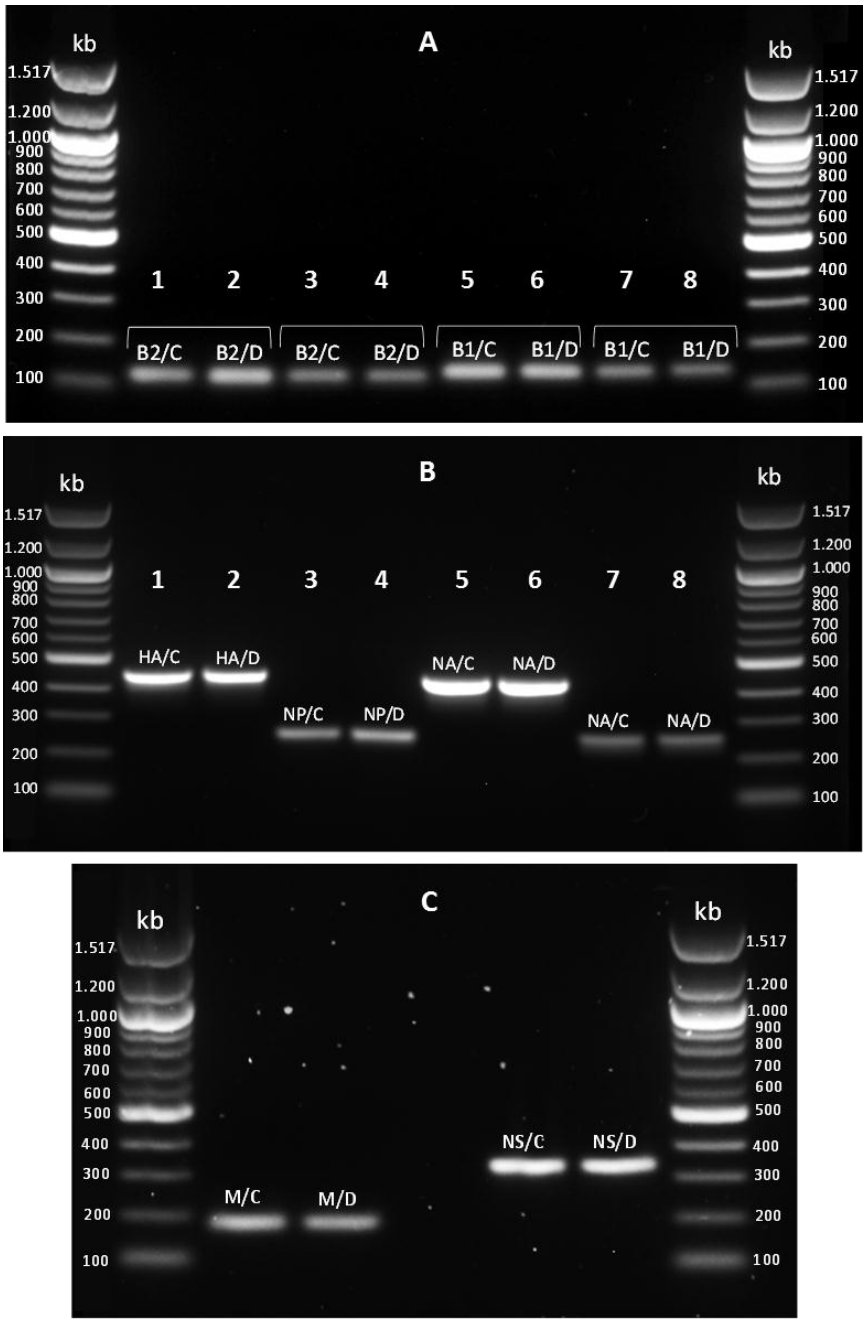

Figure 5.4–2 PCR products of small DNA amplicons of influenza virus following Nancy–520 stained agarose gel electrophoresis.

The PCR products were separated using 1% agarose gel pre–stained with 1 µg/mL Nancy–520. The genes were amplified from chicken and duck produced viruses (/C and /D). (A) Amplification at the 5´ and 3´ ends of PB2 and PB1. The bands represent amplicons located at the 5´ (1 and 2) and the 3´ ends (3 and 4) of PB2, and also the 5´ (5 and 6) and the 3´ ends (7 and 8) of PB1 of chicken and duck produced viruses (/C and /D). (B) Amplification of the 3´ end of HA (1 and 2), NP (3 and 4), NA (7 and 8) and also the 5´ end of NA (5 and 6) of chicken and duck produced viruses (/C and /D). (C) Amplification of the 3´ end of M (1 and 2) and NS (3 and 4) of chicken and duck produced viruses (/C and /D).

5.4.2 PCR sequencing

Compared with nucleotide sequences of the H2N3 virus (A/mallard duck/England/7277/06) that was used to infect chicken and duck fibroblasts, six of the viral genes (PA, HA, NA, M, NS, and NP) showed identical sequences between viruses produced from chicken and duck cells. The PB1 and PB2 nucleotide sequences from viruses grown on chicken and duck cells were aligned and compared with nucleotide sequence of the parent virus (A/mallard duck/England/7277/06). The alignment identified some nucleotide differences distributed throughout the gene sequence. However, all these differences were a consequence of non–specific amplification during PCR reaction rather than genuine mutations (Figure 5.4–3 and 5.4–4).

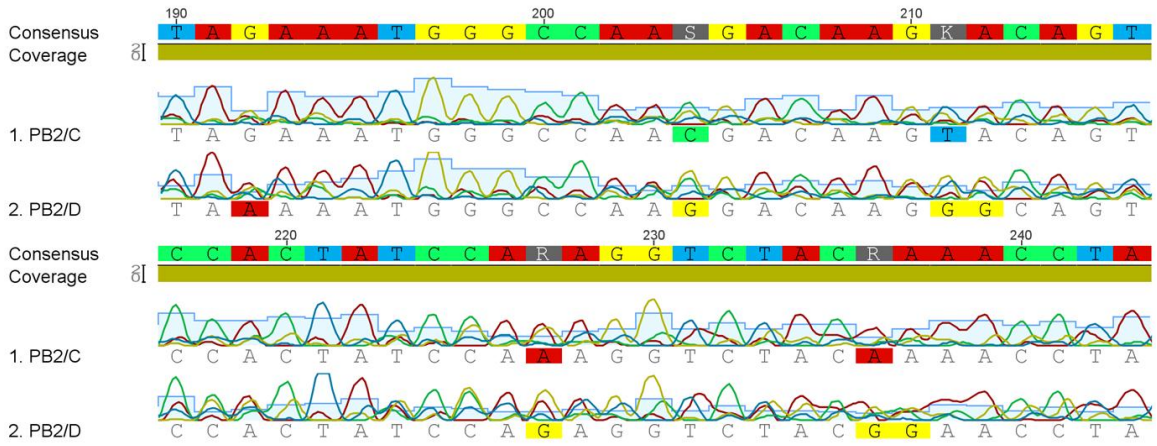

Figure 5.4–3 Polymerase basic 2 (PB2) gene alignments between chicken and duck cell grown viruses.

The figure shows a 54 nt region of the PB2 section alignment. Although, some nucleotide differences between the PB2 sequence of chicken and duck virus genes are seen, the traces show that these changes are a consequence of mixed sequence.

PB2/C: Polymerase basic 2 gene sequenced from H2N3 grown on chicken cells.

PB2/D: Polymerase basic 2 gene sequenced from H2N3 grown on duck cells.

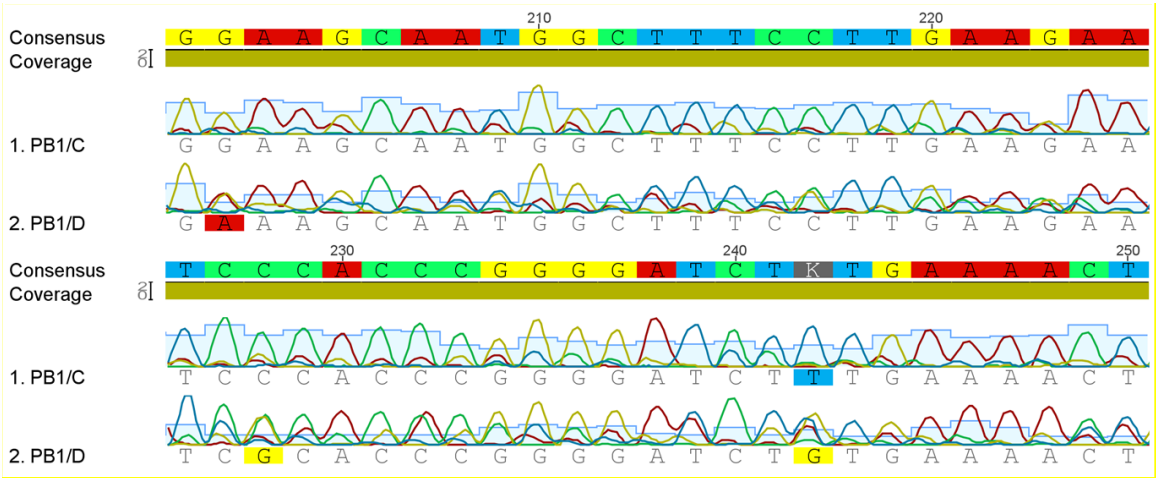

Figure 5.4–4 Polymerase basic 1 (PB1) gene alignments between chicken and duck cell grown viruses.

The figure shows a 50 nt region of the PB1 section alignment. Although, some nucleotide differences between the PB1 sequence of chicken and duck virus genes are seen, the traces show that these changes are a consequence of mixed sequence.

PB1/C: Polymerase basic 1 gene sequenced from H2N3 grown on chicken cells.

PB1/D: Polymerase basic 1 gene sequenced from H2N3 grown on duck cells.

5.4.3 Plasmid digestion

Ligation of PB1 and PB2 into pCR™ 4–TOPO vector was confirmed by digestion with the restriction enzyme EcoRI. Clones with inserts of the appropriate size were detected by loading samples on 1% agarose in TAE buffer pre–stained with Nancy–520 (Figure 5.4–5). A single band was observed for PB1, however it was slightly smaller than the expected size because of the presence of EcoRI target sequence at position 2030 of the PCR amplicon. Double bands were observed for PB2 indicating the presence of an EcoRI site within the viral sequence.

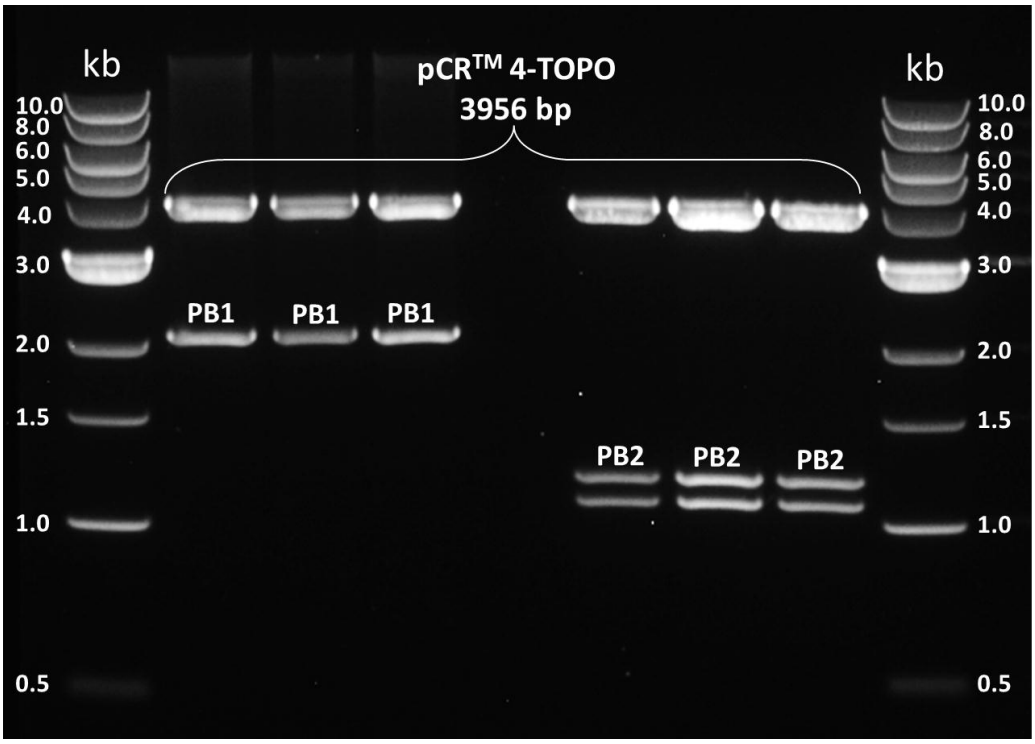

Figure 5.4–5 pCR™ 4–TOPO digestion.

Restriction digestion products were analysed on a 1% agarose gel in TAE buffer, pre–stained with 1 µg/mL Nancy–520, and the sizes of vector and digested products were measured by using 1 kb ladder. The plasmid was digested with EcoRI and the original size of the plasmid vector (3956 bp) is clearly shown following digestion. The PB1 inserts are shown with at about 2030 bp of 2274 bp (the original amplicon size) because of the presence of the target sequence of EcoRI at position 2030 of the amplicon, while the PB2 inserts show two bands of about 1100 and 1200 bp because of the presence of the target sequence for EcoRI in the middle of the PB2 amplicon.

5.4.4 Plasmid sequencing

Fifteen plasmids of the PB1 and PB2 inserted genes of both chicken and duck viruses were sequenced and aligned. The results showed very few nucleotide changes with a similar number in both chicken and duck genes. Alignment with the parent sequences obtained from viruses propagated in chicken eggs also showed no obvious difference except very few changes in some clones, which were more likely to be PCR–generated

mutations. These results confirmed that there was no fundamental difference between chicken and duck produced PB1 and PB2, and the few nucleotide differences that had been observed after PCR sequencing were due to the presence of non–specific PCR products within the sequencing reaction.

In addition, running the gel with 30 to 40 µl of PB1 and PB2 PCR products, non–specific bands are clearly observed in both reactions (Figure 5.4–6). Interestingly, the sizes of the non–specific bands correspond to the length of the genes observed in sequence chromatograms where multiple peaks were observed.

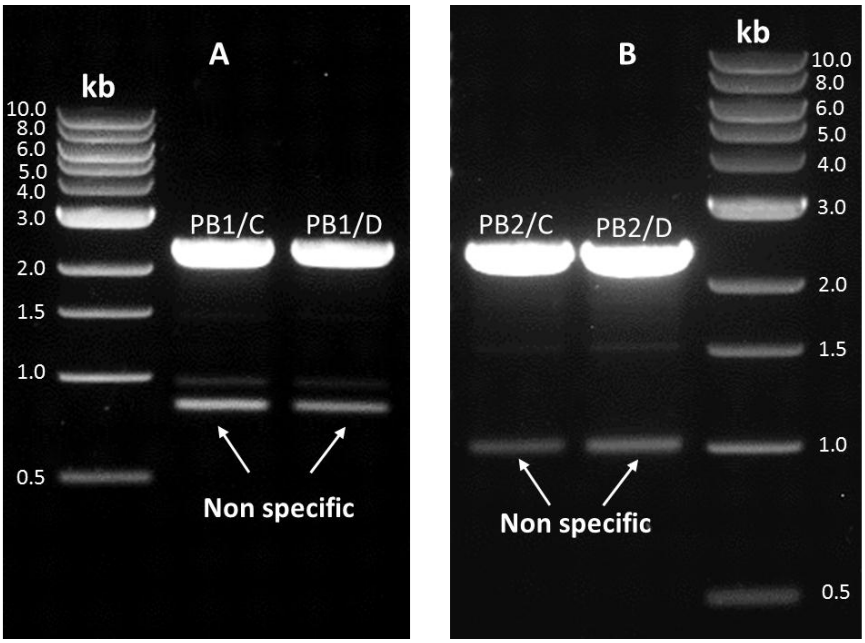

Figure 5.4–6 PCR product of PB1 and PB2 DNA amplicons visualized by Nancy–520 stained agarose gel electrophoresis.

Forty microlitres of the PCR products were separated using 1% agarose gel pre–stained with 1 µg/mL Nancy–520. Secondary bands (indicated by arrows) with similar sizes of the secondary sequences were clearly observed from both reactions. (A) Amplification of PB1 from chicken and duck produced viruses C and D. (B) Amplification of PB2 from chicken and duck produced viruses C and D.

5.5 Discussion

The nucleotide sequence of the influenza H2N3 produced in chicken and duck fibroblasts was analysed by direct sequencing, using the PCR product as a template. PB1 and PB2 sequences were confirmed by cloning of the viral genes into a vector, followed by sequencing. The overall results showed that there was no significant difference in the sequence of any of the viral genes produced from cells of the two host species.

The polymerase chain reaction (PCR) is widely used to amplify a specific region in the gene or the whole genome, to prepare products for DNA sequencing. The production of specific PCR product must be assessed by agarose electrophoresis before sequencing in order to ensure sequence specificity (Leonard et al., 1998). Detection of PCR results after applying 10 µl of the PCR products on Nancy–20–stained gel had shown single and clear bands for all the viral genes. Such a PCR product can be sequenced directly without the need for extracting bands from the gel. The initial sequencing results showed no difference in six of the virus genes (PA, HA, NP, NA, M, and NS) of viruses produced from chicken and duck cells, however, some differences were observed in PB1 and PB2 between the two host species.

There are many important factors affect virus infectivity. Mutations and deletions in any of virus genes may play a role in changing the protein structure and in eventually decreasing viral infectivity and changing the virus morphology. For example, changes in polymerase gene sequences may disrupt the functional polymerase protein and reduce viral RNA cap–snatching, endonuclease or polymerase function and consequently the infectivity of the virus (Boivin et al., 2010). In addition, deletions in the cytoplasmic tail of the M2 protein might inhibit the genome packaging and the production of infectious viruses (McCown and Pekosz, 2005). Furthermore, mutations in the M1 protein

(Burleigh et al., 2005) and deletions in the cytoplasmic tail of the HA and NA proteins (Jin et al., 1997) have been shown to play a substantial role in modulating virus morphology. These results showed that there were no mutations in any of these genes, suggesting that other factors play a role in decreasing virus infectivity in H2N3 virus derived from duck cells.

Minor nucleotide changes in influenza viruses can occur normally regardless of the type of host due to the lack of proofreading ability of the RNA polymerase, leading to incorrect ribonucleotide insertion during replication, which is termed 'antigenic drift'(Zambon, 1999). Therefore, viral polymerase plays an important role in the evolution and spread of the influenza A virus (Gabriel et al., 2013). However, no changes were detected after sequencing the whole genome of the virions. In addition, it has been shown that the amplification of DNA by thermostable polymerases using standard conditions produces errors of about 5.5×10^{-4} mutations per basepair (Spee et al., 1993). However, PCR–generated mutations are usually not detectable following sequencing of a PCR product directly. The reason for this is the presence of a large number of templates in the reaction and a mutation introduced in one PCR product in the first cycle of amplification will only be found in that one product out of thousands formed by the reaction. This means that the error is swamped by the majority of correct sequences in the PCR product and thus is not seen. As the reaction proceeds, the mutation is amplified, but so is the percentage of the non–mutated sequence at the same place in other templates. Hence, the error still only exists at a very low occurrence and is not detectable.

To conclude, according to these findings, it seems that the reduction of infectious virus production and the difference in the morphology between chicken and duck cell derived virions are most likely related to host cellular factors rather than viral genetic factors.

Further investigation is required to focus on the impact of the host cell in producing different levels of infectious viruses.

Chapter 6

Cellular factors influencing influenza virus morphology

6.1 Summary

In this chapter, virus budding and morphology were investigated by immunofluorescence. Madin Darby canine kidney (MDCK), chicken embryo fibroblast (CEF), and duck embryo fibroblast (DEF) cells were infected or mock infected with avian H2N3. A known filamentous equine influenza A H3N8 strain was used as a positive control. Cells were incubated for 8 hr in the absence or presence of 0.5 µg/mL or 5 µg/mL of cytochalasin D to inhibit actin. Following infection, cells were fixed with 4% paraformaldehyde and then stained with specific antiserum to detect viral HA antigen and with phalloidin to detect cellular actin. Following infecting cells with H2N3 in the presence or absence of actin inhibitor, MDCK and CEF cells produced spherical virions while DEF produced short filament particles. Following infecting the cells with H3N8 in the absence of an actin inhibitor, all produced filamentous viruses, and in the presence of the inhibitor, the majority of virions produced from MDCK and CEF cells were spherical while DEF cells were not markedly affected and still produced filamentous particles. These findings suggest that actin is not only the cellular factor that determines the differing morphology between viruses grown in CEF or DEF. According to a very recent published study, Microtubule–associated protein 1A/1B–light chain 3 (LC3) can play a role in the assembly of filamentous viruses. Therefore, cells were transfected with a green fluorescent protein (GFP) – LC3 expression vector and then infected or mock–infected with avian H2N3. Initial results showed that virus morphology changed from spherical to short filaments followed transfection of CEF cells with GFP–LC3. This suggests that autophagy which occurs more readily in duck cells than chicken cells might play a role in the production of filamentous virions. However, further confirmation, such as observing budding viruses under an electron microscope, is required.

6.2 Introduction

6.2.1 Host cell dependence of influenza virus morphology

The morphology of influenza virions varies considerably, ranging from spherical with a diameter of 80–120 nm to filamentous particles with a similar diameter but vastly elongated (up to 30 µm in length). They assemble and bud from the apical plasma membrane of infected epithelial cells (Nayak et al., 2004). The variation in virus morphology can be because of viral genetic factors such as differences in haemagglutinin (HA), neuraminidase (NA), matrix 1 and 2 (M1 and M2) proteins (Bourmakina and Garcia-Sastre, 2003). However, sequence analysis of viruses grown in chicken and duck embryo fibroblast cells did not reveal any gene changes that could explain the differences in morphology (Chapter 5). Host cell factors have been shown to play an important role in determining virus morphology, in particular, the filamentous form. Epithelial cells such as Madin Darby canine kidney (MDCK) cells tend to produce more filamentous particles than fibroblasts, and intact actin cytoskeleton is important for filamentous but not spherical particle formation (Roberts and Compans, 1998, Simpson-Holley et al., 2002). Actin is found inside the virions of some viruses such as the measles virus, but not in the influenza virus (Bohn et al., 1987). However, a previous study has demonstrated that both viral M1 and NP proteins interact with the actin cytoskeleton in influenza–infected MDCK cells (Avalos et al., 1997). The sensitivity of influenza filamentous virus budding to actin inhibitors such as cytochalasin D suggests that their formation depends on an intact actin cytoskeleton (Roberts and Compans, 1998). Furthermore, disruption of actin by different actin inhibitors leads to reorganization of HA, M1, and RNP proteins into annular cell–surface structures formed around a core of aggregated actin underlying the plasma membrane which results in the reduction of filamentous virion production (Simpson-Holley et al., 2002).

6.2.2 Immunofluorescence

Immunofluorescence is a histochemical laboratory staining technique that is performed to detect specific target antigens using fluorescently–labelled antibodies. It has been widely used both in clinical laboratories and scientific research. Antibodies used in this technique are tagged (labelled) with fluorescent dye such as Alexa fluor, fluorescein isothiocyanate (FITC) or tetramethyl rhodamine isothiocyanate (TRITC). They react with a specific antigen (directly or indirectly) forming an antigen–antibody complex, which is visualized using fluorescent microscopy. Some cellular components, however, can be detected using specific fluorescently–labelled compounds such as phalloidin to detect actin and 4',6–Diamidino–2–phenylindole (DAPI) to visualize the nucleus. These compounds can directly interact with the cellular components without the need of antibodies. The fluorescent signals can be quantified using an automated imaging instrument, flow cytometer, or array scanner.

Two main immunofluorescence methods have been documented: primary (direct) and secondary (indirect). The primary method uses a single fluorescent–tagged antibody that interacts directly with the antigen of interest, while the secondary method employs two antibodies; the primary antibody (unlabelled) which specifically binds to the target protein, and a secondary antibody (labelled), which recognizes the primary antibody and binds to it (Figure 6.2–1).

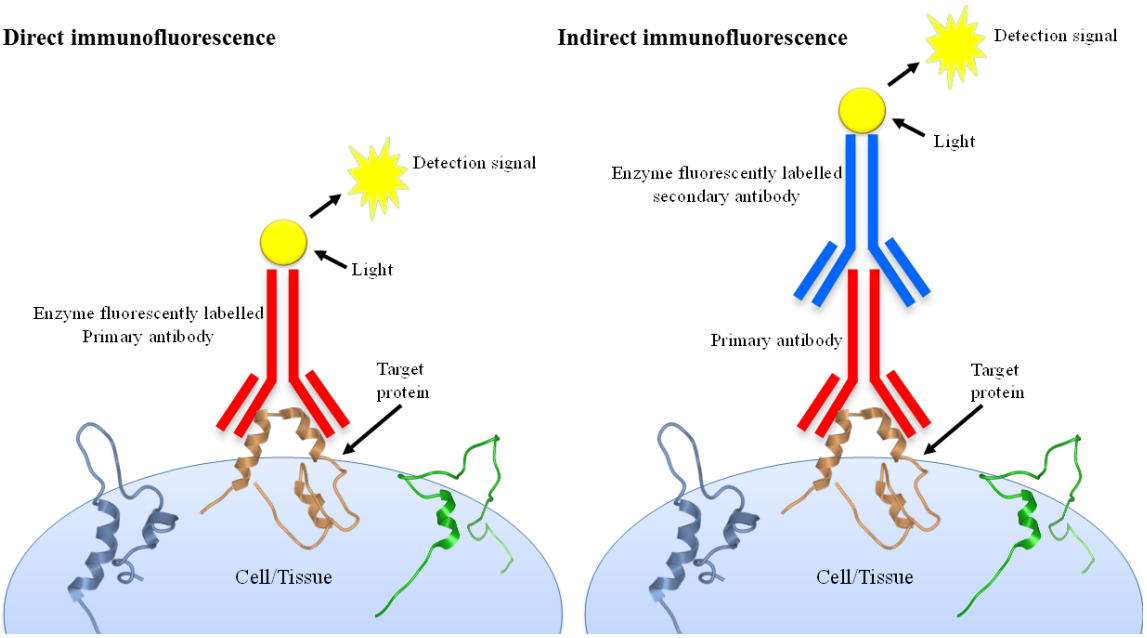

Figure 6.2–1 Schematic diagram of direct and indirect immunofluorescence.

Figure shows the mechanism of indirect (on the right) and direct (on the left) immunofluorescence. In the direct method, the primary antibody which binds to the target protein is conjugated with a fluorophore for detection by fluorescence. In the indirect method, a secondary labelled antibody with specificity against the primary antibody is employed to amplify the primary signal.

Although the direct process does not need a further step of adding labelled secondary antibody, the detection of signal may be difficult if the protein is found in small quantities. The main reason for this is because the signal is not amplified. In indirect detection, there is an amplification of the fluorescent signal as more than one labelled secondary antibody can attach to the primary antibody. Therefore, indirect immunofluorescence has been more frequently used in laboratory research because of greater sensitivity than direct immunofluorescence.

6.2.3 Immunofluorescence and influenza A virus

Immunofluorescence has been used for the detection of viral respiratory infection including influenza A virus (Blaskovic and Labzoffsky, 1973, Orstavik et al., 1984). Based on the diversity of influenza A virus surface antigens, the indirect immunofluorescence assay can be used for typing and subtyping of virus strains using specific monoclonal antibodies against surface glycoproteins, HA and NA (Johnson et al., 2012). In addition, indirect immunofluorescence can be used to detect filamentous virus budding from host cell surfaces using purified antiserum against haemagglutinin (Cox et al., 1980). Furthermore, the role of the host cell in determining the virion morphology, in particular the filamentous form, has also been observed using this technique (Roberts and Compans, 1998, Simpson-Holley et al., 2002).

6.2.4 Hypothesis

Cellular factors, for example actin, might be responsible for the morphological differences between influenza viruses grown in chicken and duck cells.

6.2.5 Aim and objectives

To study the role of host cell factors in determining virus morphology.

For this objective, chicken, duck, and MDCK cells were infected with filamentous and spherical virus strains (equine H3N8 and avian H2N3, respectively). Differences in morphology of progeny virions produced from all cells were observed via immunofluorescence microscopy, in the presence or absence of an actin inhibitor.

6.3 Materials and methods

6.3.1 Viruses

Two viral strains were used in this technique, with filamentous and spherical morphology. Influenza A/equine/Newmarket/5/03 (H3N8) was selected as a filamentous strain and avian influenza H2N3 A/mallard duck/England/7277/06 as a spherical strain. Viruses were grown in hen's eggs as described in 2.2.2.

6.3.2 Cells

Chicken and duck fibroblasts were extracted and grown following the procedure described in 2.2.3.1. MDCK cells were also used as a control and they were grown as described in 2.2.3.3.

6.3.3 Virus infection of cells

6.3.3.1 Actin disruption

MDCK, chicken and duck embryo fibroblast cells were grown on glass coverslips (19 mm in diameter) in 12–well plates in DMEM with 10% FCS and antibiotics, and then incubated at 37°C until confluent. The cells were then infected either with the filamentous virus strain (A/equine/Newmarket/5/03 (H3N8)) or with the spherical strain (A/mallard duck/England/7277/06 (H2N3)) in serum–free Ham's 12 containing 2% Ultroser G, 500 ng/mL TPCK trypsin and 1% antibiotics at a multiplicity of infection (MOI) of 1.0 for 2 hr. Control cells were incubated in serum–free Ham's 12 only. Cells

were then washed three times with PBS and fresh media was added either with cytochalasin D (5 µg/mL or 0.5 µg/mL) or without it, and further incubated for 6 hr at 37°C. They were washed three times with PBS, and incubated with 4% paraformaldehyde for 10 min, and then washed again three times with PBS. They were either kept in 4°C or processed directly for immunological staining.

6.3.3.2 LC3 transfection

Chicken and duck fibroblast cells were grown on glass coverslip (19 mm in diameter) in 12–well plates in 1 mL DMEM containing 10% FCS and antibiotics, and then incubated at 37°C until they reached 60 to 80% confluency. The medium was then removed and 1 mL of fresh media was added. In a sterile tube, 1 µg of human GFP–LC3 expression vector or GFP control vector (Cell Biolabs) was diluted in 100 µl of jetprime buffer (Polyplus transfection) and mixed by vortexing. Two microlitres of jetprime DNA transfection reagent (Polyplus transfection) were added and mixed. The mixture was spun down and incubated for 10 min at room temperature. One hundred microlitres of transfection mix were added to each well dropwise on to the cells. The plate was gently rocked back and forth and from side–to–side to distribute the complexes evenly. Two wells were left without any treatment as a control. The transfection medium was replaced after 4 hr by growth medium and the plate was then returned to the incubator. At about 40 hr after transfection, cells were infected or mock–infected with avian H2N3 (A/mallard duck/England/7277/06) in serum–free Ham's 12 containing 2% Ultroser G, 500 ng/mL TPCK trypsin and 1% antibiotics at MOI of 1.0 for 2 hr. Cells were then washed three times with PBS and fresh media, and further incubated for 6 hr at 37°C. They were washed and fixed as described above.

6.3.4 Immunological detection and imaging

Cells were first blocked with 1% bovine serum albumin (BSA, Fisher Scientific) in phosphate buffer saline (PBS) for 1 hr at room temperature. Blocking buffer was then carefully aspirated, and without washing, cells were incubated with 300 µl of primary antibodies (antibodies were typically diluted 1:500 in 1% BSA) specific to the H2 antigen (chicken H2N3 antiserum, a kind gift from Dr Ian Brown, Veterinary Laboratory Agency, UK) or specific to the H3 antigen (rabbit H3N8 antiserum, a kind gift from Dr Debra Elton, Animal Health Trust, UK) for 1 hr at room temperature. They were gently washed three times in PBS for 5 min each. Cells were then incubated in the dark for 1 hr at room temperature with a 300 µl of diluted secondary antibodies (either with goat anti–chicken or anti–rabbit IgG antibody, Invitrogen) which are labelled with green fluorescent Alexa Fluor® 488. After washing three times, cells were incubated in the dark for 1 hr with 300 µl of Alexa Fluor® 546 Phalloidin (Invitrogen) for actin staining. Cells were then washed three times with PBS, and the coverslips were removed from the wells using a combination of a curved end long needle and a pair of fine tweezers and placed facing up on a white paper towel for air drying. A spot of about 20 µl of Prolong® Gold Anti–Fade Reagent with 4',6–diamidino–2–phenylindole DAPI (Life technologies) was put on a clean glass slide; the cover slip was inverted facing down onto the mountant, and the mountant was allowed to fully spread. Coverslips were sealed by surrounding with clear nail varnish to stop the coverslip moving and prevent the cells drying out over time. They were kept at 4°C protected from light. Slides were viewed under Leica DM 5000B epifluorescence imaging system and cells were visualized and images were captured at high resolution.

For LC3–transfected cells, cells were blocked and incubated with antibodies specific for H2 antigen as described above. They were incubated in the dark for 1 hr at room

temperature with a 300 µl of diluted secondary antibody (goat anti chicken IgG antibody, Invitrogen) which is labelled with red fluorescent Alexa Fluor® 546 dye. They were washed three times with PBS, mounted with Prolong® Gold Anti–Fade Reagent with 4',6–diamidino–2–phenylindole DAPI (Life technologies), and viewed as described above.

6.4 Results

6.4.1 Virus morphology in the presence and absence of actin inhibitor

Surface HA and internal actin were examined by fluorescent microscopy. Photographs were taken in three steps, detection of viral HA (H2 or H3), actin imaging (disrupted or not disrupted), and then were merged with DAPI. Using 0.5 µg/mL of Cyt.D was sufficient to disrupt the actin without causing complete collapse of the actin cytoskeleton and rounding of the cells. The mock–infected cells showed very low levels of non–specific antibody binding of the HA–stained samples, with specific actin staining with phalloidin, in the presence or absence of cytochalasin D. The phalloidin–stained actin in untreated cells was distributed as a layer underlying the plasma membrane, while drug–treated cells showed loss of the cortical actin web which aggregated in clumps, distributed across the cell (Figures 6.4–1, 6.4–2, and 6.4–3).

In the absence of an actin inhibitor, all cells infected with H3N8 produced distinctive HA–stained filamentous structures on the cell surface which reached several microns in diameter and were distributed regularly on the cell surface. In the presence of the inhibitor, the MDCK and CEF cells produced spherical virions, while in the DEF cells, the virus morphology changed from filamentous to short filaments (Figures 6.4–4, 6.4–5,

and 6.4–6). Treatment of duck cells with a high dose of drug (5 µg/mL) showed rounding of the cells and actin collapse, although short filaments were still produced (Figure 6.3–7). Following infection of MDCK and CEF cells with H2N3, spherical virions were produced in the presence or absence of the drug with no obvious filamentous virus present. Following infection of DEF, striking short filaments were produced in the presence of the drug and elongated to pleomorphic structures were produced in the presence of 0.5 µg/ mL of the drug (Figures 6.4–8, 6.4–9 and 6.4–10). Following treatment of duck cells with a high dose of drug (5 µg/mL), some elongated virions were still produced from the cell surface (Figure 6.4–11).

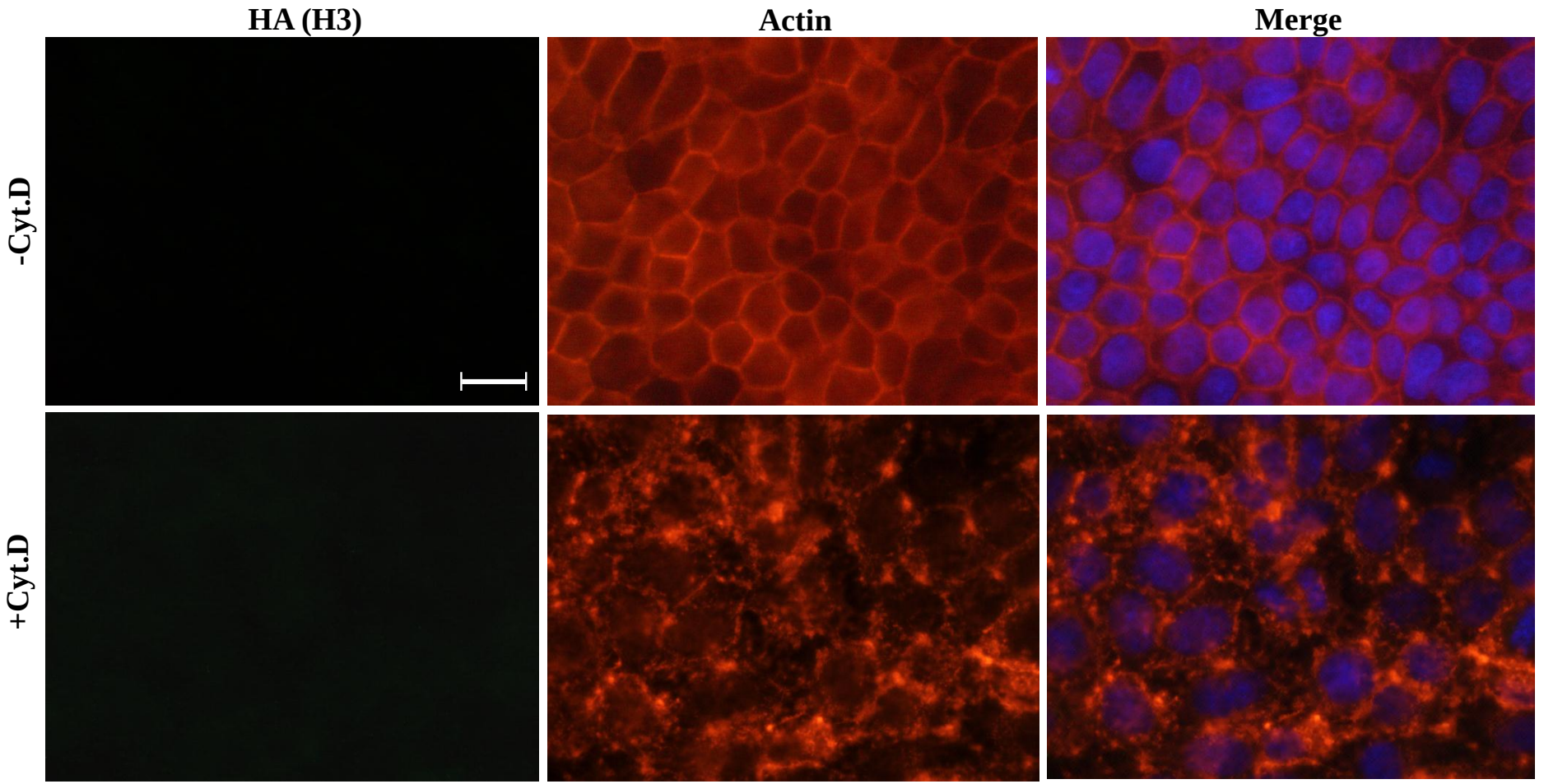

Figure 6.4–1 Effect of cytochalasin D treatment (0.5 µg/mL) on the actin of uninfected MDCK cells.

The cells were mock–infected and incubated for 8 hr with or without cytochalasin D (+Cyt.D and –Cyt.D, respectively), and stained for surface HA (green), actin (red–orange), and DNA (blue). Immunofluorescence photographs show a clear difference between the disrupted and non–disrupted actin. Scale bar 10 µm.

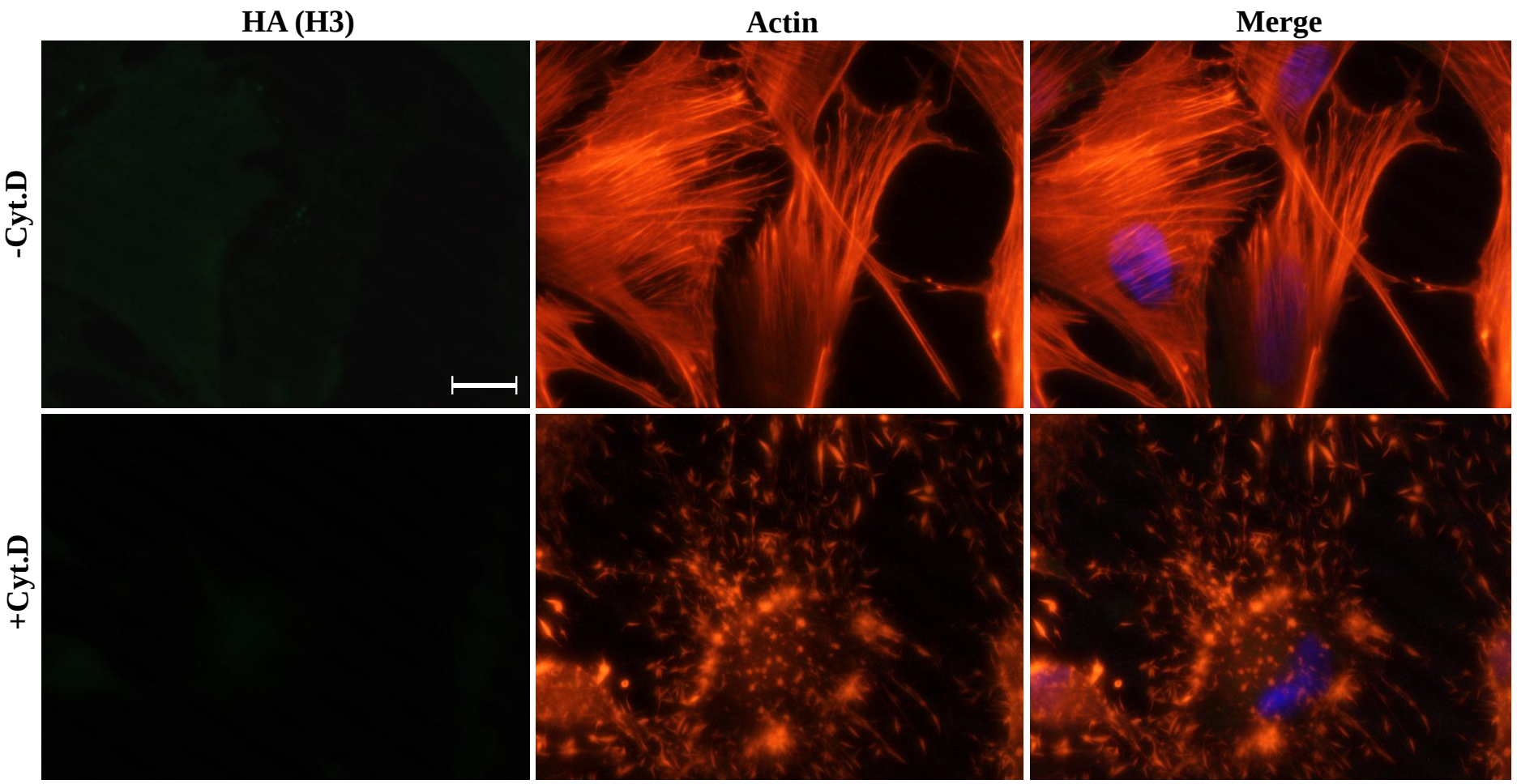

Figure 6.4–2 Effect of cytochalasin D treatment (0.5 µg/mL) on the actin of uninfected chicken embryo fibroblast cells.

The cells were mock–infected and incubated for 8 hr with or without cytochalasin D (+Cyt.D and –Cyt.D, respectively), and stained for surface HA (green), actin (red–orange), and DNA (blue). Immunofluorescence photographs show a clear difference between the disrupted and non–disrupted actin. Scale bar 10 µm.

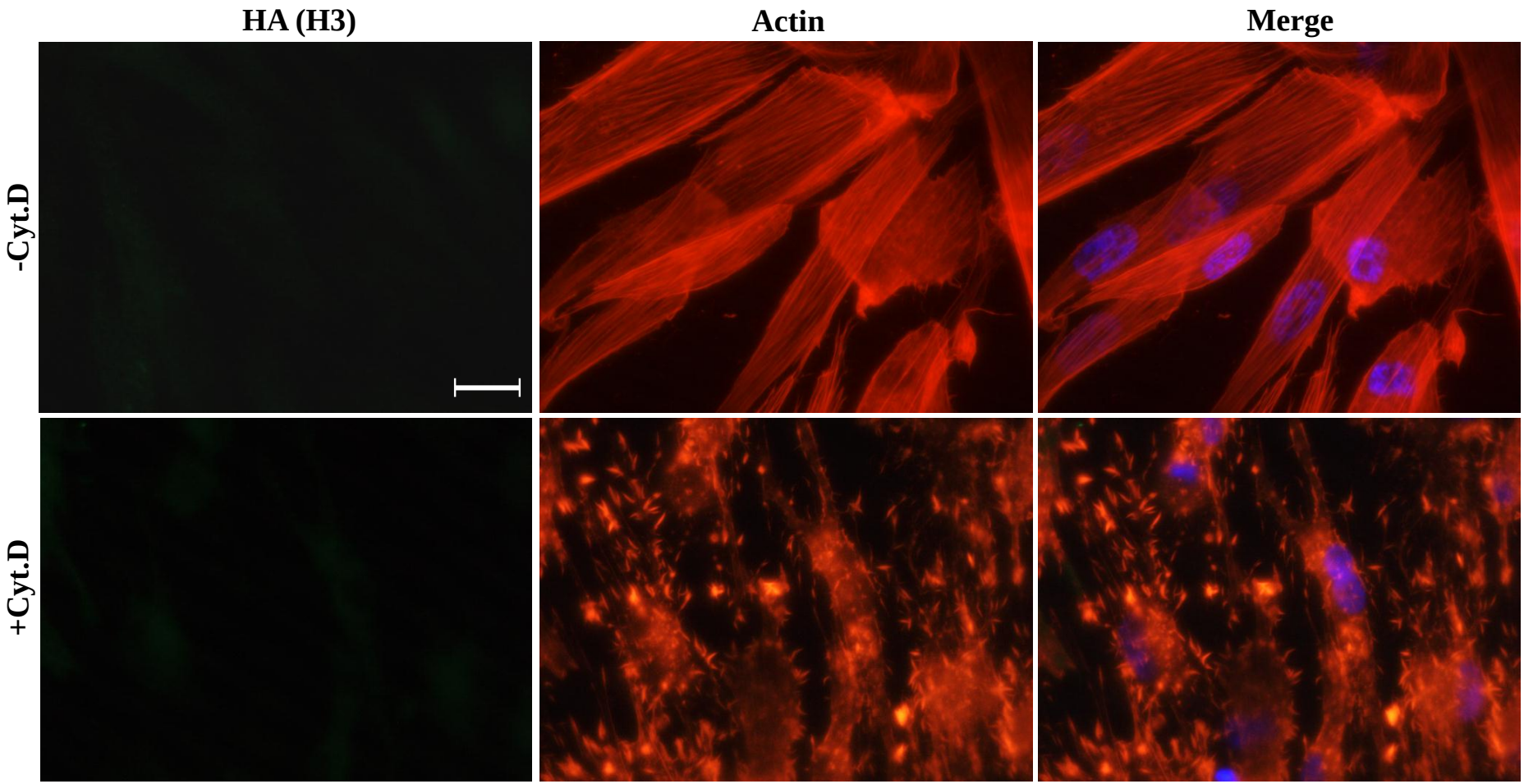

Figure 6.4–3 Effect of Cytochalasin D treatment (0.5 µg/mL) on the actin of uninfected duck embryo fibroblast cells.

The cells were mock–infected and incubated for 8 hr with or without cytochalasin D (+Cyt.D and –Cyt.D, respectively), and stained for surface HA (green), actin (red–orange), and DNA (blue). Immunofluorescence photographs show a clear difference between the disrupted and non–disrupted actin. Scale bar 10 µm.

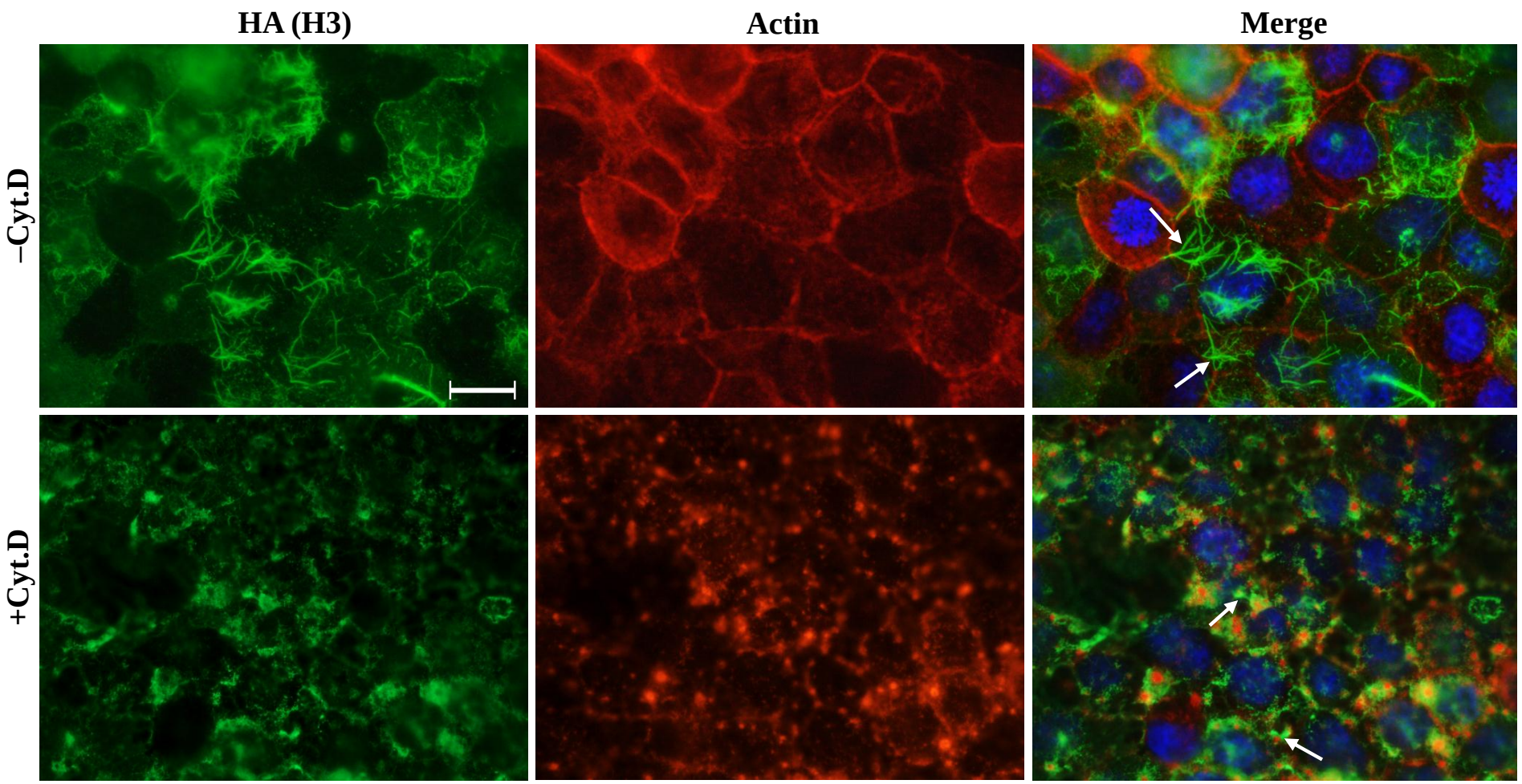

Figure 6.4–4 Differences in H3N8 morphology in MDCK cells either untreated or treated with 0.5 µg/mL of cytochalasin D. The cells were infected with the virus in the presence or absence of cytochalasin D (+Cyt.D and –Cyt.D) and stained for surface HA (green), actin (red–orange), and DNA (blue). Filamentous virions were observed on the surface of untreated cells, while spherical virions were observed following treatment (indicated by arrows). Scale bar 10 µm.

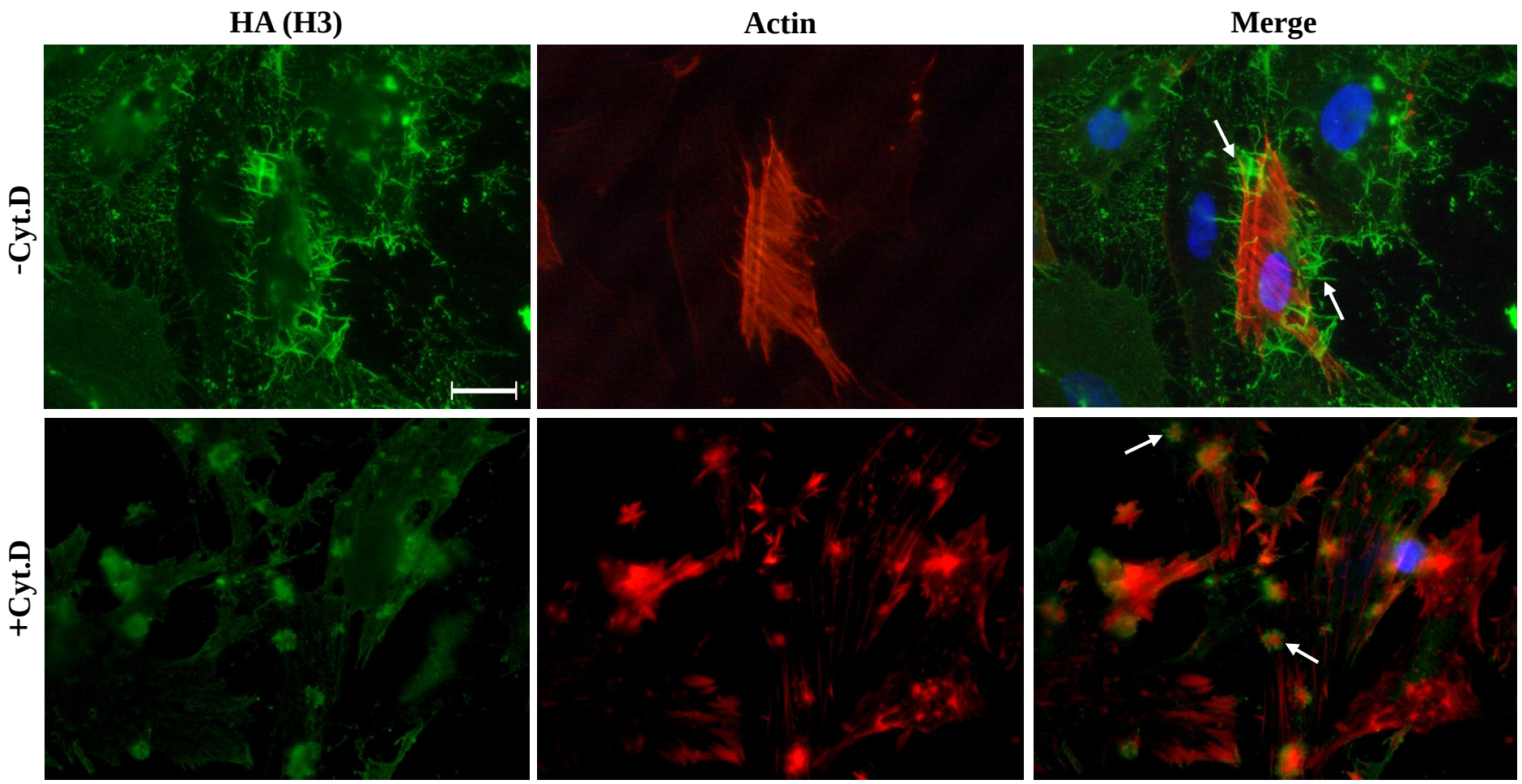

Figure 6.4–5 Differences in H3N8 morphology in chicken embryo fibroblast cells either untreated or treated with 0.5 µg/mL of cytochalasin D.

The cells were infected with the virus in the presence or absence of cytochalasin D (+Cyt.D and –Cyt.D) and stained for surface HA (green), actin (red–orange), and DNA (blue). Filamentous virions were observed on the surface of untreated cells, while significant reduction in filamentous form and increase the spherical virion production was observed following treatment (indicated by arrows). Scale bar 10 µm.

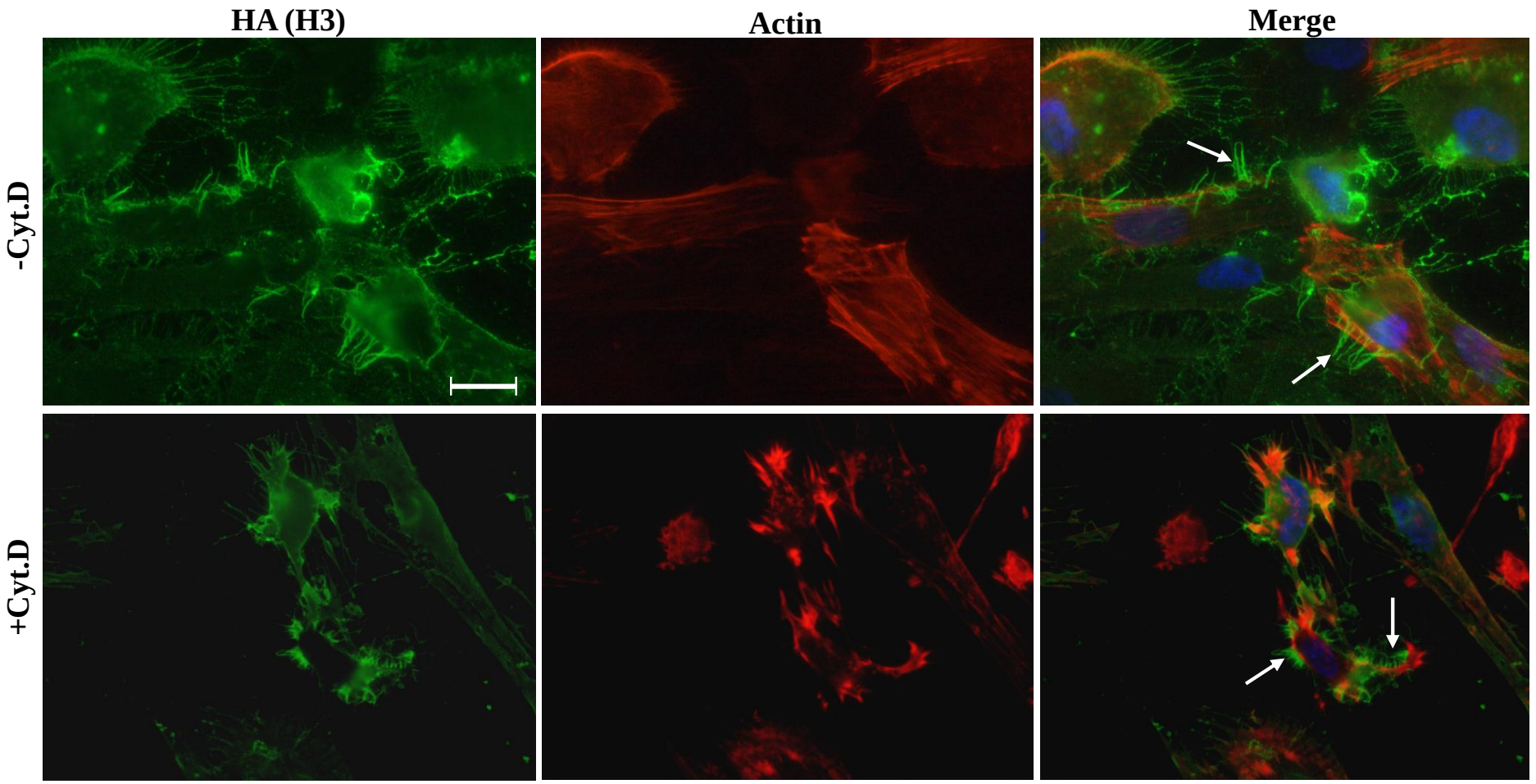

Figure 6.4–6 Differences in H3N8 morphology in duck embryo fibroblast cells either untreated or treated with 0.5 µg/mL of cytochalasin D. The cells were infected with the virus in the presence or absence of cytochalasin D (+Cyt.D and –Cyt.D) and stained for surface HA (green), actin (red–orange), and DNA (blue). Filamentous virions were observed on the surface of treated cells and short filaments were clearly noticed in untreated (indicated by arrows). Scale bar 10 µm.

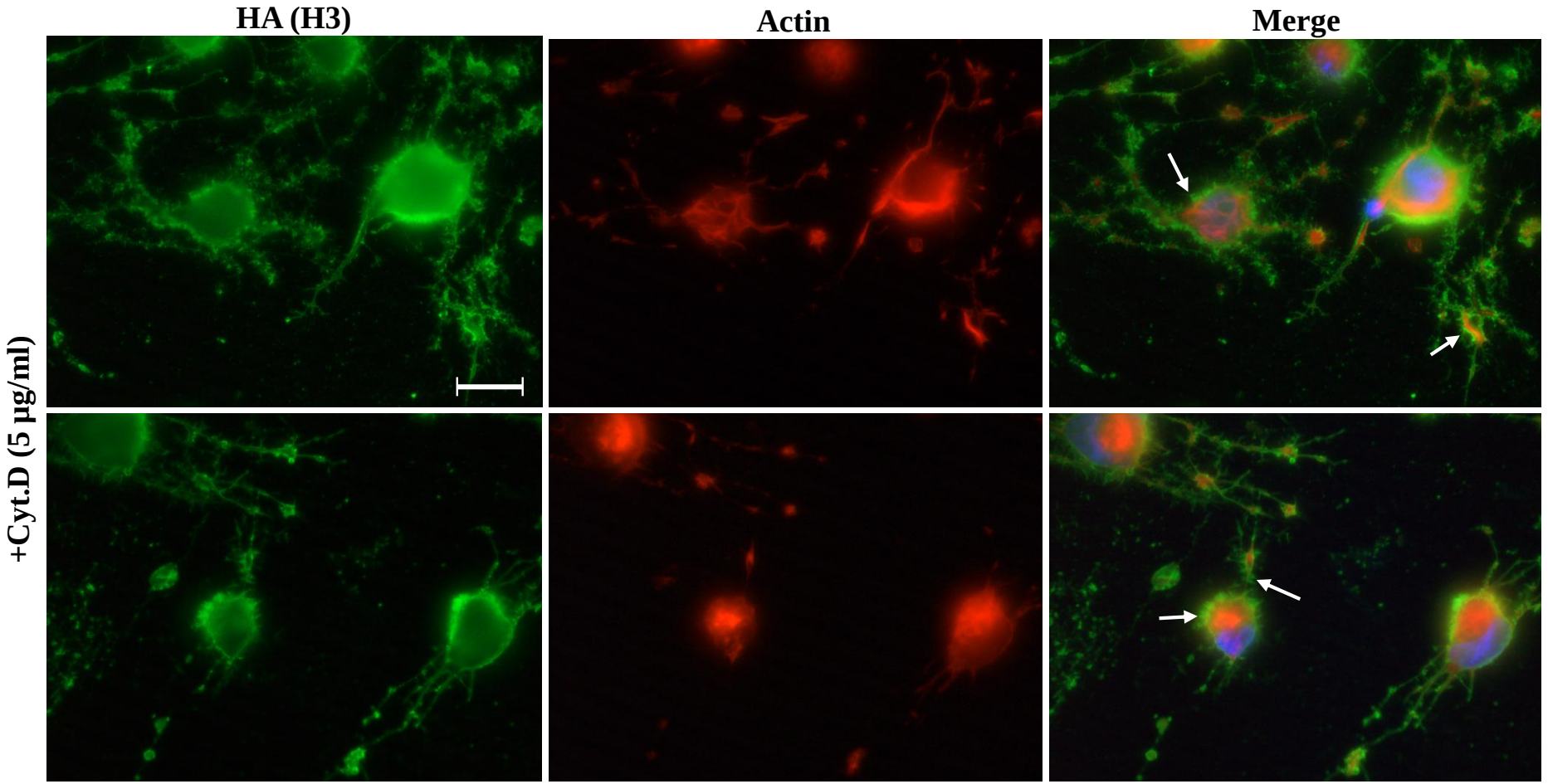

Figure 6.4–7 H3N8 morphology in duck embryo fibroblast cells treated with 5 µg/mL of cytochalasin D.

The cells were infected with the virus in the presence cytochalasin D (5 µg/mL) and stained for surface HA (green), actin (red–orange), and DNA (blue). Both elongated and short filament virions were appeared following infection of cells with the virus (indicated by arrows). Scale bar 10 µm.

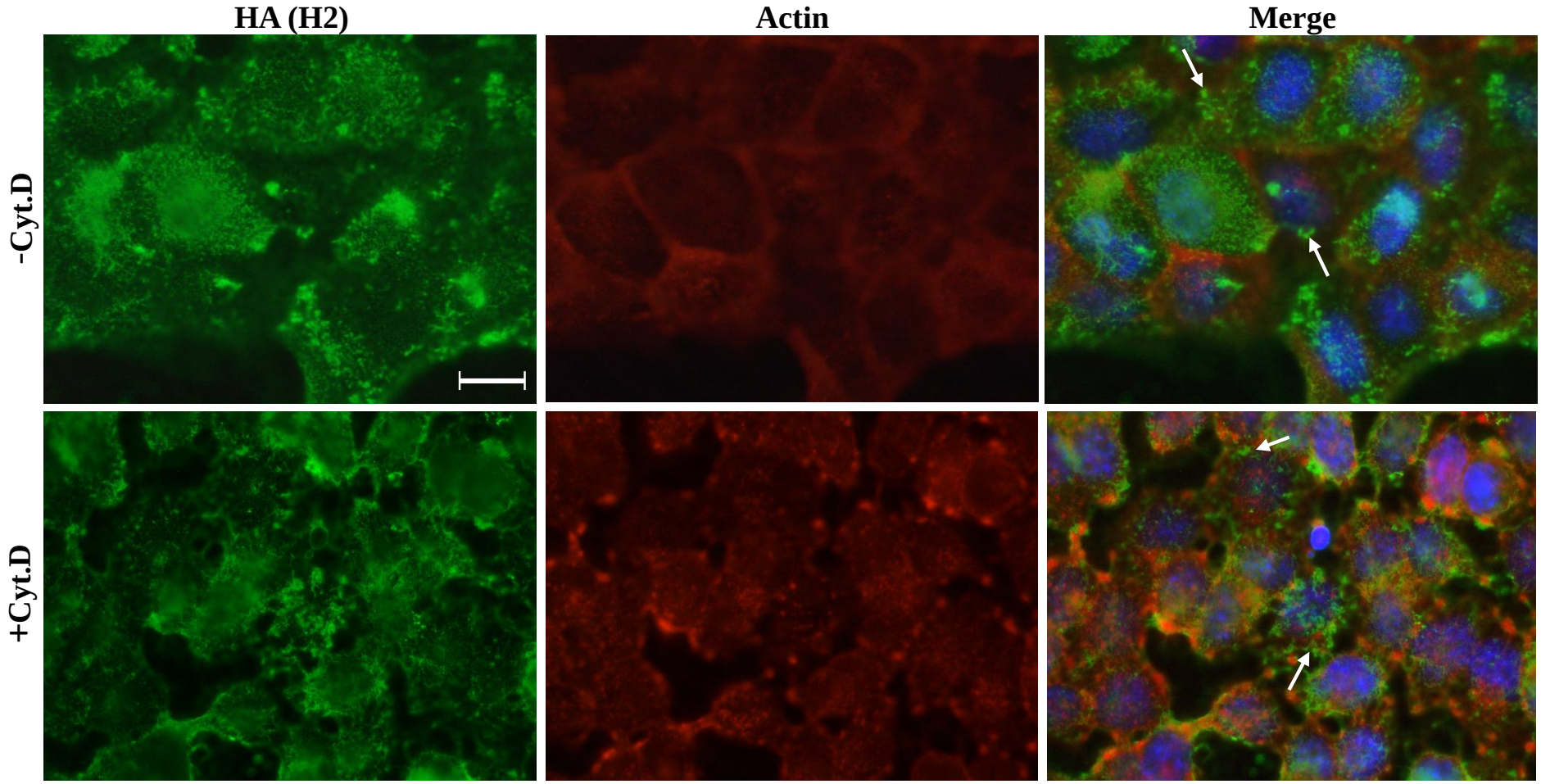

Figure 6.4–8 H2N3 morphology in untreated and treated MDCK cells with 0.5 µg/mL of cytochalasin D.

The cells were infected with the virus in the presence or absence of cytochalasin D (+Cyt.D and –Cyt.D) and stained for surface HA (green), actin (red–orange), and DNA (blue). Spherical virions were observed on the surface of treated and untreated cells (indicated by arrows). Scale bar 10 µm.

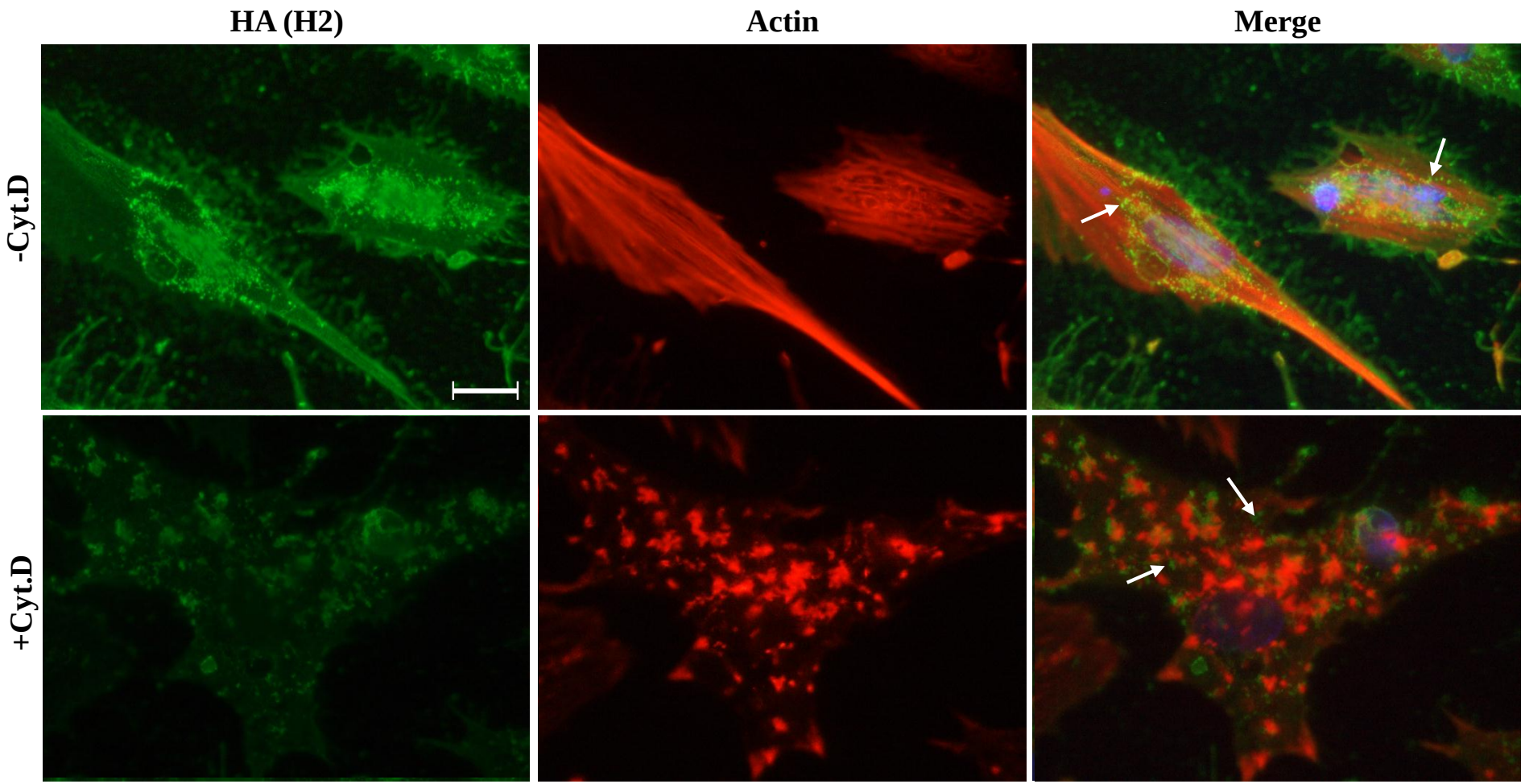

Figure 6.4–9 H2N3 morphology in untreated and treated chicken embryo fibroblast cells with 0.5 µg/mL of cytochalasin D.

The cells were infected with the virus in the presence or absence of cytochalasin D (+Cyt.D and –Cyt.D) and stained for surface HA (green), actin (red–orange), and DNA (blue). Spherical virions were observed on the surface of treated and untreated cells (indicated by arrows). Scale bar 10 µm.

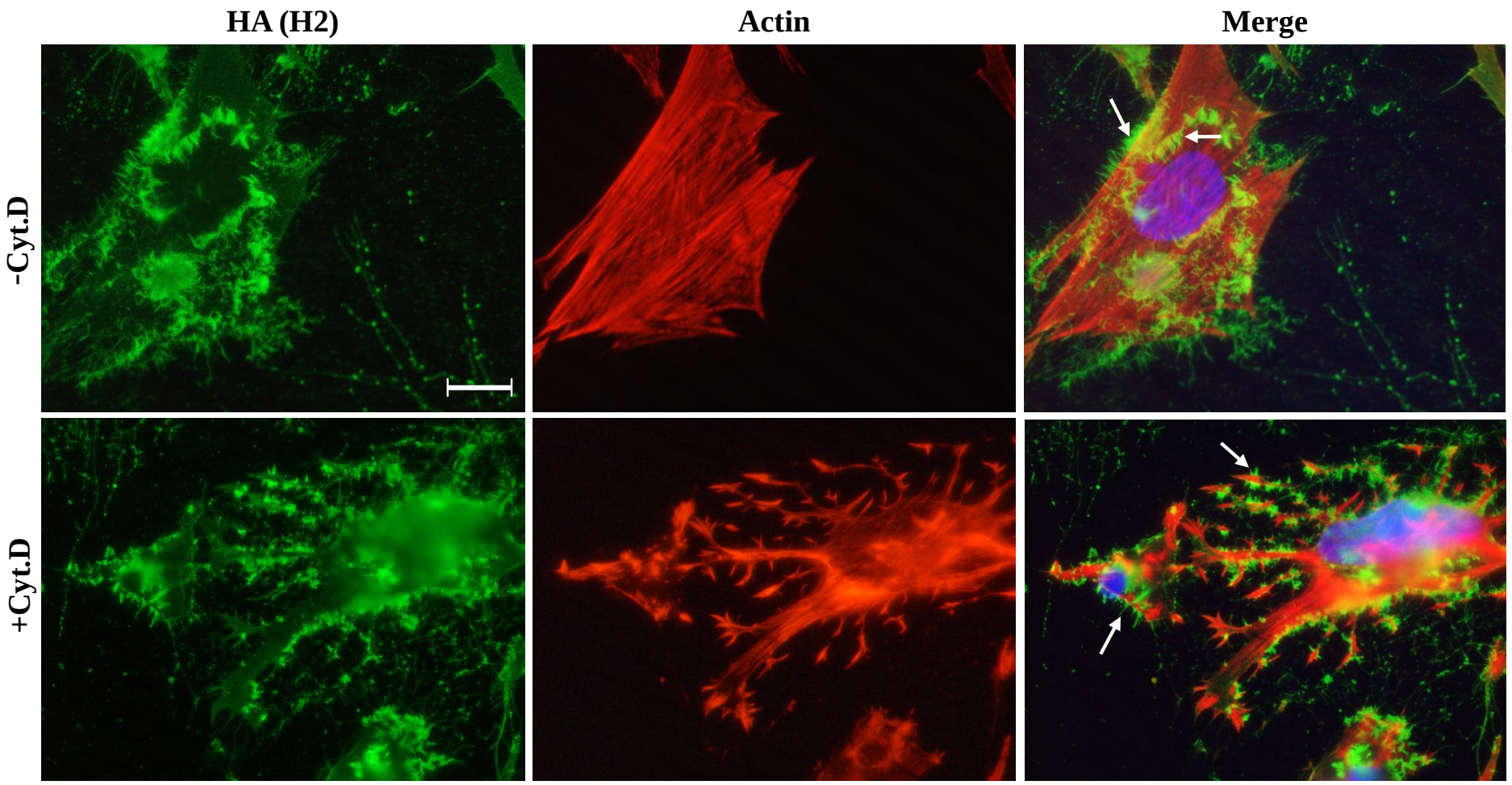

Figure 6.4–10 Differences in H2N3 morphology in untreated and treated duck embryo fibroblast cells with 0.5 µg/mL of cytochalasin D.

The cells were infected with the virus in the presence or absence of cytochalasin D (+Cyt.D and –Cyt.D) and stained for surface HA (green), actin (red–orange), and DNA (blue). Short filament and elongated virions appeared following infection of cells even after actin inhibition (indicated by arrows). Scale bar 10 µm.

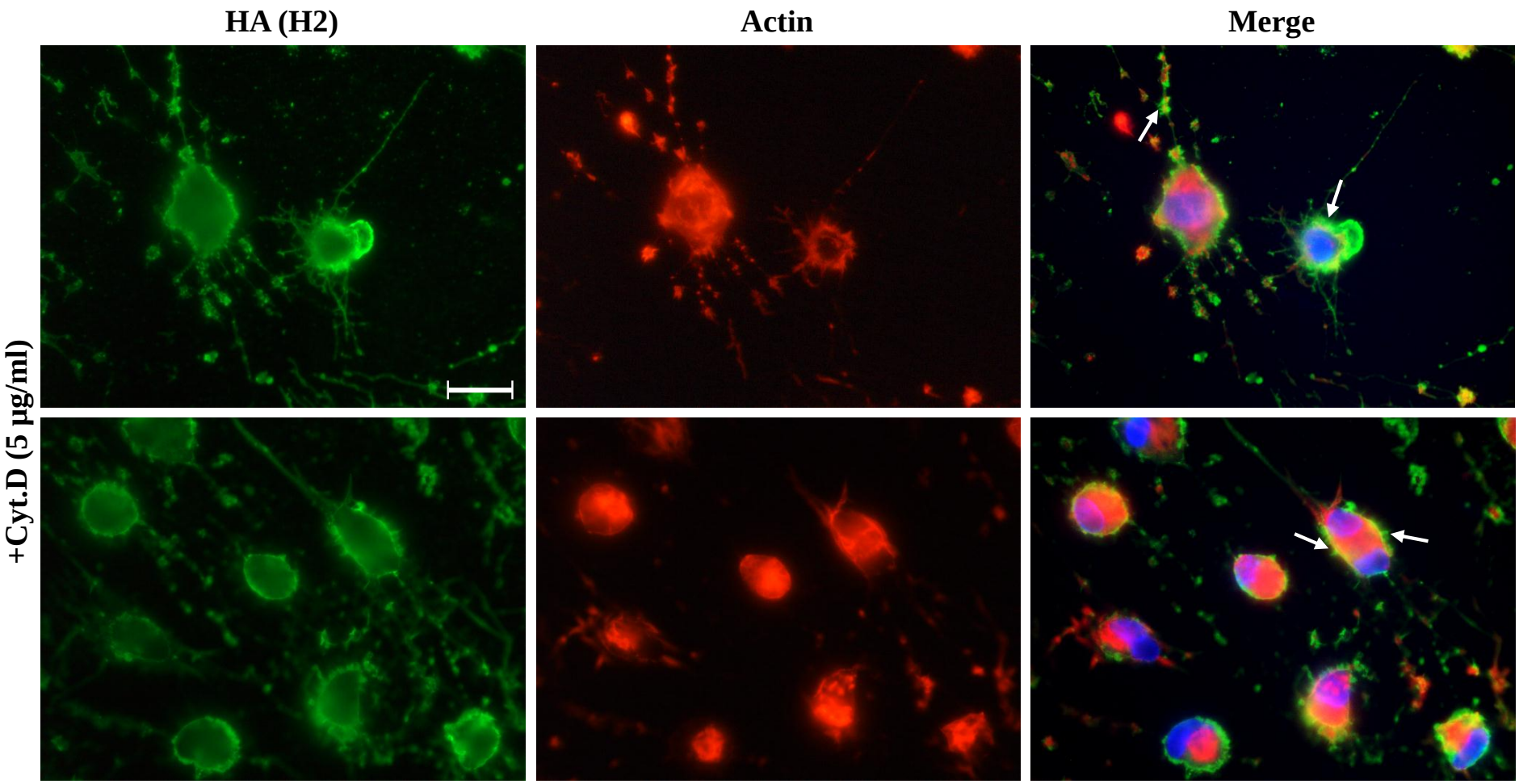

Figure 6.4–11 H2N3 morphology in treated duck embryo fibroblast cells with 5 µg/mL of cytochalasin D.

The cells were infected with the virus in the presence cytochalasin D (5 µg/mL) and stained for surface HA (green), actin (red–orange), and DNA (blue). Some elongated and pleomorphic virions also appeared following infection of cells (indicated by arrows). Scale bar 10 µm.

6.4.2 Virus morphology before and after transfection of cells with LC3

The viral HA antigen of viruses budding from the surface of chicken and duck cells was examined by immunofluorescence microscopy following the infection of cells transfected with GFP–LC3, or GFP alone as a control. Infected cells without any transfection were also examined. The results revealed that cells were transfected successfully before infection with virus (Figure 6.4.12), with some colocalization of LC3 in the perinuclear region and in the cell periphery following infection, particularly the infected chicken cells. The overall results showed a difference in virus shape before and after transfection of chicken cells with GFP–LC3. Viruses released from the untransfected chicken and duck cells were spherical and short filament, respectively, while short filaments were produced from both cells following transfection with GFP–LC3 (Figures 6.4.13, and 6.4.14).

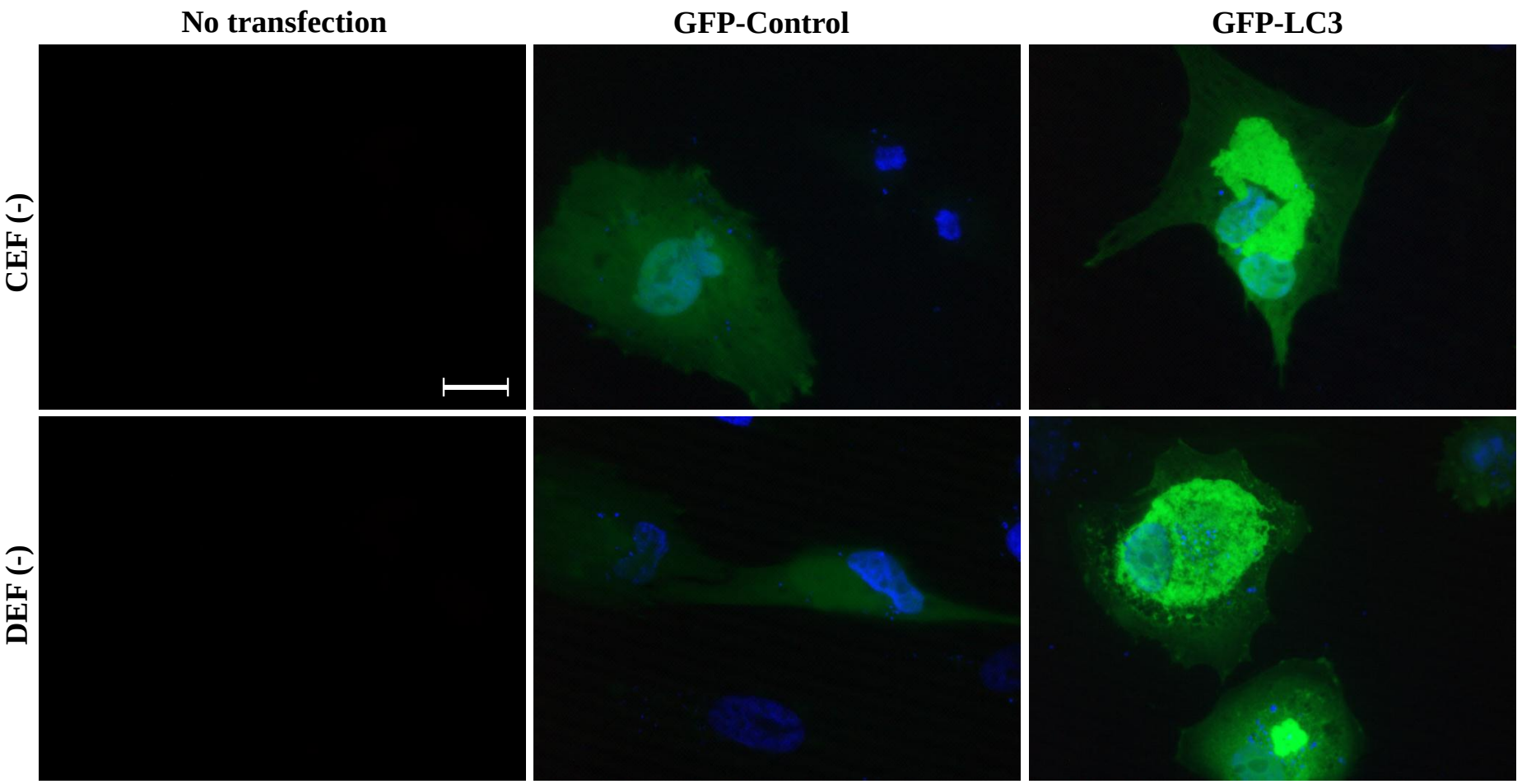

Figure 6.4.12 Transfection of uninfected chicken and duck fibroblasts with LC3 plasmid vector.

The figure shows the transfection of GFP–LC3 and GFP–Control 40 hr post transfection of the uninfected chicken and duck fibroblasts. There is a clear difference between cells transfected with GFP–LC3 and GFP–Control. Untransfected cells showed no colour. Scale bar 10 µm.

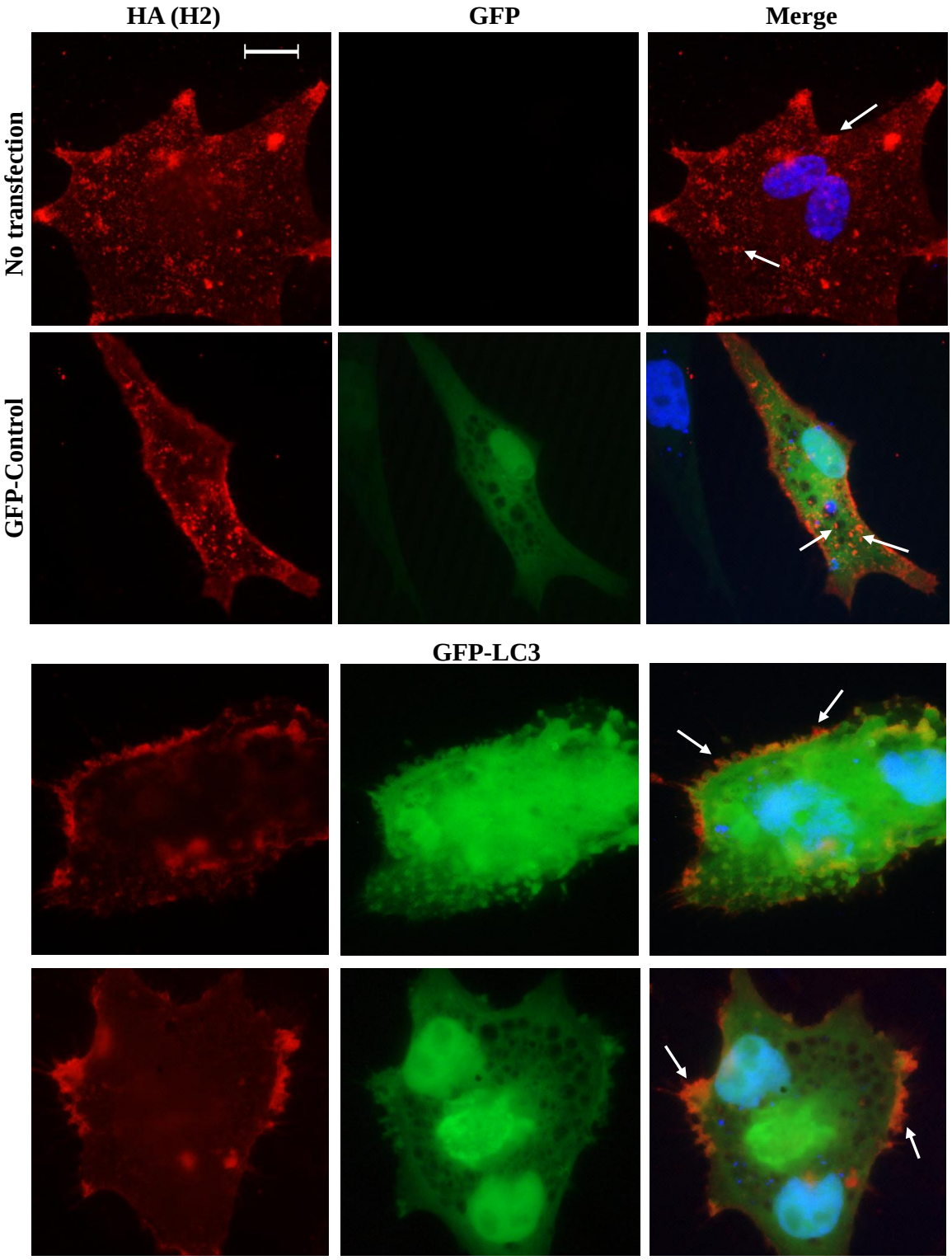

Figure 6.4.13 H2N3 morphology in GFP–LC3–transfected and untransfected chicken embryo fibroblasts. GFP–LC3 and GFP–Control transfected, and untransfected cells were infected with H2N3 for 8 hr and stained for surface HA (red) and DNA (blue), while the evidence of transfection appeared with green fluorescence. The virus morphology was detected by an immunofluorescence microscope. Spherical virions (red) were observed on the surface of untransfected cells, while short filaments were observed on the surface of transfected cells (indicated by arrows). Scale bar 10 µm.

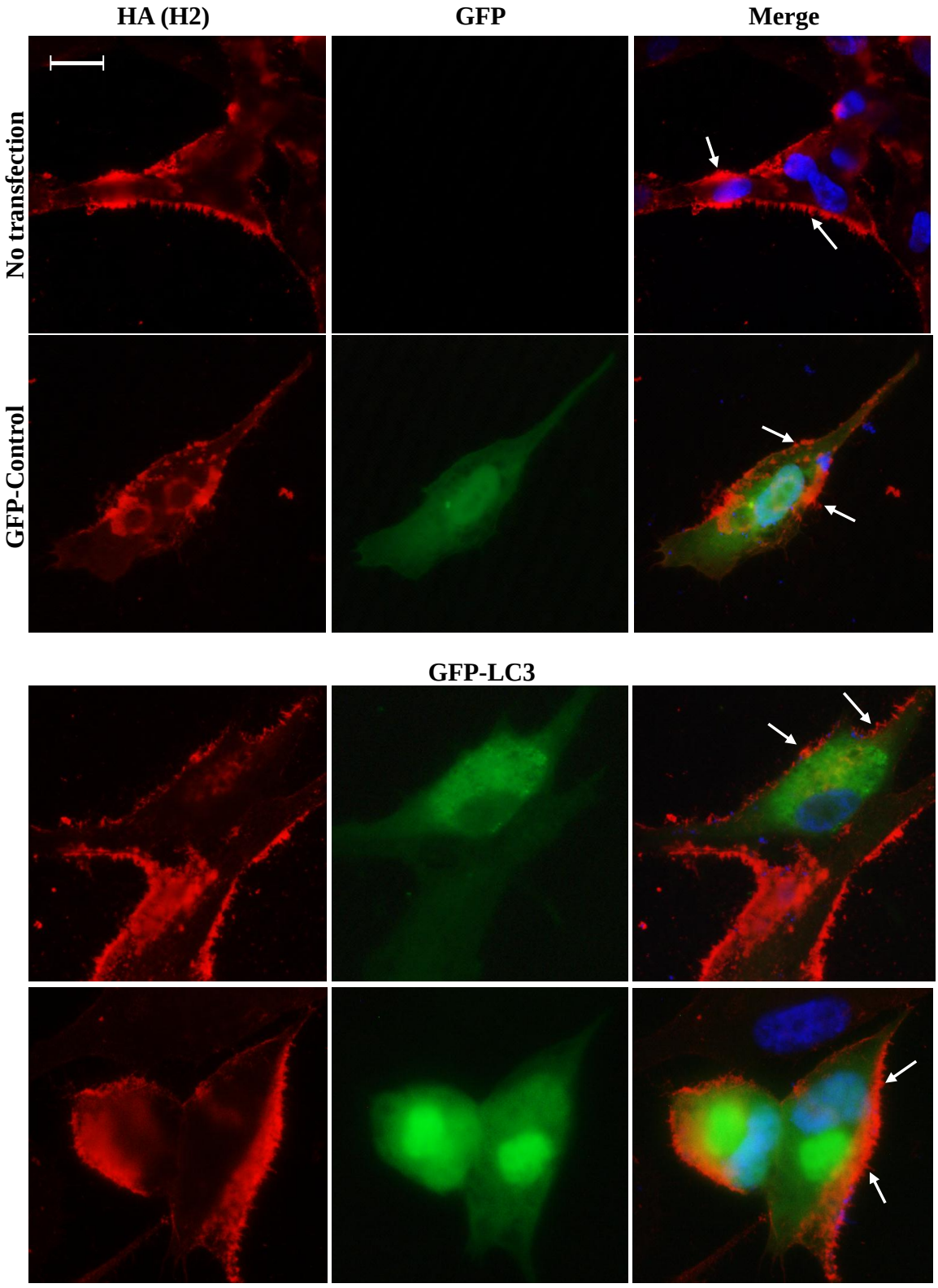

Figure 6.4.14 H2N3 morphology in GFP–LC3–transfected and untransfected duck embryo fibroblasts. GFP–LC3 and GFP–Control transfected, and untransfected cells were infected with H2N3 for 8 hr and stained for surface HA (red) and DNA (blue), while the evidence of transfection appeared with green fluorescence. The virus morphology was detected by an immunofluorescence microscope. Short filament or elongated virions (red) were observed on the surface of all cells (indicated by arrows). Scale bar 10 µm.

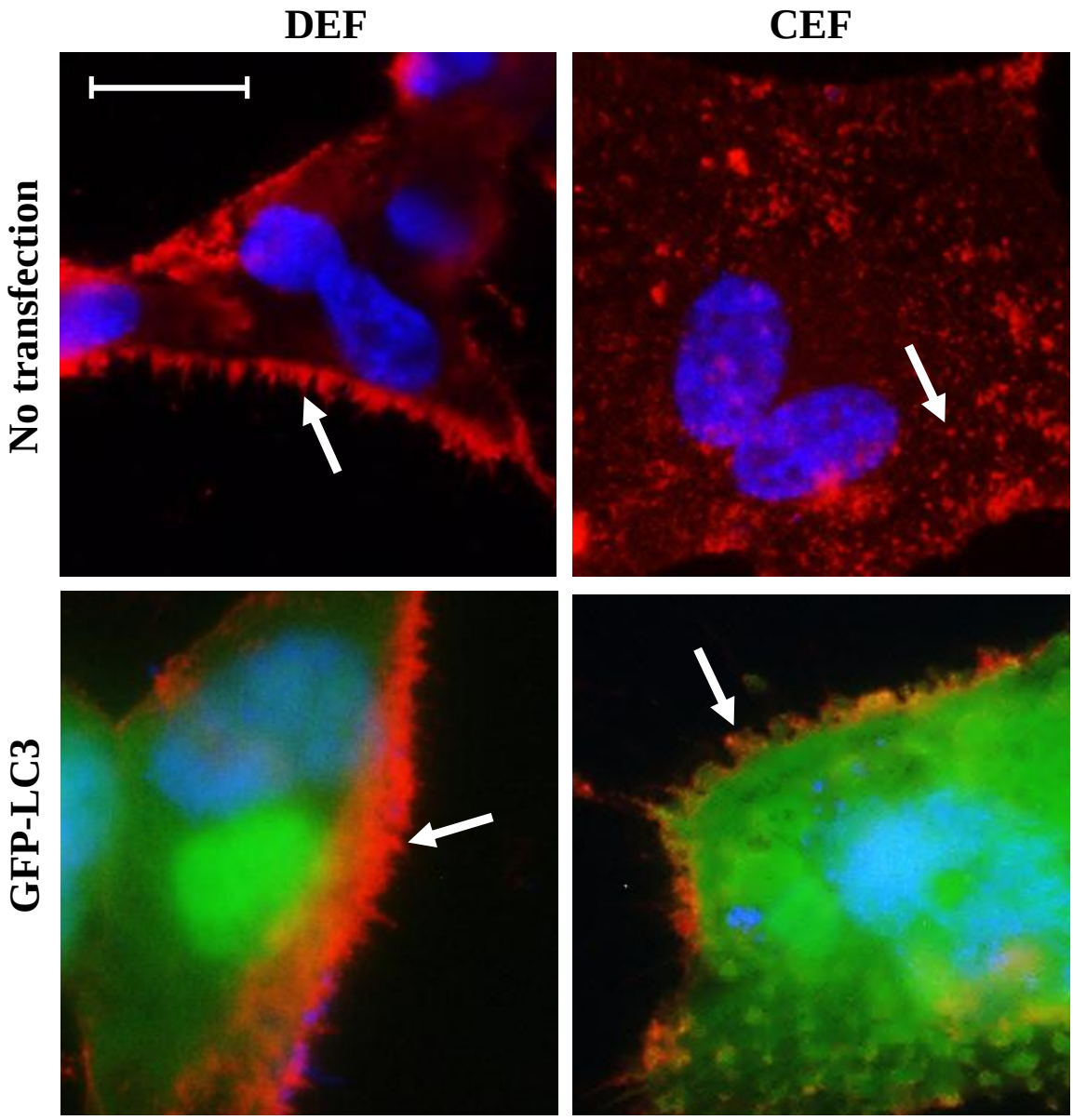

Figure 6.4.15 H2N3 morphology in GFP–LC3–transfected and untransfected chicken and duck embryo fibroblasts.

The figure shows a comparison between the morphology of H2N3 virions budding from chicken and duck fibroblasts at a high magnification. Untransfected and transfected duck cells with GFP–LC3 produce short filaments (indicated by arrows). Untransfected chicken cells produce spherical virions, while following transfection with GFP–LC3, the virus morphology shifted from spherical to short filaments (indicated by arrows). Scale bar 10 µm. DEF: duck embryo fibroblasts. CEF: chicken embryo fibroblasts.

6.5 Discussion

Differences in the morphology of influenza viruses budding from different hosts (CEF, DEF, and MDCK cells) were studied by immunofluorescence. Two virus strains were used to infect cells, spherical strain (avian H2N3) and filamentous strain (equine H3N8). The extensive production of filamentous particles by the equine influenza H3N8 strain was observed in all the infected cells. In contrast, short filament budding was restricted to DEF cells following infection with H2N3 strain, while chicken embryo fibroblasts and MDCK cells produced spherical virions, and filament formation was rarely seen. Although filamentous influenza virion assembly was proposed to depend on the actin cytoskeleton, based on their sensitivity to actin inhibitor, cytochalasin D (Roberts and Compans, 1998), duck embryo fibroblasts produced short filament virions, following infection with H3N8 and short filaments or elongated particles, following infection with H2N3, even after actin disruption.

The actin cytoskeleton has been shown to influence virus morphology. Cytochalasin D prevents actin polymerization via binding to the boarded ends of actin filaments and blocking the addition of soluble (G)–actin monomers (Schliwa, 1982). A previous study showed that cytochalasin D inhibits the production of the filamentous form of A/Udorn/72 (H3N2) virus, but not the spherical A/PR/8/34 (H1N1) virus suggesting that the assembly of filamentous particles requires an intact actin cytoskeleton (Roberts and Compans, 1998). In addition, Simpson–Holley et al. (2002) tested the effect of other actin inhibitors, jasplakinolide and latrunculin A following infecting cells with the filamentous strain A/Udorn/72 (H3N2) and the spherical strain A/PR/8/34 (H1N1). These drugs are mechanistically different inhibitors of actin. Jasplakinolide binds to F–actin and inhibits actin depolymerization (Bubb et al., 1994) and latrunculin A inhibits

actin polymerisation by sequestering G–actin monomers (Coue et al., 1987). These drugs have only been previously used to inhibit the actin cytoskeleton of MDCK cells and all were found to prevent the assembly of filamentous but not spherical virus particles. Although the use of a high dose of cytochalasin D (5 µg/mL) showed cell rounding and actin collapse, following the treatment of duck cells, short filaments were still produced, suggesting that the effect of the drug on virus morphology was not dose dependent. Using different actin inhibitors, in particular, jasplakinolide might produce a different form of disruption and might demonstrate a role for actin in changing virus shape.

Arcangeletti et al. (2008) investigated a clear difference in the fate of influenza virus infection using the same cell type from two different mammalian species, MDCK and Rhesus monkey kidney (LLC–MK2) epithelial cell lines. These cells were infected with human influenza A virus NWS/33 strain (H1N1) and the actin was disrupted using cytochalasin D. Treatment of LLC–MK2 with cytochalasin D following infection with the virus was shown to enhance virus progression and accumulation in the nuclear compartment which resulted in an increase in infection efficacy and yield of infectious virus at 24 hr post infection. On the other hand, treatment of MDCK cells with cytochalasin D had a detrimental effect on virus replication and reduced the delivery of NP to the nucleus which was accompanied by a significant decrease in virus titre at 24 hr post infection. Based on these findings, it seems that the actin cytoskeleton could play a role in the modulation of host permissiveness to viral infection; therefore, further study is required to determine the level of infectious virus produced from cells, following disruption of actin in infected CEF and DEF cells.

Following transfection of chicken cells with GFP–LC3, virus morphology shifted from spherical to short filaments. Macroautophagy, or self–eating, is considered an important defence process against influenza A infection. LC3 protein plays a critical role in

macroautophagy and is considered a suitable marker for this process (Zhou et al., 2009). However, viruses must evade autophagocytic degradation, so they can manipulate autophagy, via the interaction with LC3. This interaction is mediated by a highly conserved LC3 interacting region (LIR) motif in M2 which is required for the redistribution of LC3 to the plasma membrane in cells infected with influenza. The LC3–M2 LIR interaction supports the stability of the filamentous viruses, and mutations in M2 might inhibit LC3 interaction causing instability of virions (Beale et al., 2014). The current sequencing results showed that M2 protein sequence is identical between chicken and duck derived virions (Chapter 5). During autophagosome formation, LC3 I is converted to LC3 II. LC3–II has been shown to be rapidly upregulated in DEF cells, but only transiently upregulated in CEF cells following infection with H2N3 (Donna Fountain, personal communication). However, the higher levels of the LC3II protein could contribute to the formation of autophagosomes and eventually lyse the pathogens through lysosomes; this might support the release of filamentous particles in duck cells. The accumulation of LC3 at the cell periphery might represent the virus mobilizing lipid resources for virus budding (Beale et al., 2014). Protein colocalization was seen in the plasma membrane of the infected cells particularly chicken cells following transfection with GFP–LC3 plasmid. These preliminary results showed that virus shape changed from spherical to short filaments following transfection of chicken cells with LC3. Autophagy, which is more marked in infected duck cells than chicken cells following influenza infection (Donna Fountain, personal communication) could increase the production of filamentous virions. However, electron microscopy of infected cells is required for further confirmation of the initial observations using immunofluorescence, possibly using immunogold labelling to identify budding virions or LC3.

Chapter 7
General Discussion

7.1 General Discussion

One of the major determinants of influenza virus infection in the host is the presence of virus receptors on the host cell surface to which viral haemagglutinin can bind. Avian influenza A viruses bind to sialic acid (SA α 2,3–Gal) receptors (Connor et al., 1994). A recent study has shown that these receptors are distributed at a similar level in chicken and duck embryo fibroblasts (CEF and DEF) essentially giving them a similar affinity to infection with avian influenza viruses. Low pathogenic avian influenza (LPAI) H2N3 virus produces a comparable level of infection in both cell types (Kuchipudi, 2010). Accordingly, these cells were chosen to identify differences in the host–pathogen interaction and its impact on the nature of the virus. The aim of this research project was to elucidate the molecular and morphological differences of viruses produced from two different avian host cells, chicken and duck, following infection with low pathogenic avian influenza (LPAI) H2N3 virus. It has been shown that influenza A virus can infect a wide range of hosts, including wild and domestic birds and some mammals. Little is known about the role of the host cell type in producing different level of infectious viruses and different virus morphology following infection with the same virus strain.

It was previously reported that rapid cell death in duck cells following infection with H2N3 virus was accompanied by a reduction in the production of infectious virions but not viral RNA (Kuchipudi et al., 2011). The viral output was tested by measuring the matrix (M) gene copy number using absolute quantitative real–time PCR. This investigation may not be adequate to understand the reason behind the variation in infectious virus production between chicken and duck fibroblasts. Therefore, further techniques were employed to investigate the possible differences in the structure of viruses produced from chicken and duck cells. In the first part of this thesis, infectious virus production was extensively studied by the detection at different time points 2, 4, 6,

8, 24, and 48 hr post infection. The viruses collected from two of these time points (8 and 24 hr post infection) were used to detect the matrix protein expression of viruses produced from chicken and duck cells. These time points were selected as representative of the significant and non–significant differences in infectious virus production from chicken and duck cells.

The major part of this study was to determine the differences in virus morphology. Chicken and duck cells infected with the virus were observed by electron microscopy (EM), to determine the difference in virus morphology budding from those cells. Culture supernatants collected from chicken and duck cells infected with the virus were also observed under an electron microscope and a clear difference in virus morphology was detected. All viral genes of viruses produced from chicken and duck cells were sequenced and aligned to study the impact of any possible change in gene sequences on modulation of virus morphology and reduction in the virus titre. The role of the host cell in determining virus morphology was also studied using different virus strains (filamentous and non–filamentous) and different cell types (fibroblasts and MDCK cells).

The production of fewer infective viruses from the infected duck cells at 24 and 48 hr post infection might be the result of rapid cell death, which is an important marker induced following infection of duck cells with influenza viruses (Kuchipudi et al., 2011). However, influenza matrix gene copy number measurement by RT–PCR of viral RNA and protein expression measurement by western blotting of culture supernatants were similar between chicken and duck derived virions at this time point. The level of expression of the other genes and proteins is still unknown. The matrix protein of influenza A virus has been shown to play a major role in mediating budding of virus–like particles (VLPs), which are non–infectious and non–replicating particles. The expression

of M1 protein alone is sufficient to drive the formation of spikeless virus–like particles, which can be released from the surface of the infected fibroblast–like COS–1 African green monkey kidney cells (Gomez-Puertas et al., 2000). In addition, Latham and Galarza (2001) have reported that VLPs can be assembled and released from the surface of sf9 insect cells following expression of only four viral proteins, HA, NA, M1, and M2. The VLPs were very similar to the size and morphology of influenza virions and contained the fine structure of the surface spikes. Therefore, in future, measuring the level of all viral proteins derived from the two host species is strongly recommended. Furthermore, identification of the types and levels of incorporated cellular proteins in purified virions derived from both hosts also needs to be addressed.

To highlight the expected difference in virus assembly from chicken and duck fibroblasts, EM was employed to observe virus budding from those cells and also examine viruses from culture supernatants. Interestingly, there was a clear difference in the morphology of budding viruses with longer and pleomorphic viruses seen from duck cells in comparison with chicken cells which produced spherical virions. It is well known that influenza virus morphology can be affected by different factors. Sample preparation processes might result in the production of pleomorphic structures (Choppin et al., 1961, Sugita et al., 2011). Further, genetic factors represented by changes in M1, M2, and NA amino acid sequence (Bourmakina and Garcia-Sastre, 2003, Elleman and Barclay, 2004, Burleigh et al., 2005) or deletions in the cytoplasmic tail of HA or NA amino acid sequence (Jin et al., 1997, Zhang et al., 2000) could affect virus morphology. In addition, cellular factors play an important role in influenza virus morphogenesis.

One study has shown that influenza virus morphology is significantly affected by ultracentrifugation, which is often used to concentrate virus prior to EM. It showed that spherical or ovoid virions sometimes changed to irregular morphology following

ultracentrifugation of unfixed influenza A viruses (Sugita et al., 2011). Therefore, in the current study, viruses collected from culture supernatants were concentrated directly using an alternative system, Amicon® Ultra 100K NMWL (National Molecular Weight Limit) Centrifugal Filter Device, which should maintain virus morphology. This method was evaluated by comparing the morphology of viruses observed from the concentrated and the non–concentrated supernatants. The morphology of concentrated and non–concentrated viruses was similar. Such a procedure is recommended to be used in the future to concentrate viruses for determining virus morphology using EM.

Cellular factors such as cell polarity and actin cytoskeleton network play an important role in influenza virus morphogenesis. Polarized cells have been shown to support the production of filamentous particles up to 30 µm following infection with a filamentous A/Udorn/72 virus, while spherical to slightly elongated particles are usually observed after infection of non–polarized cells (Roberts and Compans, 1998). However, DEFs used in this study supported the production of short filaments after infecting with a non–filamentous strain (H2N3) while CEFs produced only spherical virions. Although fibroblasts are not typical host cells for influenza virus replication *in vivo*, primary fibroblasts derived from avian embryos are commonly used for culture and assay of avian influenza viruses.

In this thesis, all viral genes of the viruses derived from chicken and duck cells were amplified, sequenced, and aligned to determine whether there was a genetic basis for difference in virus morphology or to address the reason behind the reduction of infectious virus production from duck cells. However, the sequence alignments showed identical amino acid sequences of all viral genes between chicken and duck produced viruses.

Mutations and deletions in the viral genome have been shown to play a critical role in decreasing virus infectivity and changing the morphology of the virus. Minor nucleotide changes in influenza viruses can occur normally due to the lack of proofreading ability of the RNA polymerase. Here the overall results of gene sequencing were identical between the chicken and duck derived viruses. A study has shown that changes in the nucleotides of the polymerase genes might disrupt the formation of the polymerase complex protein and inhibit the polymerase functions, eventually reducing the infectivity of the virus (Boivin et al., 2010). In the current study, changes were initially detected in PB1 and PB2 following sequencing, but these were due to the presence of a secondary amplicon rather than real mutations.

The results of gene sequencing suggested that the difference in virus infectivity and morphology between chicken and duck derived viruses was due to cellular factors rather than genetic factors. Whilst much attention will be placed on the role of the host cell in modulating virus morphology, the potential importance of the role of virus genes in reducing output of infectious virus should not be overlooked. A high mutation frequency of RNA viral replication is "dangerous" for a virus because it might result in nonviable individuals. On the other hand, it could create complex quasispecies populations (mutant clouds) with potentially beneficially mutations that enable the virus to evolve and adapt to new environments during infection (Domingo et al., 2012). Using chemical mutagenesis to expand quasispecies diversity of the high–fidelity polio virus, analysing viruses provided direct evidence for complementation in sequences between members in the quasispecies. This indicates that the selection indeed occurs at the population level rather than on individual variants (Vignuzzi et al., 2006). Therefore, due to the high mutation rate of influenza A viruses, further work is required to investigate the possible changes in the viral genome which might play a role in reducing the infectivity of the

virus. For this purpose, deep sequencing of the complete genome can be a very valuable tool. Deep sequencing provides a direct way to evaluate the genome characteristics by generating massive amounts of genetic information which could be used to reveal and quantify mutations (Bidzhieva et al., 2014).

For further evaluation of the differences in virus morphology, CEF and DEF were infected with the avian H2N3 and equine H3N8 viruses. MDCK cells were also infected as a control, as most published work on influenza virus morphology is conducted in this type of cell. The principal aim was to investigate the possible role of the actin cytoskeleton in the modulation of virus morphogenesis following *in vitro* infection with the virus. In the absence of actin inhibitor, DEF cells produced filamentous or short filament particles following infection with both strains, while CEF and MDCK cells produced filamentous virions following infection with H3N8 and almost spherical particles following infection with H2N3. The assembly of filamentous particles is reported to require an intact actin cytoskeleton (Roberts and Compans, 1998). Unlike CEF and MDCK cells, DEF cells produced filaments even after disruption of actin with actin inhibitor, cytochalasin D (Cyt.D). Using other actin inhibitors such as jasplakinolide, a mechanistically different inhibitor of actin treadmilling on influenza virus infection, might produce a different form of disruption and might demonstrate a role for actin in changing virus shape. In addition, Arcangeletti et al. (2008) have reported that treatment of epithelial mammalian cells with an actin inhibitor using Cyt.D could be either advantageous or disadvantageous for virus replication following infection with human influenza A/NWS/33 virus (H1N1). The study showed treatment with the drug significantly increased the infection effectiveness in LLC–MK2 cells, while a harmful effect was detected in the MDCK cell line, which was accompanied by a significant increase or decrease in virus titre respectively. Hence, further studies are

required to explain the differential effect of Cyt.D on infection efficacy in the two avian model CEF and DEF cells.

A very recent study has shown that autophagy, which is a consequence of influenza virus infection, is manipulated by the virus itself for its benefit. This manipulation is mediated by the interaction of matrix 2 (M2) ion channel protein directly with the essential autophagy protein, LC3 (Beale et al., 2014). This interaction is mediated by a highly conserved LC3–interaction region (LIR) with M2. The M2 LIR motif causes the redistribution of LC3 to the plasma membrane at the time of virus budding. This subverts autophagy for the benefit of the virus to provide suitable resources for viral budding and to enhance virion stability. The study also showed that mutations in M2 protein abolished LC3 binding, which resulted in reduced virion stability of the filamentous influenza (Beale et al., 2014). Currently, M2 protein sequencing results are identical between chicken and duck produced viruses (Chapter 5). In addition, LC3 has been shown to be rapidly upregulated in DEF cells, but transiently upregulated in CEF cells following infection with H2N3 (Donna Fountain, personal communication). In this thesis, the preliminary findings demonstrated that transfection-mediated LC3 upregulation in CEF cells supported the production of short filaments compared with the untransfected control, which produced only spherical particles. However, observation of infected cells under an electron microscope should present a clearer image with more details about the differences in virus morphology following the transfection of cells with LC3. In addition, using high pathogenic virus strains, or a filamentous virus strain, to infect cells following transfection with LC3 could lead to new findings which will help to understand this mechanism in more detail. How this process supports the production of filaments is still not clear. However, the higher prevalence of autophagy in DEF cells, in which LC3 is a key player, could play a role in supporting filamentous virus budding.

Hence, further work may give more insights into viral morphogenesis in avian cells and possibly identify new cellular factor(s).

There is also a role for cellular Rab11 (a small GTP–binding protein involved in endocytic recycling) and Rab11–family interacting protein 3 (FIP3, which plays a role in membrane trafficking and regulation of actin dynamics) proteins in influenza virus budding and morphogenesis (Bruce et al., 2010). This study showed that both Rab11 and FIP3 proteins are required to support the formation of filamentous particles, while Rab11 is additionally involved in the final budding step of spherical virions. The reduction of Rab11 and FIP3 proteins in human embryonic kidney cells (293T) by treatment with small interfering RNA (siRNA) showed an almost complete absence of filaments following infection with the filamentous virus PR8 MUd. The level and the structure of these proteins in chicken and duck embryo fibroblasts and their impact on regulating influenza virus morphology have not been studied yet. Hence, such a study is required to address the effect these proteins may have on modulating virus morphogenesis in chicken and duck cells.

Although the embryonic chicken and duck fibroblasts are considered a good cell model to study influenza virus infection *in vitro*, they might have different growth kinetics to support the production of the influenza virus. Such a variation is also found in epithelial continuous cell lines, for example MDCK and Vero cells have different viral growth kinetics and play a role in supporting different levels of influenza virus replication (Youil et al., 2004). Further, epithelial cells of the crypts of Lieberkuhn in the large intestine of ducks represent the primary target site for replication of LPAI (Webster et al., 1978) and the epithelial cells of the upper and lower respiratory tract are the main target of virus replication in chickens (Shalaby et al., 1994, Swayne and Slemons, 1994). Although the results of this thesis affirm similar levels of virus infection in chicken and duck cells (as

evidenced by detection of viral nucleoprotein by immunohistochemical staining), there might be some differences in the growth kinetics between cells which result in the production of different levels of infective viruses. Using different cell types such as respiratory, kidney and intestinal cells of both chicken and duck is important to evaluate the role of those cells in supporting virus replication. In addition, the use of other virus strains such as highly pathogenic avian influenza (HPAI) strains to infect the same cell type of different hosts is also recommended.

7.2 Conclusions and future work

In summary, based on the findings gained from this thesis, it appears plausible that cellular factors rather than viral strain or genetic factors might play a major role in producing different titres of infectious avian H2N3 and in modulating virus morphology following the infection of embryonic fibroblasts from chickens and ducks. The hypothesis of this project was: the different outcomes of H2N3 infection in chicken versus duck cells, which are accompanied by a reduction in infectious virus titre from duck cells, may be due to changes in virus morphology, defects in the viral structure, or host cell factors. Accordingly, these findings upheld one hypothesis of this project "the role of host cell factors". However, further studies are required to identify the cellular factors, in particular the role of autophagy in modulating virus morphology. In addition, determining the level of cellular Rab11 and FIP3 in both chicken and duck fibroblasts would be worthwhile. For these purposes, using virus strains of different morphology and observation of infected cells under an electron microscope is recommended. This may further indicate some level of divergence in the mechanisms responsible for spherical and filamentous virion morphogenesis. Furthermore, studying the effect of

different actin inhibitors on virus morphogenesis and their impact on the replication of viruses is required.

On the other hand, it will be interesting to study the structure of the progeny virions in more detail, and in particular determine the level of all viral proteins following infection of CEF and DEF with the virus. This will further help in appreciating the relationship between rapid cell death which follows the infection of duck cells and the production of defective virions. At the level of the investigation conducted and findings in this thesis, no differences in virus genome were detected; however, deep sequencing of the whole virus genome may be required to reveal and quantify any possible mutations which might decrease the infectivity of the duck derived virions. Moreover, it is necessary to examine other cell types such as epithelial cells to observe the differences of virus outcome following infection. Further, the use of other virus strains such as HPAI might produce different levels of virus titre.

The kinds of approaches outlined above may lead to the potentially new findings which will help to understand the impact of the host cell on influenza virus production in more detail.

Appendices

Appendix–I: Buffers and media formulation

Tris Acetate EDTA buffer (TAE) 50X

Tris base …… 242 g

Glacial acetic acid …… 57.1 mL

0.5 M EDTA (pH 8.0) …… 100 mL

Make up the volume to 1 litre with distilled water. It can be stored at room temperature for long time.

Tris buffered saline (TBS) 10X

The following are dissolved in 800mL of distilled water

Sodium chloride (NaCl) …….. 87.66 g

Tris (Trizma) base …….. 60.55 g

Adjust the pH to 7.4 with HCl and make up the volume to one liter with distilled water.

Cell culture medium

DMEM+Gluta Max …….. 500 mL

Fetal calf serum (FCS) …… 50 mL

Penicillin–streptomycin …….. 5 mL

Infection medium (IM)

DMEM with Gluta Max and Ham's F12 …… 50 mL

Ultroser G (serum replacement) ……. 1 mL

Penstrep …….. 500 µl

TPCK trypsin ……. 2.5 µl

Media used for egg infection

Phosphate buffer Saline (PBS)…… 47 mL

Tryptose phosphate broth …… 2 mL

Penicillin Streptomycin (Pen Strep) ……1 mL

Appendix–II Influenza virus gene sequences and primer sites

Below, there are 8 viral genome sequences with their accession numbers obtained from an influenza research database (http://www.fludb.org/brc/home.do?decorator=influenza). The top and bottom yellow highlighted fragments were used for designing forward and reverse primers, respectively, to amplify the large amplicon of each gene. The forward and reverse of the start (top) of each gene are highlighted with green, while the forward and reverse of the end (bottom) are highlighted with blue. The forward and reverse primer sites used only to sequence the middle part of PB1, PB2, and PA are highlighted with red.

CY003943|A/mallard duck/ALB/353/1988 **PB2 gene**

AGCGAAAGCAGGTCAAATATATTCAATATGGAGAGAATAAAAGAACTAAGAGATCTAATG
TCGCAGTCCCGCACCCGCGAGATACTCACTAAGACCACTGTGGACCATATGGCCATAATC
AAAAAGTACACATCAGGAAGGCAAGAGAAGAACCCCGCACTCAGAATGAAGTGGATGATG
GCAATGAAATACCCAATTACAGCAGACAAGAGAATAATGGAAATGATTCCTGAGAGGAAT
GAACAAGGGCAAACCCTCTGGAGCAAAACAAACGATGCTGGCTCAGACCGAGTGATGGTA
TCACCTCTGGCCGTAACATGGTGGAATAGGAATGGACCGACAACAAGTACAGTTCACTAC
CCGAAGGTATATAAAACTTATTTCGAAAAAGTCGAAAGGTTAAAACATGGTACTTTTGGC
CCCGTCCACTTCAGAAATCAAGTTAAGATAAGAAGGAGAGTTGACATAAACCCTGGTCAC
GCAGATCTCAGTGCCAAGGAGGCACAGGATGTGATCATGGAAGTCGTTTTCCCAAATGAA
GTGGGAGCAAGAATACTAACATCAGAGTCACAGCTGACAATAACAAAAGAGAAGAAAGAA
GAGCTCCAGGATTGCAAAATTGCTCCCTTGATGGTAGCATACATGCTAGAAAGAGAGTTG
GTCCGCAAAACGAGGTTCCTCCCAGTGGCTGGTGGGACAAGCAGTGTTTATATTGAGGTG
CTGCATTTAACCCAGGGGACATGCTGGGAGCAGATGTACACTCCAGGAGGAGAAGTGAGA
AATGATGATATTGACCAAAGTTTGATTATCGCTGCTAGGAACATAGTAAGAAGAGCAACG
GTCTCAGCAGACCCATTAGCGTCTCTCTTGGAAATGTGCCATAGCACACAGATTGGAGGG
ATAAGGATGGTGGACATCCTTAGACAGAATCCAACAGAGGAACAAGCCGTAGACATATGC
AAGGCAGCAATGGGGTTGAGGATTAGCTCATCTTTCAGCTTCGGTGGGTTCACTTTCAAA
AGAACAAGCGGATCGTCAGTCAAGAAAGAAGAAGAAGTGCTCACGGGCAACCTTCAAACA

CTGAAAATAAGAGTACATGAAGGGTATGAAGAATTCACAATGGTCGGGAGAAGAGCAACA
GCTATTCTCAGAAAGGCAACCAGGAGATTGATCCAGCTAATAGTAAGTGGGAGAGACGAG
CAGTCAATTGCTGAGGCAATAATCGTGGCCATGGTATTTTCACAAGAGGATTGCATGATC
AAGGCAGTTCGGGGCGATCTGAACTTTGTCAATAGGGCAAACCAACGATTGAATCCCATG
CATCAACTCCTGAGACATTTCCAAAAAGATGCAAAAGTGCTTTTCCAGAACTGGGGAATT
GAACCTATCGACAATGTGATGGGAATGATCGGAATATTGCCCGATATGACCCCAAGTACA
GAGATGTCGCTGAGGGGAATAAGAGTCAGCAAAATGGGAGTAGATGAATACTCCAGCACG
GAGAGAGTGGTGGTGAGCATTGACCGATTTTTGAGGGTTCGGGATCAACGGGGAAATGTA
CTATTGTCTCCCGAAGAAGTCAGCGAGACACAAGGAACGGAGAAACTGACAATAACTTAT
TCGTCATCAATGATGTGGGAGATCAATGGTCCTGAGTCGGTGCTGGTCAATACTTATCAG
TGGATCATCAGGAACTGGGAGACTGTGAAAATTCAATGGTCACAAGATCCCACGATGTTG
TACAATAAAATGGAATTCGAACCATTTCAGTCTCTTGTCCCCAAGGCAGCCAGAAGTCAA
TACAGCGGATTCGTGAGGACACTGTTCCAGCAAATGCGAGATGTGCTTGGAACATTTGAC
ACTGTTCAAATAATAAAACTTCTCCCCTTTGCTGCTGCTCCACCAGAACAGAGTAGGATG
CAGTTCTCCTCACTAACTGTGAATGTGAGAGGGTCAGGGATGAGGATACTGGTAAGAGGC
AATTCTCCAGTGTTCAATTACAACAAGGCAACCAAAAGGCTTACAGTTCTTGGAAAGGAT
GCAGGTGCATTGACCGAAGATCCAGATGAAGGCACAGCTGGGGTGGAGTCTGCTGTTCTG
AGAGGATTCCTCATTCTGGGCAAAGAAGACAAGAGATATGGCCCAGCATTGAGCATCAAT
GAACTGAGCAATCTTGCAAAAGGGGAGAAGGCTAATGTGCTAATTGGACAAGGAGACGTA
GTGTTGGTAATGAAACGGAAACGGGACTCTAGCATACTTACTGACAGCCAGACAGCGACC
AAAAGAATTCGGATGGCCATCAATTAGTGTCGAATTGTTTAAAAACGACCTTGTTTCTAC
T

CY003942|A/mallard duck/ALB/353/1988 **PB1 gene**

AGCGAAAGCAGGCAAACCATTTGAATGGATGTCAATCCGACTTTACTTTTCTTGAAAGTT
CCAGCGCAAAATGCCATAAGCACCACATTCCCATATACAGGAGATCCTCCATACAGCCAT
GGAACAGGAACAGGATACACCATGGACACAGTCAATAGAACACATCAATATTCAGAAAAG
GGAAAATGGACAACAAACACAGAAACTGGAGCACCCCAACTTAACCCAATTGATGGACCA
TTACCTGAGGATAATGAGCCAAGTGGATATGCACAAACAGACTGTGTCCTGGAAGCAATG
GCTTTCCTTGAAGAGTCCCACCCAGGAATCTTTGAAAACTCGTGTCTTGAAACGATGGAA
GTTGTTCAACAAACAAGAGTGGACAAGCTGACCCAAGGGCGCCAGACCTATGATTGGACA
TTAAACAGGAATCAGCCGGCTGCAACTGCATTAGCTAATACTATAGAGGTCTTCAGATCG
AACGGTTTAACGGCTAATGAATCAGGAAGGCTAATAGATTTCCTCAAGGATGTGATGGAA

TCAATGGATAAAGAGGAAATGGAAATAACAACGCACTTCCAAAGAAAAAGAAGAGTAAGG
GACAACATGACCAAGAAAATGGTCACACAAAGAACAATAGGAAAGAAGAAACAGAGACTA
AACAAGAGAAGCTATCTAATAAGAGCACTGACACTGAACACAATGACAAAAGACGCTGAA
AGAGGCAAATTAAAAAGAAGAGCAATTGCAACACCCGGAATGCAAATCAGAGGGTTTGTG
TATTTTGTTGAAACATTGGCGAGGAGCATTTGTGAGAAACTTGAACAATCTGGACTTCCA
GTTGGAGGCAATGAAAAGAAGGCTAAACTGGCAAATGTTGTGAGAAAAATGATGACTAAT
TCACAGGATACAGAGCTCTCTTTCACAATCACTGGAGACAACACCAAATGGAATGAAAAT
CAGAACCCTAGGATGTTCCTGGCAATGATAACATACATAACAAGAAACCAACCTGAATGG
TTTAGGAATGTTTTGAGCATTGCACCTATAATGTTCTCAAACAAAATGGCAAGGCTAGGA
AAAGGGTACATGTTTGAAAGTAAGAGCATGAAACTTCGAACACAGATACCAGCAGAGATG
CTAGCAAATATTGACCTGAAATATTTCAATGAGTCAACAAGAAAAAAAATAGAGAAAATA
AGGCCTCTTCTAATAGATGGTACAGCCTCATTGAGTCCTGGAATGATGATGGGTATGTTC
AATATGCTAAGTACAGTTTTAGGAGTCTCAATCCTAAATCTAGGACAGAAGAGATATACA
AAAACAACATACTGGTGGGACGGGCTCCAATCCTCTGATGACTTTGCTCTCATCGTGAAT
GCACCGAATCATGAAGGAATACAAGCAGGAGTAGATAGATTCTATAGAACCTGCAAGCTA
GTCGGAATCAATATGAGCAAGAAGAAGTCCTACATAAACAGAACAGGGACATTTGAATTC
ACAAGCTTTTTCTATCGCTATGGGTTTGTAGCCAACTTTAGCATGGAACTGCCCAGCTTT
GGAGTGTCTGGGATTAATGAATCGGCTGACATGAGCATTGGGGTAACAGTGATAAAGAAC
AACATGATAAACAATGACCTTGGACCAGCGACGGCTCAAATGGCTCTTCAGCTGTTCATC
AAGGATTACAGGTACACGTATCGGTGTCACAGAGGGGACACACAAATTCAGACGAGGAGG
TCATTCGAGCTGAAGAAGTTGTGGGAACAAACCCGCTCAAAGGCAGGACTGCTGGTTTCA
GATGGAGGACCAAACTTATACAATATTCGGAATCTCCACATCCCGGAAGTCTGCCTGAAA
TGGGAGCTAATGGACGAAGACTATCAAGGAAGGCTTTGTAACCCATTGAACCCATTTGTC
AGCCATAAGGAGATAGAGTCTGTAAACAATGCTGTGGTGATGCCAGCTCATGGCCCAGCC
AAGAGCATGGAATATGATGCTGTTGCTACTACACATTCCTGGATCCCCAAGAGGAACCGC
TCCATCCTCAACACAAGCCAAAGGGGAATCCTTGAAGACGAACAGATGTACCAAAAGTGC
TGCAATCTATTCGAGAAATTCTTCCCTAGCAGTTCATACAGGAGACCGGTTGGAATTTCC
AGCATGGTGGAGGCCATGGTGTCTAGGGCCCGAATTGATGCACGAATTGACTTCGAGTCT
GGACGGATTAAGAAGGAGGAGTTTGCTGAGATCATGAAGATCTGTTCCACCATTGAAGAG
CTCAGACGGCAGAAATAGTGAATTTAGCTTGTCCTTCATGAAAAATGCCTTGTTTCTAC
T

CY003997|A/mallard/Alberta/79/2003 **PA gene**

AGCGAAAGCAGGTACTGATTCAAAATGGAAGATTTTGTGCGACAATGCTTCAATCCAATG
ATCGTCGAGCTTGCGGAAAAGGCAATGAAAGAATATGGGGAAGATCCAAAAATCGAGACA
AACAAATTTGCTGCAATATGCACACACTTAGAAGTGTGTTTCATGTATTCAGATTTCCAT
TTCATTGATGAACGAGGTGAGTCGATAATCGTGGAGTCTGGCGATCCAAATGCACTCCTA
AAACACCGATTTGAAATAATTGAAGGGAGAGATCGTACTATGGCCTGGACAGTAGTGAAC
AGTATTTGCAACACCACAGGAGTTGAAAAACCCAAATTTCTCCCGGATTTATACGATTAC
AAAGAGAATCGTTTCATTGAAATTGGAGTAACCAGGAGGGAGGTCCATATATACTATTTA
GAAAAGGCCAATAAGATAAAGTCTGAGAAGACACACATCCACATCTTTTCATTCACTGGG
GAAGAAATGGCTACTAAAGCAGACTACACTCTTGATGAAGAAAGTAGAGCGAGGGTCAAA
ACCAGACTATTCACCATAAGACAAGAGATGGCCAGTAGAGGCCTCTGGGATTCCTTTCGT
CAGTCCGAGAGAGGCGAAGAGACAATTGAAGAAAGATTTGAAATTACAGGAACCATGCGC
AGGCTCGCCGACCAAAGTCTCCCACCGAACTTCTCCAGCCTTGAAAACTTTAGAGCCTAT
GTGGATGGATTCGAACCGAACGGCTGCATTGAGGGCAAGCTTTCTCAAATGTCCAAAGAA
GTAAACGCAAGAATTGAACCATTTTTGAAGACAACACCACGCCCCCTGAGATTACCGGAA
GGGCCTCCTTGCTCTCAGCGGTCGAAATTTCTGCTGATGGATGCTCTGAAGCTTAGCATT
GAAGACCCGAGTCATGAAGGCGAGGGGATACCGCTGTATGATGCGATCAAATGCATGAAG
ACCTTTTTCGGCTGGAAAGAGCCTAACATTGTTAAGCCACATGAAAAGGGCATAAACCCC
AATTATCTCCTGGCTTGGAAGCAAGTGCTAGCAGAGCTACAGGATATTGAAAACGAGGAG
AAGATTCCAAAAACGAAGAACATGAAGAAAACAAGCCAATTGAAGTGGGCACTTGGTGAA
AACATGGCACCAGAGAAAGTGGACTTTGAAGATTGCAAGGATGTCAGCGATTTGAGGCAG
TATGACAGCGATGAGCCTGAGCAAAGATCACTAGCAAGTTGGATTCAAAGTGAGTTCAAC
AAAGCTTGTGAATTGACTGACTCAAGTTGGATAGAACTCGATGAAATAGGGGAGGACGTT
GCCCCAATCGAACACATTGCAAGCATGAGGAGGAATTACTTTACAGCTGAAGTGTCTCAC
TGCAGGGCAACAGAATACATAATGAAGGGAGTATACATAAACACAGCTTTGCTCAATGCT
TCTTGTGCGGCAATGGATGATTTTCAGCTGATCCCAATGATAAGCAAATGCAGAACCAAG
GAAGGGCGGCGGAAGACAAATCTGTATGGGTTCATAATAAAGGGAAGATCTCATTTGAGG
AACGATACTGATGTAGTGAATTTTGTGAGCATGGAGTTTTCTCTTACTGATCCTAGACTA
GAGCCACATAAATGGGAGAAATACTGTGTCCTTGAAATAGGGGACATGCTCCTGCGGACT
GCAATAGGCCAAGTATCGAGACCCATGTTTCTGTATGTGAGGACCAATGGAACTTCCAAG
ATCAAAATGAAATGGGGTATGGAGATGAGGCGTTGTCTTCTTCAATCCCTTCAGCAAATT
GAAAGCATGATTGAGGCCGAGTCCTCTGTCAAAGAGAAAGACATGACCAAAGAATTCTTT

GAAAACAAATCAGAGACATGGCCCATTGGGGAATCACCCAAAGGAGTAGAAGAAGGTTCC
ATTGGAAAGGTGTGCAGGACTCTGCTGGCAAAATCTGTATTCAACAGCTTGTATGCATCT
CCACAACTAGAGGGATTTTCAGCTGAGTCGAGAAAGCTGCTCCTCATTGTTCAGGCACTT
AGGGACAACCTGGAACCTGGTACCTTCGATCTTGGAGGGCTATATGAAGCAATTGAGGAG
TGCCTGATTAATGATCCCTGGGTTTTGCTTAACGCATCTTGGTTCAACTCCTTCCTCACA
CATGCACTGAAATAGTTGTGGCAATGCTACTATTTGCTATCCATACTGTCCAAAAAAGTA
CCTTGTTTCTACT

CY003992|A/mallard/Alberta/79/2003 **HA gene**

AGCAAAAGCAGGGGTTATACCATAGACAACCGAACAAAGACAATGACCATCACTTTTCTC
ATCCTCCTGTTCACAGTAGTGAAAGGGGACCAAATATGTATCGGATACCATGCCAACAAT
TCCACAGAAAAAGTTGACACAATCTTGGAACGAAACGTCACCGTGACTCATGCCAAGGAC
ATTCTTGAAAAAACGCATAATGGAAAGTTGTGCAGATTAAGCGGGATCCCTCCACTGGAA
CTGGGGGATTGCAGCATTGCAGGTTGGCTCCTTGGAAATCCGGAATGTGACCGGCTCTTA
AGTGTACCTGAATGGTCCTATATAGTGGAAAAGGAAAACCCGGTGAATGGTCTGTGCTAC
CCAGGCAGTTTCAATGATTATGAGGAATTGAAACATCTCCTCACCAGTGTGACACACTTT
GAGAAAGTTAAGATTCTGCCCAGAGATCAATGGACTCAGCACACAACAACTGGTGGTTCT
CGGGCCTGTGCAGTGTCTGGAAACCCGTCATTCTTTAGGAACATGGTTTGGCTTACAAAG
AAGGGGTCAAACTACCCAATTGCTAAAAGGTCATACAACAACACAAGTGGGGAGCAAATG
CTGGTAATCTGGGGGATACATCATCCCAATGACGATGCGGAACAAAGGACACTGTACCAG
AATGTGGGAACATATGTTTCCGTTGGGACATCAACACTAAATAAGAGGTCAATCCCTGAA
ATAGCAACAAGGCCCAAAGTCAATGGACAAGGAGGGAGAATGGAATTCTCTTGGACTCTA
TTGGAGACATGGGATGTCATAAATTTTGAGAGCACTGGTAATTTAATTGCACCAGAATAC
GGATTCAAAATATCAAAGAGAGGAAGCTCAGGAATTATGAAGACAGAGAAAACACTTGAA
AATTGTGAAACCAAATGTCAGACCCCCTTGGGGGCAATAAATACAACATTGCCCTTTCAC
AACATTCACCCATTGACAATAGGTGAGTGCCCCAAGTATGTAAAGTCAGACAGACTGGTT
TTGGCAACAGGACTAAGAAATGTCCCTCAGATTGAATCAAGGGGATTGTTTGGAGCAATA
GCTGGGTTTATAGAAGGCGGATGGCAAGGGATGGTTGATGGCTGGTATGGGTATCATCAC
AGCAATGATCAAGGATCAGGATATGCAGCAGACAAAGAATCCACTCAAAAGGCAATTGAT
GGGATAACTAACAAAGTAAATTCTGTGATTGAAAAGATGAACACTCAGTTTGAGGCTGTT
GGGAAAGAGTTCAACAATCTAGAGAGAAGACTAGAAAACTTAAATAAAAAGATGGAAGAT
GGATTTCTTGATGTATGGACATATAATGCCGAACTCCTAGTTCTAATGGAGAATGAGAGG

ACACTTGATTTCCATGACTCTAATGTGAAGAATCTGTACGATAAGGTCAGAATGCAATTA
AGAGACAATGCTAAGGAAATAGGGAACGGATGCTTTGAGTTTTATCATAAATGTGATGAT
GAATGCATGAATAGTGTCAGGAATGGAACATATGATTATCCCAAATATGAGGAAGAGTCC
AAGCTGAACAGGAACGAAATAAAAGGACTGAAATTGAGCAATATGGGGGTCTATCAAATA
CTTGCTATATACGCTACAGTTGCAGGCTCCTTGTCACTGGCAATCATGATAGCTGGGATT
TCTTTCTGGATGTGTTCTAATGGGTCTCTGCAATGCAGAATTTGCATATGACTGTAAGTC
AATTTGTAATTAAAAACACCCTTGTTTCTACT

CY003995|A/mallard/Alberta/79/2003 **NP gene**

AGCAAAAGCAGGGTAGATAATCACTCACCGAGTGACATCCACATCATGGCGTCTCAAGGC
ACCAAACGATCTTATGAACAGATGGAAACTGGTGGAGAACGCCAGAATGCAACTGAAATC
AGAGCATCTGTTGGGAGAATGGTTGGTGGAATCGGAAGGTTCTACATACAGATGTGCACT
GAACTCAAGCTCAGTGACTATGAAGGGAGGCTGATCCAAAACAGCATCACAATAGAGAGA
ATGGTTCTCTCAGCATTTGATGAGAGGAGAAACAAATATCTGGAGGAGCATCCCAGTGCT
GGAAAAGACCCTAAGAAGACTGGAGGTCCAATCTACAGGAGGAGAGATGGGAAATGGATG
AGAGAATTGATCCTATATGATAAAGAGGAGATCAGAAGGATTTGGCGTCAAGCGAATAAT
GGAGAAGACGCAACTGCCGGCCTCACCCATTTGATGATCTGGCACTCCAATCTGAATGAT
GCCACCTATCAGAGGACGAGGGCACTTGTGCGTACTGGAATGGATCCCAGGATGTGTTCT
CTGATGCAAGGCTCGACTCTTCCGAGGAGGTCTGGAGCTGCTGGAGCAGCAGTGAAAGGA
GTTGGAACAATGGTGATGGAATTGATCCGAATGATCAAGCGAGGGATCAATGATCGGAAT
TTCTGGAGAGGCGAAAATGGGCGGAGGACAAGAATTGCTTATGAGAGAATGTGCAACATC
CTCAAAGGGAAGTTTCAAACAGCGGCACAAAGAGCAATGATGGACCAGGTGAGGGAAAGC
CGGAATCCTGGGAATGCTGAAATTGAAGATCTCATCTTTCTCGCACGGTCTGCTCTCATT
CTGAGGGGATCAGTGGCTCATAAGTCTTGCCTGCCTGCTTGTGTGTATGGACTTGCTGTG
GCCAGTGGATACGACTTTGAAAGAGAGGGATACTCCCTAGTCGGAATCGATCCTTTCCGT
CTGCTCCAAAACAGTCAAGTCTTCAGTCTCATCAGACCAAACGAAAACCCAGCACATAAA
AGTCAGCTGGTATGGATGGCATGCCACTCTGCAGCTTTTGAAGATCTGAGAGTGTCAAGC
TTCATTAGAGGAACAAGAGTAGTCCCAAGAGGACAGCTATCCACCAGAGGAGTTCAGATT
GCTTCAAATGAGAACATGGAGACAATGGACTCCAGTACTCTTGAACTGAGGAGCAGATAC
TGGGCTATAAGGACCAGAAGTGGAGGAAACACTAACCAGCAGAGAGCATCCGCAGGGCAA
ATCAGCGTACAGCCCACATTCTCTGTACAGAGGAACCTCCCATTCGAGAGAGCAACCATT
ATGGCGGCATTTACAGGGAACACTGAAGGCAGAACTTCAGACATGAGAACAGAAATCATA
AGGATGATGGAAAATGCCAGACCTGAGGATGTGTCTTTCCAGGGGCGGGGAGTCTTCGAG

CTCTCAGACGAAAAGGCAACGAACCCGATCGTGCCTTCCTTTGACATGAGTAACGAAGGA
TCTTATTTCTTCGGAGACAATGCAGAGGAGTATGACAATTAAAAAAAGAAAAATACCCTT
GTTTCTACT

CY003946|A/mallard/ALB/201/1996 **NA gene**

The area which is highlighted with yellow and green is a region of overlapping between the two forward primers.

AGCAAAAGCAGGTGCGAGATGAATCCAAATCAGAAGATAATAACAATCGGGGTAGTGAAC
ACCACTCTGTCAACAATAGCCCTTCTCATTGGAGTGGGAAATTTAGTTTTCAACACAGTC
ATACATGAGAAAATAGGAGACCACCAAACAGTGATCCACCCAACAATAACGACCCCTGCA
GTACCGAACTGCAGTGACACTATAATAACATACAATAACACTGTGATAAACAACATAACA
ACAACAATAATAACTGAAGCGGAAAGGCCTTTCAAGCCTCCACTACCGCTGTGCCCCTTC
AGAGGATTCTTCCCTTTTCACAAGGACAATGCAATACGGCTGGGTGAGAACAAAGACGTC
ATAGTCACAAGGGAGCCTTATGTTAGCTGCGATAATGACAATTGCTGGTCCTTTGCTCTC
GCACAAGGAGCATTGCTAGGGACTAAACATAGCAATGGGACCATTAAAGACAGAACACCA
TATAGGTCTCTAATCCGATTCCCAATAGGAACAGCTCCAGTACTAGGAAATTACAAGGAG
ATATGCATTGCTTGGTCGAGCAGCAGTTGCTTTGACGGGAAAGAGTGGATGCATGTATGC
ATGACAGGGAACGATAATGATGCAAGTGCCCAGATAATATATGCAGGGAGAATGACAGAC
TCCATTAAATCATGGAGAAAGGACATACTGAGAACTCAGGAGTCCGAATGTCAGTGCATC
GGCGGGATTTGTGTTGTTGCTGTCACAGATGGCCCTGCTGCTAATAGTGCAGATCACAGG
ATTTACTGGATACGGGAGGGAAGAATAATGAAGTATGAAAATGTCCCCAAAACAAAGATA
CAACACTTAGAAGAGTGTTCCTGCTATGTGGACATTGATGTTTACTGTATATGTAGGGAT
AATTGGAAGGGTTCTAACAGACCTTGGATGAGAATCAACAACGAGACTATACTGGAAACA
GGGTATGTGTGTAGTAAATTTCACTCAGACACCCCCAGGCCAGCTGATCCCTCAACAATA
TCATGTGACTCCCCAAGCAATGTCAATGGAGGACCCGGAGTAAAGGGATTTGGTTTCAAA
GCCGGCAATGATGTATGGTTGGGTAGAACAGTGTCAACTAGTGGTAGATCGGGCTTTGAA
ATTATCAAAGTTACAGAGGGGTGGATCAACTCTCCCAATCATGCCAAATCAATTACACAA
ACACTGGTGTCCAACAATGATTGGTCAGGCTATTCAGGTAGCTTCATTGTCAAAACCAAG
GACTGTTTTCAGCCCTGTTTTTATGTCGAGCTTATACGAGGGAGGCCCAACAAGAATGAT
GATGTCTCTTGGACAAGCAATAGTATAGTTACTTTCTGTGGACTAGACAATGAACCTGGA
TCGGGAAATTGGCCGGATGGTTCTAACATTGGGTTTATGCCCAAGTAACAGAAAAAAGCA
CCTTGTTTCTACT

CY003945|A/mallard/ALB/201/1996 **M gene**

Pink areas represent the sites of the forward and reverse primers that were used for qPCR. Grey area represents the site of the probe.

AGCAAAAGCAGGTAGATATTGAAAGATGAGTCTTCTAACCGAGGTCGAAACGTACGTTCT
CTCTATCGTCCCGTCAGGCCCCCTCAAAGCCGAGATCGCGCAGAGACTTGAAGATGTCTT
TGCAGGAAAGAACACAGATCTTGAGGCACTCATGGAATGGCTAAAGACAAGACCAATCCT
GTCACCTCTGACTAAGGGGATTTTAGGATTTGTGTTCACGCTCACCGTGCCCAGTGAGCG
AGGACTGCAGCGTAGACGCTTTGTCCAGAATGCTCTTAATGGGAATGGAGATCCAAACAA
CATGGACAGGGCAGTCAAACTGTATAGGAAGCTCAAAAGGGAAATTACATTCCATGGGGC
CAAAGAGGTAGCACTCAGTTATTCCACTGGTGCACTTGCCAGTTGCATGGGCCTCATATA
CAACAGGATGGGAACAGTGACCACCGAAGTGGCATTTGGACTGGTGTGCGCCACATGTGA
GCAGATTGCTGACTCCCAGCATCGGTCTCACAGGCAGATGGTGACAACAACCAACCCACT
GATCAGACATGAGAACAGGATGGTACTGGCTAGTACTACGGCTAAAGCCATGGAGCAGAT
GGCAGGGTCGAGCGAACAAGCAGCAGAGGCTATGGAGGTTGCCAGTCAGGCTAGGCAGAT
GGTGCAGGCAATGAGGACCATTGGGACTCATCCTAGCTCCAGTGCCGGTCTAAAAGATGA
TCTTCTTGAAAATTTGCAGGCCTACCAGAAACGAATGGGAGTGCAAATGCAGCGATTCAA
GTGATCCTCTCGTTATTGCCGCAAGTATCATTGGGATCTTGCACTTGATATTGTGGATTC
TTGATCGTCTTTTTTTCAAATGCATTTATCGTCGCCTTAAATACGGATTGAAAAGAGGGC
CTTCTACGGAAGGAGTGCCTGAGTCTATGAGGGAAGAATATCGGCAGGAACAGCAGAGTG
CTGTGGATGTTGACGATGGTCATTTTGTCAACATAGAGCTGGAGTAAAAAACTACCTTGT
TTCTACT

CY003980|A/mallard/ALB/226/1998 **NS gene**

AGCAAAAGCAGGGTGACAAAAACATAATGGATTCCAACACTGTGTCAAGCTTTCAGGTAG
ACTGCTTTCTTTGGCATGTCCGCAAACGATTTGCAGACCAAGAACTGGGTGATGCCCCAT
TCCTTGACCGGCTTCGCCGAGATCAAAAATCTCTAAGAGGAAGAGGCAGCACTCTTGGTC
TGGATATCGAAACAGCCACTCGCTCTGGAAAGCAGATAGTGGAGAGGATTCTGGAGGAAG
AATCCGACGAGGCACTCAAAATGACTATTGCCTCTGTACCTGCTTCACGCTACCTAACTG
ACATGACTCTTGAAGAGATGTCAAGAGACTGGTTCATGCTCATGCCCAAACAAAAAGTGG
CAGGTTCCCTCTGTATCAGAATGGACCAGGCGATCATGGATAAGAATATTATACTGAAAG
CGAATTTCAGTGTGATCTTCGATCGGCTGGAGACACTAATACTACTCAGAGCTTTCACTG

AAGAAGGAGCAATTGTCGGCGAAATTTCACCATTGCCTTCTCTTCCAGGACATACTGATG
AGGATGTCAAAAATGCAATTGGGGTCCTCATCGGAGGACTTGAATGGAATGATAACACAG
TTCGAGTCTCTGAAACTCTACAGAGATTCGCTTGGAGAAGCTGTAATGAGGATGGGAGAC
CTCCACTCCCTCCAAAGCAGAAACGGAAAATGGCGAGAACAATTGAGTCAGAAGTTTGAG
GAAATAAGGTGGCTAATTGAAGAGGTGCGACATAGACTAAAGGTTACAGAGAATAGTTTT
GAACAAATAACATTTATGCAAGCCTTACAACTACTGCTTGAAGTGGAGCAAGAGATAAGA
ACTTTCTCGTTTCAGCTTATTTAATGATAAAAAACACCCTTGTTTCTACT

Appendix–III Nucleotide sequence alignments

Below, the final nucleotide sequences of the eight H2N3 viral genes of both CEF and DEF cell produced viruses. The sequences of each gene were assembled and aligned by Geneious Inspirational Software for Biologists.

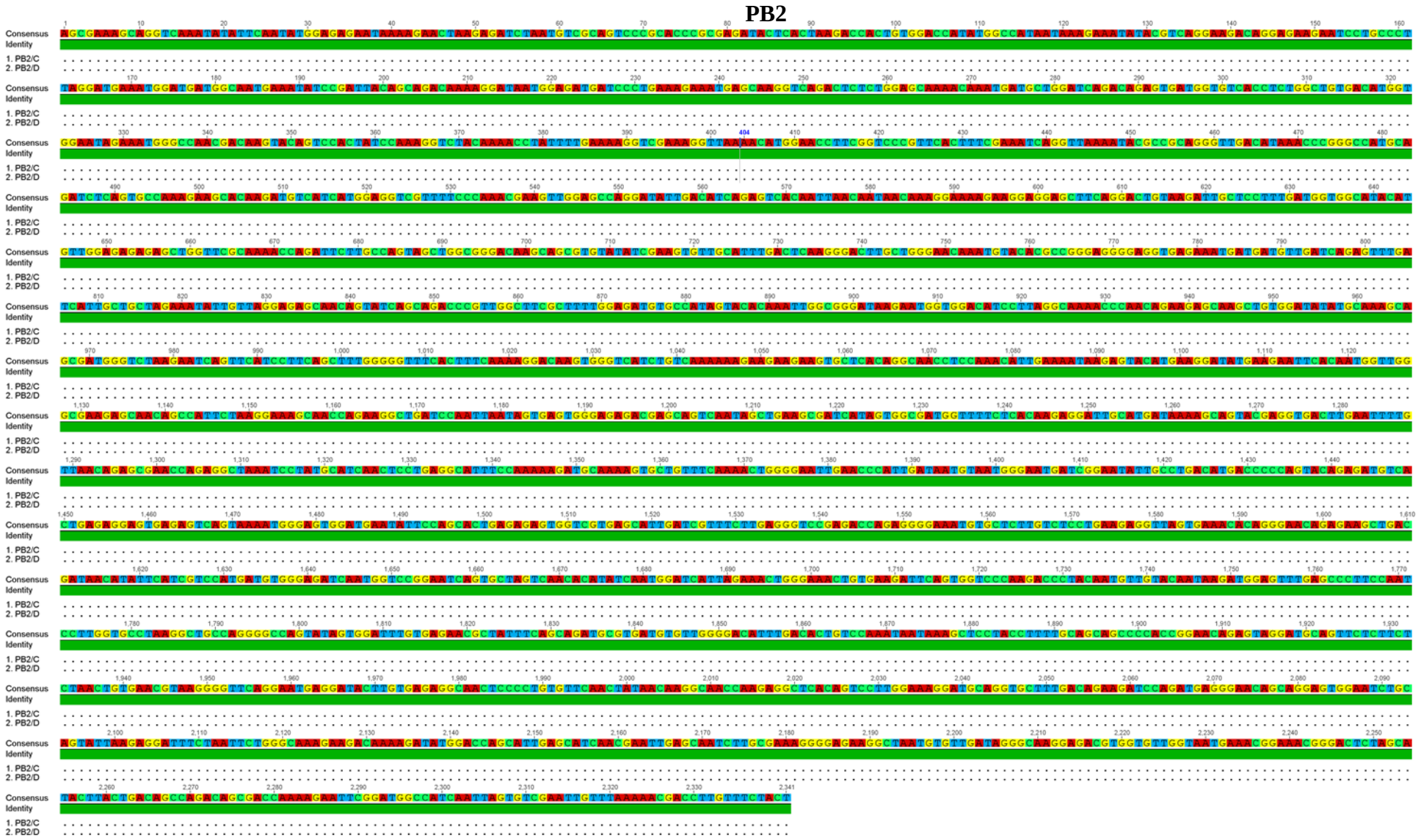

Figure III–1 Polymerase basic 2 (PB2) gene alignment between chicken and duck cell grown viruses. The figure shows identical sequences between the two PB2 genes.

PB2/C: Polymerase basic 2 gene sequenced from H2N3 grown on chicken cells.

PB2/D: Polymerase basic 2 gene sequenced from H2N3 grown on duck cells.

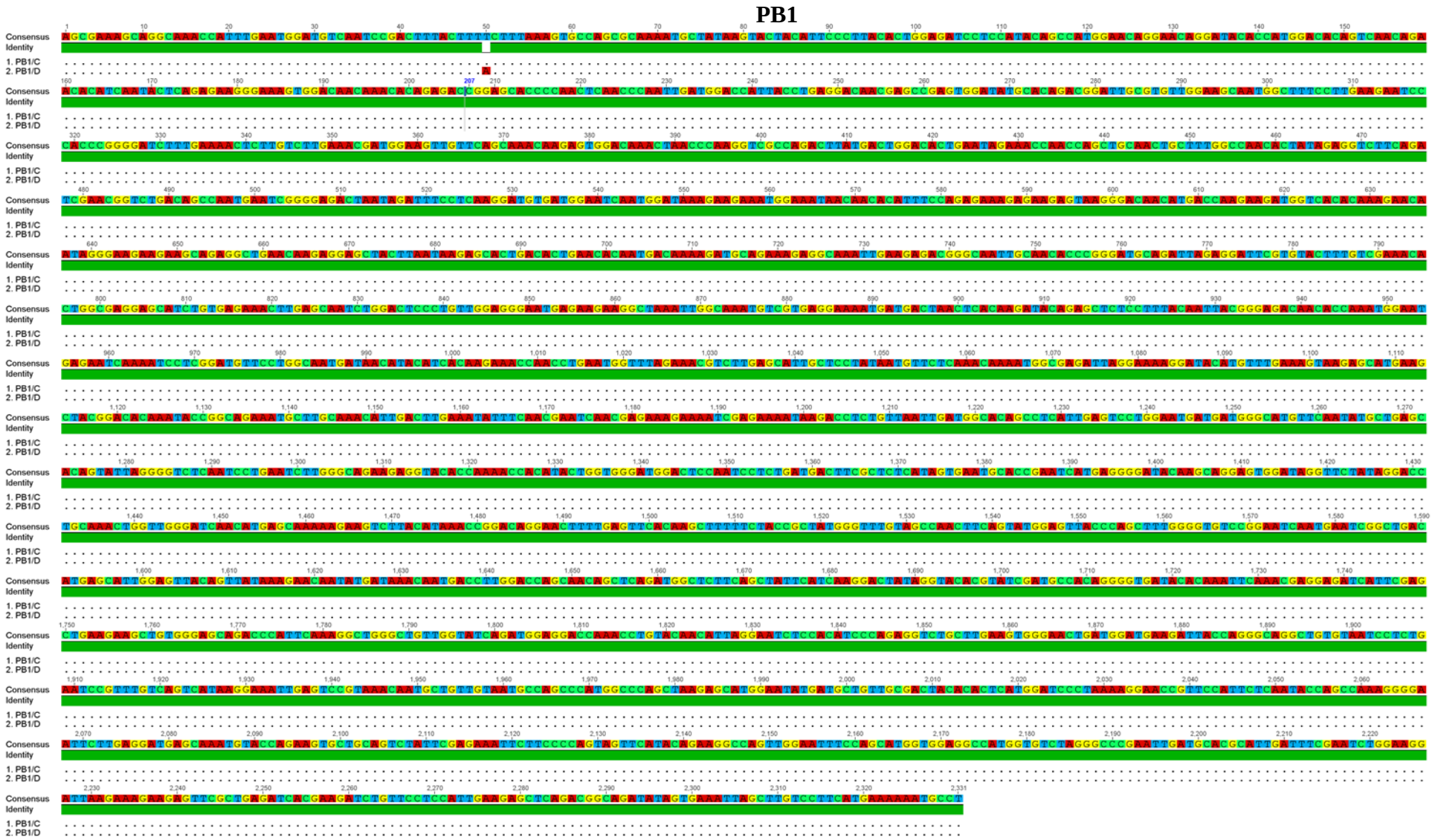

Figure III–2 Polymerase basic 1 (PB1) gene alignment between chicken and duck cell grown viruses. The figure shows identical sequences between the two PB1 genes.

PB1/C: Polymerase basic 1 gene sequenced from H2N3 grown on chicken cells.

PB1/D: Polymerase basic 1 gene sequenced from H2N3 grown on duck cells.

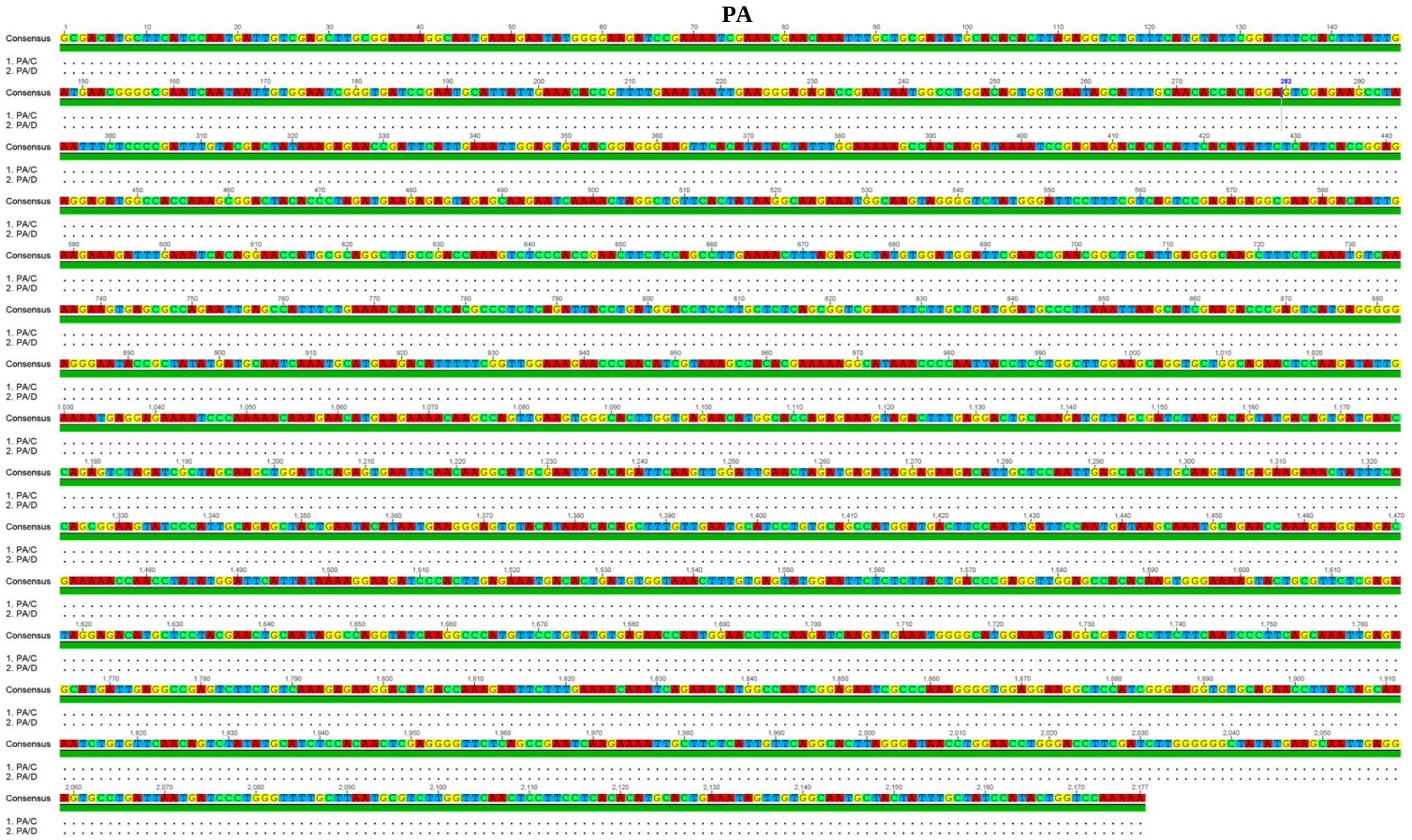

Figure III–3 Polymerase acidic (PA) gene alignment between chicken and duck cell grown viruses. The figure shows identical sequences between the two PA genes.

PA/C: Polymerase acidic gene sequenced from H2N3 grown on chicken cells.

PA/D: Polymerase acidic gene sequenced from H2N3 grown on duck cells.

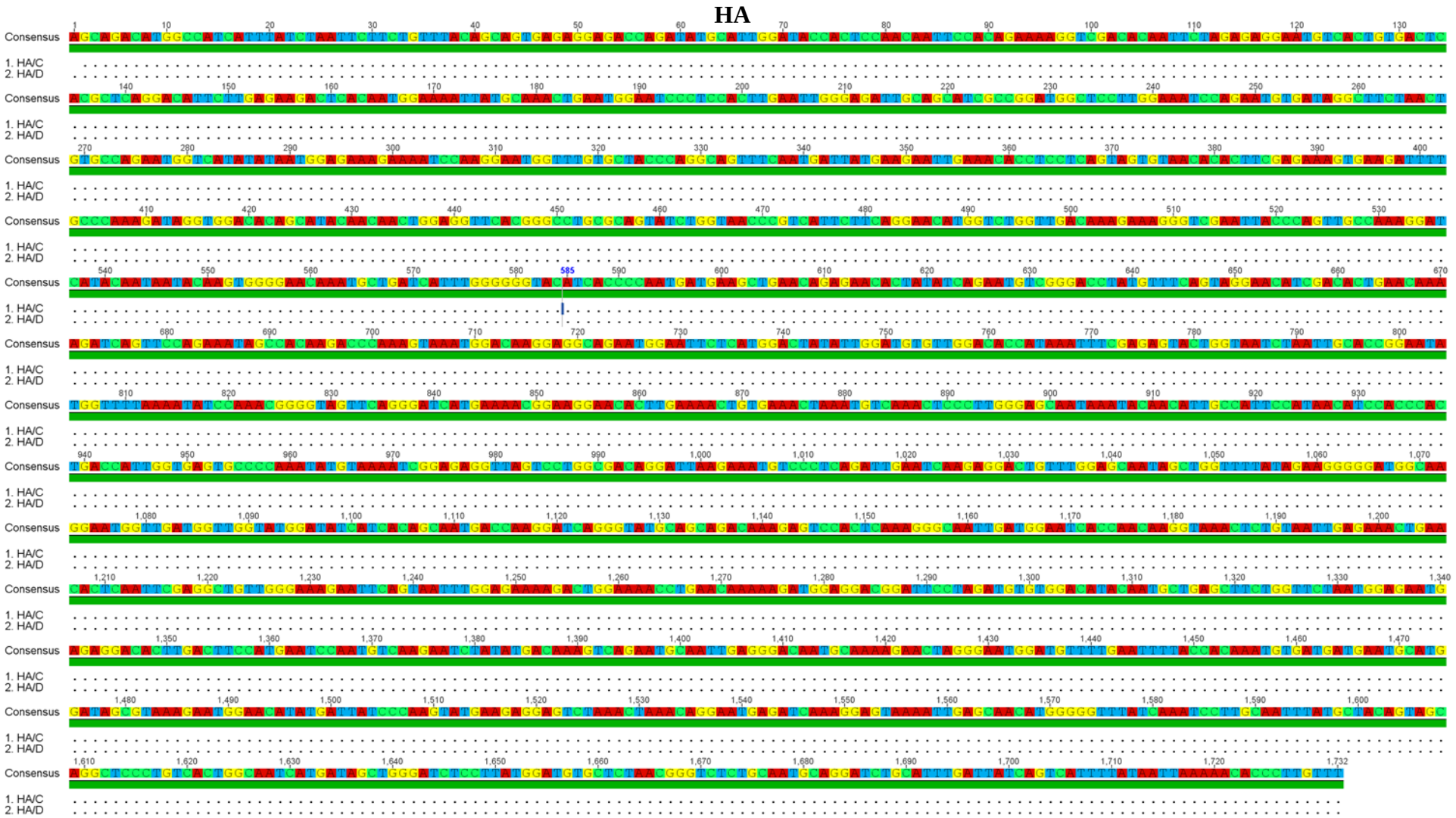

Figure III–4 Haemagglutinin (HA) gene alignment between chicken and duck cell grown viruses. The figure shows identical sequences between the two HA genes.

HA/C: Haemagglutinin gene sequenced from H2N3 grown on chicken cells.

HA/D: Haemagglutinin gene sequenced from H2N3 grown on duck cells.

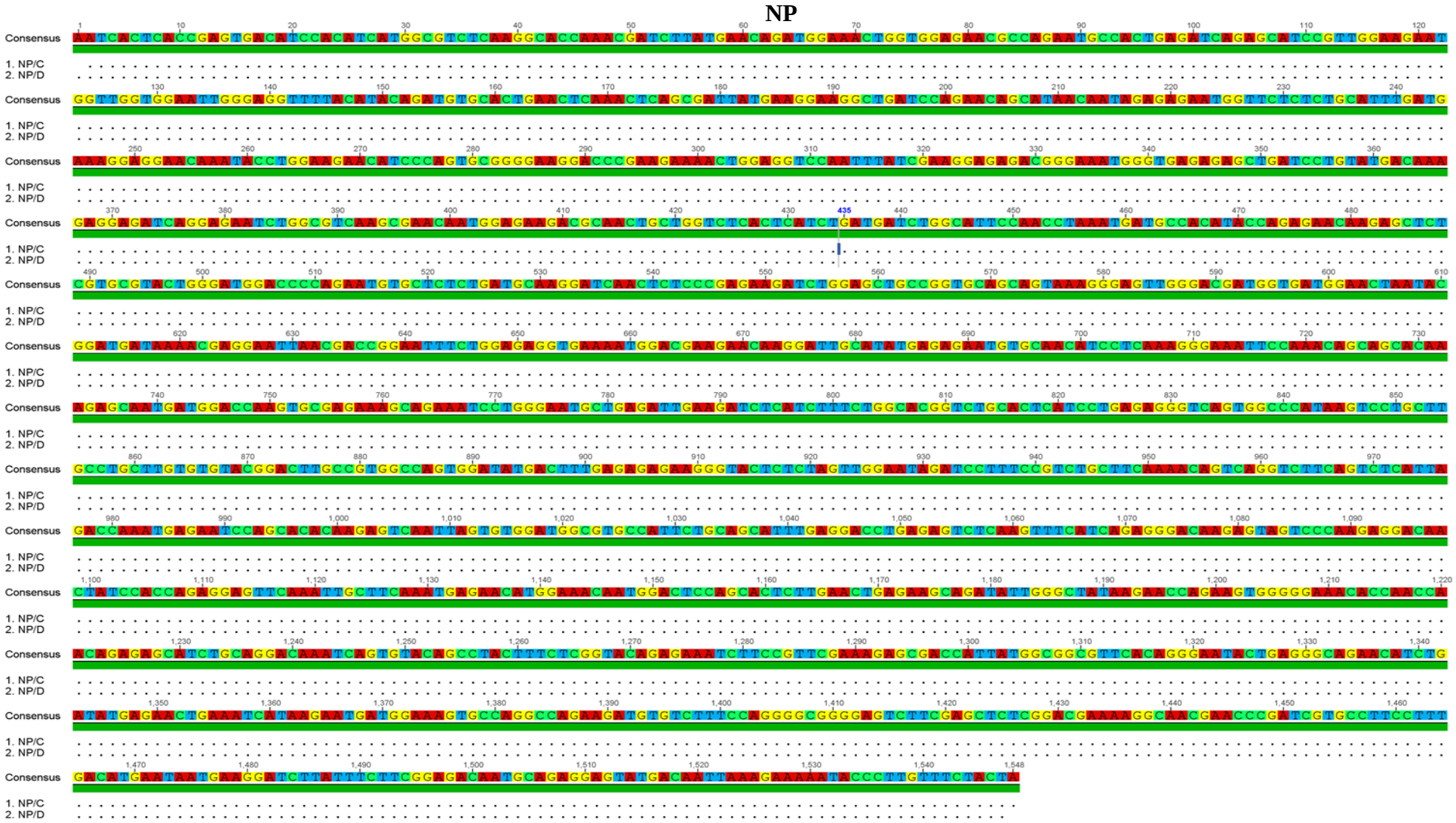

Figure III–5 Nucleoprotein (NP) gene alignment between chicken and duck cell grown viruses. The figure shows identical sequences between the two NP genes.

NP/C: Nucleoprotein gene sequenced from H2N3 grown on chicken cells.

NO/D: Nucleoprotein gene sequenced from H2N3 grown on duck cells.

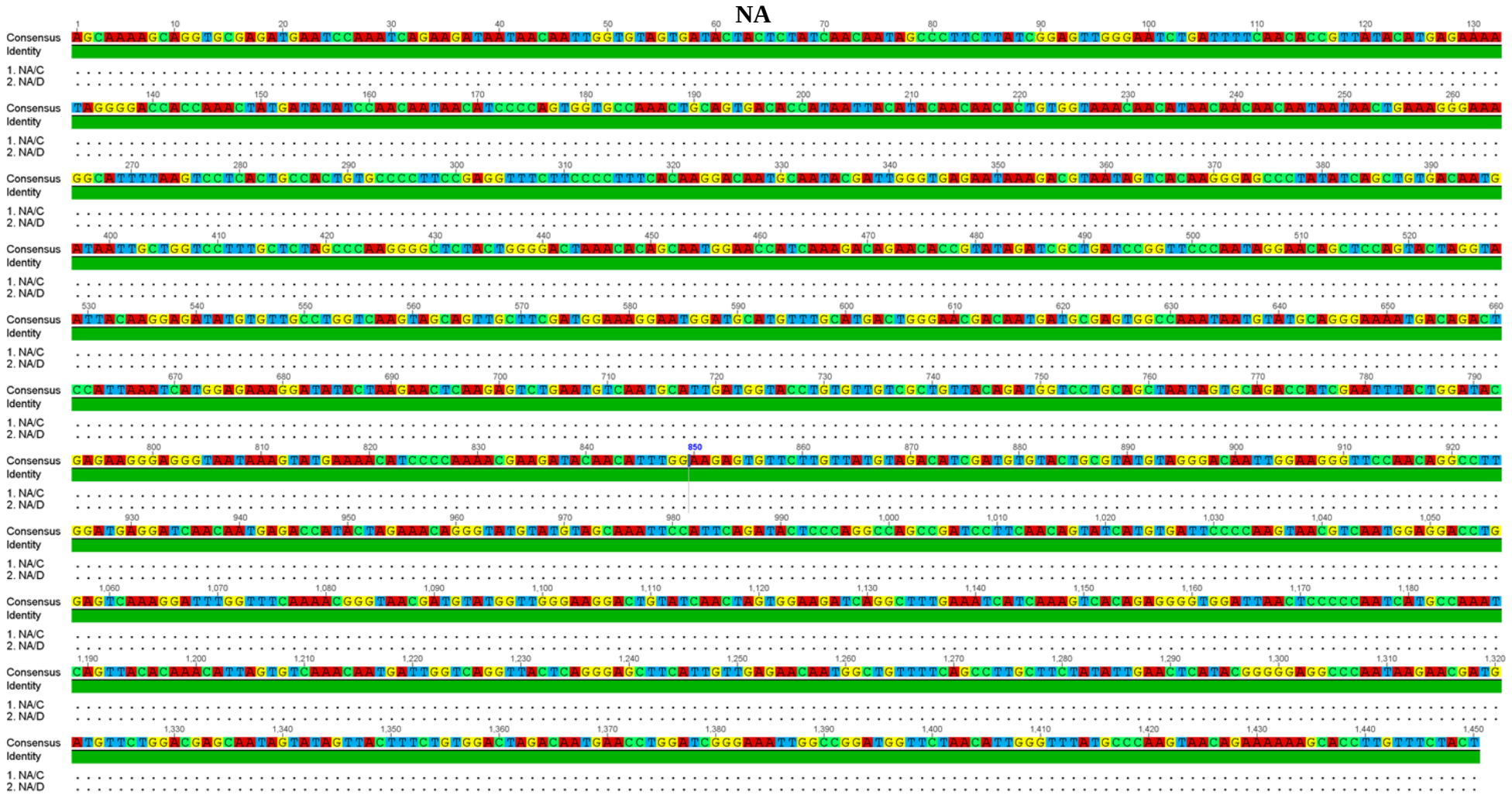

Figure III–6 Neuraminidase (NA) gene alignment between chicken and duck cell grown viruses. The figure shows identical sequences between the two NA genes.

NA/C: Neuraminidase gene sequenced from H2N3 grown on chicken cells.

NA/D: Neuraminidase gene sequenced from H2N3 grown on duck cells.

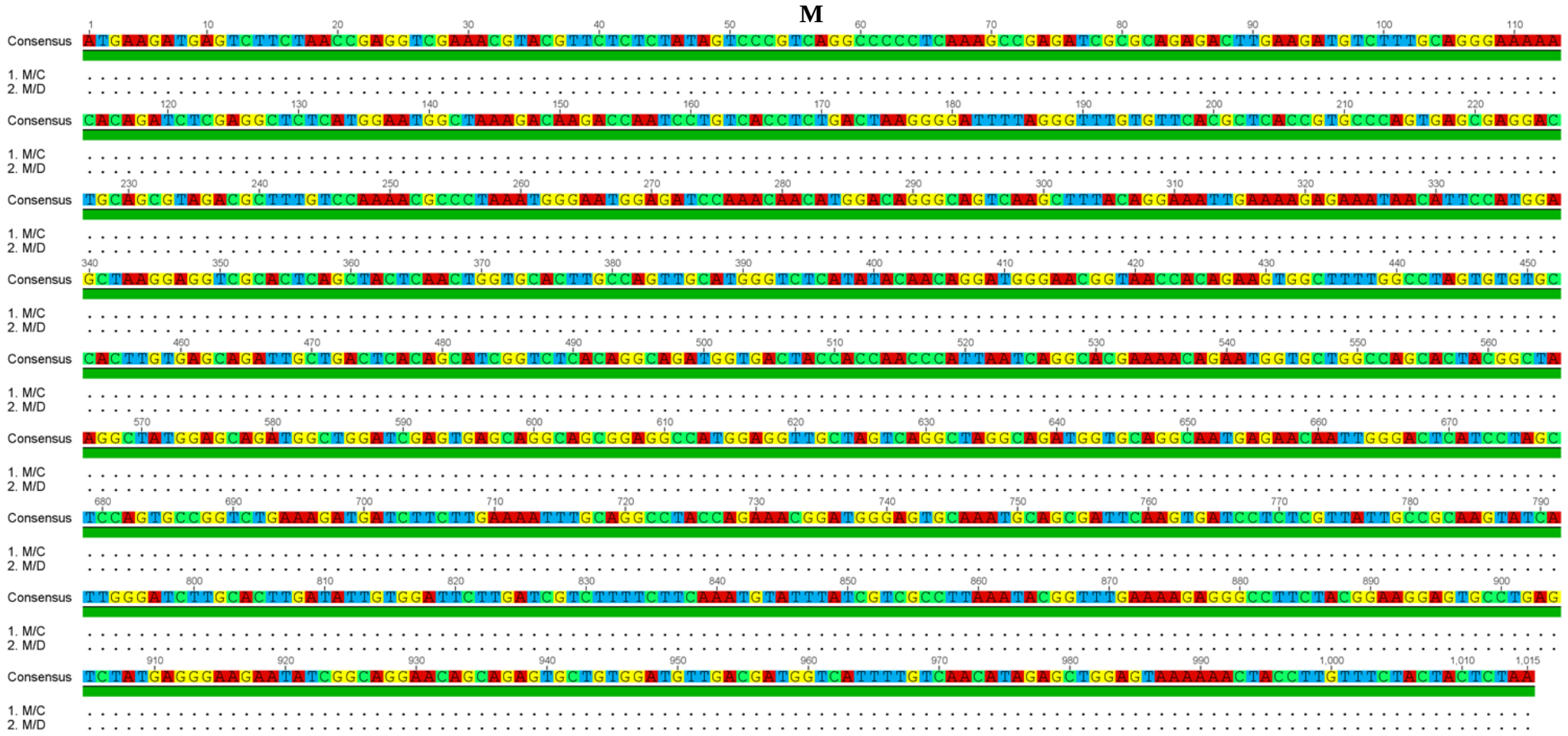

Figure III–7 Matrix (M) gene alignment between chicken and duck cell grown viruses. The figure shows identical sequences between the two M genes.

M/C: Matrix gene sequenced from H2N3 grown on chicken cells.

M/D: Matrix gene sequenced from H2N3 grown on duck cells.

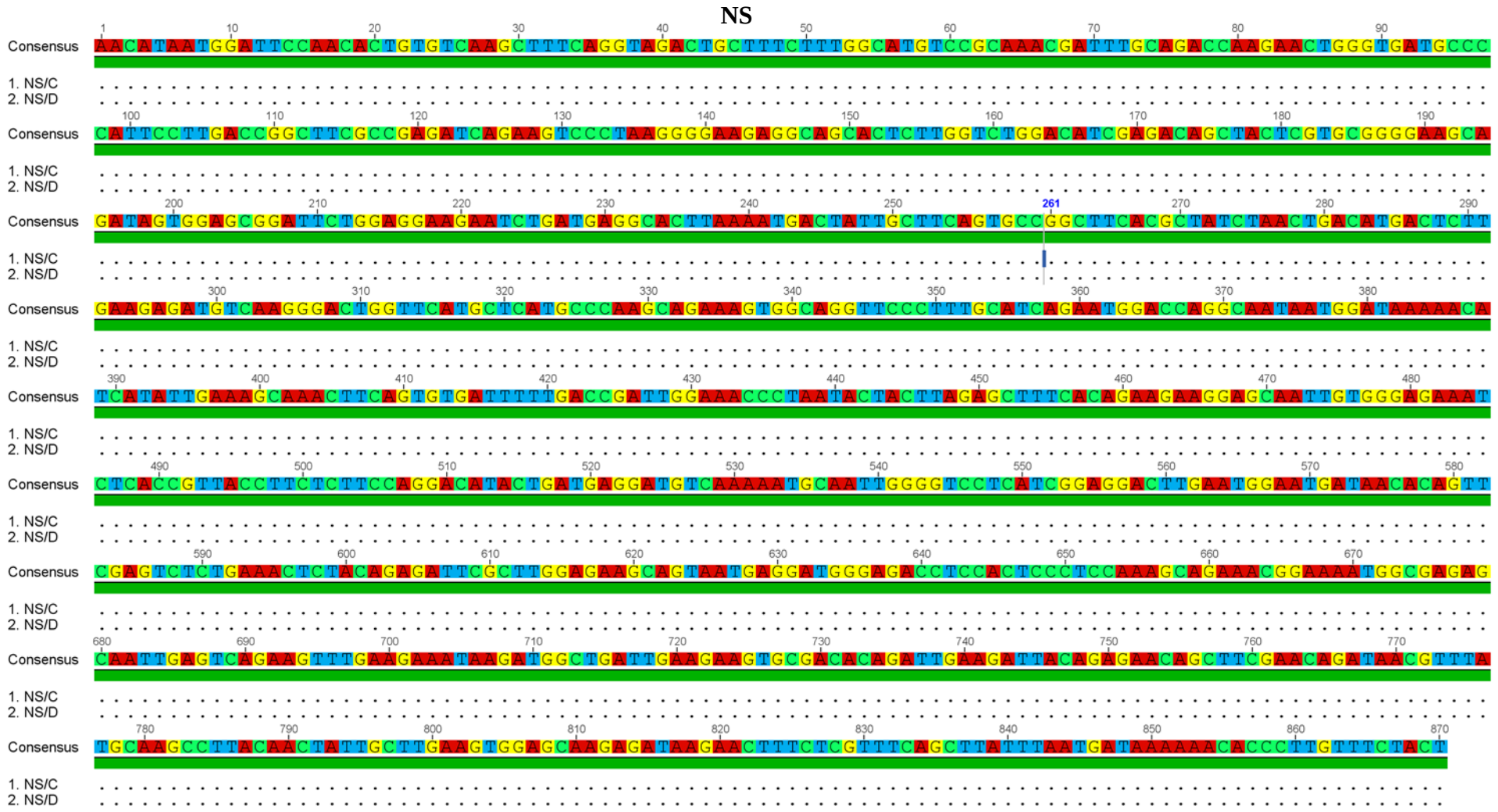

Figure III–8 Non–structural (NS) gene alignment between chicken and duck cell grown viruses. The figure shows identical sequences between the two NS genes.

NS/C: Non–structural gene sequenced from H2N3 grown on chicken cells.

NS/D: Non–structural gene sequenced from H2N3 grown on duck cells.

Appendix IV: Manufacturer's protocols

1. Viral RNA extraction

Viral RNA was extracted using QIAamp® Viral RNA Mini Kit (Qiagen) following the manufacturer's instructions. Five hundred sixty µl of AVL–carrier RNA was moved into a 1.5 mL centrifuge tube, 140 µl of allantoic fluid or culture supernatant was added to the mixture and the contents were mixed well by pulse vortexing for 15 s. The mixture was then incubated at room temperature (15 – 25˚C) for 10 min. The tube was briefly centrifuged and 560 µl of ethanol (96 – 100%) was added to the sample, mixed by pulse vortexing for 15 s.

From this mixture, 630 µl was transferred to the high filter QIAamp Mini column, and then centrifuged at 6000 xg for 1 min. The tube was placed into a clean 2 mL collection tube, and the tube containing the filtrate was discarded, then the above step was repeated. Then 500 µl of AW1 buffer was added to the QIAamp Mini column, centrifuged for 1 min at 6000 xg, then the column was placed in a clean 2 mL collection tube, and the tube containing the filtrate was discarded. Then 500 µl of buffer AW2 was added to the column and centrifuged at highest speed (20,000 xg) for 3 min to remove any residual wash buffers. The QIAamp Mini column was then inserted in a clean 1.5 mL microcentrifuge tube and viral RNA was eluted by adding 60 µl of buffer AVE, and then was centrifuged at 6000 xg for 1 min. The concentration of purified RNA was determined using a NanoDrop8000 spectrophotometer (Thermoscientific, UK) by UV absorption. Eluted viral RNA samples were stored at –80˚C until further use.

2. PCR purification

PCR product was purified using QIAquick PCR Purification Kit (Qiagen) following the manufacturer's instructions. Five volumes of buffer PB were transferred to 1 volume PCR reaction into a 1.5 mL centrifuge tube, followed by adding 10 µl of 3 M sodium acetate, pH5, to the mixture. The provided 2 mL collection tube was placed into a QIAquick column, and then the sample was added. For DNA binding, the QIAquick column containing the sample was centrifuged at 20,000 xg for 30 to 60 s. For washing, 0.75 mL of buffer PE was added to the QIAquick column, and then centrifuged at 20,000 xg for 30 to 60 s. The QIAquick column was placed in a clean 1.5 mL microcentrifuge tube. For DNA elution, 50 µl of buffer EB (10 mM Tris Cl, pH 8.5) was added to the centre of the QIAquick membrane and then the column centrifuged at 20,000 xg for 1 min. The Concentration of cleaned up DNA was determined using NanoDrop8000 spectrophotometer (Thermo Scientific, UK) by UV absorption.

3. Plasmid purification

Plasmid purification was performed using PureLink® Quick Plasmid DNA Miniprep system (Invitrogen) following the manufacturer's instructions. Five millilitres of the overnight LB culture was centrifuged at 500 xg for 5 min and the medium was removed from the tube. The pellet was re–suspended thoroughly by adding 250 µl of resuspension buffer (R3; 50 mM Tris–HCl, pH 8.0, 10 mM EDTA) with RNase A. The bacteria were lysed by adding 250 µl of pre–warmed lysis buffer (L7; 200 mM NaOH, 1% w/v SDS), mixed gently by inverting the capped tube five times and incubated at room temperature for 5 min. Three hundred and fifty microlitres of precipitation buffer were then added

and the suspension was mixed immediately by vigorously shaking the tube until the mixture was homogenous, and then centrifuged at 14000 xg for 10 min. The supernatant was then loaded onto a spin column in a 2 mL wash tube and centrifuged at 12000 xg for 1 min, the filtrate was discarded and the column was placed back into the wash tube. Five hundred microlitre of washing buffer (W10) with ethanol were uploaded into the column and centrifuged at 12000 xg for 1 min, the filtrate was discarded and the column was placed back into the washing tube. The column was then washed with W9 and ethanol by centrifuging at 12000 xg for 1 min, the filtrate was discarded and the column was centrifuged again at 12000 xg for 1 min. The spin column was then placed in a clean 1.5 mL recovery tube and 75 µl of TE buffer (10 mM Tris–HCl, pH8.0; 0.1 mM EDTA) was added to the center of the column, and incubated for 1 min at room temperature. To extract the purified plasmid, the column was centrifuged at 12000 xg for 2 min. The concentration of DNA from purified plasmid was determined using a NanoDrop8000 spectrophotometer (Thermoscientific, UK) by UV absorption.

Appendix V: List of reagents used with catalogue numbers

Reagent	Supplier and catalogue number
100 bp DNA ladder	New England BioLabs, Cat. No. N3231S
10X REACT®3	Invitrogen, Cat. No. 16303–018
1Kb DNA ladder	New England BioLabs, Cat. No. N3232S
Agar 100	Agar Scientific, Cat. No. 1043
Agarose, powder	Fisher Scientific, Cat. No. BP1356–100
Alexa Fluor® 488 Goat Anti–Chicken IgG (H+L) Antibody	Invitrogen, Cat. No. A–11039
Alexa Fluor® 488 Goat Anti–Rabbit IgG (H+L) Antibody	Invitrogen, Cat. No. A–11008
Alexa Fluor® 546 Goat Anti–Rabbit IgG (H+L) Antibody	Invitrogen, Cat. No. A11040
Alexa Fluor® 546 Phalloidin	Invitrogen, Cat. No. A22283
Amersham ECL Prime Western Blotting Detection Reagent	Scientific Laboratory, Cat. No. RPN2232
Anti–Influenza A Virus Nucleoprotein antibody (AA5H)	Abcam, Cat. No. ab20343
Anti–mouse IgG antibody, HRP–linked (for western blotting)	Cell Signaling Technology, Cat. No. 7076S
Araldite CY212 resin	TAAB, Cat. No. E006
Chloroform	Fisher Scientific, Cat. No. C/4960/PB17
Cytochalasin D	Sigma–Aldrich, Cat. No. C8273
Dibutyl phthalate	Agar Scientific, Cat. No. R1071
Dimethyl sulfoxide (DSMO), for analysis	Fisher Scientific, Cat. No. D/4121/PB08
D–MEM/F–12 (1X)	Invitrogen, Cat. No. 11039–047

Reagent	Supplier and catalogue number
DMP–30	TAAB, Cat. No. E035
Dodecenylsuccinic anhydride (DDSA)	TAAB, Cat. No. E025
Dulbecco's Modified Eagle Medium (D–MEM–1X)	Invitrogen, Cat. No. 31966–047
Dulbecco's phosphate buffered saline (DPBS)	Invitrogen, Cat. No. 31966–047
EcoRI	Invitrogen, Cat. No. 15202–013
EnVision™ + Kit HRP, Mouse (DAB+)	Dako, Cat. No. K4007
Ethidium bromide solution	Fisher Scientific Cat. No. 10375700
Fetal calf serum (FCS), qualified, heat inactivated	Invitrogen. Cat. No. 10100–147
Gel Loading Dye, Blue (6X)	New England BioLabs, Cat. No. B7021S
Glutardehyde–cocodylate buffer	Agar Scientific, Cat. No. R1010
Influenza A Matrix Protein Antibody (for western blotting)	ABD serotec, Cat. No. MCA401
JetPRIME® buffer, sterile filter 0.2 µm	Polyplus transfection, Cat No. 712–60
JetPRIME™, DNA transfection reagent	Polyplus transfection, Cat No. 114–01
Methanol	Fisher Scientific, Cat. No. M/4056/17
Nancy–520 DNA gel stain	Sigma–Aldrich, Cat. No. 01494
Novex® 14% Tris–Glycine Gels 1.0 mm, 10 well	Invitrogen, Cat. No. EC6485BOX
Novex® Tris–Glycine SDS Running Buffer (10X)	Invitrogen, Cat. No. LC2675
Nuclease–free water	Invitrogen, Cat. No. AM9937

Reagent	Supplier and catalogue number
Nutrient agar, dehydrated culture media (powder)	Thermo Scientific, Cat. No. CM0003
Nutrient broth, dehydrated culture media (powder)	Thermo Scientific, Cat. No. CM0001
Paraformaldehyde, granules	Fisher Scientific, Cat. No. P/0840/53
pCMV–GFP control vector	Cell Biolabs, Cat. No. CBA–401
pCMV–GFP–LC3 expression vector	Cell Biolabs, Cat. No. CBA–401
Penicillin–Streptomycin (penstrep), liquid	Invitrogen, Cat. No. 15140–122
Phosphate buffered saline (PBS), 1X liquid	Invitrogen, Cat. No. 10010056
Phosphate buffer saline, tablets	Invitrogen, Cat. No.18912–014
Phosphotungstic acid (2%)	Sigma, Cat. No. HT152
Prolong® Gold antifade reagent with DAPI	Invitrogen, Cat. No. P36935
Pure Link ™ Quick Plasmid meniprep kit	Invitrogen, Cat. No. K210011
QIA amp® viral RNA mini kit	Qiagen, Cat. No. 52906
QIAquick PCR Purification Kit	Qiagen, Cat. No. 28104
Reynolds lead citrate	Agar Scientific, Cat. No. R1217
SeeBlue® Pre–Stained Standard (1X)	Invitrogen, Cat. No. LC5625
SuperScript® III Platinum® One–Step Quantitative PCR System	Invitrogen, Cat. No. 11732–020
SuperScript® III Platinum® One–Step RT–PCR System with Platinum Tag High Fidelity	Invitrogen, Cat. No. 12574–030
TOPO® TA Cloning® Kit for Sequencing, with One Shot® TOP10 Chemically Competent E. coli	Invitrogen, Cat. No. K4575–J10

Reagent	Supplier and catalogue number
Tris Glycine SDS sample buffer (2X)	Invitrogen, Cat. No. LC2676
Tris Glycine SDS transfer buffer (25X)	Invitrogen, Cat. No. LC3675
Trypsin from bovine pancreas TPCK treated	Sigma–Aldrich, Cat. No. T1426
Trypsin, 2.5% (10X), liquid	Invitrogen, Cat. No. 15090–046
Tryptose phosphate broth solution	Sigma–Aldrich, Cat. No. T8159
Tween 20	Fisher Scientific, Cat. No. C58H114O26
Ultroser G, lyophilized	Pall Biosepra, Cat. No.15950–017
Urenyle acetate	AnalaR, Cat. No. 10288
Water, DNase, RNase, Protease free, 0.1 μm filtered	Sigma–Aldrich, Cat. No. W4502

References

References

ACHDOUT, H., ARNON, T. I., MARKEL, G., GONEN-GROSS, T., KATZ, G., LIEBERMAN, N., GAZIT, R., JOSEPH, A., KEDAR, E. & MANDELBOIM, O. 2003. Enhanced recognition of human NK receptors after influenza virus infection. *J Immunol,* 171**,** 915-23.

ACHENBACH, J. E. & BOWEN, R. A. 2011. Transmission of Avian Influenza A Viruses among Species in an Artificial Barnyard. *PLoS One,* 6**,** e17643.

ADA, G. L., PERRY, B. T. & ABBOT, A. 1958. Biological and physical properties of the Ryan strain of filamentous influenza virus. *J Gen Microbiol,* 19**,** 23-39.

ADAMS, S. & SANDROCK, C. 2010. Avian influenza: update. *Med Princ Pract,* 19**,** 421-32.

AIR, G. M. & LAVER, W. G. 1989. The neuraminidase of influenza virus. *Proteins,* 6**,** 341-56.

ALEXANDER, D. J. 2000. A review of avian influenza in different bird species. *Vet Microbiol,* 74**,** 3-13.

ALEXANDER, D. J. & BROWN, I. H. 2009. History of highly pathogenic avian influenza. *Rev Sci Tech,* 28**,** 19-38.

ALEXOPOULOU, L., HOLT, A. C., MEDZHITOV, R. & FLAVELL, R. A. 2001. Recognition of double-stranded RNA and activation of NF-kappaB by Toll-like receptor 3. *Nature,* 413**,** 732-8.

ALLWINN, R., PREISER, W., RABENAU, H., BUXBAUM, S., STURMER, M. & DOERR, H. W. 2002. Laboratory diagnosis of influenza--virology or serology? *Med Microbiol Immunol,* 191**,** 157-60.

ARCANGELETTI, M. C., DE CONTO, F., FERRAGLIA, F., PINARDI, F., GATTI, R., ORLANDINI, G., COVAN, S., MOTTA, F., RODIGHIERO, I., DETTORI, G. & CHEZZI, C. 2008. Host-cell-dependent role of actin cytoskeleton during the replication of a human strain of influenza A virus. *Arch Virol,* 153**,** 1209-21.

ATMAR, R. L. & KEITEL, W. A. 2009. Adjuvants for pandemic influenza vaccines. *Curr Top Microbiol Immunol,* 333**,** 323-44.

AUEWARAKUL, P., SUPTAWIWAT, O., KONGCHANAGUL, A., SANGMA, C., SUZUKI, Y., UNGCHUSAK, K., LOUISIRIROTCHANAKUL, S., LERDSAMRAN, H., POORUK, P., THITITHANYANONT, A., PITTAYAWONGANON, C., GUO, C. T., HIRAMATSU, H., JAMPANGERN, W., CHUNSUTTHIWAT, S. & PUTHAVATHANA, P. 2007. An Avian

Influenza H5N1 Virus That Binds to a Human-Type Receptor. *Journal of Virology,* 81**,** 9950-9955.

AVALOS, R. T., YU, Z. & NAYAK, D. P. 1997. Association of influenza virus NP and M1 proteins with cellular cytoskeletal elements in influenza virus-infected cells. *J Virol,* 71**,** 2947-58.

BACHI, T., GERHARD, W., LINDENMANN, J. & MUHLETHALER, K. 1969. Morphogenesis of influenza A virus in Ehrlich ascites tumor cells as revealed by thin-sectioning and freeze-etching. *J Virol,* 4**,** 769-76.

BANCROFT, C. T. & PARSLOW, T. G. 2002. Evidence for segment-nonspecific packaging of the influenza a virus genome. *J Virol,* 76**,** 7133-9.

BEALE, R., WISE, H., STUART, A., RAVENHILL, BENJAMIN J., DIGARD, P. & RANDOW, F. 2014. A LC3-Interacting Motif in the Influenza A Virus M2 Protein Is Required to Subvert Autophagy and Maintain Virion Stability. *Cell host & microbe,* 15**,** 239-247.

BIDZHIEVA, B., ZAGORODNYAYA, T., KARAGIANNIS, K., SIMONYAN, V., LAASSRI, M. & CHUMAKOV, K. 2014. Deep sequencing approach for genetic stability evaluation of influenza A viruses. *J Virol Methods***,** 68-75.

BLASKOVIC, P. & LABZOFFSKY, N. A. 1973. Immunofluorescence methods for detection of influenza and mumps antibodies using infected shedded allantoic cells and impression smears of organ cultures as the sources of antigens. *Arch Gesamte Virusforsch,* 41**,** 354-9.

BLASKOVIC, P., RHODES, A., DOANE, F. & LABZOFFSKY, N. 1972. Infection of chick embryo tracheal organ cultures with influenza A2 (Hong Kong) virus. *Arch Gesamte Virusforsch,* 38**,** 250-266.

BOHN, W., MANNWEILER, K., HOHENBERG, H. & RUTTER, G. 1987. Replica-immunogold technique applied to studies on measles virus morphogenesis. *Scanning Microsc,* 1**,** 319-30.

BOIVIN, S., CUSACK, S., RUIGROK, R. W. & HART, D. J. 2010. Influenza A virus polymerase: structural insights into replication and host adaptation mechanisms. *J Biol Chem,* 285**,** 28411-7.

BOULO, S., AKARSU, H., RUIGROK, R. W. & BAUDIN, F. 2007. Nuclear traffic of influenza virus proteins and ribonucleoprotein complexes. *Virus Res,* 124**,** 12-21.

BOULOY, M., PLOTCH, S. J. & KRUG, R. M. 1978. Globin mRNAs are primers for the transcription of influenza viral RNA in vitro. *Proc Natl Acad Sci U S A,* 75**,** 4886-90.

BOURMAKINA, S. V. & GARCIA-SASTRE, A. 2003. Reverse genetics studies on the filamentous morphology of influenza A virus. *J Gen Virol,* 84**,** 517-27.

BOUVIER, N. M. & PALESE, P. 2008. The biology of influenza viruses. *Vaccine,* 26 Suppl 4**,** D49-53.

BRUCE, E. A., DIGARD, P. & STUART, A. D. 2010. The Rab11 pathway is required for influenza A virus budding and filament formation. *J Virol,* 84**,** 5848-59.

BRYDON, E. W., MORRIS, S. J. & SWEET, C. 2005. Role of apoptosis and cytokines in influenza virus morbidity. *FEMS Microbiol Rev,* 29**,** 837-50.

BUBB, M. R., SENDEROWICZ, A. M., SAUSVILLE, E. A., DUNCAN, K. L. & KORN, E. D. 1994. Jasplakinolide, a cytotoxic natural product, induces actin polymerization and competitively inhibits the binding of phalloidin to F-actin. *J Biol Chem,* 269**,** 14869-71.

BURLEIGH, L. M., CALDER, L. J., SKEHEL, J. J. & STEINHAUER, D. A. 2005. Influenza a viruses with mutations in the m1 helix six domain display a wide variety of morphological phenotypes. *J Virol,* 79**,** 1262-70.

CADY, S. D., LUO, W., HU, F. & HONG, M. 2009. Structure and function of the influenza A M2 proton channel. *Biochemistry,* 48**,** 7356-64.

CALDER, L. J., WASILEWSKI, S., BERRIMAN, J. A. & ROSENTHAL, P. B. 2010. Structural organization of a filamentous influenza A virus. *Proc Natl Acad Sci U S A,* 107**,** 10685-90.

CAPUA, I. & ALEXANDER, D. J. 2009. Avian influenza infection in birds: a challenge and opportunity for the poultry veterinarian. *Poult Sci,* 88**,** 842-6.

CAUSEY, D. & EDWARDS, S. V. 2008. Ecology of avian influenza virus in birds. *J Infect Dis,* 197 Suppl 1**,** S29-33.

CHEN, J. & DENG, Y. M. 2009. Influenza virus antigenic variation, host antibody production and new approach to control epidemics. *Virol J,* 6**,** 30.

CHEN, W., CALVO, P. A., MALIDE, D., GIBBS, J., SCHUBERT, U., BACIK, I., BASTA, S., O'NEILL, R., SCHICKLI, J., PALESE, P., HENKLEIN, P., BENNINK, J. R. & YEWDELL, J. W. 2001. A novel influenza A virus mitochondrial protein that induces cell death. *Nat Med,* 7**,** 1306-12.

CHEUNG, T. K. & POON, L. L. 2007. Biology of influenza a virus. *Ann N Y Acad Sci,* 1102**,** 1-25.

CHOPPIN, P. W., MURPHY, J. S. & STOECKENIUS, W. 1961. The surface structure of influenza virus filaments. *Virology,* 13**,** 548-50.

CHU, C. M., DAWSON, I. M. & ELFORD, W. J. 1949. Filamentous forms associated with newly isolated influenza virus. *Lancet,* 1**,** 602.

COLLIER, L. & OXFORD, J. 2006. *Human virology : a text for students of medicine, dentistry and microbiology* Oxford : Oxford University Press.

COLOMA, R., VALPUESTA, J. M., ARRANZ, R., CARRASCOSA, J. L., ORTIN, J. & MARTIN-BENITO, J. 2009. The structure of a biologically active influenza virus ribonucleoprotein complex. *PLoS Pathog,* 5**,** e1000491.

CONNOR, R. J., KAWAOKA, Y., WEBSTER, R. G. & PAULSON, J. C. 1994. Receptor specificity in human, avian, and equine H2 and H3 influenza virus isolates. *Virology,* 205**,** 17-23.

COUCEIRO, J. N., PAULSON, J. C. & BAUM, L. G. 1993. Influenza virus strains selectively recognize sialyloligosaccharides on human respiratory epithelium; the role of the host cell in selection of hemagglutinin receptor specificity. *Virus Res,* 29**,** 155-65.

COUE, M., BRENNER, S. L., SPECTOR, I. & KORN, E. D. 1987. Inhibition of actin polymerization by latrunculin A. *FEBS Lett,* 213**,** 316-8.

COX, J. C., HAMPSON, A. W. & HAMILTON, R. C. 1980. An immunofluorescence study of influenza virus filament formation. *Arch Virol,* 63**,** 275-84.

DAIDOJI, T., KOMA, T., DU, A., YANG, C. S., UEDA, M., IKUTA, K. & NAKAYA, T. 2008. H5N1 avian influenza virus induces apoptotic cell death in mammalian airway epithelial cells. *J Virol,* 82**,** 11294-307.

DAS, K., ARAMINI, J. M., MA, L. C., KRUG, R. M. & ARNOLD, E. 2010. Structures of influenza A proteins and insights into antiviral drug targets. *Nat Struct Mol Biol,* 17**,** 530-8.

DAVID M. KNIPE, P. M. H. 2007. *Fields Virology,* Philadelphia, USA, Lippincott Williams & Wilkins (LWW).

DETJEN, B. M., ST ANGELO, C., KATZE, M. G. & KRUG, R. M. 1987. The three influenza virus polymerase (P) proteins not associated with viral nucleocapsids in the infected cell are in the form of a complex. *J Virol,* 61**,** 16-22.

DIGARD, P., ELTON, D., BISHOP, K., MEDCALF, E., WEEDS, A. & POPE, B. 1999. Modulation of nuclear localization of the influenza virus nucleoprotein through interaction with actin filaments. *J Virol,* 73**,** 2222-31.

DOMINGO, E., SHELDON, J. & PERALES, C. 2012. Viral quasispecies evolution. *Microbiol Mol Biol Rev,* 76**,** 159-216.

DU, J., CROSS, T. A. & ZHOU, H. X. 2012. Recent progress in structure-based anti-influenza drug design. *Drug Discov Today*.

DWYER, D. E., SMITH, D. W., CATTON, M. G. & BARR, I. G. 2006. Laboratory diagnosis of human seasonal and pandemic influenza virus infection. *Med J Aust,* 185**,** S48-53.

ELLEMAN, C. J. & BARCLAY, W. S. 2004. The M1 matrix protein controls the filamentous phenotype of influenza A virus. *Virology,* 321**,** 144-53.

ELLIS, J. S., FLEMING, D. M. & ZAMBON, M. C. 1997. Multiplex reverse transcription-PCR for surveillance of influenza A and B viruses in England and Wales in 1995 and 1996. *J Clin Microbiol,* 35**,** 2076-82.

ELLIS, J. S. & ZAMBON, M. C. 2002. Molecular diagnosis of influenza. *Rev Med Virol,* 12**,** 375-89.

FOUCHIER, R. A., BESTEBROER, T. M., HERFST, S., VAN DER KEMP, L., RIMMELZWAAN, G. F. & OSTERHAUS, A. D. 2000. Detection of influenza A viruses from different species by PCR amplification of conserved sequences in the matrix gene. *J Clin Microbiol,* 38**,** 4096-101.

GABRIEL, G., CZUDAI-MATWICH, V. & KLENK, H. D. 2013. Adaptive mutations in the H5N1 polymerase complex. *Virus Res*.

GAUSH, C. R. & SMITH, T. F. 1968. Replication and plaque assay of influenza virus in an established line of canine kidney cells. *Appl Microbiol,* 16**,** 588-94.

GOLDSMITH, C. S. & MILLER, S. E. 2009. Modern uses of electron microscopy for detection of viruses. *Clin Microbiol Rev,* 22**,** 552-63.

GOMEZ-PUERTAS, P., ALBO, C., PEREZ-PASTRANA, E., VIVO, A. & PORTELA, A. 2000. Influenza virus matrix protein is the major driving force in virus budding. *J Virol,* 74**,** 11538-47.

GOVORKOVA, E. A., KODIHALLI, S., ALYMOVA, I. V., FANGET, B. & WEBSTER, R. G. 1999. Growth and immunogenicity of influenza viruses cultivated in Vero or MDCK cells and in embryonated chicken eggs. *Dev Biol Stand,* 98**,** 39-51; discussion 73-4.

GRANTHAM, M. L., WU, W. H., LALIME, E. N., LORENZO, M. E., KLEIN, S. L. & PEKOSZ, A. 2009. Palmitoylation of the influenza A virus M2 protein is not

required for virus replication in vitro but contributes to virus virulence. *J Virol,* 83**,** 8655-61.

GREENBAUM, E., MORAG, A. & ZAKAY-RONES, Z. 1998. Isolation of influenza C virus during an outbreak of influenza A and B viruses. *J Clin Microbiol,* 36**,** 1441-2.

GUBAREVA, L. V., KAISER, L. & HAYDEN, F. G. 2000. Influenza virus neuraminidase inhibitors. *Lancet,* 355**,** 827-35.

HALE, B. G., RANDALL, R. E., ORTIN, J. & JACKSON, D. 2008. The multifunctional NS1 protein of influenza A viruses. *J Gen Virol,* 89**,** 2359-76.

HAMPSON, A. W. & MACKENZIE, J. S. 2006. The influenza viruses. *Med J Aust,* 185**,** S39-43.

HAY, A. J., ZAMBON, M. C., WOLSTENHOLME, A. J., SKEHEL, J. J. & SMITH, M. H. 1986. Molecular basis of resistance of influenza A viruses to amantadine. *J Antimicrob Chemother,* 18 Suppl B**,** 19-29.

HAYDEN, F. G., GWALTNEY, J. M., JR., VAN DE CASTLE, R. L., ADAMS, K. F. & GIORDANI, B. 1981. Comparative toxicity of amantadine hydrochloride and rimantadine hydrochloride in healthy adults. *Antimicrob Agents Chemother,* 19**,** 226-33.

HAZELTON, P. R. & GELDERBLOM, H. R. 2003. Electron microscopy for rapid diagnosis of infectious agents in emergent situations. *Emerg Infect Dis,* 9**,** 294-303.

HEID, C. A., STEVENS, J., LIVAK, K. J. & WILLIAMS, P. M. 1996. Real time quantitative PCR. *Genome Res,* 6**,** 986-94.

HOFFMANN, E., STECH, J., GUAN, Y., WEBSTER, R. G. & PEREZ, D. R. 2001. Universal primer set for the full-length amplification of all influenza A viruses. *Arch Virol,* 146**,** 2275-89.

HOLMES, E. C., GHEDIN, E., MILLER, N., TAYLOR, J., BAO, Y., ST GEORGE, K., GRENFELL, B. T., SALZBERG, S. L., FRASER, C. M., LIPMAN, D. J. & TAUBENBERGER, J. K. 2005. Whole-genome analysis of human influenza A virus reveals multiple persistent lineages and reassortment among recent H3N2 viruses. *PLoS Biol,* 3**,** e300.

HOLSINGER, L. J., NICHANI, D., PINTO, L. H. & LAMB, R. A. 1994. Influenza A virus M2 ion channel protein: a structure-function analysis. *J Virol,* 68**,** 1551-63.

HORIMOTO, T. & KAWAOKA, Y. 2001. Pandemic threat posed by avian influenza A viruses. *Clin Microbiol Rev,* 14**,** 129-49.

HORIMOTO, T. & KAWAOKA, Y. 2005. Influenza: lessons from past pandemics, warnings from current incidents. *Nat Rev Microbiol,* 3**,** 591-600.

HSU, M. T., PARVIN, J. D., GUPTA, S., KRYSTAL, M. & PALESE, P. 1987. Genomic RNAs of influenza viruses are held in a circular conformation in virions and in infected cells by a terminal panhandle. *Proc Natl Acad Sci U S A,* 84**,** 8140-4.

HUGHEY, P. G., ROBERTS, P. C., HOLSINGER, L. J., ZEBEDEE, S. L., LAMB, R. A. & COMPANS, R. W. 1995. Effects of antibody to the influenza A virus M2 protein on M2 surface expression and virus assembly. *Virology,* 212**,** 411-21.

HURT, A. C., HO, H. T. & BARR, I. 2006. Resistance to anti-influenza drugs: adamantanes and neuraminidase inhibitors. *Expert Rev Anti Infect Ther,* 4**,** 795-805.

HUTCHINSON, E. C., VON KIRCHBACH, J. C., GOG, J. R. & DIGARD, P. 2010. Genome packaging in influenza A virus. *J Gen Virol,* 91**,** 313-28.

INNIS, M. A., MYAMBO, K. B., GELFAND, D. H. & BROW, M. A. 1988. DNA sequencing with Thermus aquaticus DNA polymerase and direct sequencing of polymerase chain reaction-amplified DNA. *Proc Natl Acad Sci U S A,* 85**,** 9436-40.

ITO, T. & KAWAOKA, Y. 2000. Host-range barrier of influenza A viruses. *Vet Microbiol,* 74**,** 71-5.

IWATSUKI-HORIMOTO, K., HORIMOTO, T., FUJII, Y. & KAWAOKA, Y. 2004. Generation of influenza A virus NS2 (NEP) mutants with an altered nuclear export signal sequence. *J Virol,* 78**,** 10149-55.

JAGGER, B. W., WISE, H. M., KASH, J. C., WALTERS, K. A., WILLS, N. M., XIAO, Y. L., DUNFEE, R. L., SCHWARTZMAN, L. M., OZINSKY, A., BELL, G. L., DALTON, R. M., LO, A., EFSTATHIOU, S., ATKINS, J. F., FIRTH, A. E., TAUBENBERGER, J. K. & DIGARD, P. 2012. An overlapping protein-coding region in influenza A virus segment 3 modulates the host response. *Science,* 337**,** 199-204.

JEONG, O. M., KIM, M. C., KIM, M. J., KANG, H. M., KIM, H. R., KIM, Y. J., JOH, S. J., KWON, J. H. & LEE, Y. J. 2009. Experimental infection of chickens, ducks and quails with the highly pathogenic H5N1 avian influenza virus. *J Vet Sci,* 10**,** 53-60.

JIN, H., LESER, G. P., ZHANG, J. & LAMB, R. A. 1997. Influenza virus hemagglutinin and neuraminidase cytoplasmic tails control particle shape. *EMBO J,* 16**,** 1236-47.

JOHNSON, J., HIGGINS, A., NAVARRO, A., HUANG, Y., ESPER, F. L., BARTON, N., ESCH, D., SHAW, C., OLIVO, P. D. & MIAO, L. Y. 2012. Subtyping influenza A virus with monoclonal antibodies and an indirect immunofluorescence assay. *J Clin Microbiol,* 50**,** 396-400.

JUOZAPAITIS, M. & ANTONIUKAS, L. 2007. [Influenza virus]. *Medicina (Kaunas),* 43**,** 919-29.

KANG, W., PANG, W., HAO, J. & ZHAO, D. 2006. Isolation of avian influenza virus (H9N2) from emu in China. *Ir Vet J,* 59**,** 148-52.

KHANNA, M., KUMAR, P., CHOUDHARY, K., KUMAR, B. & VIJAYAN, V. K. 2008. Emerging influenza virus: a global threat. *J Biosci,* 33**,** 475-82.

KILBOURNE, E. D. & MURPHY, J. S. 1960. Genetic studies of influenza viruses. I. Viral morphology and growth capacity as exchangeable genetic traits. Rapid in ovo adaptation of early passage Asian strain isolates by combination with PR8. *J Exp Med,* 111**,** 387-406.

KIM, J. K., NEGOVETICH, N. J., FORREST, H. L. & WEBSTER, R. G. 2009. Ducks: the "Trojan horses" of H5N1 influenza. *Influenza Other Respi Viruses,* 3**,** 121-8.

KISHIDA, N., SAKODA, Y., ISODA, N., MATSUDA, K., ETO, M., SUNAGA, Y., UMEMURA, T. & KIDA, H. 2005. Pathogenicity of H5 influenza viruses for ducks. *Arch Virol,* 150**,** 1383-92.

KLENK, H. D. & GARTEN, W. 1994. Host cell proteases controlling virus pathogenicity. *Trends Microbiol,* 2**,** 39-43.

KOHHEI T. & ISHII, K. J. 2012. Adjuvants in influenza vaccines. *Vaccine,* 30**,** 7658-7661.

KONG, W. P., HOOD, C., YANG, Z. Y., WEI, C. J., XU, L., GARCIA-SASTRE, A., TUMPEY, T. M. & NABEL, G. J. 2006. Protective immunity to lethal challenge of the 1918 pandemic influenza virus by vaccination. *Proc Natl Acad Sci U S A,* 103**,** 15987-91.

KREIJTZ, J. H., FOUCHIER, R. A. & RIMMELZWAAN, G. F. 2011. Immune responses to influenza virus infection. *Virus Res,* 162**,** 19-30.

KROWCZYNSKA, A. M. & HENDERSON, M. B. 1992. Efficient purification of PCR products using ultrafiltration. *Biotechniques,* 13**,** 286-9.

KUCHIPUDI, S. V. 2010. *Studies on the cellular and molecular mechanisms of innate host susceptibility and resistance to influenza A viruses in chicken and ducks.* PhD, University of Glasgow.

KUCHIPUDI, S. V., DUNHAM, S. P., NELLI, R., WHITE, G. A., COWARD, V. J., SLOMKA, M. J., BROWN, I. H. & CHANG, K. C. 2011. Rapid death of duck cells infected with influenza: a potential mechanism for host resistance to H5N1. *Immunol Cell Biol,* 90**,** 116-123.

KUCHIPUDI, S. V., NELLI, R., WHITE, G. A., BAIN, M., CHANG, K. C. & DUNHAM, S. 2009. Differences in influenza virus receptors in chickens and ducks: Implications for interspecies transmission. *J Mol Genet Med,* 3**,** 143-51.

LAEMMLI, U. K. 1970. Cleavage of structural proteins during the assembly of the head of bacteriophage T4. *Nature,* 227**,** 680-5.

LATHAM, T. & GALARZA, J. M. 2001. Formation of wild-type and chimeric influenza virus-like particles following simultaneous expression of only four structural proteins. *J Virol,* 75**,** 6154-65.

LEONARD, J. T., GRACE, M. B., BUZARD, G. S., MULLEN, M. J. & BARBAGALLO, C. B. 1998. Preparation of PCR products for DNA sequencing. *Biotechniques,* 24**,** 314-7.

LI, I., CHAN, K., TO, K., WONG, S., HO, P., LAU, S., WOO, P., TSOI, H., CHAN, J. & CHENG, V. 2009. Differential susceptibility of different cell lines to swine-origin influenza A H1N1, seasonal human influenza A H1N1, and avian influenza A H5N1 viruses. *Journal of Clinical Virology,* 46**,** 325-330.

LIANG, Q.-L., LUO, J., ZHOU, K., DONG, J.-X. & HE, H.-X. 2011. Immune-related gene expression in response to H5N1 avian influenza virus infection in chicken and duck embryonic fibroblasts. *Molecular immunology,* 48**,** 924-930.

LIU, N., WANG, G., LEE, K. C., GUAN, Y., CHEN, H. & CAI, Z. 2009. Mutations in influenza virus replication and transcription: detection of amino acid substitutions in hemagglutinin of an avian influenza virus (H1N1). *FASEB J,* 23**,** 3377-82.

LOHMEYER, J., TALENS, L. T. & KLENK, H. D. 1979. Biosynthesis of the influenza virus envelope in abortive infection. *J Gen Virol,* 42**,** 73-88.

LUND, J. M., ALEXOPOULOU, L., SATO, A., KAROW, M., ADAMS, N. C., GALE, N. W., IWASAKI, A. & FLAVELL, R. A. 2004. Recognition of single-stranded RNA viruses by Toll-like receptor 7. *Proc Natl Acad Sci U S A,* 101**,** 5598-603.

LUPIANI, B. & REDDY, S. M. 2009. The history of avian influenza. *Comp Immunol Microbiol Infect Dis,* 32**,** 311-23.

MA, W., KAHN, R. E. & RICHT, J. A. 2008. The pig as a mixing vessel for influenza viruses: Human and veterinary implications. *J Mol Genet Med,* 3**,** 158-66.

MATROSOVICH, M. N., MATROSOVICH, T. Y., GRAY, T., ROBERTS, N. A. & KLENK, H. D. 2004. Human and avian influenza viruses target different cell types in cultures of human airway epithelium. *Proc Natl Acad Sci U S A,* 101**,** 4620-4.

MAZANEC, M. B., COUDRET, C. L. & FLETCHER, D. R. 1995. Intracellular neutralization of influenza virus by immunoglobulin A anti-hemagglutinin monoclonal antibodies. *J Virol,* 69**,** 1339-43.

MCAULEY, J. L., ZHANG, K. & MCCULLERS, J. A. 2010. The effects of influenza A virus PB1-F2 protein on polymerase activity are strain specific and do not impact pathogenesis. *J Virol,* 84**,** 558-64.

MCCAULEY, J. W. & MAHY, B. W. 1983. Structure and function of the influenza virus genome. *Biochem J,* 211**,** 281-94.

MCCOWN, M. F. & PEKOSZ, A. 2005. The influenza A virus M2 cytoplasmic tail is required for infectious virus production and efficient genome packaging. *J Virol,* 79**,** 3595-605.

MCGILL, J., HEUSEL, J. W. & LEGGE, K. L. 2009. Innate immune control and regulation of influenza virus infections. *J Leukoc Biol,* 86**,** 803-12.

METZGAR, D., MYERS, C. A., RUSSELL, K. L., FAIX, D., BLAIR, P. J., BROWN, J., VO, S., SWAYNE, D. E., THOMAS, C., STENGER, D. A., LIN, B., MALANOSKI, A. P., WANG, Z., BLANEY, K. M., LONG, N. C., SCHNUR, J. M., SAAD, M. D., BORSUK, L. A., LICHANSKA, A. M., LORENCE, M. C., WESLOWSKI, B., SCHAFER, K. O. & TIBBETTS, C. 2010. Single assay for simultaneous detection and differential identification of human and avian influenza virus types, subtypes, and emergent variants. *PLoS One,* 5**,** e8995.

MICHAELIS, M., DOERR, H. W. & CINATL, J., JR. 2009. Novel swine-origin influenza A virus in humans: another pandemic knocking at the door. *Med Microbiol Immunol,* 198**,** 175-83.

MILLER, S. E. 1986. Detection and Identification of Viruses by Electron Microscopy. *ELECTRON MICROSCOPY TECHNIQUE,* 4**,** 265-301.

MITNAUL, L. J., MATROSOVICH, M. N., CASTRUCCI, M. R., TUZIKOV, A. B., BOVIN, N. V., KOBASA, D. & KAWAOKA, Y. 2000. Balanced hemagglutinin and neuraminidase activities are critical for efficient replication of influenza A virus. *J Virol,* 74**,** 6015-20.

MONTALTO, N. J., GUM, K. D. & ASHLEY, J. V. 2000. Updated treatment for influenza A and B. *Am Fam Physician,* 62**,** 2467-76.

MONTO, A. S., MAASSAB, H. F. & BRYAN, E. R. 1981. Relative efficacy of embryonated eggs and cell culture for isolation of contemporary influenza viruses. *J Clin Microbiol,* 13**,** 233-5.

MOSCONA, A. 2005. Neuraminidase inhibitors for influenza. *N Engl J Med,* 353**,** 1363-73.

MULLIS, K. B. 1990. The unusual origin of the polymerase chain reaction. *Sci Am,* 262**,** 56-61, 64-5.

MUNDT, E., GAY, L., JONES, L., SAAVEDRA, G., TOMPKINS, S. M. & TRIPP, R. A. 2009. Replication and pathogenesis associated with H5N1, H5N2, and H5N3 low-pathogenic avian influenza virus infection in chickens and ducks. *Arch Virol,* 154**,** 1241-8.

MUNSTER, V. J., BAAS, C., LEXMOND, P., WALDENSTROM, J., WALLENSTEN, A., FRANSSON, T., RIMMELZWAAN, G. F., BEYER, W. E., SCHUTTEN, M., OLSEN, B., OSTERHAUS, A. D. & FOUCHIER, R. A. 2007. Spatial, temporal, and species variation in prevalence of influenza A viruses in wild migratory birds. *PLoS Pathog,* 3**,** e61.

NAEVE, C. W., HINSHAW, V. S. & WEBSTER, R. G. 1984. Mutations in the hemagglutinin receptor-binding site can change the biological properties of an influenza virus. *J Virol,* 51**,** 567-9.

NAFFAKH, N., TOMOIU, A., RAMEIX-WELTI, M. A. & VAN DER WERF, S. 2008. Host restriction of avian influenza viruses at the level of the ribonucleoproteins. *Annu Rev Microbiol,* 62**,** 403-24.

NAYAK, D. P., BALOGUN, R. A., YAMADA, H., ZHOU, Z. H. & BARMAN, S. 2009. Influenza virus morphogenesis and budding. *Virus Res,* 143**,** 147-61.

NAYAK, D. P., HUI, E. K. & BARMAN, S. 2004. Assembly and budding of influenza virus. *Virus Res,* 106**,** 147-65.

NELLI, R. K., KUCHIPUDI, S. V., WHITE, G. A., PEREZ, B. B., DUNHAM, S. P. & CHANG, K. C. 2010. Comparative distribution of human and avian type sialic acid influenza receptors in the pig. *BMC Vet Res,* 6**,** 4.

NELSON, M. I., EDELMAN, L., SPIRO, D. J., BOYNE, A. R., BERA, J., HALPIN, R., SENGAMALAY, N., GHEDIN, E., MILLER, M. A., SIMONSEN, L., VIBOUD, C. & HOLMES, E. C. 2008. Molecular epidemiology of A/H3N2 and A/H1N1 influenza virus during a single epidemic season in the United States. *PLoS Pathog,* 4**,** e1000133.

NELSON, M. I. & HOLMES, E. C. 2007. The evolution of epidemic influenza. *Nat Rev Genet,* 8**,** 196-205.

NEUMANN, G., CHEN, H., GAO, G. F., SHU, Y. & KAWAOKA, Y. 2009a. H5N1 influenza viruses: outbreaks and biological properties. *Cell Research,* 20**,** 51-61.

NEUMANN, G., NODA, T. & KAWAOKA, Y. 2009b. Emergence and pandemic potential of swine-origin H1N1 influenza virus. *Nature,* 459**,** 931-9.

NODA, T. 2011. Native morphology of influenza virions. *Front Microbiol,* 2**,** 269.

NODA, T. & KAWAOKA, Y. 2010. Structure of influenza virus ribonucleoprotein complexes and their packaging into virions. *Rev Med Virol,* 20**,** 380-91.

NODA, T., SAGARA, H., YEN, A., TAKADA, A., KIDA, H., CHENG, R. H. & KAWAOKA, Y. 2006. Architecture of ribonucleoprotein complexes in influenza A virus particles. *Nature,* 439**,** 490-2.

ODAGIRI, T. 1992. [Structure and function of the influenza virus genome]. *Tanpakushitsu Kakusan Koso,* 37**,** 2428-34.

ORSTAVIK, I., GRANDIEN, M., HALONEN, P., ARSTILA, P., MORDHORST, C. H., HORNSLETH, A., POPOW-KRAUPP, T., MCQUILLIN, J., GARDNER, P. S., ALMEIDA, J. & ET AL. 1984. Viral diagnoses using the rapid immunofluorescence technique and epidemiological implications of acute respiratory infections among children in different European countries. *Bull World Health Organ,* 62**,** 307-13.

OSTERHAUS, A. D., RIMMELZWAAN, G. F., MARTINA, B. E., BESTEBROER, T. M. & FOUCHIER, R. A. 2000. Influenza B virus in seals. *Science,* 288**,** 1051-3.

PALESE, P. & SHAW, M. 2007. Orthomyxoviridae: The Viruses and Their Replication. *Fields Virology***,** 1647–1689.

PALESE, P., TOBITA, K., UEDA, M. & COMPANS, R. W. 1974. Characterization of temperature sensitive influenza virus mutants defective in neuraminidase. *Virology,* 61**,** 397-410.

PANG, I. K. & IWASAKI, A. 2011. Inflammasomes as mediators of immunity against influenza virus. *Trends Immunol,* 32**,** 34-41.

PATRICK, J. V. & RICHARD, B. T. 2003. Review of Rapid Diagnostic Tests for Influenza. *Clinical and Applied Immunology,* 4**,** 151-172.

PAUL TAMBYAH & LEUNG, P.-C. 2006. *Bird flu : a rising pandemic in Asia and beyond?* , Singapore ; Hackensack, NJ : World Scientific.

PEIRIS, J. S. M., DE JONG, M. D. & GUAN, Y. 2007. Avian Influenza Virus (H5N1): a Threat to Human Health. *Clinical Microbiology Reviews,* 20**,** 243-267.

PILLAI, S. P. & LEE, C. W. 2010. Species and age related differences in the type and distribution of influenza virus receptors in different tissues of chickens, ducks and turkeys. *Virol J,* 7**,** 5.

PILLAI, S. P., PANTIN-JACKWOOD, M., SUAREZ, D. L., SAIF, Y. M. & LEE, C. W. 2010. Pathobiological characterization of low-pathogenicity H5 avian influenza viruses of diverse origins in chickens, ducks and turkeys. *Arch Virol,* 155**,** 1439-51.

PINTO, L. H. & LAMB, R. A. 2006. The M2 proton channels of influenza A and B viruses. *J Biol Chem,* 281**,** 8997-9000.

PISAREVA, M., BECHTEREVA, T., PLYUSNIN, A., DOBRETSOVA, A. & KISSELEV, O. 1992. PCR-amplification of influenza A virus specific sequences. *Arch Virol,* 125**,** 313-8.

PORTELA, A. & DIGARD, P. 2002. The influenza virus nucleoprotein: a multifunctional RNA-binding protein pivotal to virus replication. *J Gen Virol,* 83**,** 723-34.

PRINCE, H. E. & LEBER, A. L. 2003. Comparison of complement fixation and hemagglutination inhibition assays for detecting antibody responses following influenza virus vaccination. *Clin Diagn Lab Immunol,* 10**,** 481-2.

RAO, S. S., STYLES, D., KONG, W., ANDREWS, C., GORRES, J. P. & NABEL, G. J. 2009. A gene-based avian influenza vaccine in poultry. *Poult Sci,* 88**,** 860-6.

REEVE, P., GERENDAS, B. & WALZL, H. 1978. Growth of some attenuated influenza viruses in hamster tracheal organ cultures. *Med Microbiol Immunol,* 166**,** 141-150.

REINA, J., FERNANDEZ-BACA, V., BLANCO, I. & MUNAR, M. 1997. Comparison of Madin-Darby canine kidney cells (MDCK) with a green monkey continuous cell line (Vero) and human lung embryonated cells (MRC-5) in the isolation of influenza A virus from nasopharyngeal aspirates by shell vial culture. *J Clin Microbiol,* 35**,** 1900-1901.

REPERANT, L. A., RIMMELZWAAN, G. F. & KUIKEN, T. 2009. Avian influenza viruses in mammals. *Rev Sci Tech,* 28**,** 137-59.

ROBB, N. C., SMITH, M., VREEDE, F. T. & FODOR, E. 2009. NS2/NEP protein regulates transcription and replication of the influenza virus RNA genome. *J Gen Virol,* 90**,** 1398-407.

ROBERTS, K. L., LESER, G. P., MA, C. & LAMB, R. A. 2013. The amphipathic helix of influenza A virus M2 protein is required for filamentous bud formation and scission of filamentous and spherical particles. *J Virol,* 87**,** 9973-82.

ROBERTS, P. C. & COMPANS, R. W. 1998. Host cell dependence of viral morphology. *Proc Natl Acad Sci U S A,* 95**,** 5746-51.

ROBERTS, P. C., LAMB, R. A. & COMPANS, R. W. 1998. The M1 and M2 proteins of influenza A virus are important determinants in filamentous particle formation. *Virology,* 240**,** 127-37.

RODRIGUEZ BOULAN, E. & SABATINI, D. D. 1978. Asymmetric budding of viruses in epithelial monlayers: a model system for study of epithelial polarity. *Proc Natl Acad Sci U S A,* 75**,** 5071-5.

ROINGEARD, P. 2008. Viral detection by electron microscopy: past, present and future. *Biol Cell,* 100**,** 491-501.

ROSSMAN, J. S. & LAMB, R. A. 2011. Influenza virus assembly and budding. *Virology,* 411**,** 229-36.

RUSKA, H., BORRIES, B. V. & RUSKA, E. 1939. Die Bedeutung der Übermikroskopie für die Virusforschung. *Arch Gesamte Virusforsch,* 1**,** 155-169.

RUST, M. J., LAKADAMYALI, M., ZHANG, F. & ZHUANG, X. 2004. Assembly of endocytic machinery around individual influenza viruses during viral entry. *Nat Struct Mol Biol,* 11**,** 567-73.

SAMJI, T. 2009. Influenza A: understanding the viral life cycle. *Yale J Biol Med,* 82**,** 153-9.

SAVILL, N. J., ST ROSE, S. G., KEELING, M. J. & WOOLHOUSE, M. E. 2006. Silent spread of H5N1 in vaccinated poultry. *Nature,* 442**,** 757.

SCHLIWA, M. 1982. Action of cytochalasin D on cytoskeletal networks. *J Cell Biol,* 92**,** 79-91.

SCHRAMLOVA, J., ARIENTOVA, S. & HULINSKA, D. 2010. The role of electron microscopy in the rapid diagnosis of viral infections--review. *Folia Microbiol (Praha),* 55**,** 88-101.

SCHROEDER, C., HEIDER, H., MONCKE-BUCHNER, E. & LIN, T. I. 2005. The influenza virus ion channel and maturation cofactor M2 is a cholesterol-binding protein. *Eur Biophys J,* 34**,** 52-66.

SENNE, D. A., PANIGRAHY, B., KAWAOKA, Y., PEARSON, J. E., SUSS, J., LIPKIND, M., KIDA, H. & WEBSTER, R. G. 1996. Survey of the hemagglutinin (HA) cleavage site sequence of H5 and H7 avian influenza viruses: amino acid sequence at the HA cleavage site as a marker of pathogenicity potential. *Avian Dis,* 40**,** 425-37.

SHALABY, A. A., SLEMONS, R. D. & SWAYNE, D. E. 1994. Pathological studies of A/chicken/Alabama/7395/75 (H4N8) influenza virus in specific-pathogen-free laying hens. *Avian Dis,* 38**,** 22-32.

SHINYA, K., EBINA, M., YAMADA, S., ONO, M., KASAI, N. & KAWAOKA, Y. 2006. Avian flu: influenza virus receptors in the human airway. *Nature,* 440**,** 435-6.

SHOPE, R. E. 1931. SWINE INFLUENZA : III. FILTRATION EXPERIMENTS AND ETIOLOGY. *J Exp Med,* 54**,** 373-85.

SHORS, T. 2009. *Understanding viruses,* London:Barb House.

SHORTRIDGE, K. F., ZHOU, N. N., GUAN, Y., GAO, P., ITO, T., KAWAOKA, Y., KODIHALLI, S., KRAUSS, S., MARKWELL, D., MURTI, K. G., NORWOOD, M., SENNE, D., SIMS, L., TAKADA, A. & WEBSTER, R. G. 1998. Characterization of avian H5N1 influenza viruses from poultry in Hong Kong. *Virology,* 252**,** 331-42.

SIDORENKO, Y. & REICHL, U. 2004. Structured model of influenza virus replication in MDCK cells. *Biotechnol Bioeng,* 88**,** 1-14.

SIECZKARSKI, S. B. & WHITTAKER, G. R. 2002. Influenza virus can enter and infect cells in the absence of clathrin-mediated endocytosis. *J Virol,* 76**,** 10455-64.

SIMPSON-HOLLEY, M., ELLIS, D., FISHER, D., ELTON, D., MCCAULEY, J. & DIGARD, P. 2002. A functional link between the actin cytoskeleton and lipid rafts during budding of filamentous influenza virions. *Virology,* 301**,** 212-25.

SLEMONS, R. D., JOHNSON, D. C., OSBORN, J. S. & HAYES, F. 1974. Type-A influenza viruses isolated from wild free-flying ducks in California. *Avian Dis,* 18**,** 119-24.

SLOMKA, M. J., PAVLIDIS, T., COWARD, V. J., VOERMANS, J., KOCH, G., HANNA, A., BANKS, J. & BROWN, I. H. 2009. Validated RealTime reverse transcriptase PCR methods for the diagnosis and pathotyping of Eurasian H7 avian influenza viruses. *Influenza Other Respi Viruses,* 3**,** 151-64.

SMITH, G. L., W. L. IRVING, W.L. MCCAULEY & D.J., R. 2001. *New challenges to health : the threat of virus infection* Cambridge : Cambridge University Press.

SMITH W., C. H. A., P.P. LAIDLOW 1995. A virus obtained from influenza patients. *Medical Virology,* 5**,** 187-191.

SOGHOIAN, D. Z. & STREECK, H. 2010. Cytolytic CD4(+) T cells in viral immunity. *Expert Rev Vaccines,* 9**,** 1453-63.

SPACKMAN, E. & SUAREZ, D. L. 2008. Type A influenza virus detection and quantitation by real-time RT-PCR. *Methods Mol Biol,* 436**,** 19-26.

SPEE, J. H., DE VOS, W. M. & KUIPERS, O. P. 1993. Efficient random mutagenesis method with adjustable mutation frequency by use of PCR and dITP. *Nucleic Acids Res,* 21**,** 777-8.

STALLKNECHT, D. E., SHANE, S. M., KEARNEY, M. T. & ZWANK, P. J. 1990. Persistence of avian influenza viruses in water. *Avian Dis,* 34**,** 406-11.

STANLEY, W. M. 1944. An Evaluation of Methods for the Concentration and Purification of Influenza Virus. *J Exp Med,* 79**,** 255-66.

STEGMANN, T. 2000. Membrane fusion mechanisms: the influenza hemagglutinin paradigm and its implications for intracellular fusion. *Traffic,* 1**,** 598-604.

STEINHAUER, D. A. 1999. Role of hemagglutinin cleavage for the pathogenicity of influenza virus. *Virology,* 258**,** 1-20.

SUAREZ, D. L. & SCHULTZ-CHERRY, S. 2000. Immunology of avian influenza virus: a review. *Dev Comp Immunol,* 24**,** 269-83.

SUGITA, Y., NODA, T., SAGARA, H. & KAWAOKA, Y. 2011. Ultracentrifugation deforms unfixed influenza A virions. *J Gen Virol,* 92**,** 2485-93.

SUN, X. & WHITTAKER, G. R. 2007. Role of the actin cytoskeleton during influenza virus internalization into polarized epithelial cells. *Cell Microbiol,* 9**,** 1672-82.

SUPTAWIWAT, O., TANTILIPIKORN, P., BOONARKART, C., LUMYONGSATIEN, J., UIPRASERTKUL, M., PUTHAVATHANA, P. & AUEWARAKUL, P. 2010. Enhanced susceptibility of nasal polyp tissues to avian and human influenza viruses. *PLoS One,* 5**,** e12973.

SUZUKI, H., SAITO, R., MASUDA, H., OSHITANI, H., SATO, M. & SATO, I. 2003. Emergence of amantadine-resistant influenza A viruses: epidemiological study. *J Infect Chemother,* 9**,** 195-200.

SWAYNE, D. E. 2008. *Avian influenza,* Ames, lowa : Blackwell.

SWAYNE, D. E. & SLEMONS, R. D. 1994. Comparative pathology of a chicken-origin and two duck-origin influenza virus isolates in chickens: the effect of route of inoculation. *Vet Pathol,* 31**,** 237-45.

TAKIZAWA, T., MATSUKAWA, S., HIGUCHI, Y., NAKAMURA, S., NAKANISHI, Y. & FUKUDA, R. 1993. Induction of programmed cell death (apoptosis) by influenza virus infection in tissue culture cells. *J Gen Virol,* 74 (Pt 11)**,** 2347-55.

TELLIER, R. 2006. Review of aerosol transmission of influenza A virus. *Emerg Infect Dis,* 12**,** 1657-62.

TELLIER, R. 2009. Aerosol transmission of influenza A virus: a review of new studies. *J R Soc Interface,* 6 Suppl 6**,** S783-90.

THORLUND, K., AWAD, T., BOIVIN, G. & THABANE, L. 2011. Systematic review of influenza resistance to the neuraminidase inhibitors. *BMC Infect Dis,* 11**,** 134.

TIMBURY, M. C. 1997. *Notes on medical virology* Edinburgh : Churchill Livingstone.

TONG, S., LI, Y., RIVAILLER, P., CONRARDY, C., CASTILLO, D. A., CHEN, L. M., RECUENCO, S., ELLISON, J. A., DAVIS, C. T., YORK, I. A., TURMELLE, A. S., MORAN, D., ROGERS, S., SHI, M., TAO, Y., WEIL, M. R., TANG, K., ROWE, L. A., SAMMONS, S., XU, X., FRACE, M., LINDBLADE, K. A., COX, N. J., ANDERSON, L. J., RUPPRECHT, C. E. & DONIS, R. O. 2012. A distinct lineage of influenza A virus from bats. *Proc Natl Acad Sci U S A,* 109**,** 4269-74.

TONG, S., ZHU, X., LI, Y., SHI, M., ZHANG, J., BOURGEOIS, M., YANG, H., CHEN, X., RECUENCO, S., GOMEZ, J., CHEN, L. M., JOHNSON, A., TAO, Y., DREYFUS, C., YU, W., MCBRIDE, R., CARNEY, P. J., GILBERT, A. T., CHANG, J., GUO, Z., DAVIS, C. T., PAULSON, J. C., STEVENS, J., RUPPRECHT, C. E., HOLMES, E. C., WILSON, I. A. & DONIS, R. O. 2013. New world bats harbor diverse influenza A viruses. *PLoS Pathog,* 9**,** e1003657.

TOWBIN, H., STAEHELIN, T. & GORDON, J. 1979. Electrophoretic transfer of proteins from polyacrylamide gels to nitrocellulose sheets: procedure and some applications. *Proc Natl Acad Sci U S A,* 76**,** 4350-4.

TREBBIEN, R., LARSEN, L. E. & VIUFF, B. M. 2011. Distribution of sialic acid receptors and influenza A virus of avian and swine origin in experimentally infected pigs. *Virol J,* 8**,** 434.

TRIFONOV, V., KHIABANIAN, H. & RABADAN, R. 2009. Geographic dependence, surveillance, and origins of the 2009 influenza A (H1N1) virus. *N Engl J Med,* 361**,** 115-9.

UNIVERSITY JAWA STATE. 2010. *High Pathogenicity Avian Influenza* [Online]. Available: http://www.cfsph.iastate.edu/Factsheets/pdfs/highly_pathogenic_avian_influenza.pdf.

VAN-TAM, J. & SELLWOOD, C. 2010. *Introduction to pandemic influenza* Wallingford : CABI.

VAN DE SANDT, C. E., KREIJTZ, J. H. & RIMMELZWAAN, G. F. 2012. Evasion of influenza A viruses from innate and adaptive immune responses. *Viruses,* 4**,** 1438-76.

VASCELLARI, M., GRANATO, A., TREVISAN, L., BASILICATA, L., TOFFAN, A., MILANI, A. & MUTINELLI, F. 2007. Pathologic findings of highly pathogenic avian influenza virus A/Duck/Vietnam/12/05 (H5N1) in Turkeys

International Journal of Veterinary Science

6**,** 679-83.

VEERARAGHAVAN, N. & SREEVALSAN, T. 1961. Evaluation of some methods of concentration and purification of influenza virus. *Bull World Health Organ,* 24**,** 695-702.

VIGNUZZI, M., STONE, J. K., ARNOLD, J. J., CAMERON, C. E. & ANDINO, R. 2006. Quasispecies diversity determines pathogenesis through cooperative interactions in a viral population. *Nature,* 439**,** 344-8.

WANG, H., WU, X., CHENG, Y., AN, Y. & NING, Z. 2013. Tissue distribution of human and avian type sialic acid influenza virus receptors in domestic cat. *Acta Vet Hung***,** 1-10.

WANG, R. & TAUBENBERGER, J. K. 2010. Methods for molecular surveillance of influenza. *Expert Review of Anti-infective Therapy,* 8**,** 517-527.

WARD, C. L., DEMPSEY, M. H., RING, C. J., KEMPSON, R. E., ZHANG, L., GOR, D., SNOWDEN, B. W. & TISDALE, M. 2004. Design and performance testing of quantitative real time PCR assays for influenza A and B viral load measurement. *J Clin Virol,* 29**,** 179-88.

WEBSTER, R. G. 1998. Influenza: an emerging disease. *Emerg Infect Dis,* 4**,** 436-41.

WEBSTER, R. G., BEAN, W. J., GORMAN, O. T., CHAMBERS, T. M. & KAWAOKA, Y. 1992. Evolution and ecology of influenza A viruses. *Microbiol Rev,* 56**,** 152-79.

WEBSTER, R. G., YAKHNO, M., HINSHAW, V. S., BEAN, W. J. & MURTI, K. G. 1978. Intestinal influenza: replication and characterization of influenza viruses in ducks. *Virology,* 84**,** 268-78.

WHARTON, S. A., BELSHE, R. B., SKEHEL, J. J. & HAY, A. J. 1994. Role of virion M2 protein in influenza virus uncoating: specific reduction in the rate of membrane fusion between virus and liposomes by amantadine. *J Gen Virol,* 75 (Pt 4)**,** 945-8.

WHO. 2011. *Influenza fact sheet* [Online]. http://www.who.int/mediacentre/factsheets/avian_influenza/en/. 2013].

WISE, H. M., FOEGLEIN, A., SUN, J., DALTON, R. M., PATEL, S., HOWARD, W., ANDERSON, E. C., BARCLAY, W. S. & DIGARD, P. 2009. A complicated message: Identification of a novel PB1-related protein translated from influenza A virus segment 2 mRNA. *J Virol,* 83**,** 8021-31.

WISE, H. M., HUTCHINSON, E. C., JAGGER, B. W., STUART, A. D., KANG, Z. H., ROBB, N., SCHWARTZMAN, L. M., KASH, J. C., FODOR, E., FIRTH, A. E., GOG, J. R., TAUBENBERGER, J. K. & DIGARD, P. 2012. Identification of a novel splice variant form of the influenza A virus M2 ion channel with an antigenically distinct ectodomain. *PLoS Pathog,* 8**,** e1002998.

WOOD, G. W., MCCAULEY, J. W., BASHIRUDDIN, J. B. & ALEXANDER, D. J. 1993. Deduced amino acid sequences at the haemagglutinin cleavage site of avian influenza A viruses of H5 and H7 subtypes. *Arch Virol,* 130**,** 209-17.

WRIGLEY, N. G. 1979. Electron microscopy of influenza virus. *British Medical Bulleti,* 35**,** 35-38.

YEWDELL, J. W., BENNINK, J. R., SMITH, G. L. & MOSS, B. 1985. Influenza A virus nucleoprotein is a major target antigen for cross-reactive anti-influenza A virus cytotoxic T lymphocytes. *Proc Natl Acad Sci U S A,* 82**,** 1785-9.

YOUIL, R., SU, Q., TONER, T. J., SZYMKOWIAK, C., KWAN, W. S., RUBIN, B., PETRUKHIN, L., KISELEVA, I., SHAW, A. R. & DISTEFANO, D. 2004. Comparative study of influenza virus replication in Vero and MDCK cell lines. *J Virol Methods,* 120**,** 23-31.

YU, J. E., YOON, H., LEE, H. J., LEE, J. H., CHANG, B. J., SONG, C. S. & NAHM, S. S. 2011. Expression patterns of influenza virus receptors in the respiratory tracts of four species of poultry. *J Vet Sci,* 12**,** 7-13.

ZAMBON, M. C. 1999. Epidemiology and pathogenesis of influenza. *J Antimicrob Chemother,* 44 Suppl B**,** 3-9.

ZAMBON, M. C. 2001. The pathogenesis of influenza in humans. *Rev Med Virol,* 11**,** 227-41.

ZHANG, J., LESER, G. P., PEKOSZ, A. & LAMB, R. A. 2000. The cytoplasmic tails of the influenza virus spike glycoproteins are required for normal genome packaging. *Virology,* 269**,** 325-34.

ZHANG, Y., HUNG, T., SONG, J. & HE, J. 2013. Electron microscopy: essentials for viral structure, morphogenesis and rapid diagnosis. *Sci China Life Sci,* 56**,** 421-30.

ZHOU, Z., JIANG, X., LIU, D., FAN, Z., HU, X., YAN, J., WANG, M. & GAO, G. F. 2009. Autophagy is involved in influenza A virus replication. *Autophagy,* 5**,** 321-8.